

**Genetic Characterization of Selected Cyanobacteria and their Role in
Remediating Environmental Pollutants**



By

MUHAMMAD KALEEM

03041911008

**DEPARTMENT OF PLANT SCIENCES FACULTY OF
BIOLOGICAL SCIENCES
QUAID-I-AZAM UNIVERSITY ISLAMABAD, PAKISTAN**

2024

**Genetic Characterization of Selected Cyanobacteria and their Role in
Remediating Environmental Pollutants**



By MUHAMMAD KALEEM

03041911008

**A Thesis Submitted to the QUAID-I-AZAM University in Partial
Fulfilment of the Requirements for the Degree of**

DOCTOR OF PHILOSOPHY (Ph.D.)

in

PLANT SCIENCES

**DEPARTMENT OF PLANT SCIENCES FACULTY OF
BIOLOGICAL SCIENCES
QUAID-I-AZAM UNIVERSITY ISLAMABAD, PAKISTAN**

2024

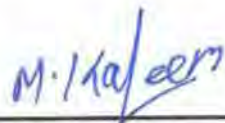


Author's Declaration

I Muhammad Kaleem hereby declare that this thesis entitled "Genetic Characterization of Selected Cyanobacteria and their Role in Remediating Environmental Pollutants" is my own work & effort and that it has not been submitted anywhere for any award/Degree. This work has not been submitted previously by me for taking any degree from Quaid-i-Azam University, Islamabad, Pakistan or anywhere else.

Where other source of information has been used, they have been properly acknowledged. Furthermore, the research work presented in this thesis was carried out by me in the Plant Genetics and Genomics Laboratory, Department of Plant Sciences.

At any time if my statement is found to be incorrect even after my Graduation the university has the right to withdraw my PhD degree.



M. Kaleem

Date: 18-09-2024

Plagiarism undertaking

I solemnly declare that research work presented in the thesis titled "**Genetic Characterization of Selected Cyanobacteria and their Role in Remediating Environmental Pollutants**" is solely my research work with no significant contributions from any other person. Small help wherever taken has been duly acknowledge and that complete thesis has been written by me.

I understand the zero tolerance policy of the HEC and University "**Quaid-i-Azam University Islamabad**" toward plagiarism. Therefore, I as an author of the above titled declare that no portion of my thesis has been plagiarized and any material used as reference is properly cited.

I undertake that if I am found guilty of any formal plagiarism in the above titled thesis even after award of Ph.D. degree, the university reserve the right to withdraw/revoke my PhD degree and that HEC has the right to publish my name on HEC/University website on which names of students are places who submitted plagiarized thesis.



Muhammad Kaleem

University ID# 03041911008

Plant Sciences

Thesis Dedication

My Father

Muhammad Hanif

For earning an honest living for us and for supporting and encouraging me to believe in myself.

My Mother

Akhtari Begam

A strong and gentle soul who taught me to trust Allah, believe in hard work and that so much could be done with little.

My Brother

Muhammad Khalid

who represented me 'living proof' of men's ability to redefine and recreate our lives despite, and maybe even because of, the tremendously constraining, oppressive and repressive situation in which we often exist.

My Brother

Muhammad Nadeem

Who have been my source of inspiration and gave me strength when I thought of giving up, who continually provide their moral, spiritual, emotional, and financial support.

My Younger Brother

Muhammad Saleem

Who always fight with me, who annoy me in every possible way, and when I really need help, when I let out loud for help, No one came forward but you, for which I owe you a big thank you. Respect you, my hero.

Special Thanks

“What we do for ourselves dies with us, what we do for other remains and are immortal”.

(Albert Pike)

*I pay my special thanks to my respected **Mother and Father** for their countless love, care, encouragement and support throughout my life.*


And

*I pay my special thanks to my supervisors **Prof. Dr. Abdul Samad Mumtaz and Dr. Muhammad Zaffar Hashmi** for their guidance, help and valuable assistance.*

APPROVAL CERTIFICATE

This is to certify that the research work presented in this thesis entitled "**Genetic Characterization of Selected Cyanobacteria and their Role in Remediating Environmental Pollutants**" was conducted by Mr. Muhammad Kaleem under the supervision of Prof. Dr. Abdul Samad Mumtaz and Dr. Muhammad Zaffar Hashmi. No part of this thesis has been submitted anywhere else for any other degree. This thesis is submitted to the Department of Plant Sciences, Quaid-i-Azam University Islamabad, Pakistan in partial fulfillment for the Degree of "**Doctor of Philosophy**" in the field of Plant Sciences.

Student Name: Muhammad Kaleem

Signature: 

Examination Committee

External Examiner 1:

Prof. Dr. Rahmatullah Qureshi
Dean, Faculty of Sciences,
PMAS-Arid Agriculture University,
Rawalpindi.

Signature: 

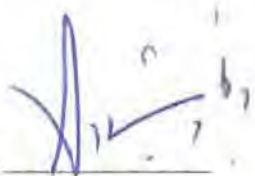
External Examiner II:

Dr. Syed Aneel Ahmad Gilani
Curator, Botanical Sciences
Division, Pakistan Museum of
Natural History, Islamabad.

Signature: 

Supervisor

Prof. Dr. Abdul Samad Mumtaz
Department of Plant Sciences,
Quaid-I-Azam University,
Islamabad.

Signature: 

Co-supervisor

Dr. Muhammad Zaffar Hashmi
Institute of Molecular Biology and
Biotechnology, The University of
Lahore.

Signature: 

Chairman

Prof. Dr. Hassan Javed Chaudhary
Department of Plant Sciences,
Quaid-I-Azam University,
Islamabad.

Signature: 

AKNOWLEDGEMENTS

Praise is to **Almighty Allah**, the cherisher and sustainer of the worlds, the most merciful, the most beneficent, who showed his countless blessing upon us. Almighty Allah enabled me to compile my humble endeavour in the shape of this dissertation. All respect goes to the **Holy prophet Hazrat Muhammad (S.A.W)** whose teaching strengthen our faith in Allah and guiding the mankind, the true path of life, who is the source of knowledge and wisdom of entire humanity, who clarified that pursuit of knowledge is a divine commandment.

I would like to express my gratitude to all those who gave me the possibility to complete this thesis & to do the necessary research work. I have a great exhilaration for my supervisor **Professor Dr. Abdul Samad Mumtaz**, Department of Plant Sciences, Faculty of Biological Sciences, Quaid-I-Azam University, Islamabad for his valuable guidance, constructive criticism, and encouragement throughout the course of my research work. I am obliged to him for extending the research facilities of the department to accomplish this work.

I would like to express my sincere gratitude to my co-supervisor **Dr. Muhammad Zaffar Hashmi**, Institute of Molecular Biology and Biotechnology, The University of Lahore, for his invaluable support and guidance throughout my PhD research. His insightful advice, encouragement and unwavering commitment have greatly contributed to the development and success of my work. I deeply appreciate his mentorship and the time he has invested in helping me grow both academically and professionally.

I greatly extend my zealous and sincerest thanks to Ph.D. scholars, **Lubna Anjum Minhas, Amber Jabeen, Farooq Inam, Amjad Khan, Khawar Majeed, Rooma Waqar, and Surat-un-Nisa**, for providing readership & ideas, paramount to the realization of this thesis. Special thanks to my time-tested colleague, **Miss Lubna Anjum Minhas** for her, care & concern, encouragement and persistent support throughout this journey.

I can never express my feelings of thanks & love to my humble father **Mr. Muhammad Hanif**, & my affectionate mother **Akhtari Begam**, for their everlasting prayers, for me to fulfil their desires and dreams in the form of compilation of my

research project. How can I say thanks and acknowledge the two personalities which are my world, my sisters, **Miss. Khalida and Miss. Samina** who always encourages and supports me by their attitude and by their prayers, helped, and encouraged me for the degree.

Last but not the least; my acknowledgements could never adequately express obligation to my amusing brothers; **Mr. Khalid, Mr. Nadeem and Mr. Saleem** and my beloved niece and nephew, **Miss. Iqra, Mr. Shaheryar**, and my sister-in-law **Mrs. Shameem Khalid** who made this journey easier with words of encouragement. I am most indebted to my family for their endless prayers, matchless love, and care.

Finally, I would like to thank everybody who was important to the successful compilation my thesis as well as I express my apology that I could not mention their names one by one. I offer my regards and blessings to all who supported me in any respect during the compilation of thesis.

Muhammad Kaleem

Thesis general info:

This thesis comprises of five chapters

- Chapter one is a general introduction of the cyanobacteria, their characteristics, characterization of cyanobacteria, environmental pollutants and their remediation.
- Chapter two is based on isolation of cyanobacteria from wastewater. Cyanobacteria culturing, purification, Identification and selection of strains for the removal of Cd and Pb.
- Chapter 3 contains the results of biosorption potential of dried biomass of *Fischerella muscicola* and *Nostoc* sp., Kinetic and Isotherm modeling of the experimental biosorption data.
- Chapter 4 describes the results of Cd and Pb toxicity assessment in two cyanobacteria, *Fischerella muscicola* and *Nostoc* sp. Biosorption potential of fresh biomass of *Fischerella muscicola* and *Nostoc* sp. in removing Cd and Pb from aqueous solutions, Kinetic and Isotherm modelling of the experimental biosorption data.
- Chapter 5 compiles the results of Iron oxide nanoparticles synthesis using metabolites extract of *Fischerella muscicola* and *Nostoc* sp., characterization of nanoparticles and their applications in the removal of Cd and Pb from aqueous solutions, Kinetic and Isotherm modelling of the biosorption experimental data.
- Combine conclusion of all the chapters (chp-2 to chp-5) and future recommendations.
- The bibliography was arranged at the end of the thesis.
- **Publications**

ABBREVIATIONS

°C	Degrees Celsius
%	Percentage
ml	Milliliters
mg	Mili gram
μL	Microliter
μm	Micrometer
μM	Micromolar
BBM	Bold's Basal Medium
BG11	Blue-Green Medium
Cm	Centimetre
CO ₂	Carbon Dioxide
DNA	Deoxyribo Nucleic Acid
DMSO	Dimethylsulfoxide
L	Liter
LM	Light microscopy
Min	Minutes
mm	Millimetre
NCBI	National Centre for Biotechnology Information
NaCl	Sodium chloride
NaNO ₃	Sodium Nitrate
OD	Optical Density
pH	Power of hydrogen
PCR	Polymerase chain reaction
Ph.D	Doctor of Philosophy
QAU	Quaid-I-Azam University Islamabad
SEM	Scanning Electron Microscope/Microscopy
sp.	Species
FTIR	Fourier Transform Infrared Spectroscopy
XRD	X-Ray diffraction

EDX	Energy-dispersive X-ray spectroscopy
Cd	Cd
Pb	Lead
IONPs	Iron Oxide Nanoparticles
U.V	Ultraviolet spectroscopy
HMs	Heavy Metals
NPs	Nanoparticles
CdCl ₂	Cd chloride
Pb(NO ₃) ₂	Lead nitrate
FeCl ₃ .6H ₂ O	Iron chloride hexahydrate
HCl	Hydrochloric Acid
NaOH	Sodium hydroxide
SPR	Surface Plasmon Resonance
FAAS	Flame Atomic Adsorption Spectrometer
JCPD	Joint Committee on Powder Diffraction Standards

Table of Contents
Table of Contents

Contents	Page no
Summary	01
Chapter 1: Introduction	
1.1. Introduction	03
1.2. Occurrence and distribution	04
1.3. Cyanobacteria culturing	05
1.4. Identification of cyanobacteria	06
1.5. Potential applications of cyanobacteria	08
1.6. Environmental pollutants	09
1.6.1. Heavy metals /In organic pollutants	11
1.6.1.1 Cd	12
1.6.1.2. Pb	13
1.6.2. Prevalence of Heavy Metals in Pakistan	14
1.7. Bioremediation	15
1.7.1. Bioaccumulation	16
1.7.2. Biosorption	16
1.7.3. Cyano-remediation	17
1.8. Nanoparticles and Nano remediation	18
1.9. Aims and Objectives	20
Chapter 2: Collection, Culturing and Screening of cyanobacteria from wastewater sites	
Summary	22
2. 1. Introduction	23
2.1.1. Cyanobacteria isolation and culturing	23
2.1.2. Identification	23
2.1.3. 16s RNA gene sequencing	25
2.1.4. Objectives	25
2.2. Materials and Methods	26
2.2.1. Study Area	26

2.2.2. Collection sites	27
2.2.3. Collection of samples	27
2.2.4. Water physico-chemical analysis	28
2.2.5. Chemicals	28
2.2.6. Microscopic observation and strains identification	28
2.2.7. Culturing	28
2.2.8. Purification in solid agar plating	29
2.2.9. Morphological characterization of axenic cultures	30
2.2.10. Molecular characterization of cyanobacteria	30
2.2.10.1. DNA Isolation	30
2.2.10.2. Gel Electrophoresis	31
2.2.10.3. Polymerase chain reaction (PCR)	31
2.2.10.4. Purification of PCR products	32
2.2.10.5. Nucleotide sequence analysis	32
2.2.10.6. Molecular Phylogenetic analysis	32
2.2.11. Initial screening of heavy metals (Cd and Pb) tolerance	32
2.3. Results	34
2.3.1. Collection sites and samples	34
2.3.2. Physico-chemical analysis	34
2.3.3. Microscopic observations	36
2.3.3.1. Initial screening of cyanobacteria	36
2.3.3.2. Culturing	36
2.3.4. Morphological, molecular and phylogenetic analysis of axenic strains	37
2.3.5. The Oscillatorales	37
2.3.6.1. <i>Desertifilum tharense</i> MK-2	37
2.3.6.2. <i>Phormidium</i> sp. MK-3	39
2.3.6.3. <i>Nodosilinea nodulosa</i> strain MK-4	41
2.3.7. The Nostacales	43
2.3.7.1. <i>Desikacharya</i> sp. MK-7.	43
2.3.7.2. <i>Fischerella muscicola</i> MK-8	45

2.3.7.3. <i>Westiellopsis prolifica</i> MK-9	47
2.3.7.4. <i>Nostoc</i> sp. MK-11	49
2.3.8. The Chroococcales	51
2.3.8.1. <i>Synechocystis fuscopigmentosa</i> MK-13	51
2.3.8.2. <i>Gloeocapsa</i> sp. MK-14	53
2.3.8.3. <i>Synechococcus elongatus</i> strain MK-16	55
2.3.9. Screening of strains against Cd and Pb	57
2.3.10. Discussion	58
Chapter 3. Cd and Pb Biosorption capacity in dried biomass of <i>Fischerella muscicola</i> and <i>Nostoc</i> sp.: Kinetics and Isotherm modeling	
Summary	69
3.1. Introduction	70
3.2. Materials and Methods	72
3.2.1. Chemicals	72
3.2.2. Culturing	72
3.2.3. Biomass production and harvesting	72
3.2.4. Batch biosorption experiments	72
3.2.5. Biosorbent characterization	74
3.2.6. Desorption and reusability	74
3.2.7. Data analysis	74
3.3. Results and Discussion	76
3.3.1. Characterization of biomass	76
3.3.1.1. Fourir transform infrared spectroscopy	76
3.3.1.2. Scaning electron microscopy	77
3.3.2. Effect of pH	78
3.3.3. Effect of contact time	80
3.3.4. Biosorption kinetics	81
3.3.5. Effect of initial metal concentrations	85
3.3.6. Biosrption Isotherms	86
3.3.7. Desorption and reusability	89

Chapter 4: Comparative studies on growth and biosorption of Cd and Pb from contaminated aqueous solutions by fresh biomass of *Fischerella muscicola* and *Nostoc* sp.: Kinetic and Isotherm modeling

Summary	93
4.1. Introduction	94
4.2. Materials and Methods	97
4.2.1. Culturing and assessment of Cd and Pb toxicity effects on growth	97
4.2.2. Measurement of photosynthetic pigments	97
4.2.3. Measurement of dry weight	97
4.2.4. Batch biosorption experiments	98
4.2.5. Biosorbent characterization	98
4.2.6. Data analysis	99
4.3. Results and Discussion	100
4.3.1. Effects of Cd and Pb on growth of <i>Fischerella muscicola</i> and <i>Nostoc</i> sp.	100
4.3.2. Effects of Cd and Pb on biomass	103
4.3.3. Effects of Cd and Pb on the photosynthetic pigments	105
4.3.4. FTIR	107
4.3.5. Effect of pH on biosorption of Cd and Pb	109
4.3.6. Effect of contact time on biosorption of Cd and Pb	110
4.3.7. Kinetic study	112
4.3.8. Effect of initial metal concentrations on biosorption	114
4.3.9. Isotherm study	115

Chapter 5: Fabrication of Iron oxide nanoparticles using *Fischerella muscicola* and *Nostoc* sp. extracts and adsorption of Cd and Pb from contaminated aqueous solutions: Kinetic and Isotherm modeling

Summary	123
5.1. Introduction	124
5.2. Materials and Methods	126
5.2.1. Chemicals	126

5.2.2. Biogenic synthesis of cyanobacteria extract mediated IONPs	126
5.2.3. Physio-chemical Characterizations of IONPs	127
5.2.4. Adsorption Batch study	128
5.2.5. Desorption and reusability	128
5.3. Results and Discussion	129
5.3.1. Physiochemical Characterizations	129
5.3.1.1. Colour indication	129
5.3.1.2. UV-visible spectroscopy	130
5.3.1.3. FTIR	130
5.3.1.4. X-ray diffraction	132
5.3.1.5. Energy dispersive X-Ray and Scanning electron microscopy	133
5.3.2. Impact of pH on the adsorption of metals	134
5.3.3. Impact of contact time on adsorption	135
5.3.4. Kinetic modeling of the experimental data	137
5.3.5. Impact of initial metal concentrations on adsorption of Cd and Pb	139
5.3.6. Isotherm study	141
5.3.7. Desorption and Reusability	144

List of Figures

Sr. No	Title	Page no
Chapter 1		
1.1	Overview of the potential of cyanobacteria in different fields of science and development	08
Chapter 2		
2.1	Map of the study area: (a) map of Pakistan; (b) map of Punjab; (c) map of Islamabad and Rawalpindi	26
2.2	Collection sites of algal samples: (a-j) e-waste polluted water, Park road Islamabad; (k-o) sewage water, I-9 sector Islamabad; (p) sewagewater, Gojar khan, Rawalpindi.	27
2.3	Growth patterns of cyanobacteria in BG-11 agar media: (a) <i>Desertifilum tharense</i> MK-2; (b) <i>Phormidium</i> MK-3; (c) <i>Nodosilinea nodulosa</i> MK-4; (d) <i>Desikacharya</i> sp. MK-7; (e) <i>Fischerella muscicola</i> MK-8; (f) <i>Westiellopsis prolifica</i> MK-9; (g) <i>Nostoc</i> sp. MK- 11; (h) <i>Synechocystis fuscopigmentosa</i> MK-13 (i); <i>Gloeocapsa</i> sp. MK14; (j) <i>Synechococcus elongatus</i> strain MK-15	36
2.4	Micrographs of <i>D. tharense</i> MK-2: (a1) Cells longer than wide (arrow), (a2) isodiametric cells (arrow); (b) Filaments with transparent sheath at the apical cell (arrow); (c) aerotypes in the cells (arrow).	37
2.5	NJ analysis of 16S rRNA data of strain MK-2.	38
2.6	Micrographs of <i>Phormidium</i> sp. MK-3: (a) densely packed filaments; (b) Trichome surrounded by a colorless sheath and sheath at the tip(arrow); (c) necridia development in the trichome (arrow).	39
2.7	NJ analysis of 16S rRNA data of strain MK-3.	40
2.8	Micrographs of <i>Nodosilinea nodulosa</i> strain MK-4 under the light microscopy: (a) mature filaments forming spiral arrangements of the cells (arrow); (b) characteristic nodule (arrow); (c) nodules forming on BG-11 agar media (arrow).	41
2.9	NJ analysis of 16S rRNA data of strain MK-4.	42

2.10	Micrographs of <i>Desikacharya</i> sp. MK-7 under the light microscopy; (a) Irregular shaped colony on agar BG-0 media; (b) coiled trichomes; (c) intercalary elliptical heterocyst; (d) terminal, slightly oval shaped heterocyst; (e) terminal sub-spherical heterocyst	43
2.11	NJ analysis of 16S rRNA data of strain MK-7.	44
2.12	Micrographs of Strain <i>Fischerella muscicola</i> MK-8 under the light microscope: (a) T-type branches (arrow); (b) bi-seriate condition (arrow); (c) round shaped terminal cells (arrow); (d) heterocysts in main filaments (arrow) and branches (arrow); (e) Intercalary heterocyst in main filaments (arrow).	45
2.13	NJ analysis of 16S rRNA data of strain MK-8.	46
2.14	Micrographs of Strain <i>Westiellopsis prolifica</i> MK-9: (a) T-type branches (arrow); (b) barrel shaped heterocyst (arrow); (c) elongated cylindrical heterocyst (arrow); (d) pseudohormocyte showing transverse and longitudinal cell division (arrow).	47
2.15	NJ analysis of 16S rRNA data of strain MK-9.	48
2.16	Micrographs of <i>Nostoc</i> sp. MK-11 under light microscope: (a) colorless sheath (arrow); (b) granulated cells (arrow); (c) heterocysts sub-spherical in shape present at both ends end of the trichome (arrows); (d) intercalary heterocyst (arrow).	49
2.17	NJ analysis of 16S rRNA data of strain MK-11.	50
2.18	Micrographs of <i>Synechocystis fuscopigmentosa</i> MK-13: (a1) oval shaped cells (a) (arrow); (b) colorless cells (arrow); (c) thin mucilage around the cells (arrow); (d) cell constricted at the middle (arrow).	51
2.19	NJ analysis of 16S rRNA data of strain MK-13	52
2.20	Micrographs of <i>Gloeocapsa</i> sp. MK1-4 under the light microscope: (a) Colony of cells enclosed by mucilage (arrow); (b) colorless mucilage around the cells of the colony (arrow); (c) dispersion of cells from the colonies	53
2.21	NJ analysis of 16S rRNA data of strain MK-14.	54

2.22	Micrographs of <i>Synechococcus elongatus</i> MK-15 under the light microscope (a) elongated cells; (b) bluish-green color of the cells; (c) Growth on BG-11 agar media.	55
2.23	NJ analysis of 16S rRNA data of strain MK-15	56
Chapter 3		
3.1	Diagrammatic depiction of batch-mode investigations designed to explore the biosorption of metal ions using dried biomass of <i>F. muscicola</i> and <i>Nostoc</i> sp.	73
3.2	(a) FTIR spectra of non-treated, Cd and Pb treated dry biomass of <i>F. muscicola</i> ; (b) FTIR spectra of non-treated, Cd and Pb treated dry biomass of <i>Nostoc</i> sp.	77
3.3	SEM images of biomass: (A) SEM images of <i>F. muscicola</i> : (a) dull surface of raw biomass; (b) bright surface of biomass saturated by Cd; (c) bright surface of biomass saturated by Pb. (B) SEM images of <i>Nostoc</i> sp.: (a) dull surface of raw biomass b) bright surface of biomass saturated by Cd; bright surface of biomass saturated by Pb.	78
3.4	(a) Effect of pH on Pb and Cd ions biosorption by dried biomass of <i>F. muscicola</i> ; (b) Effect of pH on Pb and Cd ions biosorption by dried biomass of <i>Nostoc</i> sp.	80
3.5	(a) Effect of contact time on Pb and Cd ions biosorption by dried biomass of <i>F. muscicola</i> ; (b) Effect of contact time on Pb and Cd ions biosorption by dried biomass of <i>Nostoc</i> sp..	81
3.6	(a) Pseudo first order; (b) Pseudo second order; (c) Intraparticle diffusion, kinetics for the biosorption of Cd and Pb by dried biomass of <i>F. muscicola</i>	82
3.7	(a) Pseudo first order; (b) Pseudo second order; (c) Intraparticle diffusion kinetics for the biosorption of Cd and Pb by dried biomass of <i>Nostoc</i> sp.	83

3.8	(a) Effect of initial metal concentrations on the biosorption of Cd and Pb by dried biomass of <i>F. muscicola</i> ; (b) Effect of initial metal concentrations on the biosorption of Cd and Pb ions by dried biomass of <i>Nostoc</i> sp.	85
3.9	(a) Langmuir isotherm; (b) Freundlich isotherms; (c) Temkin isotherm models for the biosorption of Cd and Pb by dried biomass of <i>F.muscicola</i> .	87
3.10	(a) Langmuir; (b) Freundlich; (c) Temkin, isotherm models for the biosorption of Cd and Pb by dried biomass of <i>Nostoc</i> sp.	87
Chapter 4		
4.1	Visuals of Cd and Pb stress on growth of cyanobacteria strains: (a) Growth (12 days culturing) visuals of <i>F. muscicola</i> in BG ₁₁ media with different Cd concentrations; (b) Growth (12 days culturing) visuals of <i>F. muscicola</i> in BG ₁₁ media with different Pb concentrations; (c) Growth (12 days culturing) visuals of <i>Nostoc</i> sp. in BG ₁₁ media with different Cd concentrations; (d) Growth (12 days culturing) visuals of <i>Nostoc</i> sp. in BG ₁₁ media with different Pb concentrations.	100
4.2	Microscopic images of Cd and Pb stress on the morphology of cyanobacteria strains: (a) Morphology of <i>F. muscicola</i> (4 days culturing) in BG ₁₁ media with Cd (0mg/L); (b) Morphology of <i>F. muscicola</i> (4 days culturing) in BG ₁₁ media with Cd (3 mg/L); (c) Morphology of <i>F. muscicola</i> (4 days culturing) in BG ₁₁ media with Pb (120 mg/L); (d) Morphology of <i>Nostoc</i> sp. (4 days culturing) in BG ₁₁ media with Cd(0 mg/L); (e) Morphology of <i>Nostoc</i> sp. (4 days culturing) in BG ₁₁ media with Cd (3mg/L); (f) Morphology of <i>Nostoc</i> sp. (4 days culturing) in BG ₁₁ media with Pb (120 mg/L).	101

4.3	Growth curves of two cyanobacteria strains: (a) growth curve of <i>F. muscicola</i> under control and various concentrations of Cd; (b) growth curve of <i>F. muscicola</i> under control and various concentrations of Pb; (c) growth curve of <i>Nostoc</i> sp. under control and various concentrations of Cd; (d) growth curve of <i>Nostoc</i> sp. under control and various concentrations of Pb.	103
4.4	Effect of different initial concentrations of Cd and Pb on biomass of two cyanobacteria strains: (a) effect of different initial concentrations of Cd on biomass of <i>F. muscicola</i> ; (b) Effect of various Pb concentration on biomass of <i>F. muscicola</i> ; (c) effect of various initial Cd concentrations on biomass of <i>Nostoc</i> sp.; (d) effect of different initial Pb concentration on biomass of <i>Nostoc</i> sp.	104
4.5	Effects of different concentrations of Cd and Pb on the photosynthetic pigments of two cyanobacteria strains: (a) effect of different Cd concentration on chlorophyll <i>a</i> content of <i>F. muscicola</i> ; (b) effect of various concentrations of Pb on chlorophyll <i>a</i> content of <i>F. muscicola</i> ; (c) effect of different Cd concentration on carotenoids content of <i>F. muscicola</i> ; (d) effect of various concentrations of Pb on carotenoids content of <i>F. muscicola</i> .	106
4.6	Effects of different concentrations of Cd and Pb on the photosynthetic pigments of two cyanobacteria strains: (a) effect of different Cd concentration on chlorophyll <i>a</i> content of <i>Nostoc</i> sp.; (b) effect of various concentrations of Pb concentration on chlorophyll <i>a</i> content of <i>Nostoc</i> sp.; (c) effect of different Cd concentration on carotenoids content of <i>Nostoc</i> sp.; (d) effect of different concentrations of Pb on carotenoids content of <i>Nostoc</i> sp.	107
4.7	FTIR spectra of two cyanobacteria fresh biomass: (a) FTIR spectra of <i>F. muscicola</i> fresh biomass; (b) FTIR spectra of <i>Nostoc</i> sp. fresh biomass.	109

4.8	(a) Effect of pH on the biosorption of Cd and Pb by fresh biomass of <i>F. muscicola</i> ; (b) Effect of pH on the biosorption of Cd and Pb by fresh biomass of <i>Nostoc</i> sp.	110
4.9	(a) Effect of contact time on the biosorption of Cd and Pb by the fresh biomass of <i>F. muscicola</i> ; (b) Effect of contact time on the biosorption of Cd and Pb by fresh biomass of <i>Nostoc</i> sp.	111
4.10.	(a) Pseudo first order; (b) Pseudo second order; (c) Intraparticle diffusion kinetics for the biosorption of Cd and Pb by fresh biomass of <i>F. muscicola</i> .	112
4.11.	(a) Pseudo first order; (b) Pseudo second order; (c) Intraparticle diffusion kinetics for the biosorption of Cd and Pb by fresh biomass of <i>Nostoc</i> sp.	113
4.12.	(a) Effect of initial metal concentrations on the biosorption of Cd and Pb ions by the fresh biomass of <i>F. muscicola</i> ; (b) Effect of initial metal concentrations biosorption of Cd and Pb ions by fresh biomass of <i>Nostoc</i> sp.	115
4.13	(a) Langmuir; (b) Freundlich; (c) Temkin, isotherm models for the biosorption of Cd and Pb by fresh biomass of <i>F. muscicola</i>	16
4.14	(a) Langmuir isotherm; (b) Freundlich isotherm; (c) Temkin, isotherm models for the biosorption of Cd and Pb by fresh biomass of <i>Nostoc</i> sp.	116
Chapter 5		
5.1	Biogenic synthesis of IONPs	127
5.2	(aA) Extract of <i>F. muscicola</i> ; (aB) Iron chloride hexahydrate salt solution; (aC) dark brown IONPs; (bA) extract of <i>Nostoc</i> sp.; (bB) Iron chloride hexahydrate salt solution; (bC) dark brown IONPs; (c) Biological reduction mechanism of Iron Oxide NPs using <i>F. muscicola</i> and <i>Nostoc</i> sp. extracts.	129

5.3	U. Vis spectra of IONPs: (a) U.V spectra of IONPs (<i>F. muscicola</i> mediated IONPs); (b) U.Vis spectra of IONPs (<i>Nostoc</i> sp. mediated IONPs).	130
5.4	FTIR spectra of biogenic IONPs: (a) FTIR spectra of <i>F. muscicola</i> extract mediated IONPs; (b) FTIR spectra of <i>Nostoc</i> sp. extract mediated IONPs.	132
5.5	(a) XRD pattern of <i>F. muscicola</i> mediated IONPs; (d) Size calculation of <i>F. muscicola</i> mediated IONPs; (c) XRD pattern of <i>Nostoc</i> sp. mediated IONPs; (d) Size calculation of <i>Nostoc</i> sp. mediated IONPs.	133
5.6	(a) EDX spectrum of <i>F. muscicola</i> mediated IONPs; (b) EDX spectrum of <i>Nostoc</i> sp. mediated IONPs; (c) SEM image of <i>F. muscicola</i> mediated IONPs; (d) SEM image of <i>Nostoc</i> sp. mediated IONPs	134
5.7	(a) Impact of pH on adsorption of Cd and Pb ions onto the <i>F. muscicola</i> mediated IONPs; (b) Impact of pH on adsorption of Cd and Pb ions onto the <i>Nostoc</i> sp. mediated IONPs.	135
5.8	(a) Impact of contact time on the adsorption of Cd and Pb ions onto the <i>F. muscicola</i> mediated IONPs; (b) Impact of contact time on adsorption of Cd and Pb ions onto the <i>Nostoc</i> sp. mediated.	136
5.9	Pseudo 1 st order; (b) Pseudo 2 nd ; (c) Intraparticle diffusion, kinetics for the adsorption of Cd and Pb onto the <i>F. muscicola</i> mediated IONPs.	138
5.10	Pseudo 1 st order; (b) Pseudo 2 nd ; (c) Intraparticle diffusion, kinetics for the adsorption of Cd and Pb onto the <i>Nostoc</i> sp. mediated IONPs.	138
5.11	Impact of initial metal concentrations on the adsorption of Cd and Pb ions onto the <i>F. muscicola</i> mediated IONPs; (b) Impact of initial metal concentrations on the adsorption of Cd and Pb ions onto the <i>Nostoc</i> sp. mediated IONP.	140

5.12	(a) Langmuir; (b) Freundlich; (c) Temkin, isotherms for the adsorption of Cd and Pb onto the <i>F. muscicola</i> mediated IONPs	141
5.13	Langmuir; (b) Freundlich; (c) Temkin, isotherm for the adsorption of Cd and Pb onto the <i>Nostoc</i> sp. mediated IONPs.	141
5.14	(a) Reusability of <i>F. muscicola</i> mediated IONPs; (b) Reusability of <i>Nostoc</i> sp. mediated IONPs.	145

List of Tables

Sr. No	Title	Page no
Chapter 2		
2.1	The collection sites and associated field data	34
2.2	Physio-chemical parameters of water samples	35
2.3	Heavy metals detected in the water from three different sites of Rawalpindi and Islamabad.	35
2.4	Screening of strains exposed to different concentrations of Cd and Pb in aqueous solutions	57
Chapter 3		
3.1	Parameters of kinetic models	84
3.2	Parameters of Isotherm models	89
3.3	Biosorption-Desorption of Cd and Pb by dried biomass of <i>F. muscicola</i> and <i>Nostoc</i> sp.	90
3.4	Comparison of maximum biosorption capacities of <i>F. muscicola</i> and <i>Nostoc</i> sp. dried biomass with other biosorbents	90
Chapter 4		
4.1	Parameters of kinetic models	114
4.2	Parameters of Isotherm models	118
4.3	Comparison of maximum biosorption capacities of <i>F. muscicola</i> and <i>Nostoc</i> sp. fresh biomass with other biosorbents	119
Chapter 5		
5.1	Parameters of the pseudo first order, pseudo second order and intraparticle diffusion kinetic models	139
5.2	Parameters of Langmuir, Freundlich and Temkin isotherm models	143
5.3	Comparison of maximum adsorption capacities of <i>F. muscicola</i> and <i>Nostoc</i> sp. -mediated IONP with other adsorbents	143
Synthesis and Conclusions		146
Future Recommendations		148

Bibliography	149
List of Publications	211
Appendices	214

Summary

Bioremediation using microorganisms such as bacteria, cyanobacteria, microalgae, yeasts, and fungi is efficient, cost-effective, and eco-friendly. Among these, cyanobacteria can carry out oxygenic photosynthesis, fix atmospheric nitrogen and pose flexibility to sustain a range of harsh conditions. These also offer the promise for treating environmental pollutants found in soil and water. Despite huge prospects little or no work is available on indigenous/local cyanobacterial species of Pakistan. Therefore, this research was initiated to isolate and assess the potentials of local cyanobacterial strains capable of remediating heavy metals especially Cadmium (Cd) and Lead (Pb). Three different sites were surveyed for the collection of algal samples. Initially 45 different taxa were isolated belonged to the group: cyanobacteria, green algae and diatoms. Among these, ten axenic strains of cyanobacteria were obtained. Six taxa were identified up to species level while four were identified to the genus level. Six taxa have been reported for the first time from Pakistan, viz. *Desertifilum tharensense* MK-2, *Nodosilinea nodulosa* MK-4, *Fischerella muscicola* MK-8, *Westiellopsis prolifica* MK-9, *Desikacharya* MK-7, *Synechocystis fuscopigmentosa* MK-13.

The purified strains were screened for Cd and Pb tolerance. Since obtained from sewage sites, most of the strains showed tolerance to Cd and Pb concentrations. Screening results further showed that *Nostoc* sp. MK-11 was the most tolerant followed by *F. muscicola* MK-8. Therefore, these two strains were selected for further analysis. Cells of *Nostoc* sp. and *F. muscicola* were cultured and their biomass was harvested, dried and ground to fine powder. The dried biomass of *Nostoc* sp. revealed highest biosorption of Pb and Cd at 60-minute contact time, with maximum biosorption capacities of 75.757 mg/g for Cd and 83.963 mg/g for Pb. Biosorption of Pb and Cd on dried biomass of *Nostoc* sp. followed the Pseudo second order Kinetics and Langmuir isotherm models indicating chemisorption mechanism in homogeneous manner. Biosorption-desorption tests showed above 90% metal recovery besides the fact that the dried biomass of *Nostoc* sp. holds the potential of reusability, thus, are cost-effective and eco-friendly in nature. Dried biomass of *F. muscicola* displayed rapid kinetic biosorption at 60 and 90 minutes for Cd and Pb, respectively, with maximum biosorption at pH 7 and 5. Langmuir isotherm modeling revealed biosorption capacities of 63.5 mg/g for Cd and 70.2 mg/g for Pb, signifying

effective biosorption in homogeneous manner. Biosorption of metals onto the dried biomass of this strain also followed the pseudo-second-order kinetics showing the chemisorption of metals. Functional groups responsible for heavy metal binding, highlighting hydroxyl, amine, carbonyl, carboxyl, and sulfoxide groups crucial for metal ion complexation, showed biosorbent potential for Cd and Pb, while the Scanning electronmicroscopy highlighted the altered morphology after the biosorption process. Furthermore, desorption of Cd and Pb using 0.1 M Hydrochloric acid showed efficient metal desorption with a recovery rate of 90%.

Iron oxide nanoparticles (IONPs) synthesized using extracts of two cyanobacteria (*F. muscicola* and *Nostoc* sp.) and parallel analyses were carried out. The Langmuir isotherm calculated maximum adsorption capacities for *F. muscicola* based IONPs as 94.161 and 93.370 mg/g for Pb and Cd, respectively. Similarly, Langmuir isotherm calculated maximal adsorption capacities of *Nostoc* sp. mediated IONPs as 105.932 and 118.764 mg/g for Cd and Pb, respectively. The recyclability of IONPs revealed retention of their adsorption efficiency. Hence, this study indicated that *Nostoc* sp. has higher potentials of adsorbing Cd and Pb ions compared to *F. muscicola*, both these strains are derived from the indigenous algal flora thriving in polluted water.

The study recommends exploring diverse ecological niches and hybrid water treatment systems, advancing genetic engineering, and improving biosorption methods, with field trials needed to validate the feasibility and ecological safety of cyanobacteria-based solutions.

CHAPTER 1

Introduction and Review of Literature

1.1. Introduction

Cyanobacteria also known as Blue-green algae form a natural group by virtue of being the only group of prokaryotic algae. These organisms have an outer plasma membrane enclosing protoplasm containing 70s ribosomes, DNA fibrils not enclosed in a separate membrane and photosynthetic thylakoids. Chlorophyll *a* is the major photosynthetic pigment and oxygen is evolved during photosynthesis (Lee, 2018). It has been hypothesized that cyanobacteria evolved in freshwater around 2.5 billion years ago (Blank, 2013). In eukaryotes, the photosynthetic organelle is believed to have possibly emerged from the process of endosymbiosis between a cyanobacterium and a photoautotrophic host (Löffelhardt and Bohnert, 1994). There are morphologically diverse types of cyanobacteria that exist as: filamentous, unicellular, colonial, benthic or planktonic (Whitton and Potts, 2007; Burja et al., 2001). These are among the most common photosynthetic organisms found in nature. Cyanobacteria survive in a variety of ecologies including freshwater, marine, and terrestrial habitats. These are well-known for their potential to carry out several metabolic processes and can quickly change from one mode to another (Stal, 1995). All cyanobacteria possess the capability of oxygenic photosynthesis while some cyanobacterial species can shift to sulfide-dependent anoxygenic photosynthesis (Cohen et al., 1986). In dark or under anoxic conditions, cyanobacteria can carry out fermentation for energy generation (Stal, 1997). Heterocysts are specialized cells that some filamentous cyanobacteria have evolved for nitrogen fixation (Capone et al., 2005).

Lee (2018) classified cyanobacteria into three major orders: (1) Chroococcales, which are either single celled or loosely bound together in slimy irregular colonies. *Synechococcus*, *Synechocystis* and *Micocystis* are some of the genera included in this group; (2) Oscillatoriales are long, thread-like cyanobacteria and represented by *Oscillatoria*, *Phormidium*, *Lyngbya*, *Trichodesmium*, *Anthrospira* (*Spirulina*) and *Hydrocoleus*; and (3) Nostocales, another thread-like algae with special heterocysts (Lee, 2018). Due to their abundance, variety and ecological function, unicellular cyanobacteria play a vital role in aquatic environments (Hallenbeck, 2017). These microorganisms had a significant impact in the initial increase of atmospheric oxygen approximately 2.3 billion years ago (Holland, 2002). More recently, cyanobacteria have earned attention for their potential in bioenergy production and the synthesis of

valuable biocompounds. As a result, during the past 20 years, cyanobacterial engineering has been a hot topic of research (Hallenbeck, 2017).

The unicellular freshwater cyanobacterium *Synechocystis* is a remarkable model organism in the field of single-cell research for genetics, physiological investigations of photosynthesis, and energy studies (Ikeuchi and Tabata, 2001; Lindberg et al., 2010). Remarkably, the complete genome sequencing of *Synechocystis* sp. PCC 6803 marked a significant milestone, as it was the first phototrophic organism and the fourth organism overall to undergo such comprehensive sequencing back in 1996 (Ikeuchi and Tabata, 2001; Kaneko et al., 1996).

According to Humbert and Fastner, (2016) cyanobacteria exhibit a range of morphologies, including filamentous forms that are multicellular, colonial, and unicellular. Their cell size spans a wide range, from less than 1 μm in diameter for *picocyanobacteria* to as much as 100 μm for certain tropical *Oscillatoria* species (Jasser et al., 2017; Schulz-Vogtet et al., 2007). Unicellular cyanobacteria have diverse cell shapes such as spherical, ovoid, or cylindrical, and they can aggregate into colonies held together by a mucous matrix, or mucilage, secreted during colony growth (Chorus and Welker, 2021; Mur et al., 1999). The number of cells development and growth (Kumar et al., 2010) and they are essential for motility and symbiotic colonization of hosts (Meeks and Elhai, 2002; Adams and Duggan, 2008; Meeks and Elhai, 2002; Uyeda et al., 2016; Wong and Meeks, 2002). Heterocysts, which can be observed in multicellular cyanobacteria like *Anabaena* and *Nostoc*, are enormous, spherical cells with a thicker cell membrane than vegetative cells. They have potential in fixing nitrogen (Kumar et al., 2010). Akinetes are long-lasting cells that resemble spores and emerge when growth circumstances are unfavorable, such as cold or drought (Kumar et al., 2010) and akinetes, similar to heterocysts, possess a robust cell wall (Uyeda et al., 2016). It has been postulated that akinetes could serve as evolutionary precursors to heterocysts (Wolk et al., 1994).

1.2. Occurrence and distribution

Cyanobacteria have captivated the attention of ecologists owing to their broad presence and considerable influence in various ecosystems. These microorganisms inhabit a wide array of environments, spanning from freshwater bodies to marine habitats, and even extreme niches like hot springs and deserts (Whitton, 2012). The distribution of cyanobacteria is intricately tied to numerous environmental factors,

encompassing nutrient availability, water, temperature, light intensity, and pH levels (Paerl and Paul, 2012). The interplay of these factors contributes to the diverse patterns of cyanobacteria distribution across ecosystems. Freshwater systems stand as primary cyanobacteria habitats, encompassing both stagnant and flowing environments. In nutrient-rich waters, cyanobacterial blooms frequently occur, disrupting ecological equilibrium and impacting water quality (Paerl et al., 2016). The emergence of these blooms is often linked to excessive nutrient inputs, particularly phosphorus and nitrogen, which provide nourishment for cyanobacterial growth (Chorus and Bartram, 1999). Cyanobacteria also showcase adaptability in marine ecosystems, flourishing in nutrient-deficient waters by utilizing strategies such as diazotrophy to fix atmospheric nitrogen and sustain their growth. This distinctive trait allows them to occupy ecological niches that might be less accessible to other primary producers.

Cyanobacteria put significant influence on global carbon and nitrogen cycles, impacting nutrient availability and primary productivity within aquatic systems (Stal, 2012). Presence of cyanobacteria is not confined solely to benign environments. They have been documented in extreme habitats, illustrating their remarkable resilience. For example, cyanobacterial mats in hot springs and hypersaline lakes underscore their ability to withstand extreme temperatures, salinities, and pH levels (Nandagopal et al., 2021). This adaptability is facilitated by their potential to synthesize specialized metabolites and pigments that offer protection against harsh conditions. However, the prolific growth of cyanobacteria can have adverse repercussions. The development of harmful algal blooms (HABs) is a notable concern due to the production of toxins like microcystins and anatoxins, which pose threats to aquatic organisms and human health (Chorus and Bartram, 1999).

1.3. Cyanobacteria culturing

Cyanobacteria play an important role in global primary production and biogeochemical cycling, adapting to a wide spectrum of growth conditions that shape their physiology, metabolism, and ecological functions. To cultivate cyanobacteria effectively, scientists manipulate diverse parameters to mimic natural habitats. Light, crucial for photosynthesis, is regulated by adjusting light intensity and photoperiod to match strain-specific requirements (Huang et al., 2018). Temperature, another key factor, varies among strains but generally falls within the 20 to 30°C range (Singh et

al., 2017). Agitation and aeration replicate native hydrodynamics and enhance nutrient exchange (Huang et al., 2018).

Culturing media formulation is equally significant. BG₁₁ and BG₀ media offer essential nutrients and trace metals, with BG₁₁ designed for general cultivation and BG₀ lack combined nitrogen for nitrogen fixation studies (Stanier and Cohen-Bazire, 1977; Rippka et al., 1979). Solid media like agar plates aid in isolating and purifying colonies, crucial for obtaining axenic strains (Rajaniemi et al., 2005). Conversely, liquid cultures allow large-scale growth in various vessels, from Erlenmeyer flasks to photobioreactors, enabling controlled conditions like light, temperature, and aeration (Singh et al., 2017). pH serves as a critical culturing parameter impacting cyanobacteria growth. Different strains have varying optimum pH, necessitating the maintenance of the appropriate pH range to achieve optimal growth rates and metabolic activities (Rajaniemi et al., 2005). pH influences nutrient availability, enzyme activities, and cellular processes in cyanobacteria, making it a crucial consideration in culturing conditions. Recent research by Hagemann and Hess (2018) underscores the role of carbon availability, especially inorganic sources like CO₂ and HCO₃⁻ which influence photosynthetic rates and carbon assimilation strategies in cyanobacteria. Understanding and managing these multifaceted culturing conditions are pivotal for successful cyanobacterial cultivation and for advancing our comprehension of their diverse ecological functions and potential application.

1.4. Identification of cyanobacteria

Traditionally, the identification, enumeration, and classification of cyanobacteria have relied upon light microscopy, wherein morphological characteristics like cell size, cell division pattern, width of trichome, terminal cells morphology, presence of specialized cells (e.g., akinetes and heterocytes), and the occurrence of aerotopes have been key criteria (Castenholz, 2015; Radkova et al., 2020; Tan et al., 2023). This approach is contingent upon easily discernible features that remain recognizable even when using light microscopy at lower magnifications. Nevertheless, it often proves challenging, particularly for groups lacking distinctive attributes and featuring small cell sizes. Furthermore, phenotypic plasticity among cyanobacteria, especially in groups like picocyanobacteria, further complicates identification. For instance, the categorization of unicellular organisms that are less than 2-3 μm in size as species belonging to *Synechococcus* or *Cyanobium*, along with those of equivalent

dimensions that form colonies and produce mucilage, is ascribed to species of *Aphanocapsa*, *Anathece* or *Aphanothece*. According to studies by Huber et al. (2017) and Jezberová and Komárková (2007), *Cyanobium* species are capable of generating colonies in response to grazing pressure that exhibit morphological characteristics resemble those of *Anathece*. The close affinities between these two genera have been established by 16S rRNA phylogenetic analysis (Komárek et al., 2011).

The identification of simple coccoid cyanobacteria is made more difficult by the fact that only a small number of morphological characteristics at the cellular level (Komárek et al., 2014). According to Komárek et al. (2014), higher-order cyanobacteria have more morphological variety and can have specialized characteristics like heterocytes, branched trichome, or akinetes. Consequently, many simple coccoid species confront identification through light microscopy, potentially harboring cryptic diversity or leading to misinterpretations. Consequently, it is considerably less viable to infer any conclusions regarding the potential of cyanobacterial communities solely from their morphological characteristics (Palinska and Surosz, 2014; Tanabe et al., 2009; Komárek, 2016).

The reliance on morphological traits for cyanobacteria classification poses challenges since these traits can be influenced by environmental and developmental factors, hindering strain diversity characterization in cultures under selective growth conditions. These constraints underscore the need for molecular techniques in cyanobacterial identification (Lyra et al., 2001). The 16s rRNA gene is generally employed as molecular markers in identifying microorganisms and revealing their interrelationships. While this gene encompasses evolutionarily conserved regions, it also contains variable sequences that are species-specific. Species-level identification can be achieved by amplifying these variable regions through PCR (Lefler et al., 2023). Studies have demonstrated precise identification of *Oscillatoria limnetica* and *Geitlerinema* strain PCC9452 by amplifying their 16S rRNA genes (Boyer et al., 2001). Additionally, the terminal heterocysts and akinetes of *Cylindrospermum* have allowed differentiation from the *Nostocaceae* family, enabling the identification of 45 taxa within this genus (Johansen et al., 2014; Karan et al., 2017). Although less frequently utilized, some researchers have explored alternative gene regions, including *nifH*, *recA*, *rpoD1*, *rpoC1*, *rpoB* and, for phylogenetic analysis of cyanobacteria (Premanandh et al., 2006). In certain studies, phylogeny-based

determination of *Synechococcus* strains has been accomplished by utilizing phycocyanin gene sequences (Robertson et al., 2001).

1.5. Potential applications of cyanobacteria

Cyanobacteria have become progressively prominent due to their promising applications in various fields of biotechnology (Abed et al., 2009). The secondary metabolites of cyanobacteria, which include vital vitamins, enzymes, and toxins, serve as large reservoirs of bioactive substances and are crucial to several biotechnological fields (Amadu et al., 2021). The manufacturing of bioplastics using cyanobacterial polyhydroxy alkanoates (PHA) is one industry where these chemicals are used (Afreen et al., 2021; Koller, 2022). A promising resource for the synthesis of bioplastics with characteristics like polyethylene and polypropylene is the intracellular accumulation of PHA in a number of cyanobacterial species (Koller, 2022). Additionally, a wide variety of cyanotoxins are produced by cyanobacteria. These cyanotoxins have distinct properties that have sparked attention among scientists regarding their potential use on a worldwide industrial scale (Kurmayer et al., 2016). A summary of all possible applications of cyanobacteria is presented in Figure 1.1.

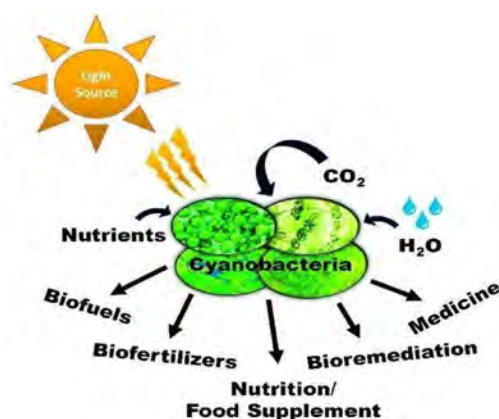


Figure 1.1: An overview of the possible applications of cyanobacteria in several scientific and developmental domains (Zahra et al., 2020).

Due to their effective photosynthesis, cyanobacteria have a prospective advantage in the manufacture of biofuels. They convert carbon dioxide and sunlight into biomass and lipids that can be converted into biofuels (Nozzi et al., 2013; Singh et al., 2023). Cyanobacteria produce secondary metabolites from natural sources generating enzymes, pigments, vitamins, and other beneficial co-products. These

include biocatalysts for the transformation of CO₂ into fuels and chemicals. Examples include the major cyanobacterial pigments carotenoids and phycobili proteins, which are utilized extensively in the bio-industry (Deb et al., 2021; Pekkoh et al., 2023).

They are used as nutritional sources and dietary supplements, comprising intricate carbohydrates, amino acids, proteins, phycocyanin, bioactive enzymes, beta-carotene, chlorophyll, minerals, essential fatty acids, vitamins and carbohydrates. The term "*spirulina*" is used to refer to *Arthrospira maxima* and *Arthrospira platensis*. Common uses for *A. platensis* include whole foods and dietary supplements. The poultry, aquarium, and aquaculture sectors utilize it as a feed additive and it is grown all over the world (Zhu et al., 2022; Liu et al., 2021; Grossmann et al., 2020). In a range of agricultural and ecological settings, cyanobacteria can serve as natural biofertilizers, contributing to enhanced agricultural productivity (Chittora et al., 2020; Hamed et al., 2022; Rezasoltani and Champagne, 2023). They contain secondary metabolites that have potential biotechnological applications in the field of medicine (Chaubey et al., 2022; Saeed et al., 2022).

They can perform bioremediation by absorbing and metabolizing pollutants like heavy metals and organic contaminants from various environments, aiding in environmental cleanup. Their rapid growth and self-sustaining nature further enhance their potential as effective and eco-friendly agents for addressing pollution and restoring ecosystems (Devi et al., 202; Encarnação et al., 2023). They also offer distinct advantages in nanoparticle synthesis due to their ability to produce and secrete bioactive compounds that can facilitate the formation and stabilization of nanoparticles. This natural approach not only simplifies the nanoparticle production process but also holds potential for developing environmentally friendly and biocompatible nanomaterials for various applications including medicine and catalysis (Ali Anvar et al., 2023; Mandhata et al., 2022).

1.6. Environmental pollutants

A major threat to human health globally is environmental pollution. The swift progression of urbanization, agricultural practices, and industrial activities, coupled with the increasing demand for enhanced quality of life, has led to the unavoidable discharge of various organic chemicals, pesticides, persistent organic pollutants (POPs), antibiotics, and inorganic contaminants, including metal ions like Hg, Cd, As, Pb, and Cr into natural ecosystems (Wang et al., 2022b; Huang et al., 2022; Liu et al.,

2022; Chen et al., 2022c; Liu et al., 2022). Their prolonged presence in the environment can be attributed because they are difficult to eradicate from ecosystems or to degrade. Because these environmental toxins can enter the body and accumulate throughout the food chain, they are hazardous to human health even at extremely low amounts. For instance, Pb(II) poisoning may harm the cardiovascular and cranial nerve systems, while the detrimental effects of Cd(II) poisoning on skeletal and renal functions have been documented in the literature (Rouhani and Morsali, 2018; Zhao et al., 2011). In the mean time, organic chemicals exposure in the environment may also cause nervous system toxicity (Liu et al., 2021a).

The quality of the water has a fundamental impact on the health of all living organisms on Earth. The expanding human population, industry, urbanization, and chemically enhanced agriculture are all contributing to the rapid contamination of water supplies. Nowadays, a lot of people have trouble getting access to clean water, which has a negative impact mostly on underdeveloped countries (Waheed et al., 2021). The features of modern civilization have led in an abrupt rise in the quantity of pollutants in water bodies, which has reduced the availability of drinkable water. Water bodies are being contaminated by a wide range of inorganic and organic contaminants, including industrial wastes, agricultural runoff, and domestic wastes. Both point and diffuse sources are the source of these pollutants (Qiu et al., 2022).

Electronic waste (e-waste) is contributing significantly to the escalation of environmental issues as a consequence of advancements in computing and information technology, leading to the production of electronic components and an increase in the quantity of products characterized by reduced life durations (Robinson, 2009; Mmereki et al., 2016; Awasthi et al., 2016). Given that e-waste comprises a heterogeneous assortment of materials, such as glass, plastics, organic compounds, metalloids, precious metals, and various heavy metals, the recycling of e-waste presents an opportunity for lucrative commercial enterprise. However, the implementation of safe recycling methodologies incurs substantial costs and poses potential hazards to both human health and environmental integrity. The predominant flow of e-waste is from established nations to developing countries, where the regulatory framework concerning its disposal is comparatively negligent. For example, a considerable proportion of the global e-waste generated per annum is exported for disposal to nations in Asia and Africa (Efthymiou et al., 2016; Iqbal et

al., 2015; Adaramodu et al., 2012). Inappropriate recycling and disposal practices associated with e-waste intensify the elevated heavy metals levels present in the environment (Pradhan and Kumar, 2014; Song and Li, 2014).

1.6.1. Heavy metals /Inorganic pollutants

According to Ferguson (1990), metallic elements with densities higher than water are classified as heavy metals (HMs). These are naturally occurring elements with significant atomic weights and densities at least five times greater than water (Tchounwou et al., 2012). Notably, HMs includes metalloids like arsenic (As), which may cause toxicity at low exposure levels while having a relatively smaller mass (Duffus, 2002). Cd, chromium (Cr), copper (Cu), nickel (Ni), Pb, zinc (Zn), mercury (Hg) and arsenic (As) are certain heavy metals classified in this group and are known for their biological significance and negative effects on aquatic ecosystems (Jacob et al., 2018).

Hazardous metals, particularly HMs, are often associated with anthropogenic activities, such as those in the nonferrous metallurgical, tanning leather, mining, electroplating, mineral processing and chemical sectors (Sarker et al., 2023). Heavy metals, inherent in earth's crust since its origin, have witnessed a notable escalation in their prevalence within terrestrial and aquatic domains due to the substantial surge in their utilization (Briffa et al., 2020; Gautam et al., 2016). Human activities encompass a spectrum of processes including metal mining, smelting operations, foundry activities, and various metal-centric industries. Moreover, heavy metals find their way into the environment through mechanisms such as metal leaching from diverse sources, including landfills, waste disposal sites, biological excretions, livestock and poultry manure, urban runoff, vehicular emissions, and road construction. Furthermore, the agricultural industry plays a role in secondary heavy metal contamination due to the use of various substances, including pesticides, insecticides, fertilizers, and other associated chemicals. Natural occurrences further intensify the heavy metals contamination problem, with volcanic eruptions, the corrosion of metallic surfaces, volatilization of metals from soil and aquatic bodies, sediment resuspension, soil erosion, and geological weathering all playing roles in this complex ecological challenge (Walker et al., 2012; Masindi and Muedi, 2018).

Heavy metals occur naturally within the ecosystem and can be beneficial to human health when found in low concentrations. However, their entry into the human

body, primarily through ingestion and inhalation, can lead to adverse effects when exposed to high levels (Genchi et al., 2020). Toxicity levels associated with these hazardous substances are contingent upon the concentration and duration of exposure experienced by living organisms. Prolonged exposure to heavy metals may result in a variety of illnesses in humans and other organisms. These routes include skin contact, eating contaminated food, and inhalation (Anyanwu et al., 2018). Heavy metals toxicity has become a major worldwide concern because of growing industry and its multiple environmental releases (Rathi et al., 2021).

1.6.1.1. Cd

Cd is one of the heavy metals that is relatively common in both natural environments (such as air, living things, soil, sediment, and water) and human-influenced spheres (such as agricultural crops, food, and sewage sludge), and it has an active affinity for uptake by plants. This inclination is concerning since it poses serious threat to human health, even at trace doses (Schaefer et al., 2020; Hayat et al., 2019; Billah et al., 2019; Chuanwei et al., 2015; Feng et al., 2020). Cd has been used in fertilizers, electroplating, battery manufacturing and mineral processing (Wan et al., 2023). The sources of Cd can be both natural, as in the case of Cd concentrations in the natural environment and anthropogenic, due to the utilization of phosphate fertilizers, mining activities, and the release of Cd via municipal wastewater. Furthermore, mixed mechanisms of Cd pollution involve the atmospheric transport of Cd releases activated by human activities, followed by deposition (Moreno-Jiménez et al., 2014).

Cd stands as a profoundly toxic heavy metal, officially acknowledged as a human carcinogen by reputable entities like The International Agency for Research on Cancer and US National Toxicology Program (Suhani et al., 2021; Congeevaram et al., 2007). The harmful impacts of Cd are attributed to its potential to inhibit the synthesis of essential biomolecules, including DNA, RNA and proteins, culminating in the malignant transformation of normal epithelial cells. Extended exposure to Cd in human populations has been strongly associated with the development of lung cancer and the infliction of renal damage. Furthermore, Cd can disturb vital elements such as zinc, iron, calcium, magnesium, and selenium, thereby inducing functional and morphological alterations in various organs and disrupting secondary metabolic pathways. Manifestations of Cd toxicity include pneumonia, asthenia, fever, thoracic

discomfort, and, in severe instances, fatality. It is noteworthy that females exhibit a high vulnerability to Cd exposure, given their elevated dietary absorption of Cd (Bhattacharyya et al., 2021; Mala et al., 2006).

Cd is notably responsible for the disorder known as Itai-Itai disease, which predominantly affects women, inflicting impairment upon tubular and glomerular kidney functions and resulting in multiple bone fractures attributable to osteoporosis and osteomalacia. Moreover, when Cd reacts with hydrochloric acid within the stomach, it forms chlorides, precipitating acute gastrointestinal inflammation. Cd also exerts disruptive effects on the immune system, with a primary focus on natural killer cells, T cells, macrophages and B cells. Interaction with Metallothionein, a protein pivotal in the regulation of free radicals and zinc homeostasis, can induce hypertension and elevate the generation of reactive oxygen species (ROS), thereby impacting the cardiovascular system. Inhalation of Cd can culminate in respiratory distress syndrome. Furthermore, Cd detrimentally influences reproductive functionality by interfering with testicular and prostatic function, perturbing hormonal dynamics, and diminishing male fertility (Choo et al., 2006).

1.6.1.2. Pb

Pb is another noxious heavy metal capable of prompting pronounced physiological effects even at minimal concentrations (Collin et al., 2022). This metal, ranking as the second most hazardous metal, exists in the earth's crust in a scant proportion of 0.002%, occurring naturally in limited quantities. Nevertheless, human activities, notably industrial processes, automotive emissions, and the manufacturing of batteries, have made substantial contributions to lead contamination, thereby affecting both environment and human health (Tripathy et al., 2022). Principal sources of Pb exposure include particulate matter, automobile emission, emissions stemming from battery operations, remnants of lead-based paint, mining, smoking, wastewater and the consumption of contaminated foodstuffs (Tripathy et al., 2022; Obasi and Akudinobi, 2020).

Pb exposure can manifest through various avenues, including inhalation, ingestion, and dermal absorption. It is noteworthy that Pb can effortlessly traverse the placental barrier, giving rise to specific concerns regarding the development of fetuses, with more pronounced toxic effects noted in younger fetuses, including the occurrence of cerebral edema (Goyer, 1990). Upon inhalation, Pb preferentially

accumulates in various bodily tissues, encompassing the circulatory system, soft tissues, hepatic structures, pulmonary organs, skeletal framework, and various organ systems, including the cardiovascular, nervous, and reproductive systems. In adults, Pb exposure may result in symptoms such as reduced concentration, impairment of memory faculties, as well as muscular and articular discomfort (Goyer, 1990). In contrast, children and infants exhibit extraordinary susceptibility, even to minute Pb doses, attributable to Pb neurotoxic properties, which can give rise to learning disabilities, deficits in memory, hyperactivity, and the potential for cognitive impairment (Farhat et al., 2013). High environmental lead concentrations also have detrimental consequences for plant growth and crop development. Neurological effects have been observed in vertebrates and animals associated with high Pb concentrations (Assi et al., 2016).

1.6.2. Prevalence of Heavy Metals in Pakistan

In several regions of Pakistan, such as Kasur, Salt Range, Mianwali and Bahawalpur groundwater has been identified as containing elevated fluoride levels, with concentrations ranging from 65 to 12 mg/L. Furthermore, analyses of groundwater in districts like Sargodha, Jhelum and Gujarat have revealed arsenic concentrations surpassing the WHO permissible limit of 10 µg/L (Rasheed et al., 2021). A recent study covering 11 cities in Punjab has drawn attention to excessive arsenic and fluoride concentrations in the water supply systems of six cities, including Bahawalpur, Multan, Kasur, Sheikhpura, Lahore, Gujranwala and. It is important to note that over 2 million people live in these cities and are potentially exposed to groundwater polluted with arsenic (PCRWR, 2016).

Furthermore, high levels of nitrates, microbial contaminants, fluorides and arsenic ions are recognized as significant pollutants in water supply systems across various regions of Pakistan. Several research studies have pointed out that several physiochemical parameters of water quality in major cities do not follow to the safety standards established by WHO/PSQCA for potable water (PCRWR, 2016). The Pakistan Council of Research on Water Resources evaluated the water quality of 23 main cities in Pakistan in 2016 which revealed that out of 369 monitored sites; only 31% (116) met the criteria for safe drinking water, while the remaining 69% (253) were deemed unsafe. It is worth noting that in Islamabad, the capital city, only 32% of water sources were found to provide safe drinking water, with the remaining 68%

categorized as unsafe. Similarly, in Rawalpindi 62% of water sources were considered unsuitable for consumption (PCRWR, 2016). In addition, a study conducted in the Sargodha district identified soil with the highest Cd concentration at 6.74 mg/kg, the findings suggest a possible risk of Cd infiltrating the food chain, as evidenced by the observed accumulation of Cd in forage plants, which ranged from 1.14 to 4.20 mg/kg (Khan et al., 2011).

Islamabad and Rawalpindi, situated in the northern region of Pakistan, are twin cities known for their significant presence of automotive workshops. These workshops engage in a range of activities related to auto-mechanical repairs, which can introduce heavy metals in environment, including soil, surface water, and groundwater, primarily through processes such as percolation (Ashraf et al., 2020). In Islamabad, soil samples and road dust along the Islamabad expressway recorded concentrations of Cd ranging from 5.8 to 6.1 mg/kg and 4.5 to 6.8 mg/kg, respectively. These values exceed levels found in many global cities and are comparable to those observed on highways in Aqaba Shuna (Jordan) and Istanbul (Turkey) (Faiz et al., 2009; Khashman, 2007). At present, the amount of Pb in the urban atmosphere of Islamabad has demonstrated a reduction in recent years, due to the usage of lead-free gasoline. Nevertheless, Pb levels remain notably high, ranging from 0.002 to 4.7 $\mu\text{g}/\text{m}^3$ (Shah et al., 2004). These harmful water contaminants may seriously harm human health since they can accumulate in living beings and other environmental media. There is an urgent demand for materials and technologies that are chemically robust, easy to use, inexpensive, eco-friendly, transportable, and economically efficient in order to meet the massive global need for safe water. Pollution toxicity negatively affects food chains, biological systems, the global economy, and the environment (Selvasembian et al., 2021).

1.7. Bioremediation

Bioremediation is an environmentally sustainable and cost-effective technology employed to ameliorate contaminated sites or industrial effluents through biological processes (Kertesz et al., 1994; Sharma et al., 2022). Bioremediation employs microorganisms such as bacteria, algae, and fungi; and phytoremediation that employ plants; both stand as significant biological techniques to facilitate the remediation process (Chang et al., 2008; Dhaliwal et al., 2020). Different mechanisms of action are identified within the field of bioremediation, including biosorption,

bioaccumulation, biomineralization, bioleaching. Although metal toxicity can damage cell membranes, microbes have developed defense mechanisms to prevent such injury. Recombinant DNA technology, a form of genetic engineering, is used to increase the effectiveness of metal removal by microorganisms (Verma and Kuila, 2019).

1.7.1. Bioaccumulation

Bioaccumulation is acknowledged as an active biological process (Ardal, 2014), where living biomass plays a pivotal role in the detoxification of contaminants (Kumar et al., 2015). This process depends on biomass ability to absorb materials and vital nutrients across its surfaces (Ratte, 1999). Depending on the specific biomass involved, compounds are either accumulated within the biomass or metabolized (Ardal, 2014). According to Hoffman et al. (2002) and Mustafa et al. (2002), bioaccumulation is the process by which both inorganic and organic pollutants, such as pesticides, heavy metals, sulfates, nitrates and phosphates are transported into the living cells. The bioconcentration factor measures the pollutant concentration inside the biomass as compared to the surrounding medium (Ratte, 1999). *E. acus*, *C. vulgaris*, *O. bornettia* and *P. curvicauda* have been used in studies on the bioaccumulation of Al, Cd, Zn, Cu and Fe. Notably, *Oscillatoria* had the highest metal concentration factors, with Zn, Fe, Cu, and Cd values of 0.306, 0.302, 0.091, and 0.276, respectively (Abirhire and Kadiri, 2011).

1.7.2. Biosorption

Biosorption is an important method for the elimination of heavy metals from wastewater; it includes a variety of different methods, involving adsorption ion exchange, surface complexation, chelation and precipitation (Bhatt et al., 2022). According to De Philippis and Micheletti (2017) Mota et al. (2016), cyanobacteria cell walls often include an excess of negatively charged groups that can serve as binding sites for heavy metals. Metal ions may rapidly bind to the cell surface in the initial phases. Active transporters and carriers then aid in the transfer of metal ions into cells, where they may be changed into less harmful forms or confined within vacuoles. Various genera of cyanobacteria, including *Arthrospira*, *Anabaena*, *Cyanothece*, *Cyanobium*, *Synechocystis*, *Nostoc*, *Leptolyngbya* and *Microcystis* have demonstrated considerable efficacy in removing heavy metals including Cd, Zn, Cr, Cu, Cr, Pb, Co, Hg or Ni across a range of initial concentrations, from a few mg/L to

150-200 mg/L (Bloch and Ghosh, 2022; Mota et al., 2016; Pandey et al., 2022; Yadav et al., 2020; Zinicovscaia et al., 2018). Maximum metal uptake typically falls within the 15–80 mg/g dry weight range although certain studies have reported values exceeding 300 mg/g dry weight (Cui et al., 2022).

Biosorption is thought to be a more practical method for removing heavy metals than bioaccumulation because of its faster kinetics and the ability of the cells to withstand large quantities of potentially harmful heavy metals. Nonetheless, the biosorption process is subject to several influencing factors, including pH, temperature, biosorbent dosage, and pretreatment, necessitating careful consideration to enhance adsorption capabilities (AlAmin et al., 2021). The possibility for numerous desorption/adsorption cycles, which increase the shelf-life of the biosorbents and their economic viability, is another benefit of biosorption. Different solutions, such as strong acids or bases, EDTA, or water, may be employed during the desorption process depending on the physical and mechanical resilience of the biosorbents and the strength of the interaction between the metal ions and the binding groups (Agarwal et al., 2020; Chatterjee and Abraham, 2019; Satya et al., 2021).

1.7.3. Cyano-remediation

Cyanobacteria offer a viable biological tool to meet modern circular economy and sustainability requirements. They may function as bio-factories for a range of substances with applications in the nanotechnology and bioremediation sectors (Ciani and Adessi, 2023). Cyanoremediation, utilizes cyanobacteria, serves as a method to eliminate diverse contaminants including heavy metals, dyes, or pesticides from wastewater. Cyanobacteria are essential in mitigating the impacts of industrial effluents generated by sectors such as sugar production, paper manufacturing, brewing, distillation, oil refining, dye production, and pharmaceuticals. Species of cyanobacteria, including *Synechococcus* sp., *Oscillatoria* sp., *Cyanothece* sp., *Nostoc* sp., and *Nodularia* sp., are predominant within the microbial communities found in these industrial effluents. Some cyanobacterial species, including *Anabaena*, *Nostoc*, *Nodularia*, *Microcystis*, *Synechococcus*, *Oscillatoria*, and *Oscillatoria* exhibit the ability to break down lindane residues (El-Bestawy et al., 2007).

Removal of pollutants from diverse sources of industrial, domestic, and synthetic wastewater has been successfully achieved through the use of microbial consortia that include members of the Chroococcales order (such as *Gloeocapsa* and

Cyanothece), diazotrophic Nostocales (*Nostoc*, *Anabaena*, *Cylindrospermum*, *Calothrix*, *Rivularia*, and *Tolypothrix*), as well as other taxa like *Hapalosiphon*, *Stigonema*, and *Mastigocladus*. Additionally, they aid in the tertiary treatment of urban and agro-industrial effluents, reducing bioaccumulation and eutrophication in aquatic and terrestrial environments (Vilchez et al., 1997). In a subsequent investigation, a range of organophosphorus insecticides, organochlorine and herbicides were effectively degraded by species such *Anabaena* sp., *Microcystis aeruginosa*, *Anacystis nidulans*, *Lyngbya* sp. *Synechococcus elongatus* and *Nostoc* sp. (Vijayakumar, 2012). *Spirulina* sp. demonstrated the capability to eliminate glyphosate herbicide (Lipok et al., 2007). A consortium of cyanobacteria-bacteria comprising *Microcoleus chthonoplastes* and *Phormidium corium* has demonstrated considerable potential for the degradation of n-alkanes in oil-contaminated water and soil. This consortium has effectively addressed isolates from the oil-rich sediments of the Arabian Gulf (Al-Hasan et al., 1998; Sorkhoh et al., 1995). The culturing of cyanobacteria in wastewater presents a promising approach for the neutralization of contaminants, thus alleviating pollution challenges. Genera of cyanobacteria such as *Synechococcus* sp., *Aphanocapsa* sp., *Plectonema terebrans* and *Oscillatoria salina* from mats in aquatic and semi-aquatic environments, and are being utilized in the global remediation of oil spills and petroleum (Raghukumar et al., 2001; Cohen, 2002).

1.8. Nanoparticles and Nano-remediation

Nanotechnology (NT) holds a prominent position in the realm of nanomaterial development, finding applications across diverse scientific and technological domains (Ali et al., 2022). Conventional methods to synthesize nanoparticles often involve hazardous chemicals and require large amounts of physical and chemical energy. These traditional methods include microwave-assisted combustion, chemical and direct precipitation. The methodologies encompass electro-deposition wet chemical techniques, thermal evaporation, chemical micro-emulsion processes, spray pyrolysis, molecular beam epitaxy and pulsed laser deposition (Mitra et al., 2015; Yuvakkumar et al., 2015). In contrast, biological methods offer a more environmentally friendly method that requires less energy and employs non-toxic chemicals (Devi et al., 2020). Biogenic synthesis applies a variety of microorganisms as reducing agents, such as fungus, bacteria, viruses, plants, and algae (Sathiyavimal et al., 2021; Vasantharaj et

al., 2019). Due to their several biological potentials, including NP synthesis, wastewater bioremediation, bioenergy production, and the creation of commercial goods such as pigments and medicines, algae have drawn the attention among these (Chaudhary et al., 2020). Algae are rich in functional groups that are necessary for the synthesis of metal NPs, such as hydroxyls, carboxyls, and aminos (Caf, 2022). Consequently, they have emerged as a contemporary and sustainable alternative for biogenic NP synthesis (Mahdavi et al., 2013; Salam et al., 2012). In recent years, cyanobacteria have gained importance as a promising avenue for nanoparticle synthesis in the biomedical sciences, offering economic and eco-friendly advantages. Numerous cyanobacterial species including *Calothrix* sp., *Plectonema boryanum*, *Anabaena*, *Spirulina platensis*, *Lyngbya majuscula*, *Phormidium valderianum*, *Microcoleus chthonoplastes*, *S. platensis* have revealed their potential in synthesizing nanoparticles (Lengke et al., 2006).

Nano-remediation is an innovative approach employing nanoparticles to address polluted soil, water, or air (Hussain et al., 2022). This emerging remediation technique has demonstrated remarkable effectiveness in removing contaminants through processes involving adsorption, catalysis, and the reduction of toxic valences to stable metallic states. The nanoscale dimensions of these particles result in significantly increased surface areas, rendering them well-suited for adsorption and catalytic reactions (Pak et al., 2019). A diverse range of nanoparticles is employed in nano-remediation, including carbon-based nanoparticles such as carbon dots (CDs), graphene oxides (GOs), and carbon nanotubes (CNTs), as well as non-carbon-based nanoparticles like nanoscale zero-valent iron (nZVI) and zeolites. However, it is essential to note that certain nanoparticles used in nano-remediation, such as GOs, reduced GOs (rGOs), and CNTs, have exhibited potential toxicity toward human cells, especially in lung and breast tissues. This toxicity is attributed to the reactive surfaces of nanoparticles, which feature exchangeable ions and small particle sizes. To address these concerns, efforts have been made to modify the reactive surfaces of nanoparticles with functional surfactants, making them safer for environmental applications such as remediation (Pak et al., 2019).

Iron (Fe) stands as one of the vital elements, owing to its extensive utility in both biological and geological contexts (Abdollahi et al., 2019). Iron oxide nanoparticles (IONPs), characterized by their small size, non-toxicity, magnetism, high reactivity, large surface area, robust thermal and electrical conductivity, and

dimensional stability, find application in various domains. Notably, they play a pivotal role in drug delivery (Batool et al., 2021). Iron oxide nanoparticles have been used extensively among all nanoscale materials for the removal of heavy metals from polluted water because of their higher surface area, small size, biocompatibility, and super paramagnetic qualities, which make it simple to separate adsorbents from the system (Wu et al., 2008; Xu et al., 2012). IONPs have a wide range of uses outside of the environmental sector, including material engineering, biomedicine, cosmetics, therapies, and diagnostics (Abbasi et al., 2019).

1.9. Aims and Objectives

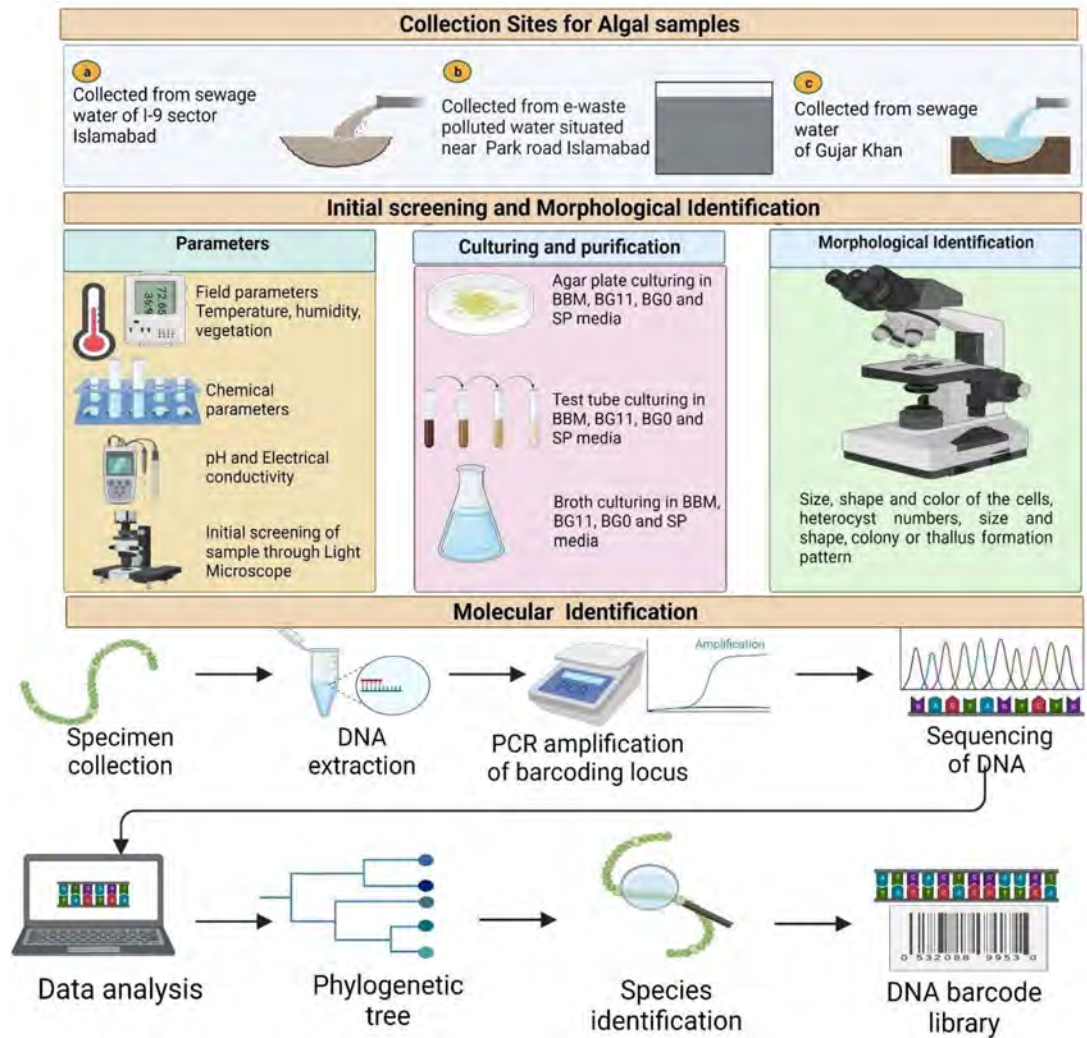
This thesis has following objectives:

1. To isolate cyanobacteria samples from various wastewater sites in twin cities of Rawalpindi and Islamabad
2. To purify, culture and isolate cyanobacteria in synthetic culturing media
3. To observe morphologically diverse strains of cyanobacteria and the 16s rRNA based analyses for species identification.
4. To screen heavy metals (Cd and Pb) tolerant strains under metal stress conditions and their potentials for bioremediation in dried (non-living) and fresh (living) forms.
5. To synthesize Iron oxide nanoparticles using extracts of the same strains and reassess/compare their heavy metals remediation capacity.

CHAPTER 2

Collection, Culturing and Screening of Cyanobacteria from wastewater sites

Graphical Abstract



Schematic presentation of collection, culturing and screening of cyanobacteria.

Summary

Environmental samples were collected from wastewater sites of Islamabad and Rawalpindi. All samples were subjected to isolation, cultivation and characterization of cyanobacteria and other algal types. A total of 45 distinct strains were successfully isolated. Among these cyanobacteria were identified as: *Desertifilum tharensense* MK-2, *Phormidium* sp. MK-3 and *Nodosilinea nodulosa* MK-4 of the order **Oscillatoriales**; *Desikacharya* sp. MK-7, *Fischerella muscicola* MK-8, *Westiellopsis prolifica* MK-9 and *Nostoc* sp. MK-11 of the order **Nostocales**; *Synechocystis fuscopigmentosa* MK-13, *Gleocapsa* sp. MK-14 and *Synechococcus elongatus* MK-15 of the order **Chroococcales**. In initial culturing all isolated cyanobacteria showed growth response in the BG₁₁ media and green algal isolates showed growth response in the BBM media. Strains of order Nostocales showed growth response both in BG₁₁ and BG₀ media. Furthermore, some isolates of cyanobacteria also responded in the SP medium. The morphological and molecular data-based identification revealed six taxa; *Desertifilum tharensense* MK-2, *Nodosilinea nodulosa* MK-4, *Fischerella muscicola* MK-8, *Westiellopsis prolifica* MK-9, *Desikacharya* sp. MK-7, *Synechocystis fuscopigmentosa* MK-13; as the new records from Pakistan. A subset of purified strains was screened for Cd and Pb tolerance. *Nostoc* sp. MK-11 exhibited best tolerance while *Fischerella muscicola* MK-8 was the second best in tolerating Cd and Pb stress and studied for their bioremediation potential.

2. 1. Introduction

Cyanobacteria are a diverse group of prokaryotic organisms that are found in every environment with enough light and carry out oxygenic photosynthesis (Singh et al., 2021). According to Schaechter (2009), cyanobacteria can be found in a variety of habitats, such as desert, soil, glaciers, fresh and brackish water, hot springs, oceans, and they can also be found in symbiosis with plants, lichens, and primitive creatures. They are important primary producers in the microbial world (Chisholm et al., 1988). The oxygen that they generate through oxygenic photosynthesis is essential to the worldwide biogeochemical cycling of metals that are sensitive to redox, such as carbon, nitrogen, and sulphur. As a result, both the past and present biogeochemical cycles and microbial populations have been significantly impacted by cyanobacteria (Sanchez-Baracaldo et al., 2005).

2.1.1. Cyanobacteria isolation and Culturing

It is essential to obtain axenic cultures for proper morphological description, experimental analyses and for genetic base identification. Isolation of microalgae into culture is well established via traditional techniques, beginning with the practice of Miquel (1890–1893) and Beijerinck (1890). Some algae species, often referred to as seaweed, are easy to isolate, while others particularly microalgae are challenging in this regard. The first step towards effective isolation is often to understand the environmental contexts (temperature, pH, salinity) that occur naturally. Similarly, it may be essential to have taxonomic understanding of the target species. The subsequent phase in the successful isolation process entails the elimination of contaminants, particularly those that may compete with the desired species. The concluding phase necessitates sustained growth following sub-culturing. It is not a typical for the target species to exhibit growth during the initial stages post-isolation, yet subsequently perish after one or several transfers to fresh liquid medium. This phenomenon frequently indicates that a particular nutrient is deficient in the culture medium, which may not be readily apparent. Consequently, the maintenance of the isolated strain under culturing conditions emerges as a critical and delicate stage that demands heightened attention.

2.1.2. Identification

Correct identification and quantification of the species present in an ecosystem, is necessary for bio-assessment programs (McElroy et al., 2020). Traditional analyses

are carried out by proficient taxonomists who classify organisms based on their morphological and structural characteristics, such as the arrangement, size, and shape of both their specific cells and general cells (Vuorio et al., 2020). Algal cell identification and counting are still often accomplished using light microscopy (Li et al., 2019). Although acknowledged, the procedure is seen to be difficult, requiring knowledge and the examination of taxonomic literature, which might differ amongst analysts and result in observer bias (Bailet et al., 2020). Concerning the availability of taxonomic knowledge is the fact that there is a shortage of recently qualified taxonomists compared to the demand (Santi et al., 2021).

Although the technique was widely used, there were significant technical constraints outlined here (Abad et al., 2016; Esenkulova et al., 2020). The presence of cryptic species (Li et al., 2020; Vuorio et al., 2020; Esenkulova et al., 2020), of cyanobacteria that do not exhibit distinctive characteristics, along with filament-clustering bloom-forming species, pose challenges for taxonomic differentiation based solely on morphological traits (Li et al., 2019). Finally, divergent identifications, including those of reference strains, may result from phenotypic variation brought on by changing environmental and culturing conditions (Lee and colleagues, 2014; Komarek, 2006).

Molecular genetic methods provide an effective alternative to the limitations of micromorphology, as they facilitate quicker and more efficient sample processing, enable the identification of rare and diminutive species and are generally considered a more economical option (Santi et al., 2021). With the introduction of such molecular technologies, the taxonomy of cyanobacteria is constantly being reorganized (Komárek, 2016a, b). The identification of cyanobacteria taxa and elucidation of their biodiversity patterns typically rely on meta-barcoding techniques that target the 16s rRNA gene or internal transcribed spacer region (Woodhouse et al., 2016). Furthermore, genotypic analyses have the potential to reveal cryptic species (Callahan et al., 2017). Nonetheless, each step of the meta-barcoding process presents certain limitations and biases, which include water sampling, method of DNA extraction (Vasselon et al., 2017), choice of marker genes (Kermarrec et al., 2013), PCR amplification (Bailet et al., 2020), and sequence clustering level (Tapolczai et al., 2019). Moreover, reliable species classification is often limited and unclear due to inadequate taxonomic representation or incorrect labels in DNA reference databases

(Cordonier et al., 2017; Pawlowski et al., 2018). Additionally, life stages cannot be distinguished using molecular techniques (Costa et al., 2016).

2.1.3. 16s RNA gene sequencing

The 16S rRNA gene provides a detailed and accurate depiction of the evolutionary affiliations among cyanobacteria when compared with morphology alone (Komárek et al., 2014). Through the utilization of 16S rRNA gene sequencing, taxonomists are able to delineate monophyletic clades predicated on evolutionary connections, as opposed to relying solely on morphological resemblances, thereby facilitating a more effective resolution of polyphyletic cryptic taxa (i.e., taxa that exhibit morphological similarities yet possess distinct genetic identities) (Bonthond et al., 2021; Lefler et al., 2021; Mai, 2016). Over the past two decades, the implementation of 16S rRNA gene phylogenies has led to the publication of hundreds of new taxa, either as novel classifications or as amendments to previously recognized polyphyletic taxa (Komárek et al., 2014; Mai, 2016). Recent attention has been increasingly directed towards orders and families (Berthold et al., 2022; Berthold et al., 2021), notwithstanding the fact that many existing taxonomic hierarchies were established based on morphological assessments. Employing both phylogenomic and 16S rRNA gene analyses, various studies (Berthold et al., 2022; Mareš., 2018; Sendall and McGregor, 2018) have elucidated the polyphyletic characteristics of these taxa. Through comprehensive phylogenomic analyses, Strunecký et al. (2023) have revised the classification of orders and families within cyanobacteria, thereby enhancing our comprehension and addressing the polyphyletic nature of these classifications. Furthermore, the 16S rRNA gene sequences phylogenetic analysis has substantiated several systematic findings that emerged from phylogenomic studies.

2.1.4. Objectives

Objectives for this study are:

- Collection of samples from wastewater sites of Islamabad and Rawalpindi.
- Assessment, isolation, and culturing of cyanobacterial strains.
- Morphological and molecular (16s rRNA sequence based) identification of isolates.
- Screening of isolated strains for Cd and Pb tolerance.

2.2. Materials and Methods

2.2.1. Study Area

Islamabad is the capital of Pakistan and a center for culture, education, business, and social life with rich and extensive history, positioned at 33.738°N latitude and 73.084°E longitude spreads across an area spanning 906 km², boasting altitudes ranging from 457 to 1240 meters above mean sea level. The city experiences an average annual rainfall of approximately 980 millimeters (38.6 inches). Rawalpindi, situated in the Punjab province, and covers an area of 5,286 km². Positioned at a latitude of 33.626° N and a longitude of 73.071° E and at an elevation of 512 meters. The average rainfall is 1,346.8 millimeters (53.02 inches), most of which falls in the monsoon season. Both Islamabad and Rawalpindi are twin cities (Figure 2.1).

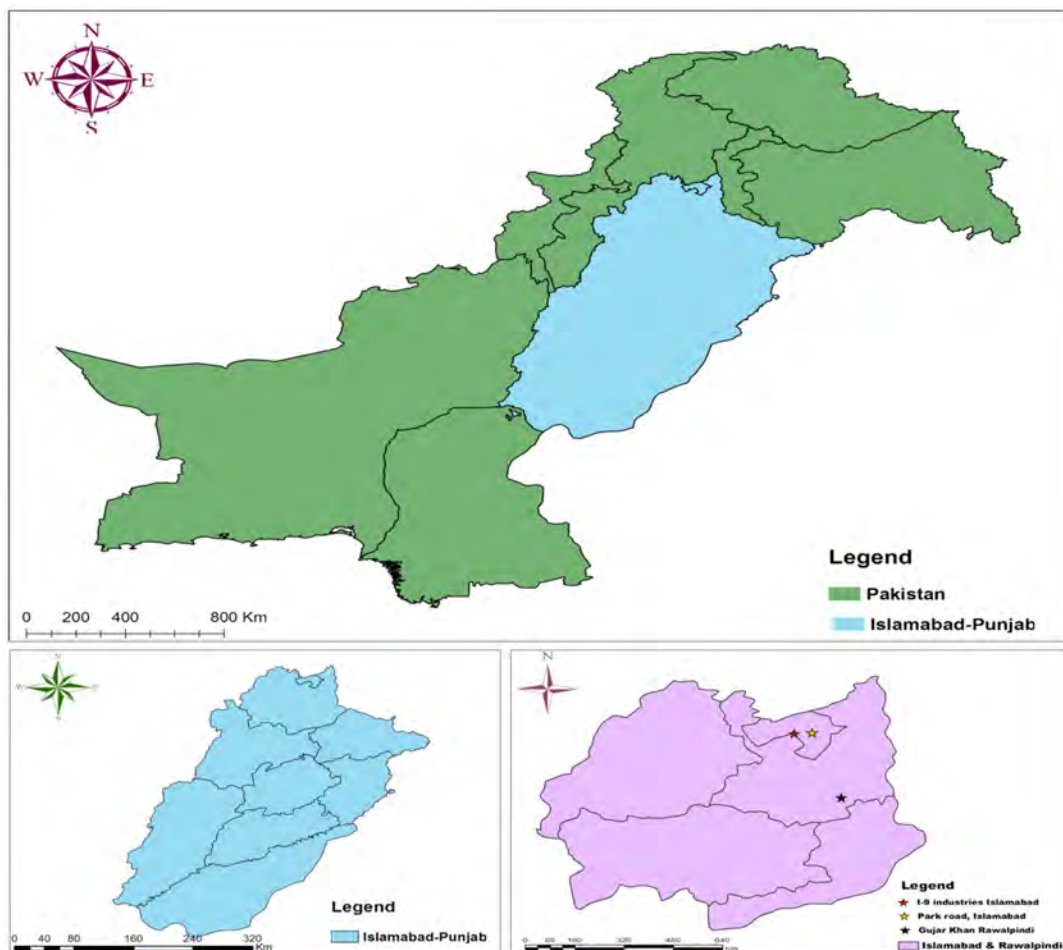


Figure 2.1: Map of the study area: (a) map of Pakistan; (b) map of Punjab (c) map of Islamabad and Rawalpindi.

2.2.2. Collection sites

The sample collection was conducted during the years 2020 and 2021. Three different wastewater sites of Islamabad and Rawalpindi were sampled. Fourteen samples were collected from a site with electronic waste (also called e-waste) at Park Road Islamabad; twenty-five samples were collected from sewage water from sector I/9 Islamabad; and one sample was collected from sewage water in Gujar Khan, Rawalpindi as shown in Figure 2.2.



Figure 2.2: Collection sites of algal samples: (a-j) e-waste polluted water, Park Road Islamabad; (k-o) sewage water, sector I/9 Islamabad; (p) sewage water, Gojar khan.

2.2.3. Collection of samples

All algal samples were collected from the natural habitat. Forceps, gloves, notebook, thermometer, EC meter, humidity meter, permanent markers, polythene bags, and 50 ml falcon tubes were used for the purpose of collection and to note the field data. Various field parameters, such as substrate color, temperature, humidity, and habitat were noted during the sample collection process. When the samples arrived in the lab, the pH and electrical conductivity (EC) were determined. Following this, collected samples were shifted to conical flasks and stored at 25 °C in a growth chamber for further studies.

2.2.4. Water physico-chemical analysis

The physico-chemical characteristics of water samples were inspected at the Chemical Testing Laboratory, Qarshi Research International (Pvt) Ltd., Haripur, Pakistan. Heavy metals analyses of collected water samples were conducted using Flame atomic absorption spectrometer (Agilent Technologies, MC187906, Malaysia) at Quaid-i-Azam University Islamabad, Pakistan.

2.2.5. Chemicals

Different solvents and media components used in current research were purchased from Sigma-Aldrich (U.S) and Merck (Germany) with analytical grade. The recipe and different media components have been described in the appendices section.

2.2.6. Microscopic observations and strain identification

Light microscope (LM) (Nikon Labophot II phase-contrast microscope, Japan) was employed to study the morphological characteristics of the algal isolates. Rigorous light microscopy was conducted during the process of purification to ensure the absolute purity of the axenic cultures. A field manual (Prescott, 1978) was used for preliminary identification of algal cultures. Isolates were assessed morphologically as described in section 2.3 below and the available identification keys in previous literature (Andersen, 2005).

2.2.7. Culturing

Algal samples were cultured in the laboratory using four different media, *viz*, Blue Green medium with (BG₁₁) and without (BG₀) nitrogen source; Bold Basal medium (BBM); and Spirulina medium (SP). Initially all algal samples were cultured on the solid agar BG₁₁, BG₀, BBM and SP media. The composition of culture media is described below:

- **BG₁₁ Media**

Stock solutions of the BG₁₁ media were prepared according to the recipes (Rippka, 1979). About 10 ml of stock 1, 10 ml stock 2, 10 ml of stocks 3 and 1 ml of stock 4 (trace metals) were mixed in an Erlenmeyer flask. The total volume of the medium was raised to 1L by adding distilled water. The carbonates and nitrates were provided by the addition of 0.02g of NaCO₃ and 1.5g of NaNO₃, respectively. The pH of the BG₁₁ media was adjusted to 7.3 and was autoclaved at 15 psi. and 121°C for 45 min.

Recipes of all the stock solutions are described in the appendices.

- **BG₀ media**

Ingredients of the BG₀ media were similar to the BG₁₁ media, except that the BG₀ media was devoid of NaNO₃ (as a nitrate source). Nitrate source was the only difference between BG₁₁ and BG₀ media (Rippka, 1979).

- **BBM Media**

BBM media was prepared using five distinct stock solutions. Approximately 10 ml of stock solution 1, 1 ml of stock solution 2, 1 ml of stock solution 3, 1 ml of stock solution 4, and 1 ml of stock solution 5 were combined in an Erlenmeyer flask, and the total volume was subsequently adjusted to 1000 ml through the incorporation of distilled water. The pH of the solution was meticulously calibrated to 6.8, and the medium underwent autoclaving at a temperature of 121°C and a pressure of 15 psi for duration of 45 minutes (Bischoff, 1963). The formulations for all stock solutions are described in the appendices.

- **SP media**

SP media was prepared using two stock solutions with different pH. Stock 1 was prepared in 500 ml of distilled water with pH 9.0 ± 0.2 and stock 2 was prepared in 500 ml distilled water with a pH of 3.8 ± 0.2 . After cooling, the both stocks were autoclaved separately and mixed. 1ml of the trace metals solution was added and final pH was adjusted to 9.2 and again autoclaved. Recipes of all the stock solutions are described in the appendices.

2.2.8. Purification in solid agar plating

Growth on solid agar media is a precondition for the isolation and purification of any microorganism (Rippka, 1988). Therefore, to isolate various species of cyanobacteria from water samples, solid agar plating technique was used. For this purpose, agar based BG₀, BG₁₁, BBM and SP media were prepared by adding 1.5 % agar in liquid media. 25 ml of agar media was poured in autoclaved Petri plates. Water samples with algal biomass were poured and streaked on the media in Petri plates. To maintain an aseptic environment, all these procedures were performed in a laminar flowhood. Petri Plates were incubated in a growth chamber at 25 °C under continuous LED light. After culturing on agar plate, first observation under light

microscope was carried out after four to five days and purified colonies were picked with the help of a sterilized loop and inoculated to the respective liquid media. The process of agar plate culturing of cyanobacteria and its microscopy was rigorously carried out to achieve strain purification. After getting pure cultures on media, the strains were shifted to the respective broth cultures in a test tube. After 5 to 6 days of culturing in the test tubes, cyanobacteria strains were observed again under a microscope to check any contamination or mixing with other algal stains. This is to avoid any cross-contaminating bacteria and fungi. When the strain purity was confirmed in the test tubes, the cultures were shifted to 250 ml flasks and purity was confirmed by following the same steps as mentioned above. The pure/axenic isolates thus obtained were preserved in triplicates: on solid agar media (in petri plates), in test tube with broth media and in flasks with broth media. The pure isolates were kept in a growth chamber under continuous LED light at 25 ± 2 °C.

2.2.9. Morphological characterization of axenic cultures

All axenic cultures were observed under the dissecting and light microscopes at 10X, 40X and 100X magnifications. Microscopic observations were carried out for twenty days, to observe morphological characters stage by stage with time. The features studied in detail for the isolates were: size, shape, color of the cells; heterocyst numbers, position, size and shape; thallus or colony formation pattern (solitary trichomes or their groups, hemispherical colonies); texture (hard, soft or gelatinous); filaments (trichomes arrangements, hairs, heterogeneity, trichomes width ; sheath morphology); frequency and trichomes, type of false branching (Prescott, 1978; Anderson, 2005; Lee, 2018).

2.2.10. Molecular characterization

2.2.10. DNA Isolation

The CTAB (Cetyltrimethylammonium bromide) method (Doyle and Doyle, 1987) with some modifications was used for DNA extraction of strains. Sterile pestle and mortar were used to grind the 400 mg wet cyanobacteria biomass. Ground biomass was shifted into 1.5 ml eppendorf tube. Later, 600 μ L of CTAB buffer, 1% polyvinylpyrrolidone (PVP) 50 μ l, 0.1% β -mercaptoethanol 20 μ L and 4 μ l proteinase k were added to the Eppendorf tubes. The mixture was vortexed properly for 1-2 minutes followed by an incubation of 1 hour and 30 minutes in water bath at 65°C. Mixture was cooled down at room temperature for five to six minutes.

Chloroform-isoamylalcohol (24:1) 500 μ L was added to the mixture and mixed gently for 1-2 minutes. After that, the mixture was centrifuged for ten minutes at 12000 rpm. This step was repeated twice. Supernatant was shifted into new eppendorf tube, and the pellet was discarded. Afterwards, 100 μ L of 5M NaCl and 500 μ L chilled isopropanol were added to the supernatant. Subsequently, the mixture was centrifuged at 12000 rpm for 10 minutes. Pellet was retained and the supernatant was discarded. After that, the pellet was mixed with 500 μ L of 70% ethanol and centrifuged for 10 minutes at 6000 rpm. After that, the pellet was allowed to air dry for one to two hours at room temperature. After drying, 50 μ l of RNAase, DNAase free PCR water was added to dissolve the DNA pellet.

2.2.10.2. Gel Electrophoresis

To visualize the extracted DNA, 1% agarose gel was used. Powdered agarose was heated with distilled water (dH_2O) in an oven for 2 minutes at 100°C to dissolve the agarose completely. After 2 minutes of heating, mixture was allowed to attain room temperature and ethidium bromide (2 μ L) was added to stain the gel. The gel was poured in a casting tray, combs were applied. Once the gel got solidified, combs were removed gently and placed in 1X TBE buffer. 2 μ l of DNA from each sample and 2 μ l of 6x loading dye were loaded into the wells. Gel was allowed to run for 40 to 45 minutes at constant voltage (95 volts). After the stipulated time the gel was visualized in a Gel documentation system (Bio-RAD, Milan, Italy).

2.2.10.3. Polymerase Chain Reaction (PCR)

PCR was carried out for the amplification of 16s rRNA locus using cyanobacteria specific primers, CYA 106 F^c (5'-CGG ACG GGT GAG TAA CGC GTG A-3') as forward and CYA781R (a)^c (5'-GAC TAC TGG GGT ATC TAA TCC CAT T-3') as reverse primer (Nübel et al., 1997).

- **Reaction mixture and conditions**

A 19.6 μ l of PCR reaction mixture was prepared: 11.39 μ l PCR water, 2.5 μ l 10X PCR buffer, 2.2 μ l MgSO_4 (25 mM), 0.86 μ l dNTPs, 0.86 μ l (10pmol each) of forward and reverse primers, 0.33 μ l of Taq polymerase, 0.6 μ l DMSO and 2 μ l (50ng/ μ l) of template DNA. Amplification of the 16 rRNA gene was conducted by following the conditions: Preheating at 99°C for 1min, denaturing at 94°C for 2 min, followed by 30 cycles of 94°C for 1min; 55°C for 1 min and 72°C for 3min; a final

extension at 72°C for 10 min, and an optional holding at 4°C.

2.2.10.4. Purification of PCR Products

To purify PCR products gene jet PCR purification kit (Thermo Scientific Lithuania, Europe) was used. In 15 µL PCR samples, 30 µL of DNA binding buffer was added (PB) and was mixed well. The mixture was put to the column and centrifuged at 12,000 rpm for 1 minute. After centrifugation, the filtrate was removed. A 600 µL washing buffer was applied to each column and was centrifuged at 12,000 rpm for 1 minute. The column along with collection tube was subsequently centrifuged at 12000 rpm for 1 minute. Afterwards, the column was transferred to a new Eppendorf tube and 30 µL of elution buffer (EB) was added to elute the DNA and was allowed to stand at room temperature for 2 minutes. Then the centrifuged for 1 minute at 12,000 rpm. 1 % agarose gel was used to visualize the purified PCR products. The purified PCR products were sequenced commercially from Eurofins (USA).

2.2.10.5. Nucleotide sequence analysis

The sequences thus obtained were studied through BioEdit software. The sequences were cleaned through online software JustBio (<http://www.justbio.com/hosted-tools.html>) and compared with the sequence in Gene databank using National Center for Biotechnology Information (NCBI; <https://www.ncbi.nlm.nih.gov/>). The omology of nucleotide sequences was established via BLAST-ntool (<https://blast.ncbi.nlm.nih.gov/Blast.cgi>).

2.2.10.6. Molecular phylogenetic analysis

The phylogenetic analyses were conducted in MEGA (version 11) (Tamura et al., 2011). The diversity of strains was verified with previously reported genes sequences in NCBI database. The phylogenetic trees were constructed using the Neighbor-Joining (NJ), Maximum Likelihood (ML) and Maximum Parsimony (MP) methods. The topologies derived in NJ analysis have been presented in the results.

2.2.11. Initial screening for heavy metals (Cd and Pb) tolerance

The axenic cyanobacterial strains were cultivated in different initial concentrations of Cd (0, 0.25, 0.5, 0.5, 0.75, 1.0, 1.25, 1.5, 2, 2.5, 3 and 5 mg/L) and Pb (0, 5, 10, 15, 20, 25, 30, 25, 40, 45, 60, 90 and 120 mg/L). Experiments were carried out using the 96-Well Polypropylene MicroWell™ Plates. Each microliter

plate contained 200 μL BG₁₁ media with various concentrations of Cd and Pb and inoculated with actively growing 50 μL of axenic culture. Incubation was carried out in a growth chamber for 12 days under constant white LED lights at 25 °C. Visual observations were taken to assess the growth of the strains. The optical density (OD) at 750 nm (OD₇₅₀) was measured at specific intervals to monitor the increase in biomass (Oyebamiji et al., 2019).

2.3. Results

2.3.1. Collection sites and samples

All samples were collected in summer, therefore the recorded temperatures during this time of collection were above 30°C with profound growth of cyanobacteria, green algae and diatoms observed in field samples. The sites were found teaming with cyanobacteria mostly in floating and suspended form. Further details of the collection sites have been described in Table 2.1.

Table 2.1: The collection sites and associated field data

Site No.	Site	Sample description	Temp.	Location	Collection date
Site 1	Park road, Islamabad	Wastewater from electronics waste	32°C	33° 39' 56.8" N 73° 9' 4.71" E	06-5-2020
Site 2	I-9 industries Islamabad	Sewage water/effluents from industrial waste	31°C	33° 39' 36.52" N 73° 3' 19.02" E	07-9-2020
Site 3	Gujar Khan Rawalpindi	Sewage water from domestic waste	38°C	33° 15' 14.79" N 73° 18' 15.58" E	05-07-2021

2.3.2. Physico-chemical and Heavy metal analyses of wastewater

As expected, the sewage water samples collected from these sites were turbid with grey, brown to black in colour. Average temperatures were found maximum (38 °C) at site 3 (located in Gujar Khan, Rawalpindi) as it was mostly exposed to direct sunlight while average temperature at site 2 was 31°C (located in I-9, Islamabad). pH of these samples was mostly around 7 and therefore neutral, however for some samples of Islamabad the pH ranged was slightly acidic while a sample collected from site 3 (located in Gujar Khan, Rawalpindi) showed a slightly basic pH (>7). The range of the total dissolved solids (TDS) was 203–236 mg/L., the values were more than average at site 2, and less than average at site 3. Among electrolytes, the nitrates were in the range of 3.0–3.18 mg/L; magnesium 4.62–6.50 mg/L; Chlorides 33–39 mg/L. Calcium 6.86-11.49 mg/L; sulphates 1.8-3.01 mg/L etc. For the electrolytes, the values were high at site 1 (e-waste, Park Road, Islamabad). Similarly, the sodium concentration was 25.21-30.11 mg/L. At site 1, the average recorded values were lower compared to the average, while at site 2 these were recorded as high compared to the average. Potassium values varied from 9.93 to 15 mg/L. At site 2, these values were found higher whereas at site 1 these were recorded in low quantities. The physico-chemical properties of domestic, industrial and e-

wastewater has been described further in Table 2.

Table 2.2: Physio-chemical parameters of water samples. Site details are given in table 2.1.

Site names	Site 1	Site 2	Site 3
Appearance	Turbid	Turbid	Turbid
Color	Dark brown, black	Grayish	Grayish
Odor	Pungent	Pungent	Pungent
pH	7.15	7.33	6.57
Electrical Conductivity ($\mu\text{S}/\text{cm}$)	810	795	788
Turbidity (NTU)	17.7	15.02	14.67
Alkalinity (mg/L)	209	217	200
TDS (mg/L)	223	236	203
Chloride (mg/L)	33.9	39	35.09
Sulphates (mg/L)	1.8	2.71	3.01
Nitrates (mg/L)	3.01	3.88	3.77
Calcium (mg/L)	6.86	11.49	9.23
Magnesium (mg/L)	4.62	6.5	5.91
Sodium (mg/L)	25.21	35.45	30.11
Potassium (mg/L)	9.93	15	10.61
BOD (mg/L)	7.95	8.15	8.19

Different heavy metals have also been detected in the water samples collected from three sites of Islamabad and Rawalpindi. The details of heavy metals and their concentrations (mg/L) are described in Table 2.3.

Table. 2.3. Heavy metals detected in the water from three different sites of Rawalpindi and Islamabad.

Heavy metals (mg/L)	Site 1	Site 2	Site 3
Pb	0.3	0.25	1.10
Zn	0.034	0.09	0.228
Cd	0.51	0.321	0.83
Mn	0.19	0.16
Fe	0.149	0.08	1.01
Co	1.45	0.15
Cu	0.011	0.135	0.126
Cr	0.02
Ni	0.10	0.07

2.3.3. Microscopic Observations

2.3.3.1. Initial Screening of Cyanobacteria

Based on the morphological observations, the cyanobacterial species were identified mostly to the genus level, however, where morphological characters were clear the species were also identified.

2.3.3.2. Culturing

Most of the cyanobacteria showed response in BG₁₁ and to an extent in BG₀. On the contrary, none showed growth response in BBM. All heterocytous types responded well in BG₁₁ and BG₀. Some cyanobacterial isolates also responded in the SP media. In addition, the green algae responded well in BBM media but some species of green algae also responded in BG₁₁ media e.g., *Chlorella* and *Scenedesmus*. It has also been observed that different species of different genera responded differently. For instance, some preferred slightly acidic conditions (for instance pH 6.5 to 6.9) while others responded well above pH 7.0. Figure 2.3 shows the colony pattern of the ten axenic cyanobacterial strains cultivated in BG₁₁ agar medium. The colony shape was either spreading, compact, spherical, or irregular in shape. The colony shape was a stable character having diagnostic value for species identification.

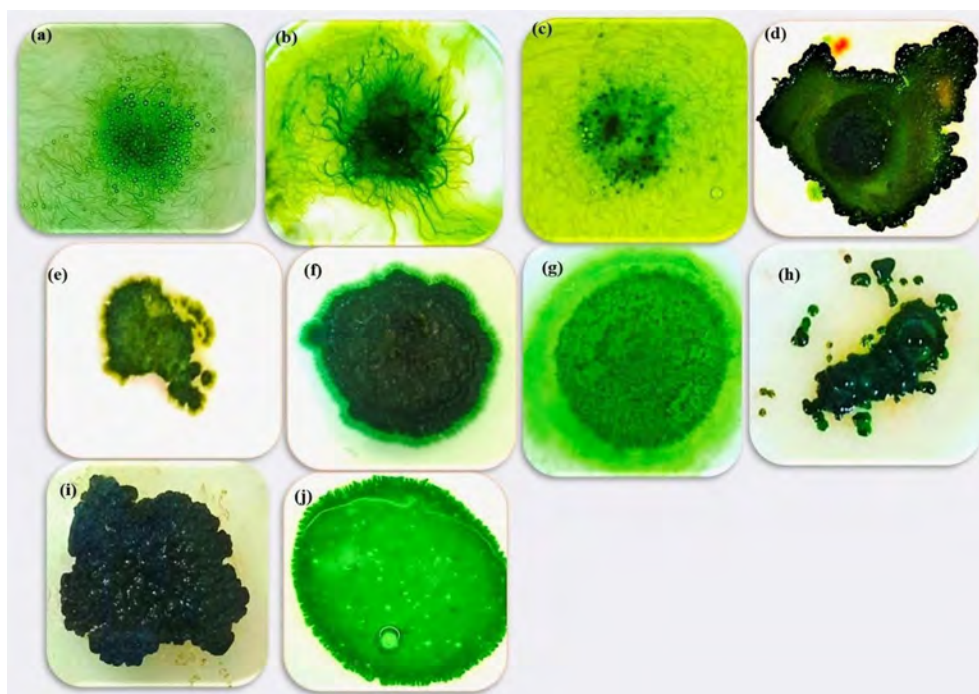


Figure 2.3: Growth pattern of cyanobacteria in BG-11 agar media: (a) *Desertifilum*

tharen MK-2; (b), *Phormidium* MK-3; (c) *Nodosilinea nodulosa* MK-4; (d) *Desikacharya* sp. MK-7; (e) *Fischerella muscicola* MK-8; (f) *Westiellopsis prolifica* MK-9; (g) *Nostoc* sp. MK-11; (h) *Synechocystis fuscopigmentosa* MK-13 (i); *Gloeocapsa* sp. MK14; (j) *Synechococcus elongatus* MK-15.

2.3.4. Morphological, Molecular and Phylogenetic analysis of axenic strains

2.3.5. The Oscillatorales

2.3.6.1. *Desertifilum tharense* MK-2

- **Taxonomic Characters:** The morphological observations were based on cultured samples.

The isolated strain was a free-floating filamentous type with a mat-forming thallus of blue green color. Cells are mostly longer than wide and few are isodiametric (Fig. 2.4a1 and 2.4a2). Cell width 2.1-3.7 μm and 3.2-5.9 μm long. Filaments solitary, wavy or straight and a few entangled. Oscillation was observed in filaments. Apical cells were long and conical to round. A transparent sheath present at the tip of apical cells (Fig. 2.4b). Cells with homogeneous content and high number of granules were found in older filaments and aerotypes were present in cells (Fig 2.4c).

- **Diagnostic characters:** Cells longer than wide, isodiametric and presence of aerotypes.
- **Site detail and habitat:** This strain was collected from sewage water. Other taxa found in the sample: *Oscillatoria*, *Cosmarium*, *Pseudoanabaena*, and *Cymbella*.
- **Culturing Conditions:** *Desertifilum tharense* MK-2 strain responded well in BG₁₁ medium.

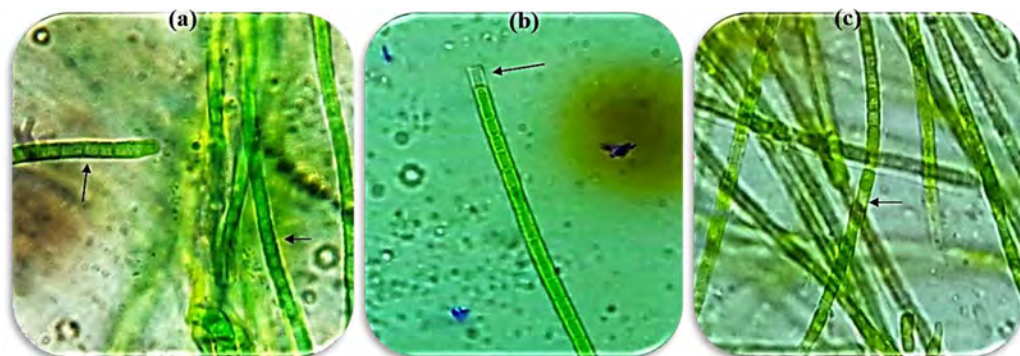


Figure 2.4: Micrographs of *D. tharense* MK-2: (a1) Cells longer than wide (arrow);

(a2) iso-diametric cells (arrow); (b) filaments with transparent sheath at the apical cell (arrow); (c) aerotypes in the filaments (arrow).

- **Molecular and Phylogenetic analysis**

The NCBI blast analysis of 16S rRNA gene sequences (633 bp) received for the strain MK-2 showed 99% similarity with *Desertifilum tharense* PD2001/TDC4 and 98% similarity with *Desertifilum dzianense* strain PMC 872.14. A NJ tree constructed using 16s rRNA sequences of this strain compared to those downloaded from NCBI, showed resemblance with *D. tharense* PD2001/TDC4 with 100 bootstrap value (Fig 2.5). Maximum parsimony and Maximum Likelihood also showed the same clustering pattern (Figures not shown here). NCBI searches and Phylogenetic analysis supported similarity of MK-2 strain with the genus *Desertifilum*.

Based on strong morphological evidence, molecular and phylogenetic analysis, strain MK-2 was identified as *Desertifilum tharense*.

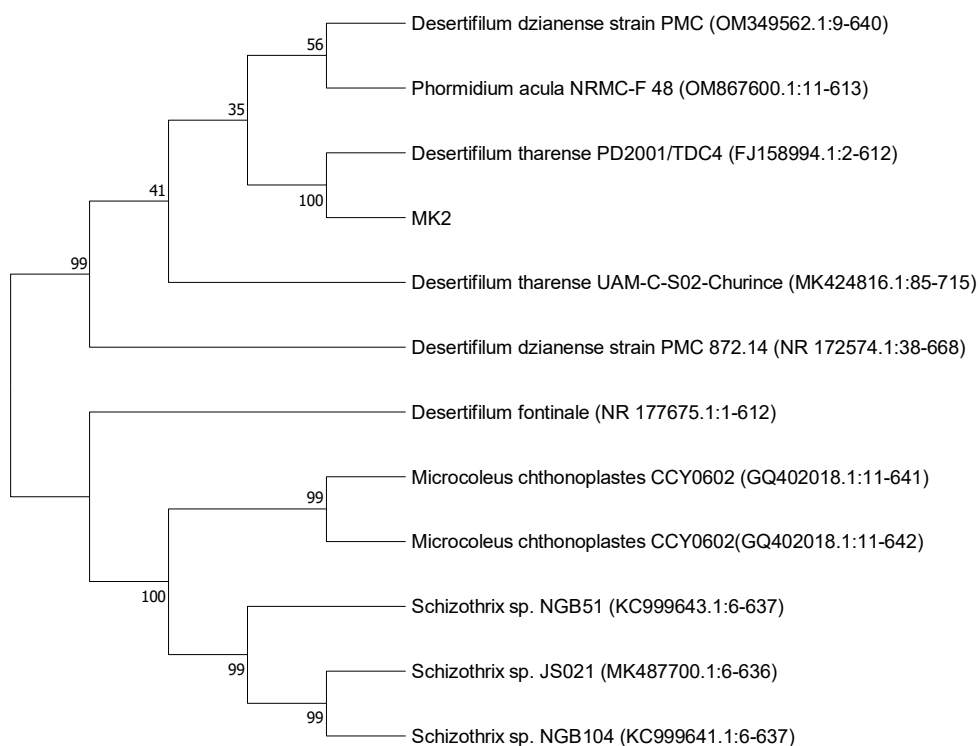


Figure: 2.5: NJ analysis of 16S rRNA data of strain MK-2.

2.3.6.2. *Phormidium* sp. MK-3

- **Taxonomic Characters:**

Densely packed filaments (Fig 2.6a), trichomes long, cells 2.9-5.3 μm wider and 1.3-2.4 μm long; isopolar; trichomes end with round epical cells and surrounded by a thin colorless sheath (Fig. 2.6b), variously curved and brightly colored. Necridia development occurs in the trichome (Fig. 2.6c) supporting the reproduction. Cells at the cross wall were constricted sometimes not; gas vesicles absent.

- **Diagnostic characters:** Densely packed filaments and necridia development
- **Site details and habitat:** Collected from sewage water with prominent growth along with other taxa including *Pinnularia*, *Spirogyra*, *Rhizoclonium*, *Chlorella*.
- **Culturing conditions:** *Phormidium* sp. MK-3 responded well in BG11 medium.

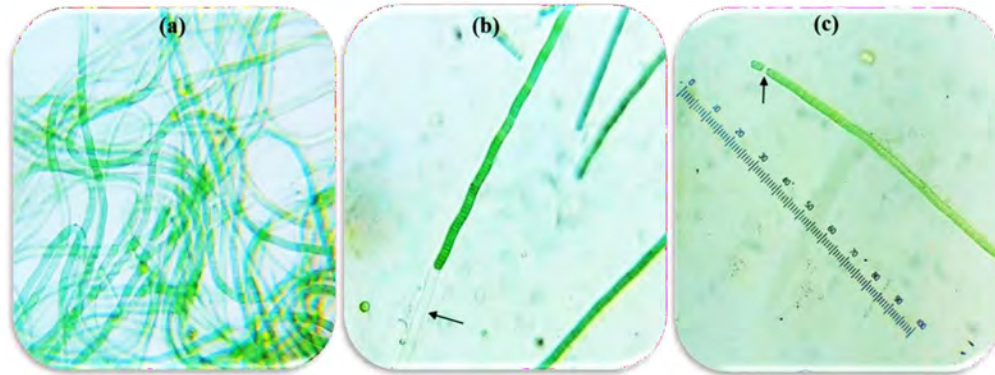


Figure 2.6: Micrographs of *Phormidium* sp. MK-3; (a) densely packed filaments; (b) Trichomes surrounded by a colorless sheath and sheath at the tip (arrow); (c) necridia development in the trichome (arrow).

Sequence Analysis: In BLAST analysis of 16S rRNA gene sequences (670 bp), the strain MK-3 revealed 96.9% similarity with *Phormidium* sp. CENA270 and the cluster analysis also revealed its clustering similarity with *Phormidium* sp. CENA270 with a bootstrap support of 63. Neighbor joining phylogenetic analysis constructed with 18 sequences of cyanobacteria obtained from NCBI is shown in Figure 2.7. Maximum likelihood and Maximum parsimony phylogenetic analysis also showed similar clustering results (data not shown). On the basis of morphological evidence, molecular and phylogenetic analysis, strain MK-3 was identified as *Phormidium* sp. MK-3.

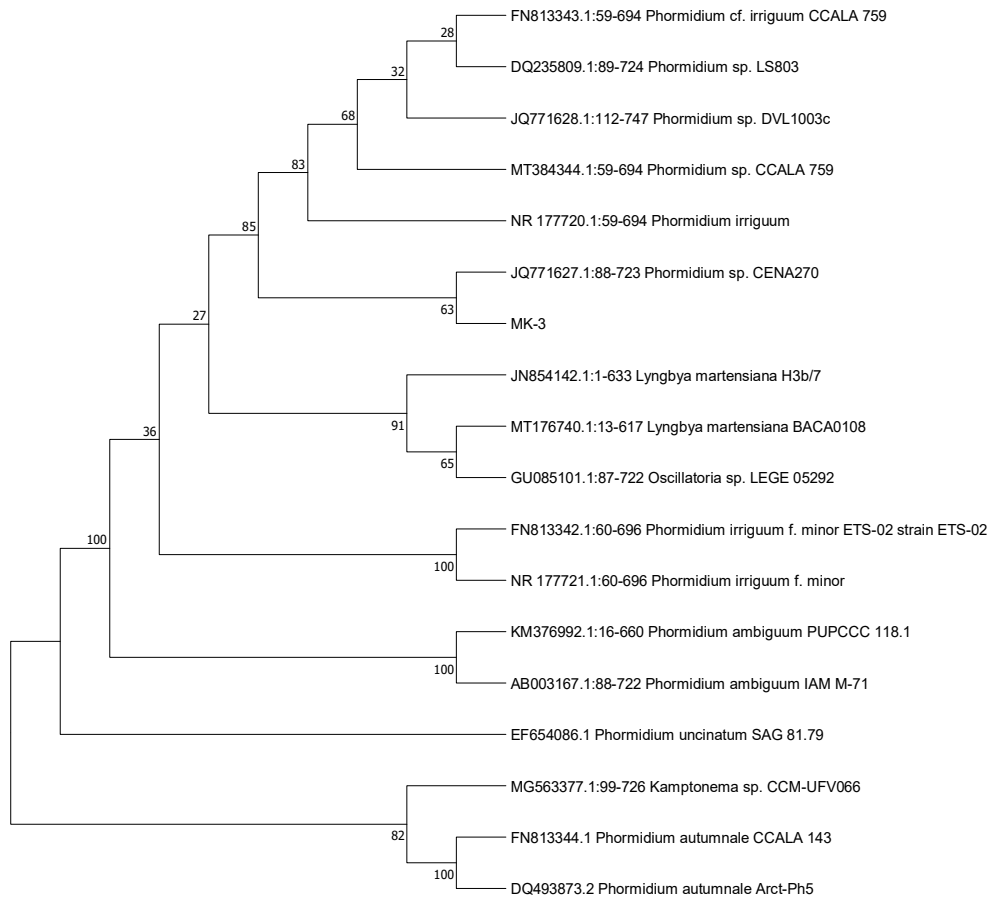


Figure 2.7: NJ analysis of 16S rRNA data of strain MK-3.

2.3.6.3. *Nodosilinea nodulosa* strain MK-4

- **Taxonomic Characters:**

Filaments mostly with single trichome, sometime multiseriate. Mature filaments form spiral arrangement of the cells (Fig. 2.8a) and nodules formation observed in the mature filaments (Fig. 2.8b). Trichomes long or short, straight or bent sometimes present circular growth, soft, thin, colorless sheath. Indication of nodule formation was observed on agar BG₁₁ growth media (Fig. 2.8c).

- **Diagnostic characters:** Nodules development
- **Site detail and habitat:** Strain MK-4 was collected from the e-waste standing dark brown water with pungent smell along with other tax including *Leptolyngbya*, *Syneccoccus*, *Calothrix*, *Anabeana*.
- **Culturing Conditions:** Strain-MK-4 responded in BG₁₁ medium.

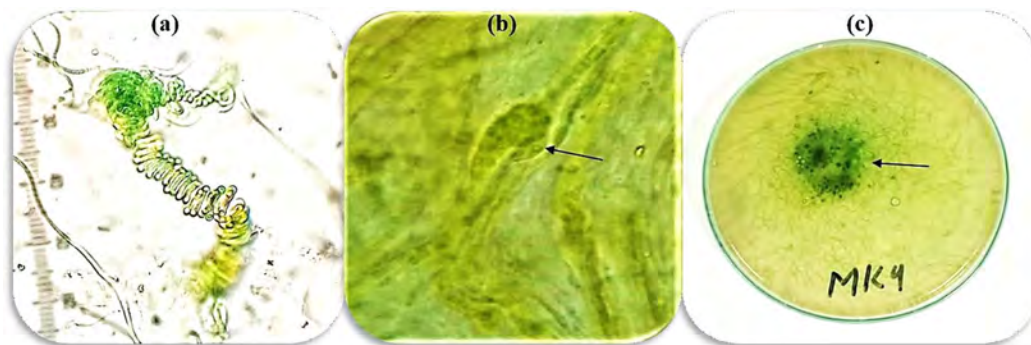


Figure 2.8: Micrographs of *Nodosilinea nodulosa* strain MK-4 under the light microscopy: (a) mature filaments forming spiral arrangements of the cells (arrow); (b) characteristic nodule (arrow); (c) nodules forming on BG-11 agar media (arrow).

Sequence Analysis: In BLAST analysis of 16S rRNA gene sequences (687 bp), the strain MK-4 revealed 94.15% similarity with *Nodosilinea nodulosa* strain UTEX B 2910 and the cluster analysis also revealed the clustering similarity with *Nodosilinea nodulosa* strain UTEX B 2910 with a bootstrap support of 72. Neighbour joining phylogenetic analysis constructed with 18 sequences of cyanobacteria obtained from NCBI as shown in Figure 2.9. Maximum likelihood and Maximum parsimony phylogenetic analysis also showed similar clustering results (data not shown). On the basis of morphological evidence, molecular and phylogenetic analysis, strain MK-4 was identified as *Nodosilinea nodulosa* MK-4.

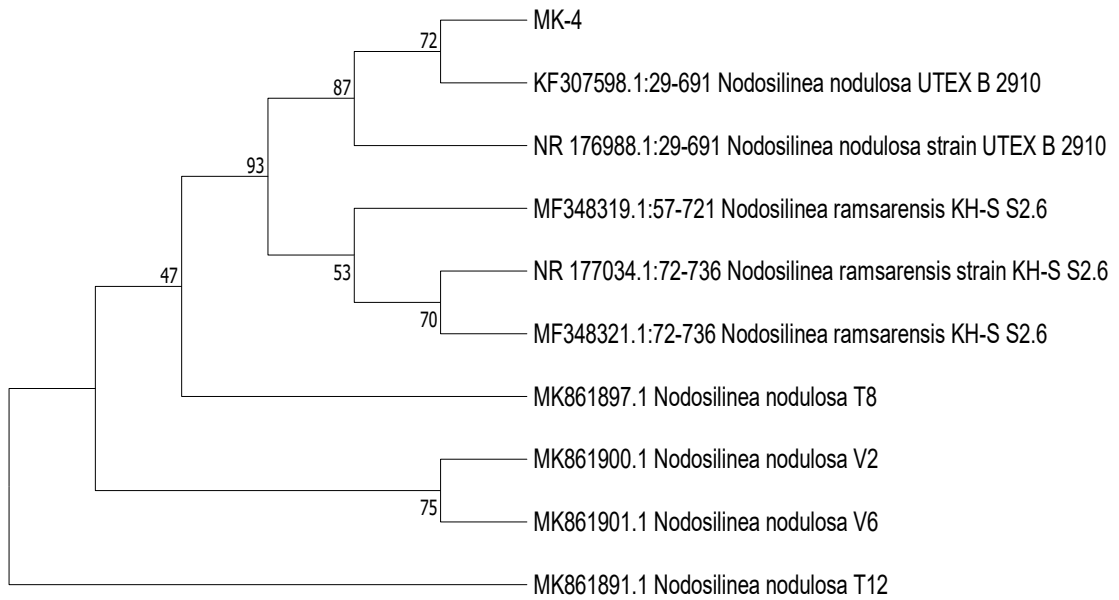


Figure 2.9: NJ analysis of 16S rRNA data of strain MK-4.

2.3.7. The Nostocales

2.3.7.1. *Desikacharya* sp. MK-7.

- **Taxonomic Characters:** Irregular shape colony (Fig.2.10a), Trichome slightly coiled (Fig. 2.10b), isopolar, mucilage present around the filaments. Thallus dark green and slightly yellow green in color, terminal cells slightly large with curved ends, 3.4 to 4.6 μm wide and 3.7 to 4.8 μm long. The vegetative cells are square to cylindrical. Heterocysts intercalary, elliptical (Fig. 2.10c), slightly oval (Fig. 2.10d), terminal and sub-spherical in shape (Fig. 2.10e).
- **Diagnostic characters:** Trichome less coiled, heterocysts sub-spherical to elliptical in shape.
- **Site detail and habitat:** Strain MK-7 was collected from the e-waste polluted standing water. Growth of the MK-7 strain was not prominent at the time collection. It appeared during the culturing in laboratory conditions. Other taxa found in the sample were: *Gleotheca*, *Aphanocapsa*, *Zygnema*, *Phormidium*
- **Culturing conditions:** Strain MK-7 showed response in BG₁₁ and BG₀ media.

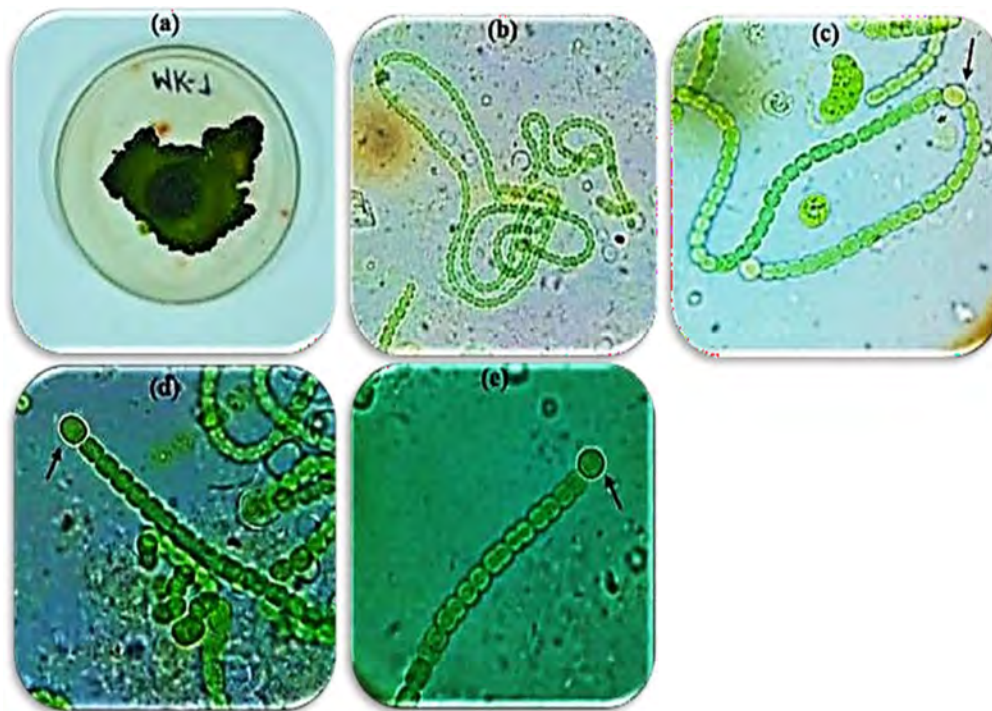


Figure 2.10: Micrographs of *Desikacharya* sp. MK-7 under the light microscopy; (a) Irregular shaped colony on agar BG-0 media; (b) coiled trichomes; (c) intercalary elliptical heterocyst; (d) terminal, slightly oval shaped heterocyst; (e)

terminal sub-spherical heterocysts.

Sequence Analysis: In BLAST analysis of 16S rRNA gene sequences (661 bp), the strain MK-7 revealed 98.2% similarity with *Desikacharya* sp. NS2000 and the cluster analysis also revealed the clustering similarity with *Desikacharya* sp. NS2000 with a bootstrap support of 72. Neighbour joining phylogenetic analysis constructed with 18 sequences of cyanobacteria obtained from NCBI as shown in Figure 2.11. Maximum likelihood and Maximum parsimony phylogenetic analysis also showed similar clustering results (data not shown). On the basis of morphological evidence, molecular and phylogenetic analysis, strain MK-11 was identified as *Desikacharya* sp. MK-11.

The morphological and 16S rRNA gene sequence analysis of MK-7 stain revealed its identification as *Desikacharya* sp.

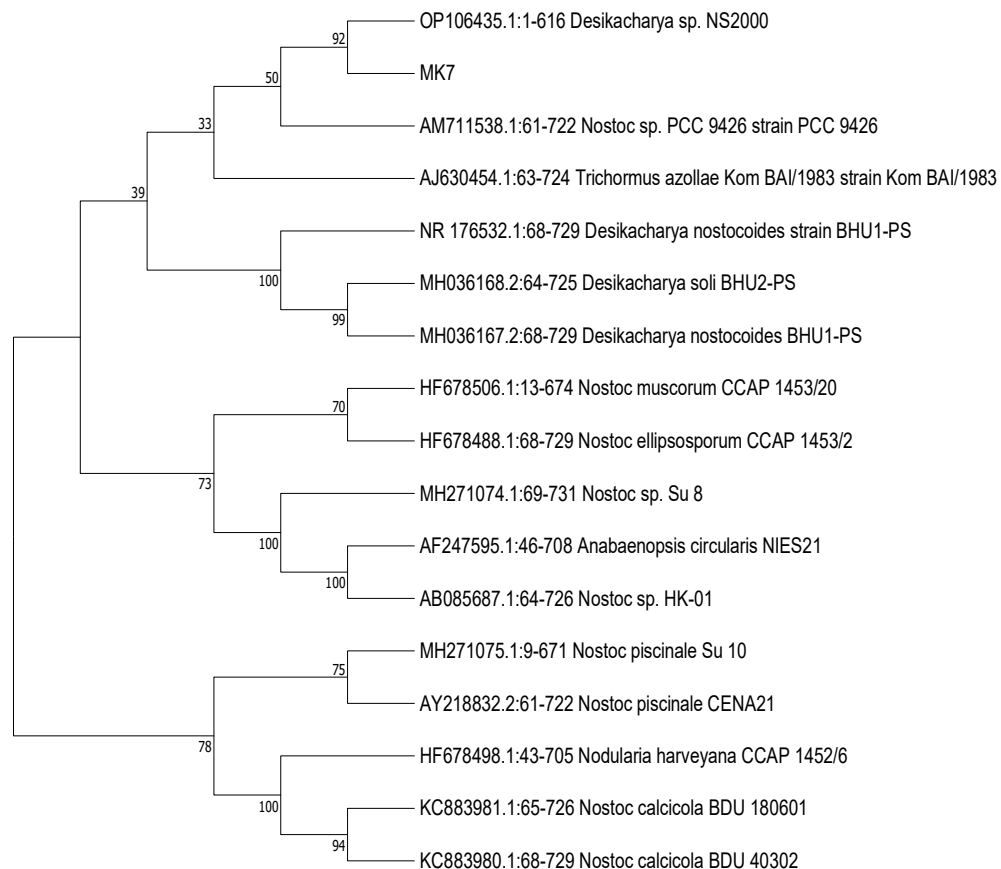


Figure 2.11: NJ analysis of 16S rRNA data of strain MK-7.

2.3.7.2. *Fischerella muscicola* MK-8

- **Taxonomic Characters:**

Heterocystous branched filamentous cyanobacterium. Main filament creeping, dark green branched, interwoven, flexuous, T-type branches (Fig 2.12a). Mostly filaments in uniseriate condition and some biseriata (Fig 2.12b). Main filaments cells sub-spherical, sub-quadrata, 6.2-8 μm broad and 6.6-7.4 μm long, constricted at the cross wall. Terminal cells round (Fig 2.2c). Lateral branches straight, erect, and different from the primary filament. Cells light green colored, closely compressed, and rectangular, round apical portion. Intercalary heterocyst in the branches as well as in the main filaments, yellowish in color, sub-spherical, 6.99-8.7 μm broad and 5.67-7.89 μm long (Fig 2.12d). Intercalary heterocyst in the main filaments (Fig 2.12e).

- **Diagnostic characters:** T-type branches, uniseriate and biseriata filaments.
- **Site detail and habitat:** Strain MK-8 was collected from the sewage water. At the time of collection biomass of the stain was prominent and was easily collected for laboratory analysis. Other species found in the sample were *Oscillatoria*, *Leptolyngbya*, *Achnantheidium*.
- **Culturing Conditions:** Strain MK-8 showed response in BG₁₁ and BG₀ culturing media.

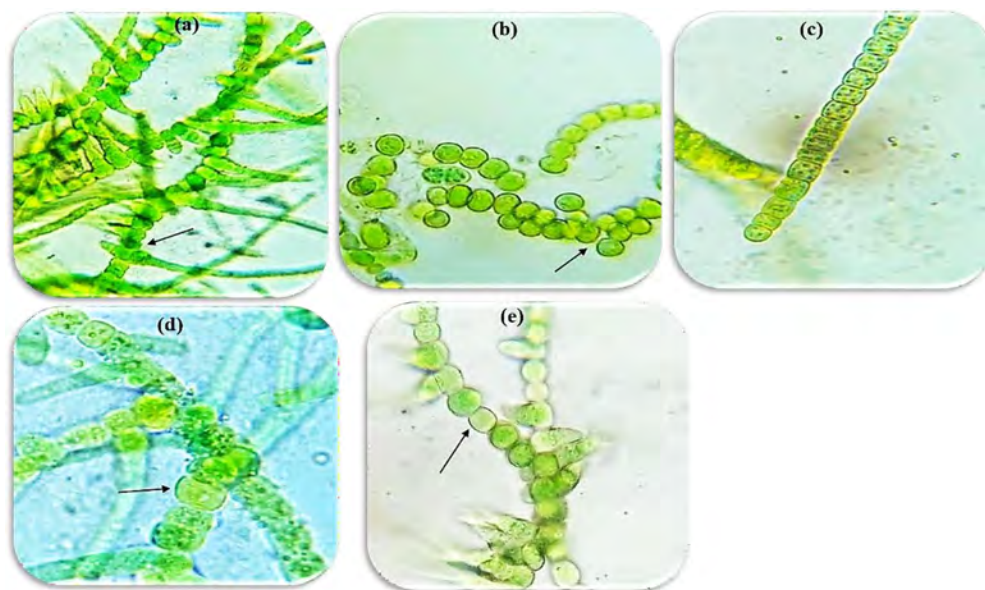


Figure 2.12: Micrographs of Strain *Fischerella muscicola* MK-8 under the light microscope: (a) T- type branches (arrow); (b) bi-seriate condition (arrow); (c) round shaped terminal cells (arrow); (d) heterocysts in main filaments (arrow) and branches (arrow); (e) Intercalary heterocyst in main filaments (arrow).

Sequence analysis: In this study, 679 bp sequences were obtained for the strain MK-8 showed 99.21% similarity with *Fischerella muscicola* UTEX 1829 with 100 % query coverage. In phylogenetic analysis strain MK-8 clustered with the *Fischerella muscicola* UTEX 1829. Phylogenetic tree was constructed with Neighbor joining method using the sequences of cyanobacteria strains is shown (Figure 2.13).

Morphological, similarity of 16s rRNA gene sequence and phylogenetic analysis confirm its identity as *Fischerella muscicola* MK-8.

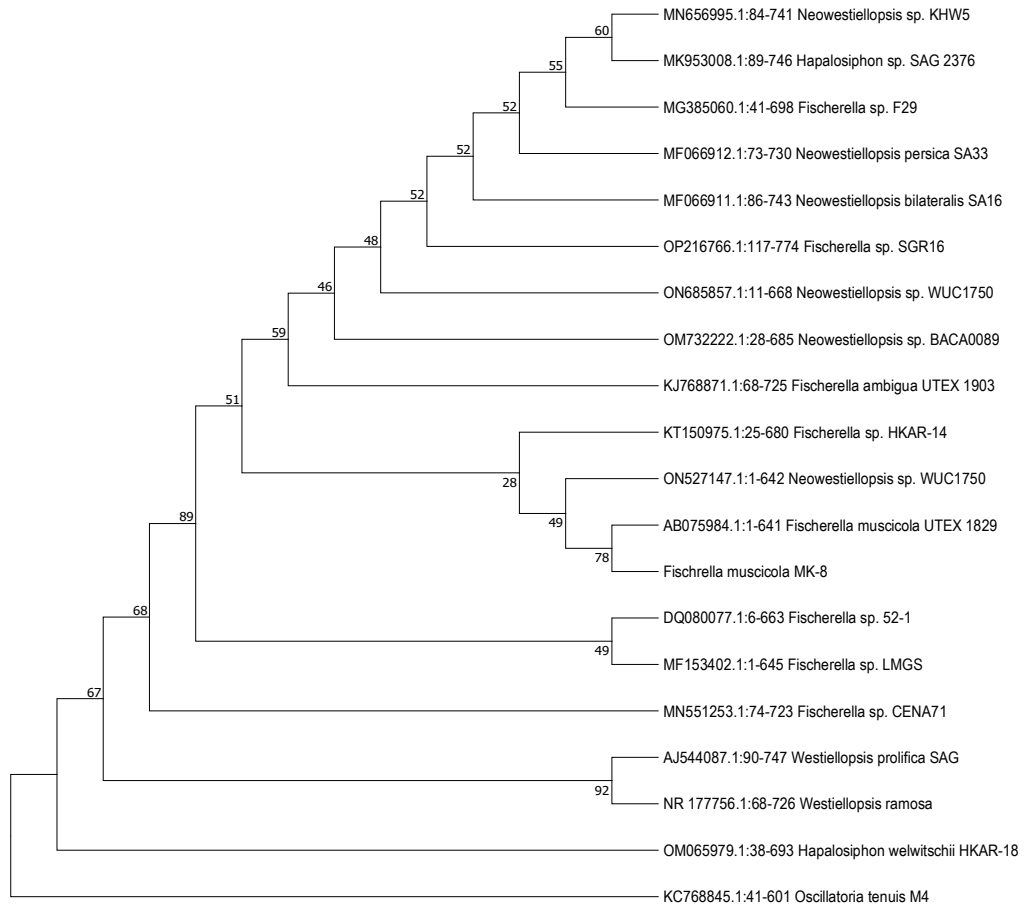


Figure 2.13: NJ analysis of 16S rRNA data of strain MK-8.

2.3.7.3. *Westiellopsis prolifica* MK-9

- **Taxonomic Characters:**

Heterotrichous filaments, T-type branches (Fig. 2.14a), thallus blue-green. Main filaments flesuous monoseriate, and constricted at cross walls. Barrel shaped granulated cells, 8.5-10.3 broad and 7.5-12.8 μm long. Lateral branches erect thinner than main filaments distinctly constricted in the basal parts. In the upper parts cells not constricted and cells usually elongated. Heterocyst intercalary, solitary, barrel shaped (Fig. 2.14b), short to elongate-cylindrical (Fig. 2.14c). Monocytes reproductive structures spherical, single, 4.9-6.1 μm in diameter, liberate from the pseudohormocytes which formed at the lateral branches end as a result of multiple longitudinal and transverse cell divisions (Fig. 2.14d).

- **Diagnostic characters:** Monoseriate, main filament prostrate, constricted at the cross-walls and Pseudohormocytes development.
- **Site detail and habitat:** Strain MK-9 was collected from the sewage water. Other species isolated along the sample were *Leptolyngbya*, *Chlorella*, *Chroococcus*, *Ulothrix* and *Scenedesmus*.
- **Culturing Conditions:** MK-9 strain showed growth response in BG₀ and BG₁₁ media.

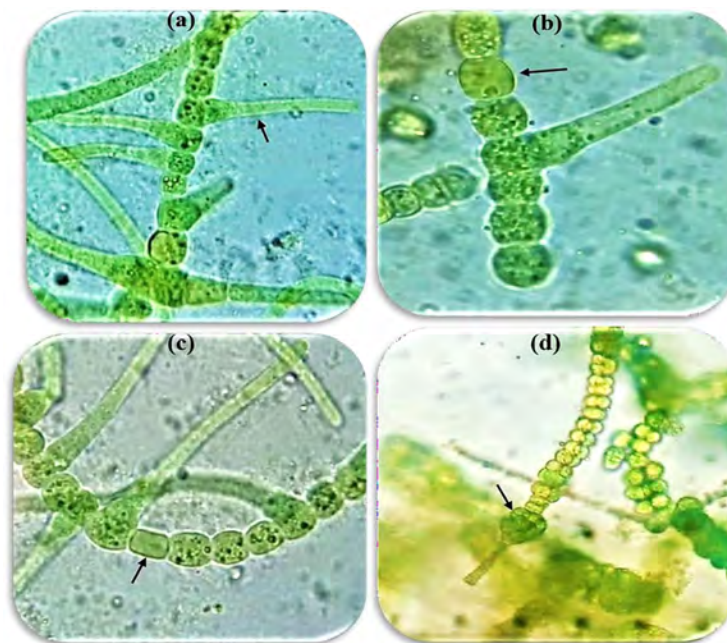


Figure 2.14: Micrographs of Strain *Westiellopsis prolifica* MK-9: (a) T-type branches

(arrow); (b) barrel shaped heterocyst (arrow); (c) elongated cylindrical heterocyst (arrow); (d) pseudohormocyte showing transverse and longitudinal cell division (arrow).

Sequence Analysis: In this study, 16S rRNA gene sequences of 679 bp obtained for the strain MK-9 showed 96.71%, 96.71%, and 99.1% similarity with *Neowestiellopsis persica* SA33, *Neowestiellopsis bilateralis* SA16 96.71 %, *Westiellopsis prolifica* AUS- JR/SD/MS-028, respectively. A NJ tree constructed with 23 sequences of cyanobacteria strains from NCBI along with the sequences of MK-9 strain exhibited a close cluster with *Westiellopsis prolifica* AUS-JR/SD/MS-028 with a bootstrap value of 93 (Fig 2.15). MP and ML also showed the similar results with slight differences in the bootstrap values.

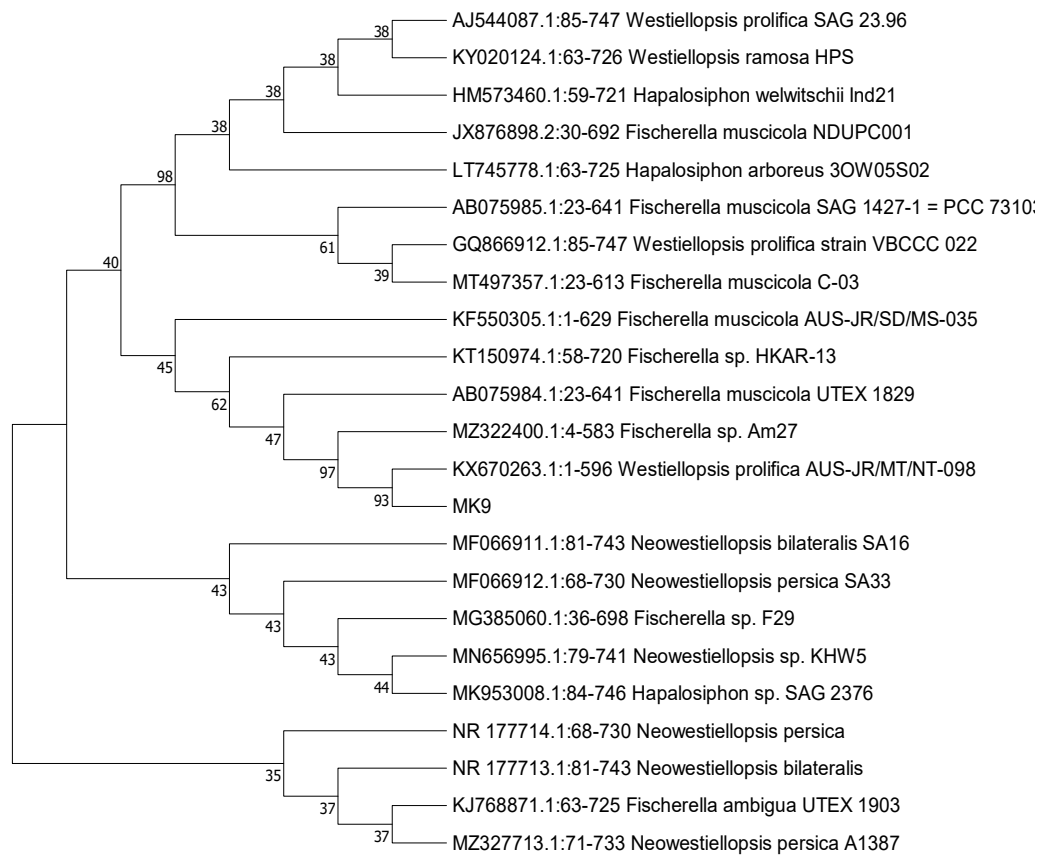


Figure 2.15: NJ analysis of 16S rRNA data of strain MK-9.

2.3.7.4. *Nostoc* sp. MK-11

- **Taxonomic Characters**

Small size colonies, mostly irregular in shape, appearing dark green, long loosely associated trichomes and cells were surrounded by high mucilaginous sheath (Fig. 2.16a). Cells mostly granulated (Fig. 2.16b), 4.4 μm long, 2.3 μm wide, terminal cells large in size, 4.7 μm long and 2.4 μm wide, heterocysts sub-spherical and elliptical in shape present at both ends end of the trichome (Fig. 2.16c) and also intercalary position (Fig. 2.16d).

- **Diagnostic characters:** High mucilaginous sheath around the filaments, prominent heterocysts
- **Site detail and habitat:** Strain-MK-11 was isolated from the e-waste polluted water with pungent smell. Other species isolated from the same site were: *Oscillatoria*, *Synechocystis*, and *Rhizoclonium*
- **Culturing Condition:** Strain, MK-11 responded to BG₁₁ and BG₀ media

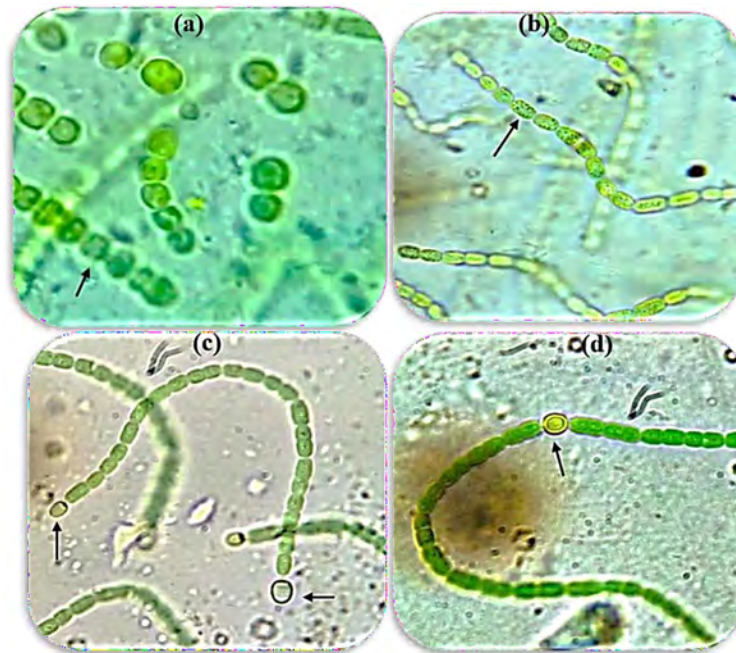


Figure 2.16: Micrographs of *Nostoc* sp. MK-11 under light microscope: (a) colorless sheath (arrow); (b) granulated cells (arrow); (c) heterocysts sub-spherical in shape present at both ends end of the trichome (arrows); (d) intercalary heterocyst (arrow).

Sequence Analysis: The NCBI blast analysis of 633 base pair 16S rRNA gene sequences was of strain MK-11 showed 100% query coverage with 100% identity with *Nostocales cyanobacterium* NapMSIm13. The phylogenetic trees constructed using the NJ, ML, and MP methods revealed similar results. A NJ tree constructed with this strain and the sequences obtained from NCBI exhibited a close clustering with *Nostocales cyanobacterium* NapMSIm13 with bootstrap value 100% (Fig.2.17). Strain MK-11's morphological and molecular characteristics suggest that it belongs in the genus *Nostoc*.

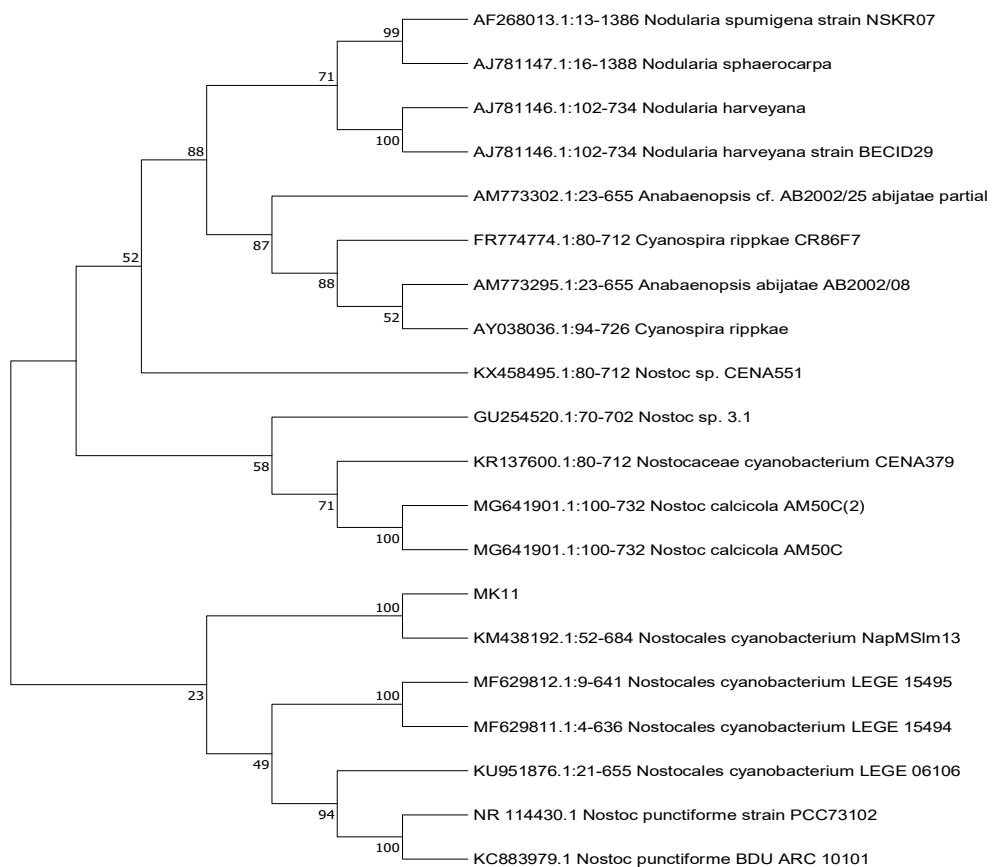


Figure 2.17: NJ analysis of 16S rRNA data of strain MK-11.

2.3.8. The Chroococcales

2.3.8.1. *Synechocystis fuscopigmentosa* MK-13

- **Taxonomic Characters**

Cells spherical, mostly oval and after cell division they become hemispherical shape (Fig. 2.18a). Cell color pale blue-green, olive-green and a few cells were colorless (Fig. 2.18b) and homogeneous cell content. Cells diameter, 3.1 to 5.4 μm , very fine mucilage around the cells (Fig. 2.18c) and the cells were solitary or present together. During cell division cells increase in size and constrict in the middle (Fig. 2.18d), separate from each other and each cell divide into two cells.

- **Diagnostic characters:** Oval, spherical shaped cells, cell size and color
- **Site detail and habitat:** Strain MK-13 was collected from the e-waste standing polluted water. Other species found in the sample were *Oscillatoria*, *Phormidium* and a unicellular green alga.
- **Culturing Conditions:** Strain MK-13 showed response in BG₁₁ medium.

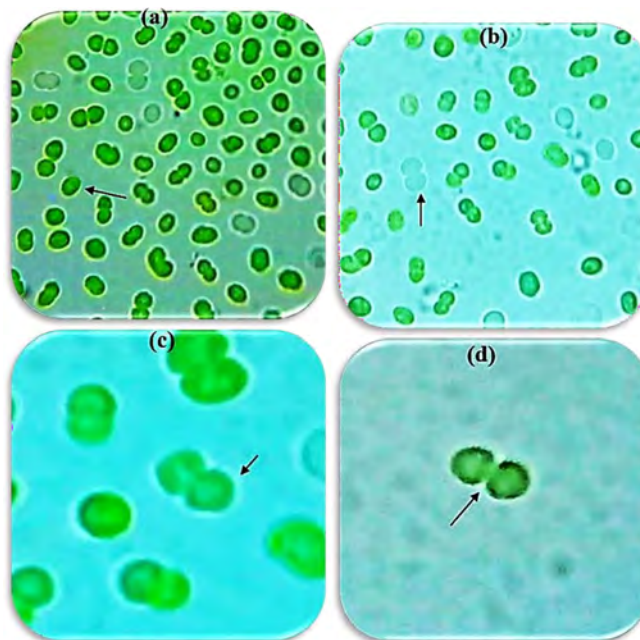


Figure 2.18: Micrographs of *Synechocystis fuscopigmentosa* MK-13: (a) oval shaped cells (a)(arrow); (b) colorless cells (arrow); (c) thin mucilage around the cells (arrow); (d) cell constricted at the middle (arrow).

Sequence Analysis: BLASTn analysis based on gene sequences of 16S rRNA and 637 bp obtained for the strain MK-13 revealed 97.58 % similarity with query coverage 90% to *Synechocystis* sp. CR_L29 and 97.44 % similarity with query coverage 97% to *Geminocystis* sp. CENA526 and 95.53% similar with 97% query coverage to *Synechocystis fuscopigmentosa* CCALA 810. The phylogenetic trees constructed with NJ, ML, and MP analysis showed similar results. A NJ tree (Fig.2.19) constructed with sequences of cyanobacterial strains obtained from NCBI revealed clustering of MK-13 with *Synechocystis* sp. CR_L29 and also showed close clustering with *Synechocystis fuscopigmentosa* CCALA810.

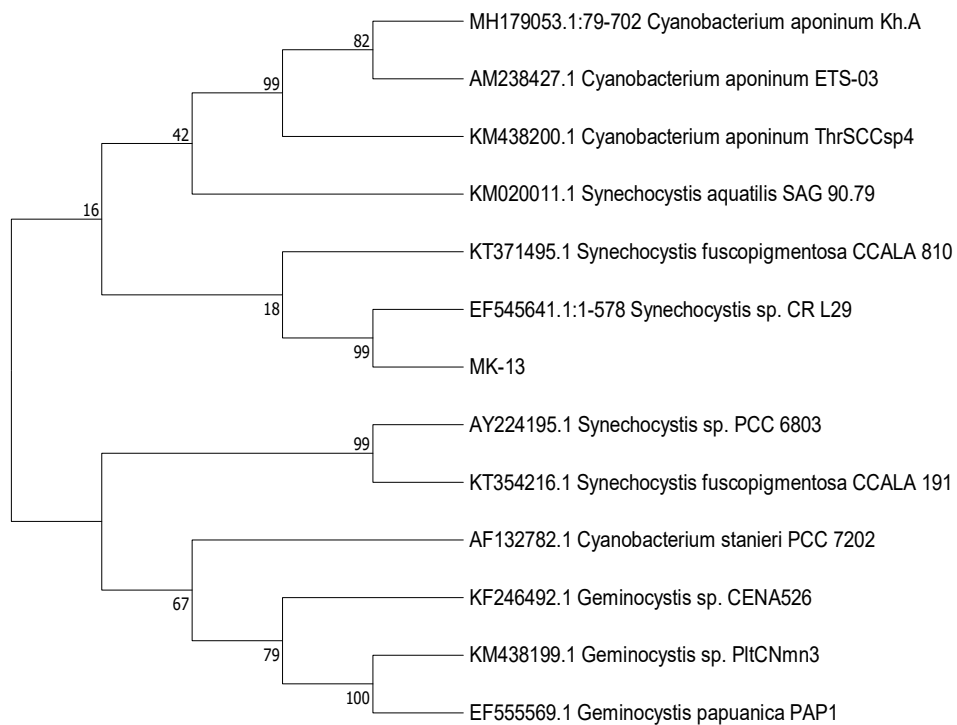


Figure 2.19: NJ analysis of 16S rRNA data of strain MK-13

2.3.8.2. *Gloeocapsa* sp. MK 14

- **Taxonomic Characters**

Colonies spherical and sometime become irregular in shape and enclosed by mucilage (Fig 2.20a). Cells arrangement in the colony was not regular. Cells, elliptical, oval or spherical, 2.5-3.6 μm broad, 3-5.2 μm long. Mucilaginous sheath wrapped the cells together and formed the colonies. Each cell in the colony was separated from other cell by a colorless sheath (Fig 2.20b). Cells are granulated and the color of the cells was pale blue green. After division the cells develop their mucilage envelops and grow into original shape. When the cells mature, they are release from the mucilaginous colony and then they start to divide further and develop a new colony of cells (Fig 2.20c).

- **Diagnostic characters:** Cells enclosed by mucilage. In the colony, separation of cells from each other by a colorless sheath.
- **Site detail and habitat:** Strain MK-14 was isolated from the sewage running water. Other taxa found in the sample were: *Phormidium*, *Nostoc*, *Pseudoanabaena* and *Chlorella*, *Scenedesmus*.
- **Culturing Conditions:** *Gloeocapsa* sp. MK-14 responded in BG₁₁ medium.

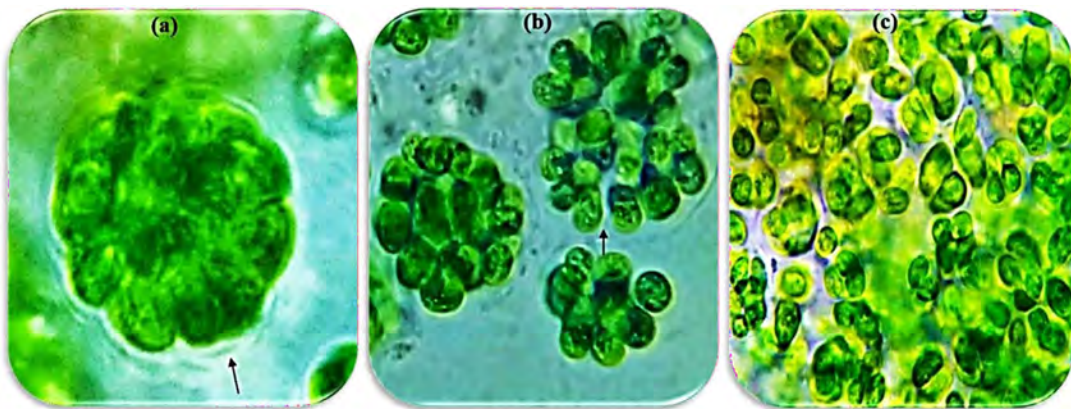


Figure 2.20: Micrographs of *Gloeocapsa* sp. MK1-4 under the light microscope: (a) Colony of cells enclosed by mucilage (arrow); (b) colorless mucilage around the cells of the colony (arrow); (c) dispersion of cells from the colonies.

Sequence Analysis: A total of 671 bp of 16S rRNA gene sequences were received for the MK-14. The similarity of obtained sequences assessed at NCBI showed 95.25% similarity with *Gloeocapsa* sp. Ryu1-8DN_B9 and 93.58% similarity with *Gloeotheca citriformis*. The phylogenetic trees constructed using the NJ, ML, and MP methods revealed similar topologies. The NJ tree constructed with the sequences of strain MK-14 and those downloaded from NCBI showed its close resemblance with *Gloeocapsa* sp. Ryu1- 8DN_B9 with a bootstrap support of 86 (Fig. 2.21).

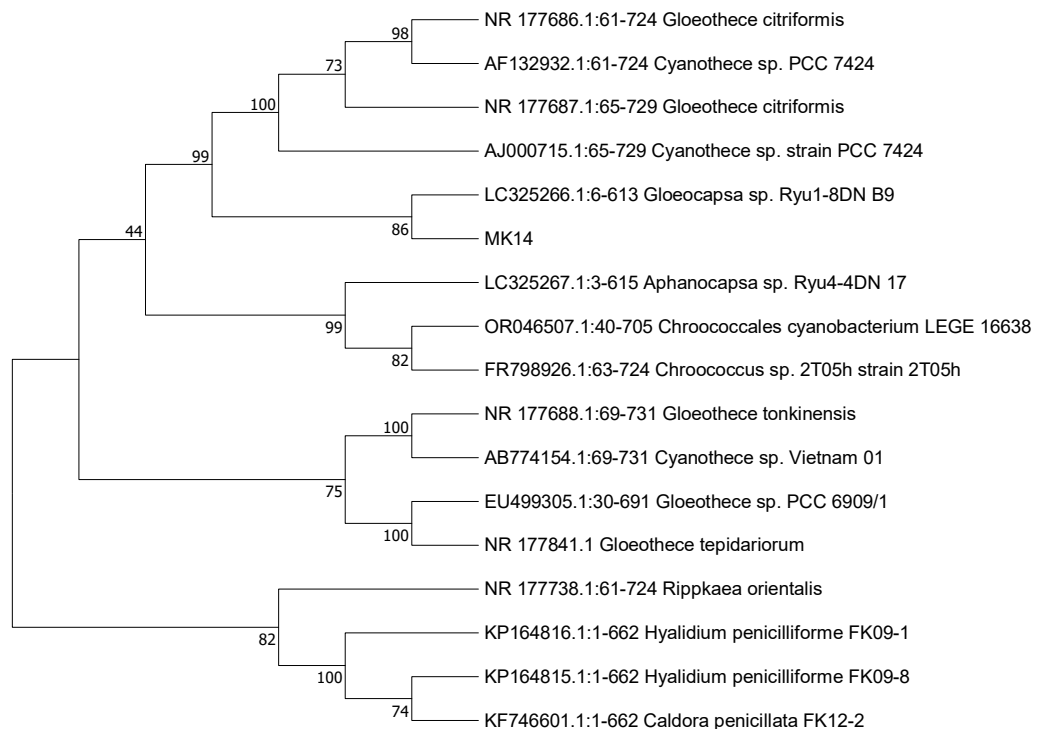


Figure 2.21: NJ analysis of 16S rRNA data of strain MK-14.

2.3.8.3. *Synechococcus elongatus* strain MK-15

- **Taxonomic Characters**

Cells solitary or in pairs but do not form distinct colonies and no mucilage envelope around the cells. Cells cylindrical to elongated shape (Fig 2.22a). Homogeneous cell content, light blue green in color (Fig 2.22b), 1.4 μm broad and 2.3-4.8 μm long in size. Gas vesicles not present in the cells. Cells divide by perpendicular binary fission. On BG₁₁ agar media cells colony grows in circular shape (Fig 2.22c).

- **Diagnostic characters:** Cylindrical to elongated shape cells.
- **Site detail and habitat:** Strain MK-15 was collected from sewage water of Islamabad.

Other taxa found in the sample were: *Phormidium* and *Chlorella*, *Scenedesmus*, *Cosmarium*,

- **Culturing Conditions:** *Synechococcus elongatus* MK-15 responded in BG₁₁ medium.

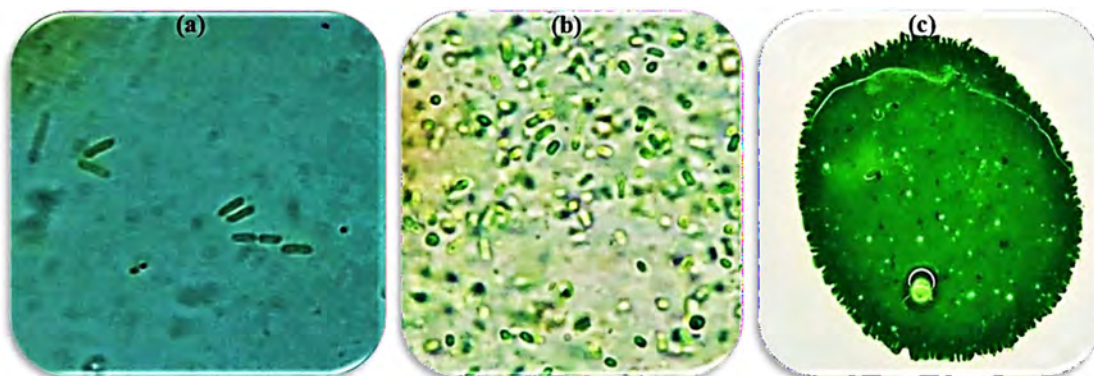


Figure 2.22: Micrographs of *Synechococcus elongatus* MK-15 under the light microscope: (a) elongated cells; (b) bluish-green color of the cells; (c) Growth on BG-11 agar media.

Sequence Analysis: In this study, 16S rRNA gene sequence of 638 bp were received for the strain MK-15. The sequence homology of MK-15 sequences assessed at NCBI with BLASTn analysis showed 97% query coverage with 94.49% identity to *Synechococcus elongatus* PCC 11801. A NJ tree constructed for the investigated strain MK-15 and the sequences downloaded from NCBI, exhibited close clustering of strain MK-15 with *Synechococcus elongatus* PCC 11801 with bootstrap value 42% (Fig. 2. 23).

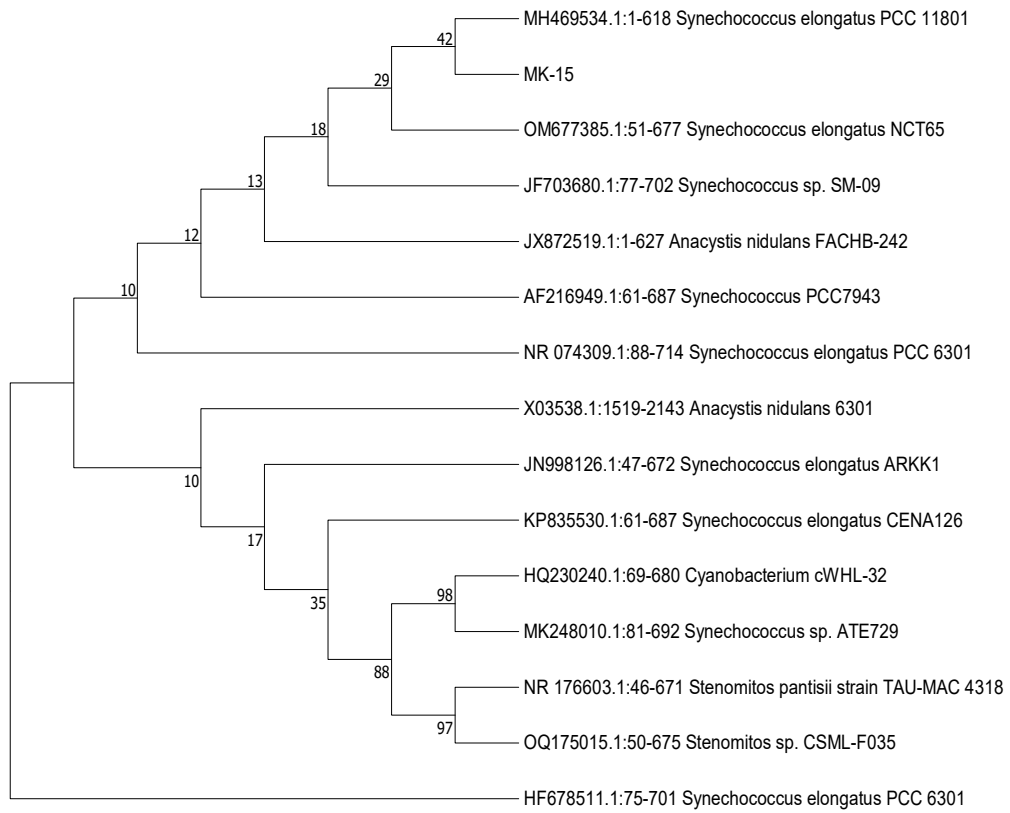


Figure 2.23: NJ analysis of 16S rRNA data of strain MK-15.

2.3.9. Screening of strains against Cd and Pb

Cyanobacteria strains isolated from the various environments were screened with different concentrations of Cd and Pb to check their maximum tolerance level against these toxic metals. Screening results showed that all the strains were able to grow at low concentrations of the Cd and Pb. *Nostco* sp. MK-11 showed the highest level of tolerance to Cd and Pb stress and *F. muscicola* MK-8 was the second best in tolerating the highest stress of Pb and Cd. **Table 2.4** shows the tolerance of different cyanobacteria strains against different initial concentrations of Pb and Cd. The biomass of selected tolerant strains was scaled up to 150ml, 250ml and 500ml. In the Table 2.4, symbols “+” and “-” show the tolerance and no tolerance, respectively to the Cd and Pb stress.

Table 2.4: Screening of strains exposed to different concentrations of Cd and Pb in aqueous solutions

Strains	MK-2	MK-3	MK-4	MK-7	MK-8	MK-9	MK-11	MK-13	MK-14	MK-15
Cd mg/L										
0.25	+	+	+	+	+	+	+	+	+	+
0.5	+	+	+	+	+	+	+	+	+	+
0.75		+	+	+	+	+	+	+	+	+
1	-	-	+	+	+	+	+	+	+	+
1.25	-	-	-	+	+	+	+	+	-	-
1.5	-	-	-	-	+	+	+	-	-	-
1.75	-	-	-	-	-	-	+	-	-	-
2	-	-	-	-	-	-	-	-	-	-
2.5	-	-	-	-	-	-	-	-	-	-
3	-	-	-	-	-	-	-	-	-	-
5	-	-	-	-	-	-	-	-	-	-
Pb mg/L										
0	+	+	+	+	+	+	+	+	+	+
5	+	+	+	+	+	+	+	+	+	+
15	+	+	+	+	+	+	+	+	+	+
20	-	-	+	+	+	+	+	+	+	+
25	-	-	+	+	+	+	+	+	+	-
30	-	-	-	-	+	-	+	+	-	-
35	-	-	-	-	-	-	+	-	-	-
45	-	-	-	-	-	-	+	-	-	-
60	-	-	-	-	-	-	-	-	-	-
90	-	-	-	-	-	-	-	-	-	-
120	-	-	-	-	-	-	-	-	-	-

2.3.10. Discussion

Consequent to eutrophication in wastewater, cyanobacteria and algae thrive quickly in wastewater. Yet in extreme cases cyanobacteria and other algal types produce blooms, sometimes referred to as HABs (Glibert, 2017), causing serious environmental problems. The ecological impacts due to the presence of different strains in wastewater are less known. To probe this, the current research was commissioned to investigate cyanobacterial diversity in the wastewater of Islamabad and Rawalpindi, Pakistan. Previously, there is only very little data offering little understanding into the biodiversity of cyanobacteria in wastewater eco-system and their advantages for instance in tackling the issue of heavy metals through phycoremediation. Here evidence showed high levels of cyanobacterial diversity and therefore offers good prospects of finding such strains as discussed in the following sections.

Many studies show that physicochemical constituents are important for the growth and abundance of Cyanobacteria, as this play a significant role in defining species composition (Kohler, 1994; Chellappa et al., 2003; Prasanna et al., 2012). In this study a detailed analysis of the physico-chemical analysis was conducted. The Biochemical Oxygen Demand (BOD) (Table 2.2) analysis indicated that wastewater at different sites contained primarily inorganic materials (Lee and Nikraz, 2014), which is likely due to an excess concentration of soluble salts (Ghaly et al., 2014). The calcium level in sewage water at site 1 was 6.86 mg/L and at site 2, 11.49 mg/L. It is well known that the concentration of calcium affects the population abundance of cyanobacteria (Sarojini, 1996). Furthermore, the concentrations of nitrates and sulphates at three different sample collection sites were significantly higher than the World Health Organization's (WHO) permitted discharge limits. Release of these nutrients into the environment usually results in eutrophication in natural water bodies, as they are important nutrients for photosynthetic organisms (Oyebamiji et al., 2019).

In the sewage and e-waste water sulphates, calcium, magnesium, potassium, nitrates, and sodium, electrolytes were abundant and readily absorbed by the cyanobacteria and algae (Olguín and Sánchez-Galván, 2012). Physicochemical constituents showed a correlation of algal diversity with physicochemical constituents. An earlier study showed that higher level of physico-chemicals supported the

diversity of phytoplankton in Kinjhar Lake, Pakistan (Nazneen, 1980).

At site 1 to be more specific, a total of 16 strains were found including 13 cyanobacteria, 2 green algae and 1 diatom. At this site cyanobacteria diversity was high which showed that nutrients at this site sufficiently favored the growth of cyanobacteria. Substantial presence of oxidizable organic matter, along with detectable levels of dissolved oxygen and significant concentrations of nitrates and phosphates in the effluents, has been identified as conducive to the proliferation of cyanobacteria. This assertion is supported by the findings of Venu et al. (1984), Venkateswarlu (1969a), Rai and Kumar (1977), Boominathan (2005), Vijayakumar et al. (2005) and Murugesan (2005).

Singh (1969) and Venkateswarlu (1976) indicated that elevated concentrations of chemical oxygen demand, phosphates, biochemical oxygen demand and nitrates are more conducive to the proliferation of cyanobacteria compared to other algal species. This assertion was corroborated by the research conducted by Vijayakumar et al. (2005), Boominathan (2005) and Jeganathan (2006), which examined effluents from the dairy, dye, and oil refinery industries, respectively. In the current investigation, all analyzed effluents exhibited significant levels of nitrates and phosphates, alongside heightened BOD values.

Another important factor which plays role in the cyanobacteria diversity is pH. At site 1 the pH of the water was 7.15 and at site 2 the pH of the water was 7.33. Range of the pH of water samples was very close to the pH used by Ripka et al. (1998) in BG-11 for culturing cyanobacteria in laboratory settings. This may explain the robust proliferation of cyanobacteria observed in the examined contaminated water locations.

The abundance or biomass of cyanobacteria may increase in ecosystems that are polluted and characterized by high nutrient concentrations. Research conducted by Kim et al. (2004) identified a positive relationship between the occurrence of cyanobacteria and pollution levels in reservoir water. This study highlighted several species, including *Anabaena*, *oscillarioides*, *Anabaena azollae*, *Chroococcus limneticus*, *Aphanothece microscopic*, *Chroococcus turgidus*, *Gloeocapsa*, *Chroococcus tenax*, *Phormidium* and *Lyngbya*. Rai et al. (2021), reported maximum numbers of heterocystus cyanobacteria; *Nostoc*, *Nodularia*, *Scytonema*, and *Aphanizomenon* than non-heteroscystous cyanobacteria in urban areas (one of the

causes of environmental pollution) and highlighted that urbanization reduced the abundance of non-heterocystous filamentous cyanobacteria and increased the diversity of heterocystous filamentous cyanobacteria.

Analysis of water samples showed that the concentrations of heavy metals were higher in the e-waste and sewage polluted water than the permissible limit set by The US Environmental Protection Agency (EPA) (Table 2.3). EPA has established the maximum contamination levels for arsenic (As), Cd, chromium (Cr), mercury (Hg) and Pb in water as: 0.015, 0.01, 0.1, 0.002 and 0.015 respectively (Leong and Chang, 2020). Cyanobacteria screening in response to Cd and Pb toxicity (Table 2.4) showed that heterocystous unbranched filamentous *Nostoc* sp. was the highest Cd and Pb tolerant cyanobacterium. Its higher level of tolerance could be due to the presence of heterocysts, mucilage and in addition to the possible presence of metal tolerant genes. Branched heterocystous filamentous cyanobacteria, *Fischerella muscicola* MK-8, *Westiellopsis prolifica* MK-9 were second in row to bear the Cd and Pb toxicity.

The unicellular cyanobacteria (*Synechocystis fuscopigmentosa* MK-13, *Gloeocapsa* sp. MK-14 and *Synechococcus elongatus* MK-15) were tolerant to Cd and Pb toxicity. Least tolerant were the filamentous non heterocystous cyanobacteria (*Desertifilum tharense* MK-2 and *Phormidium* sp. MK-3. *Nodosilinea nodulosa* MK-4 non-heterocystous filamentous strain showed tolerance close to unicellular cyanobacteria in response to Cd and Pb stress. It might be due to development of nodules which play role in nitrogen fixation and might also assist in Cd and Pb toxicity resistance.

Cyanobacteria strains collected from site 1 were more tolerant to Pb and Cd stress compared to the strains collected from site 2. This could be due to the higher number and concentration of heavy metals at site 1. As result, the study revealed that site 1 was more toxic than other sites (Table 2.3) which show that high toxic conditions have comparatively lower diversity of cyanobacteria. But most of the cyanobacteria strains collected from this e-waste site were found more tolerant as compared to the cyanobacteria strains collected from the sewage wastewater site (site 2).

Culturing of cyanobacteria and green algae was carried out using various *in vitro* culturing media. Different strains exhibited varied responses, for instance green

algae species, showed preference for BBM media, indicating adaptable growth tendencies within specific green algae species (Riani and Futeri, 2023). Certain cyanobacteria species displayed limited or no response to BBM but showed favorable growth in BG₁₁ and BG₀ media. Different cyanobacteria isolates exhibited diverse nutritional preferences, with some preferring SP media. The isolation of species from solid media for subsequent cultivation in liquid media is a crucial step in achieving axenic cultures (Skeffington et al., 2020). This meticulous isolation process provides a controlled environment for individual species to proliferate and allows further characterization and experimentation (Huang et al., 2021). Tailored culture conditions and nutritional requirements are important for cultivating pure cultures of green algae and cyanobacteria, as there can be subtle variations in growth preferences within and between species (Vu et al., 2018). Understanding these variations is crucial for comprehending the ecological significance and potential applications of these organisms (Finger et al., 2022). Maintenance of cyanobacterial axenic (pure) cultures was a difficult task which required more focused concentrations. One of the biggest problems in the fields of basic and applied microbiology is the production and preservation of axenic cultures of various microorganisms, including cyanobacteria (Alain and Querellou, 2009; Ashida et al., 2010; Ishii et al., 2013; Joint et al., 2010).

Traditionally, cyanobacteria taxa are classified based on ecological and morphological characters. However, the whole taxonomic system of cyanobacteria (species, genera, families, orders) has performed an extensive restructuring and revision in recent years with the advent of phylogenetic analyses based on molecular sequence data, and it is expected that there will be further changes in the future (Komárek, 2014). The polyphasic approach, mostly using morphological features and DNA sequences, has emerged as the most suitable method to characterize cyanobacteria taxa as well as a resolution to the cyanobacteria taxonomic problem (Comte et al., 2007; Sciuto et al., 2011). Elucidating evolutionary processes in cyanobacteria taxonomy based on the molecular phylogenetic research has led to description of more genera since 2000 (Komárek et al., 2014), especially in the non-heterocystous filamentous cyanobacterial group. The use of two distinct nomenclatural codes, namely the Botanical and Bacteriological codes, has led to substantial confusion, and molecular phylogenetics is actively assisting in resolving this issue (Lee, 2016). Furthermore, two major challenges arise: firstly, the identification of

numerous strains stored in international culture collections rely solely on morphological characteristics. Secondly, many nucleotide sequences present in public database, originate from environmental DNA extracted from cyanobacteria that have not been observed under a microscope (Rajaniemi et al., 2005; Wilmotte and Herdman, 2001). Therefore, in this research project, a comprehensive approach combining cyanobacteria strains cultivation, light microscopy, and 16S rRNA gene sequencing was used to ensure the precise identification.

Oscillatoriales include filamentous, photosynthetic cyanobacteria characterized by their unbranched trichomes or filaments (Gomont, 1892). They are commonly found in diverse habitats such as freshwater, marine environments, and even terrestrial habitats like damp soil and rocks. The cells in the filaments often show a gliding movement, which gives these cyanobacteria their name "Oscillatoriales," derived from their oscillatory motion (Hamouda and El-Naggar 2021). Trichomes are devoid of true branching and lack specialized cells such as heterocysts and akinetes (Geitler and Rabenhorst, 1932; Gomont, 1892). Morphologically, Oscillatoriales species exhibit notable variations in their filamentous forms, ranging from uniseriate (single row of cells) to multiseriate (multiple rows of cells) arrangements (John et al., 2002). Their trichomes can be either straight or spiral-shaped, with cells typically containing prominent granules of cyanophycin or glycogen as reserve materials. Furthermore, some Oscillatoriales species form colonies held together by mucilaginous sheaths secreted by the cells, aiding in adhesion to substrates. This morphological diversity within Oscillatoriales underscores their adaptability to various habitats, contributing significantly to primary production and ecological functions in aquatic and terrestrial ecosystems (Komárek 2005; Whitton and Potts, 2012).

Desertifilum, a new Oscillatoriales genus, was recently established based on isolates from the Thar Desert in western India (Dadheech et al., 2012). *Desertifilum tharense*, the type species, was found in black and dark-blue biological crusts on dry and moist sand dunes with only 25 cm of annual precipitation. Trichomes are isodiametric, with a colourless sheath. Despite its benthic habitat, this species has gas vesicles. Another *Desertifilum* species, *Desertifilum fontinale* was later described from a warm spring of East Africa. The habitat, morphology and molecular characteristics of the latter species differ from those of *D. tharense*. As a result, the *Desertifilum* genus now has more diversity in morphology, physiology, and

ecological habitats (Dadheech et al., 2014). In the current study, *Desertifilum tharense* MK-2 was isolated from the sewage water and showed the morphological characteristics which were consistent with *D. tharense* (Dadheech et al., 2012). There were differences between the natural habitat of the *D. tharense* MK-2 and *Desertifilum* strains described in the literature. Phylogenetically, *D. tharense* MK-2 strain was also associated with the *D. tharense* clade. The Investigated strain also showed similarities with *Desertifilum dzianense* (PMC 872.14) collected from the Stromatolites, Mayotte (Cellamare et al., 2018). But the difference between these was existence of aerotypes which were present in the *D. tharense* MK-2 strain and absent in the *Desertifilum dzianense* collected from the desert. Morphological characters of strain MK-2 also matched with *Desertifilum salkalinema* but there were some differences. Cell width of MK-2 strain was 2.4-3.5 μm and filaments were straight, slightly wavy, solitary or entangled while cell width of *Desertifilum salkalinema* was 2.08 and filaments were elongated, straight, slightly wavy and entangled (Cai et al., 2017). The genus *Phormidium* has been characterized in botanical literature based on morphological traits such as thin, transparent sheaths that are partially diffused or completely dissolved. These characteristics cause the filaments to adhere together in layered mats. This genus included numerous species found in both freshwater and marine environments, exhibiting variations in cell sizes, proportions, apical cells, and degrees of constrictions at cross-walls (Palinska et al., 2011). Morphological features like entangled filaments, colorless sheath around the filaments and necridia development of *Phormidium* sp. MK-3 showed close resemblance with the *Phormidium* sp. SENA270 (Shishido et al., 2013). Phylogenetically it also made clustering with the *Phormidium* sp. SENA270 as described above.

Species of *Nodosilinea* usually have filaments with a single trichome, however they can occasionally have several serrations. Trichomes show constriction at the cross-walls and are immotile. Furthermore, their sheaths are often thin, delicate, and colorless. With peripheral thylakoids, the cells appear to be roughly isodiametric or longer than wide. Several species can fix nitrogen (Casamatta, 2011). When the genus is morphologically identical to *Leptolyngbya*, the nodules are usually not visible and there are only a few individual trichomes detected in the wild. As a result, it is likely that this genus will only be identified upon the availability of strain sequence data (Vazquez-Martinez et al., 2018). Morphological characters of the investigated *Nodosilinea nodulosa* MK-4 like nodules formation and spiral arrangements of the

filaments showed strong resemblance with the *Nodosilinea nodulosa* strain (Strunecky et al., 2020). In contrast the literature show that *N. nodulosa* was isolated from marine plankton in the South China Sea (Li and Brand 2007), while the strain *Nodosilinea nodulosa* MK-4 was collected from the e-waste polluted water of Islamabad, Pakistan which show the difference of their local environments. Development of nodules helps these cyanobacteria species in nitrogen fixation. This feature in cyanobacteria strongly suggests their utility as biofertilizers.

Nostocales encompasses filamentous cyanobacteria that possess the capability to undergo cellular differentiation into akinetes or hormogonia (reproductive trichomes), which are suitable for perennation and possess nitrogen-fixing heterocysts (Mandhata et al., 2023). In accordance with classical taxonomic classification, the genus *Anabaena* is characterized by a substantial gelatinous sheath, the genus *Nostoc* is defined by filaments composed of moniliform cells devoid of a sheath, and *Aphanizomenon* is categorized within the Nostocaceae family (Komárek and Anagnostidis, 1989; Rippka et al., 1979). Their trichomes are helically (spirally) formed, straight, or curved, and feature noticeable cross-wall constrictions. In most species, the widths of the flat, cylindrical, elliptical, or spherical cells vary from 2 to 10 μm , but in some, they can reach 20 μm (Desikachary, 1959). With the exception of certain terminal conical heterocysts observed in specific taxa, both intercalary and terminal heterocysts generally exhibit a spherical to cylindrical morphology with rounded ends. The position of akinetes varies depending on the species, however they are usually found within trichomes. Individual akinetes lack a sheath but have a common mucilaginous layer covering them.

It is notable that the genus *Desikacharya* is another recently described genus that shows the typical *Nostoc*-like morphology. Hence, the members of this genus with typical *Nostoc*-like morphology were differentiated using phylogenetic tools. *Desikacharya constricta* SA10 is distinguished by the presence of constricted cells along with having spherical/globose heterocytes at both the terminal and intercalary positions (Kabirnatay et al., 2020). The filaments appear long with a slight tendency for coiling. Light-colored mucilaginous sheath surrounds all the amorphous colonies but is not truly mat in the natural conditions; light mucilaginous sheath is also present across the trichomes even at the ends. Vegetative cells barrel-shaped to cylindrical vegetative cells are curved at the ends. Hormogonia formation was also observed with the trichome having around nine vegetative cells and no heterocytes. Akinetes large;

solitary; prominently intercalary; barrel shaped with length greater than width (Kabirataj et al., 2020, Saraf et al., 2019). *Desikacharya* MK-7 investigated in this study showed close resemblances both morphologically and phylogenetically to the genus *Desikacharya*. Despite the fact the difference in color might be due to culturing conditions. Morphological characters of the *Desikacharya* MK-7 strain were very similar to *Desikacharya* sp. NS2000 (Ngo et al, 2022) and phylogenetic analysis also strongly supported the resemblance of *Desikacharya* MK-7 and *Desikacharya* NS2000. Thus, the strain MK-7 was identified as *Desikacharya* sp. MK-7

Branched cyanobacteria strain *Fisherella muscicola* MK-8 was isolated from the sewage water and its morphological characters closely matched with *Fisherella muscicola* (Thuret) Gom and *Fisherella muscicola* NDUPC001 (Mishra et al., 2019). *F. muscicola* MK-8 also showed some characters like the *Neowestiellopsis bilateralis* SA16 which has bilateral branches, but the main difference was biseraite condition which was observed in *F. muscicola* MK-8 strain and no such condition was reported in the *Neowestiellopsis bilateralis* SA16 (Kabirataj et al., 2020). Phylogenetically, MK-8 strain was also closer to the *Fisherella muscicola* with 77 % bootstrap value. Another branched cyanobacterium *Westiellopsis prolifica* MK-9 was isolated from the sewage water and its morphological character matched with the *Westiellopsis prolifica* as described in the literature. The most important characteristics of the *Westiellopsis* strains is the presence of pseudo-hamocyte which is important taxonomic character of these branched cyanobacteria and help in identification and reproduction (Saber et al., 2017; Abed et., 2013). The phylogenetic analysis also showed the close relationship of *W. prolifica* MK-9 strains to the *Westiellopsis prolifica* and the morphology also supported identification of strain MK-9 and the strain identification was confirmed as *Westiellopsis prolifica* MK-9.

Species of the genus *Nostoc* show un-branched trichomes, barrel-shaped cells with rounded or sub- spherical heterocyst (Desikachary, 1959). *Nostoc* sp. MK-11 was identified under LM as a species of the genus *Nostoc* Vaucher ex Bornet and Flahault 1886. Morphologically the investigated strain showed strong morphological and phylogenetic resemblances with *Nostoc* strain NapMSIm13 (Bravakos et al., 2016). Molecular phylogeny placed strain *Nostoc* sp. MK-11 in a clade in close proximity to *Nostoc* NapMSIm13. *Nostoc* sp. MK-11 also showed some similar characteristics to *Nostoc calcicola* Brebisson BDU 40302 and *Nostoc calcicola*

Brebisson BDU 180601 in having similar type of heterocysts specifically at the tips of the filaments (Thangaraj et al., 2017).

Order Chroococcales, and the Chroococcaceae family, are distinguished by the unicellular or non-differentiated colonial cyanobacteria. These organisms possess cells that are usually spherical or ovoid in shape, occasionally forming clusters or colonies embedded within a mucilaginous sheath. Unlike some other cyanobacteria orders that form filaments or chains of cells, Chroococcales species lack this filamentous structure, consisting of individual cells or aggregates. The absence of specialized motility organelles such as flagella or gas vesicles further characterizes these organisms (Rippka et al., 1979). Instead, their dispersal often relies on passive means like water currents or attachment to surfaces via their gelatinous coatings. This order's morphological homogeneity and the absence of complex cellular differentiation pose taxonomic challenges, emphasizing the significance of genetic analysis and biochemical traits in identifying and classifying Chroococcales species within the cyanobacterial phylum (Whitton and Potts, 2012).

The cyanobacteria *Synechocystis fucospigmentosa* MK-13, *Gloeocapsa* sp. MK-14 and *Synechococcus elongatus* MK-15 belonging to Chroococcales were isolated, purified and identified on morphological and molecular basis. *Synechocystis* 6803 is a model strain of the genus *Synechocystis* which has the diameter of range 1.67-2.46 μm (Zavřel et al., 2017). Genus, *Geminocystis* is characterized by spherical cells like cells of *Synechocystis* but with slightly larger dimensions ($\sim 3.5 \mu\text{m}$ to $\sim 6.2 \mu\text{m}$) (Korelusova et al., 2009). *Synechocystis fucospigmentosa* MK-13 cells dimensions were larger than then the *Synechocystis* 6803 and close to *Synechocystis fucospigmentosa* (KovAcIK 1988) and also in close clade in phylogenetic tree. Phylogenetically strain *Synechocystis fucospigmentosa* MK-13 was in close proximity with *Synechocystis* sp. CR_L29 and low clustering (18 % bootstrap value) with *Synechocystis fucospigmentosa*. Although the bootstrap values of *Synechocystis fucospigmentosa* MK-13 was low but its due to strong morphological characters its identification was confirmed with morphology observations. Therefore, morphology plays important role alongside genetics for accurate identifications of the cyanobacteria. Therefore, strain MK-13 Identification was confirmed by morphology, molecular sequence data and phylogenetic position. *Gloeocapsa* in the order Chroococcales, show the physical appearance that cells are either single or cluster of cells enclosed in concentric layers of mucilage. Strain,

Gloeocapsa MK-14 showed the close characteristics with the genus *Gloeocapsa*. Phylogenetically the strain showed close proximity in the same clad with *Gloeocapsa* sp. Ryu1-8DN_B9 with 86 % bootstrap value. *Synechococcus elongatus* MK-15 was isolated from the sewage water lake Islamabad. *Synechococcus elongatus* is a Gram-negative, photosynthetic microorganism that is commonly found in freshwater and marine environments. It is a model organism for studying photosynthesis, nitrogen fixation, and cell cycle regulation. Remarkably elongated, these cells measure 5 μm in width and 34 μm in length, making them approximately 6 to 7 times longer than their width (Bhakta et al., 2016).

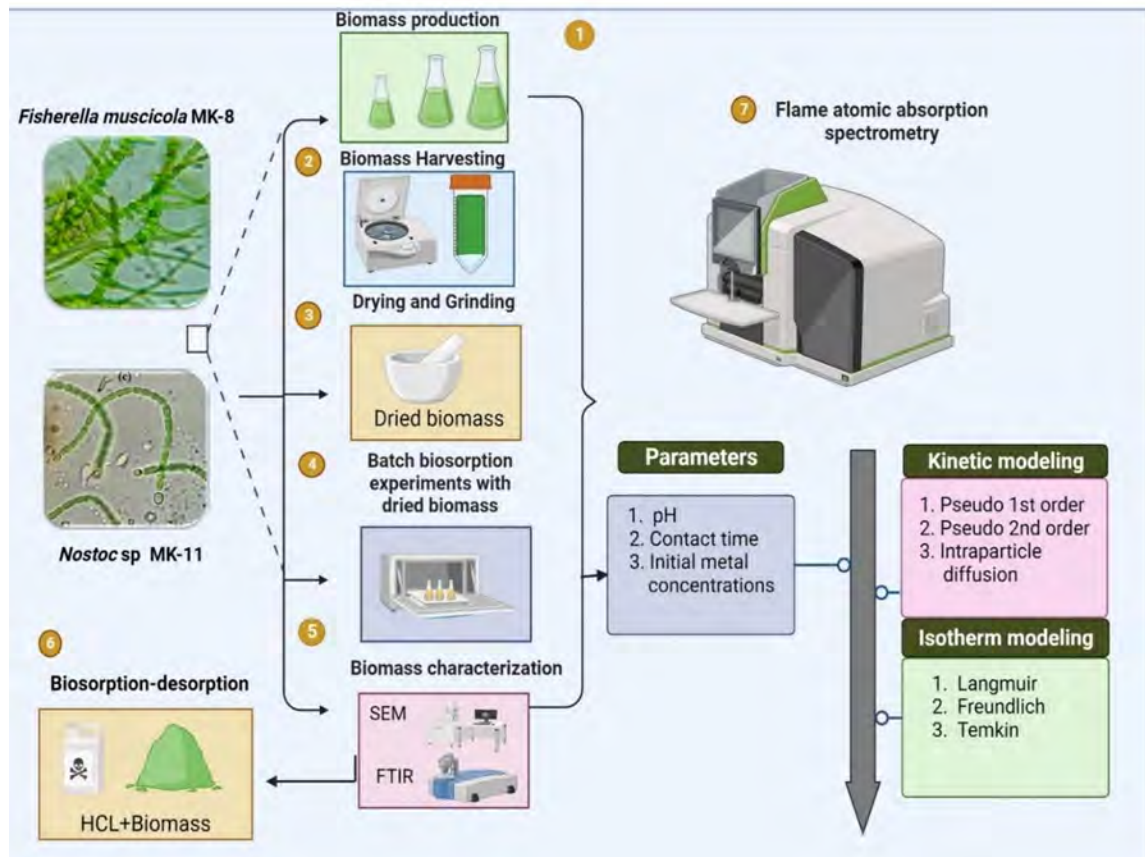
Conclusions

- Sewage and e-wastewater/sites in Islamabad and Rawalpindi have elevated concentration of heavy metals, especially Pb and Cd.
- These sewage water sites are a rich source of cyanobacteria. Six species for instance: *Desertifilum tharense* MK-2, *Nodosilinea nodulosa* MK-4, *Fischerella muscicola* MK-8, *Westiellopsis prolifica* MK-9, *Desikacharya* sp. MK-7, *Synechocystis fuscopigmentosa* MK-13 have been recorded for the first time from Pakistan.
- Maintenance of cyanobacteria as axenic cultures is challenging and requires a careful and focused approach.
- Several species showed tolerance to Cd and Pb. Among these, *Nostoc* sp. MK-11 was the most tolerant species followed by *F. muscicola* MK-8.

CHAPTER 3

Cd and Pb Biosorption capacity in dried biomass of *Fischerella muscicola* and *Nostoc* sp.: Kinetics and Isotherm modeling

Graphical Abstract



Graphical Abstract: Graphical depiction of Pb and Cd biosorption by dried biomass of *Fischerella muscicola* and *Nostoc sp.*

Summary

In the current study two cyanobacteria strains, *Fischerella muscicola* and *Nostoc* sp. isolated from wastewater have been investigated as dried biosorbents to remove Pb and Cd from the aqueous solutions. Biosorption properties of cyanobacterial biomass were studied as a function of pH, time and initial metal concentrations. Initially metal biosorption rate was high which gradually decreased with time. Three distinct kinetic models (Pseudo first order, Pseudo second order, and intraparticle diffusion) along with three isotherm models (Langmuir, Freundlich, and Temkin) were employed on the experimental data to study the mechanism and rate of biosorption. The analysis of the experimental modeling indicated that the Pseudo second-order kinetic model and the Langmuir isotherm model exhibited a strong correlation with the experimental data, thereby illustrating the phenomena of chemisorption and uniform interaction. Based on the modeling of the Langmuir isotherm, the maximum biosorption capacity (q_{\max}) of *F. muscicola* dried biomass was determined to be 70.274 and 63.572 mg/g for Pb and Cd, respectively. In a similar fashion, the Langmuir isotherm assessed the q_{\max} of *Nostoc* sp. dried biomass as 83.963 and 75.757 mg/g for Pb and Cd, respectively. Results of biosorption showed that the dried biomass of *Nostoc* sp. holds higher potential in removing Cd and Pb compared to the *F. muscicola* biomass. FTIR analyses revealed carboxyl, hydroxyl, amine and sulfoxide functional groups in the dried biomass of *F. muscicola* which may have made complexation with metals during the process of biosorption. Similarly, in the dried biomass of *Nostoc* sp., hydroxyl, amines, sulfoxide, and carbonyl functional groups were detected. SEM results showed changes in the surface appearance of the biomass after the metals biosorption which indicated binding of Cd and Pb on the surface of biomass. Metals desorption from the dried biomass of both the cyanobacteria using Hydrochloric acid (0.1 M) was stretched up to 90%. After three cycles of biosorption-desorption, the ability of the dried biomass from the cyanobacterial strains to biosorb significantly high which showed their potential of reusability.

3.1. Introduction

Water contamination is one of the main global issues of the twenty-first century. The issue must be addressed to improve water quality and reduce negative effects on both human and ecological health. Several water contaminants are produced because of industrialization, climate change, and the growth of urban areas (Zamora-Ledezma et al., 2021). Discharge of heavy metals-containing effluents may have an impact on all natural resources as well as living things in the receipt water (Igwe and Abia, 2006; Kadirvelu et al., 2001). Due to its prevalence, low degradability, and ease of bioaccumulation, heavy metals pollution in the environment has drawn attention on a global scale (Cui et al., 2021; Jupp et al., 2017). Despite low concentrations, heavy metals and associated products are highly poisonous, mutagenic, carcinogenic and pose major health hazards (Mezynska and Brzóska, 2018; Ayangbenro and Babalola, 2017). The United States Environmental Protection Agency has set forth maximum allowable levels of contamination for arsenic (As), Cd, mercury (Hg), chromium (Cr) and Pb in water as: 0.015, 0.01, 0.1, 0.002 and 0.015, respectively (Leong and Chang, 2020).

Cd and Pb are considered the most hazardous and toxic to the environment (Sari and Tuzen, 2008). Their contamination is alarming environmental problem that has harmful impact on aquatic eco-systems and health of humans (Liu et al., 2022). Pb is used extensively in paints, pigments, batteries, cables, steel and alloys, metal, plastic industries and glass (Selatnia et al., 2004). Pb is thought to be dangerous at high concentrations and is regarded as a cumulative toxin. Its toxicity can harm liver, kidneys, immunological system, circularity system and gastrointestinal tract (Ghaedi et al., 2018; Yu et al., 2020). While Cd comes primarily from the battery, paint, pigment, fertilizers and refinery industries. Humans exposed to Cd develop renal and cancer problems (Padmaja et al., 2018). Exposure to Cd may have also teratogenic consequences, hepatic injury, hypertension, renal failure, and lungs damage (Hajjaligol et al., 2006).

Conventional chemical and physical methods to remove heavy metals are often expensive and insufficiently successful, and they also generate a lot of harmful sludge (Cheng et al., 2019, Sun et al., 2018). In the previous decades, the hunt for affordable technologies for the eco-management of wastewaters containing metals has attracted a lot of attention (Dhir, 2014; Dixit et al.,

2015). To make the process of treatment environment friendly and economic, bioremediation via microalgae, bacteria, fungi and yeasts has developed into a successful method, particularly for heavy metals at low concentrations (Leong and Chang, 2020; Cheng et al., 2019). Since last few years, the utilization of advanced biosorption technology by non-living and/or alive biosorbents for the heavy metals bioremediation and recapture has been well-thought-out (Leong and Chang, 2020). Algae are inherently abundant, require few nutrients, and are autotrophic. These organisms are superior to other biosorbents because they cause less harm to the environment and create a large amount of biomass (Das et al., 2008).

Cyanobacteria are the only prokaryotic organisms capable of carrying out oxygenic photosynthesis (Das et al., 2018) and several of them can fix atmospheric nitrogen (N_2) (Heimann and Cires, 2015). This strength enables them to thrive in diverse harsh environments, making them a promising candidate for addressing environmental issues such as wastewater treatment, soil remediation, and environmental pollutants degradation (Singh et al., 2016). Remarkably, owing to their strong attraction and abundant heavy metal binding sites cyanobacteria are anticipated to be highly efficient in the heavy metals bioremediation. An explanatory example of this is the utilization of EPS-producing cyanobacteria as chelating agents to remove Cr, Pb and Cd from the aqueous solutions (Jiang et al., 2016; Shane et al., 2018). Blue-green algae including *Arthrospira platensis*, *Dunaliella*, *Anabaena*, *Nostoc* and *Synechococcus*, are typical demonstrations of biosorbents with the potential to remove heavy metals from the wastewater (Al-Homaidan et al., 2015; Donmez and Aksu, 2002; Zinicovscaia et al., 2018). Cyanobacteria possess distinct advantages compared to other microbes, such as their expanded surface area, increase volume of mucilage with robust binding capabilities and simple nutrients requirements (Roy et al., 1993). These organisms are simple to grow in high quantities in lab cultures, offer cheap biomass for the biosorption process (Abdel-Aty et al., 2013). However, only a few experiments have been carried out employing cyanobacterial non-living material. Current study reports for the first-time the biosorption of Pb and Cd ions from the aqueous solutions using dried biomass of newly isolated cyanobacteria, *Fischerella muscicola* and *Nostoc* sp.

The current study aimed at: investigating the prospects of using dried biomass of newly identified cyanobacteria (*F. muscicola* and *Nostoc* sp.) as biosorbents to

remove Cd and Pb from the wastewater; analyzing the impact of pH, initial metal concentrations and the contact time on the biosorption of metals; investigating the kinetic and isotherm behaviour of the biosorption process; and assessing the desorption and reusability potential of the investigated dried biomass.

3.2. Materials and Methods

3.2.1. Chemicals

Lead nitrate ($\text{Pb}(\text{NO}_3)_2$) and Cd chloride (CdCl_2) were used to synthesize metal solutions for the biosorption experiments. HCL and NaOH were used to adjust the pH of the media and other solutions.

3.2.2. Culturing

Cyanobacteria, *F. muscicola* and *Nostoc* sp. were isolated and purified from the efflux of wastewater in Rawalpindi and Islamabad, Pakistan. BG₁₁ media (Rippka et al., 1979) was used for culturing of cyanobacteria. Cultures and BG₁₁ media were inoculated in the Erlenmeyer flasks and were maintained at a temperature of 25 ± 2 °C under white LED lights.

3.2.3. Biomass production and harvesting

For the production of biomass, the cultures were grown in multiple Erlenmeyer flasks of varying sizes: 250 ml, 500 and 1000 ml with corresponding volumes of BG₁₁ media set at 200, and 350 ml, 750 ml, respectively. All the flasks carrying cultures were kept in a growth chamber at 25 ± 2 °C under continuous white LED lights. At optimum growth, cultures were harvested by centrifugation at 4000 rpm for 15 min. Upon harvesting, the biomass was washed three times with double distilled to remove the adsorbed media ingredients from the surface and pellet of biomass was left air dried. To achieve an amorphous state, dried biomass was finely ground and passed through 100 μm mesh.

3.2.4. Batch biosorption experiments

Biosorption studies were performed using dried biomass of *F. muscicola* and *Nostoc* sp. as biosorbents and Pb and Cd ions as adsorbates. One gramme of the biosorbent was dissolved in 100 milliliters (ml) of an aqueous solution containing metal ions at a concentration of 100 milligrams (mg) per liter in a 250 ml conical flask. In the current study, effect of different factors such as pH (ranging from 2-8), initial metal ions concentration (20- 120 mg/L) and contact time (5-120 minutes) on

the biosorption of metal ions onto the biosorbents were studied. Mixture of metal ions and biosorbents were stirred at 150 rpm using an orbital shaker for a predetermined period at 25 °C. Whatman-40 filter paper was used to filter the solution and Initial and final metal concentrations in the filtrate were determined using Agilent Flame Atomic Adsorption Spectrometer (FAAS). Biosorption capacity (mg/g) of dried biomass was calculated using equation 1.

$$q_e = \frac{(C_i - C_e)}{W} \times V \quad (1)$$

In equation 1, q_e is biosorption capacity of biomass (mg/g), C_e indicates the equilibrium metal concentrations, expressed in mg/l, C_i denote the the initial concentration of metal ions in the solution (mg/l), W stands for the biomass weight in g and V stands for the solution volume in L.

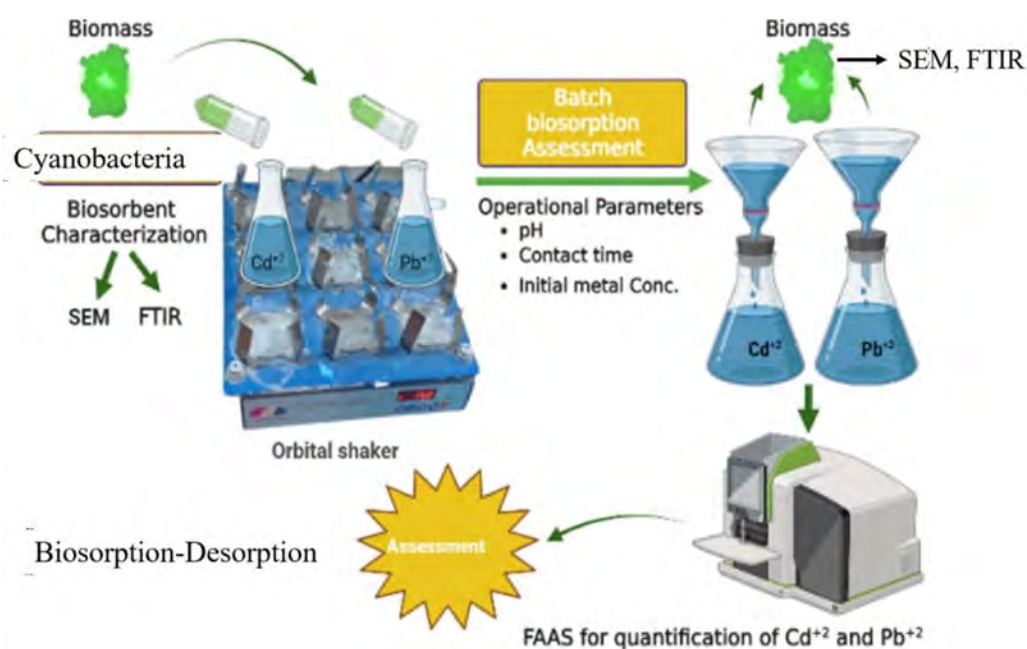


Figure 3.1: Diagrammatic depiction of batch-mode investigations designed to explore the biosorption of metal ions utilizing the dried biomass of *F. muscicola* and *Nostoc* sp.

3.2.5. Biosorbent characterization

Employing scanning electron microscopy (SEM) (JSM5910 model JEOL, Tokyo, Japan), alongside Fourier transform infrared spectroscopy (FTIR) (PerkinElmer Spectrum 65), cyanobacteria biomass was characterized before and after the biosorption process. FTIR technique was used to characterize the surface functional groups of biomass and to investigate its chemical properties related to the capacity for binding metallic ions (Raize et al., 2004). SEM was used to observe the morphology of both untreated and metal-treated biomass.

3.2.6. Desorption and reusability

For the desorption and reusability studies, Cd and Pb loaded dried biomass were dissolved in 0.1 M hydrochloric acid (HCL) solution for 1 hour at 100 rpm. Metals-loaded biomass was rinsed three times with distilled water before to the desorption investigation to eliminate any loosely attached Cd and Pb ions from the surface of the biosorbents. Following the desorption investigation, supernatant was collected for further analysis and biomass was carefully washed with distilled water after each cycle to neutralize and re-condition them with saline solution for further biosorption and desorption studies (Tüzün et al., 2005b). Initial and final metal concentrations in the solution were determined using Flame Atomic Adsorption Spectrometer. Desorption of metals was determined on the basis of amount of metals biosorbed by the biomass and concentrations of metals in desorption media. The efficiency of desorption (ED) was evaluated using Equation (2), as described below:

$$ED = \frac{q_D}{q_B} \times 100 \quad (2)$$

In Equation 2, the term q_D (mg/g) and q_B (mg/g) shows the desorbed metal ions quantity from the biomass and the quantity of biosorbed metal ions by the biomass, respectively.

3.2.7. Data analysis

Each experiment was performed in triplicates and the results were presented as the mean of three values. The data shown in (Fig. 3.4; 3.5; Fig. 3.6; Fig. 3.7; Fig. 3.8; Fig. 3.9; 3.10 and Table 3.1; Table 3.2; Table 3.3) describe the average values plus or minus the standard deviations (SD) calculated from all the repeated

measurements. The statistical analysis of the data was achieved utilizing OriginPro 8.5 (OriginLab Corporation, Northampton, Massachusetts, USA) and Microsoft Office Excel (2010) software.

3.3. Results and Discussion

3.3.1. Characterization of biomass

3.3.1.1. Fourir transform infrared spectroscopy

Figure. 3.2a and 3.2b describes the FTIR spectra of the *F. muscicola* and *Nostoc sp.* native biomass as well as those treated with Cd and Pb. Various main peaks at 1016, 1533, 1689, 2150, 2364, 2868, 2987, 3560 cm^{-1} were observed in the FTIR spectra of non-treated *F. muscicola* biomass. Similarly, in the biomass of *Nostoc sp.*, main peaks at 1068, 1346, 1652, 2096, 2434, 2978, 3525 cm^{-1} were detected. When dry biomass of *F. muscicola* and *Nostoc sp.* were loaded with metals, shifting of peaks occurred. The alteration of peak positions following the biosorption of metals can be attributed to the development of bond between the metals and the biomass's functional groups.

The dry biomass of *F. muscicola* exhibited a peak at 3560 cm^{-1} , which was associated with the stretching of the hydroxyl group (OH). Additionally, the peaks observed in the range of 2800 to 3000 cm^{-1} were attributed to the stretching of C-H; peak at 1533 cm^{-1} associated with nitroso group, stretching; 1016 S=O (sulfoxide) strong to stretching. The peak at 2150 cm^{-1} corresponds to S-C \equiv N (thiocyanate); peak at 1689 is associated to C=O (Carboxyl, stretching) as shown in Fig. 3.2a.

Amine (N-H) and hydroxyl (O-H) functional groups present in the biomass of *Nostoc sp.* were associated with the prominent peak observed in the FTIR spectra at 3525 cm^{-1} . Additionally, the peak located between 2800 and 3000 cm^{-1} , corresponding to the asymmetric and symmetric stretching vibrations of aliphatic chains (C-H), indicated the stretching distribution of CH₂ and CH₃ groups. Peak at 2096 cm^{-1} is indicative of an alkyne with C–C stretching. Asymmetric vibration of the C=O functional group was observed in the peak at 1652 cm^{-1} . The peak at 1346 cm^{-1} corresponds to S=O sulfoxide stretching, whereas the Peak at 1068 cm^{-1} relates to S=O (Fig. 3.2b).

Peak shifting was observed subsequent to the biosorption of Cd and Pb. The alteration of spectral peaks is associated with functional groups like carbonyl, sulfoxide, hydroxyl, and amines, thereby affirming the removal of Pb and Cd ions from the aqueous medium. This observation implies the occurrence of interactions between the functional groups of biomass and metal ions. In previous studies it was described that the metal biosorption by the dried biomass of the cyanobacteria

happens due to different physicochemical interactions that involve cationic exchange, chemical chelation, and ionic bonds (Bon et al., 2021). Literature indicates that functional groups such as hydroxyl, carboxyl, sulfoxide and amines predominantly play a role in the process of metal biosorption (El-Sheekh et al., 2019a; Satya et al., 2020). FTIR analysis indicates that the dry biomass of *F. muscicola* and *Nostoc* sp. could be beneficial for the biosorption of Pb and Cd ions. Similar outcomes were explained in earlier research (Goher et al., 2016; Kumar et al., 2018a; Sheng et al., 2004).

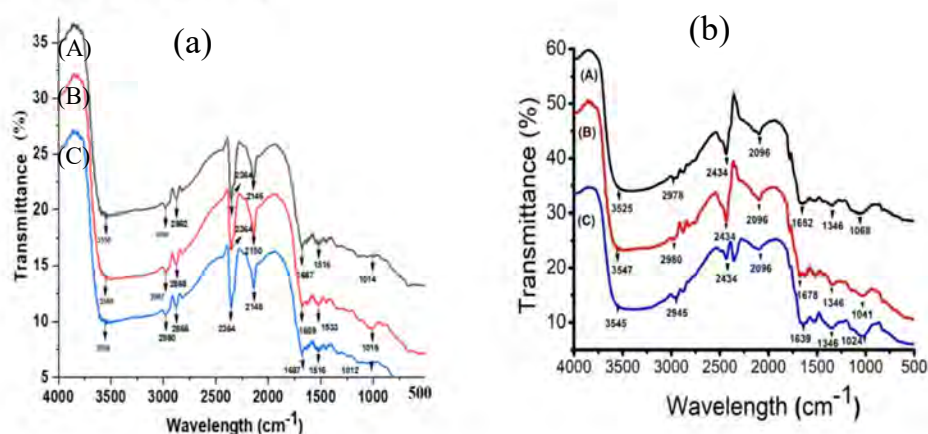


Fig. 3.2: (a) FTIR spectra of untreated, as well as Cd and Pb-treated dried biomass of *F. muscicola*; (b) FTIR spectra of untreated, Cd and Pb-treated dried biomass of *Nostoc* sp.

3.3.1.2. Scanning electron microscopy (SEM)

Appearance of non-treated and Pb and Cd treated dried of *F. muscicola* and *Nostoc* sp. was investigated using SEM (Fig. 3.3Aa, Fig. 3.3Ab, Fig. 3Ac, Fig.3Ba, Fig. 3Bb, Fig. 3Bc). The dried biosorbents surface looked dull prior to the biosorption of metals, whereas the biosorbents were seen bright, rough, and sharp ended after the biosorption of metals. Surface of the dry biomass loaded with Pb (Fig. 3.3Ac and Fig. 3.3Bc) was brighter compared to Cd loaded (Fig. 3.3Ab and Fig. 3Ba). This was due to the more Pb ions biosorption as compared to Cd ions. Surface precipitation of metals alters the surface morphology of the biosorbent. The shape of cells suggests that the metals lowered the surface porosity of the cyanobacterial biomass. This might be explained by the cross-linkage between the metals and functional groups of the biomass (Arief et al., 2008). Changes in morphology showed the metals precipitation due to biosorption. Previously, it has been reported that the surface morphology of the

Parachlorella sp. biomass changed during the removal of the Cd (Dirbaz and Roosta, 2018). Similar phenomenon was also observed in case of silica monolith synthetic particles (Alam et al., 2021).

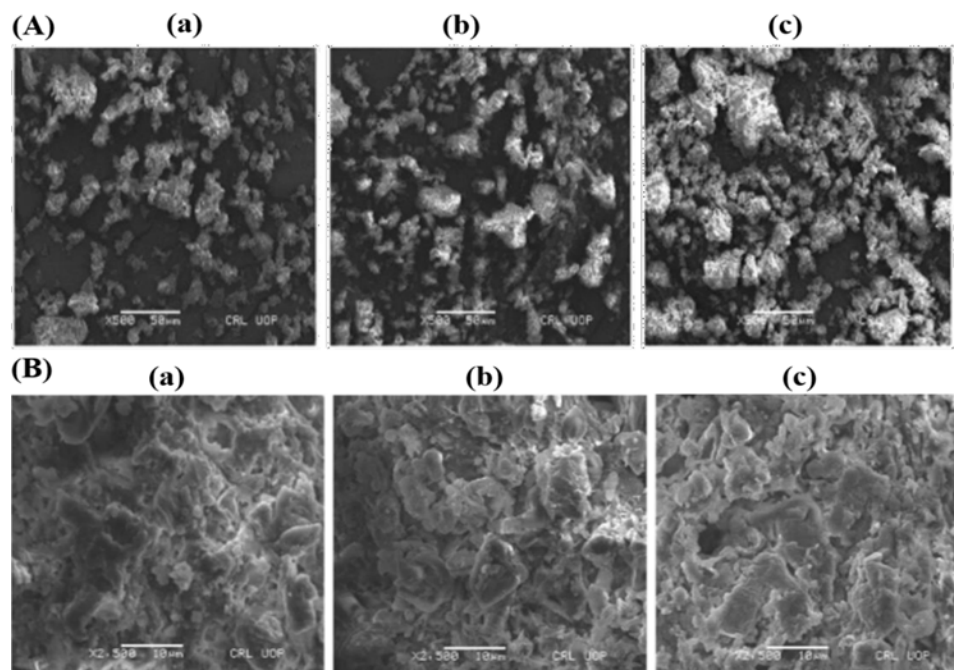


Figure 3.3: SEM images of biomass: (A) SEM images of *F. muscicola*: (a) dull surface of raw biomass; (b) bright surface of biomass saturated by Cd; (c) bright surface of biomass saturated by Pb. (B) SEM images of *Nostoc* sp.: (a) dull surface of raw biomass; (b) bright surface of biomass saturated by Cd; (c) bright surface of biomass saturated by Pb.

3.3.2. Effect of pH

pH of the solution is an important factor for biosorption. In the literature it has been described that polysaccharide cell wall of algae contains a high concentration of carboxyl groups from guluronic and mannuronic acids, changes in the pH of the solution may have an impact on the biosorption process (Matheickal and Yu, 1999). Effect of pH was investigated from 2-8 (Fig. 3.4a and 3.4b) using 1g/L biomass, 100 mg/L metals concentrations at specific intervals of contact time. Metals biosorption on to the dry biomass of *F. muscicola* was improved with the increase in the pH of the solution from 2 to 7 for Cd and 2 to 5 for Pb. At pH 6-8, Pb ions biosorption started to decline while the Cd ions biosorption declines after pH 7 (Fig. 3.4a). The

highest level of biosorption for Pb and Cd was 70.01 and 62.9 mg/g, respectively. While the maximum biosorption of Cd and Pb by dried biomass of *Nostoc* sp. was at pH 5 and 4, respectively. Therefore, pH 4 and 5 were selected for the biosorption Pb and Cd on to the dry biomass of *Nostoc* sp. Biosorption of Pb started to decrease when the pH level exceeded 4 (Fig. 3.4b). Similarly, Biosorption of Cd started to decrease when the pH level exceeded 5 (Fig. 3.4b). Because of repulsion force, the rise in positive charge on the biomass surface at low pH levels (2-3) limited the approach of metal cations. The decrease in biosorption at low pH can be attributed to the increased concentration of hydrogen ions, which interact with metal ions on the surface of the biosorbent (Singh et al., 2007).

This study shows that solution pH has a significant role in the biosorption of metal ions from the aqueous solution. In previous research it was described that the solution pH affects the metal ions chemistry, sorbent metal binding sites and ultimately affects the sorption of metals (Katrırcıoğlu et al., 2008). In principle, during the sorption of metals the solution pH has a significant role. It affects ionic competition, biomass functional groups activity, and the metal species solubility in the solutions. Most of the functional groups, like carboxyl are acidic and pH of the solution affects their propensity to adsorb heavy metal ions. Hydrogen ions (H^+) and metal ions compete in acidic conditions to produce the ligand at the surface of cells (Mehta and Gaur, 2005).

Furthermore, high Cd and Pb biosorption occurred at various pH levels. This is because the metals have various characteristics, like size, electronegativity, or the accessibility of additional metal ions, which adsorb better on adsorption sites (Chen et al., 2008). Cd maximum biosorption took place at pH 5 and 7 onto the dead biomass of *F. muscicola* and *Nostoc* sp., respectively. The highest levels of Pb biosorption were observed at pH 5 for *F. muscicola* and at pH 4 for *Nostoc* sp. The biosorption of same metal at different pH might be due to the differences in biomass composition. This corroborates to Mack et al. (2007) who described characteristics of metal ions biosorption generally happening at the pH 3 to 7. It was described that maximum biosorption of Cd by dry biomass of *Chlamydomonas reinhardtii* and *Anabaena doliolum* also occurred at pH 7 (Adhiya et al., 2002; Goswami et al., 2015). In another study it was reported that maximum biosorption of Pb by *C. reinhardtii* occurred at pH 5 (Tuzun et al., 2005b).

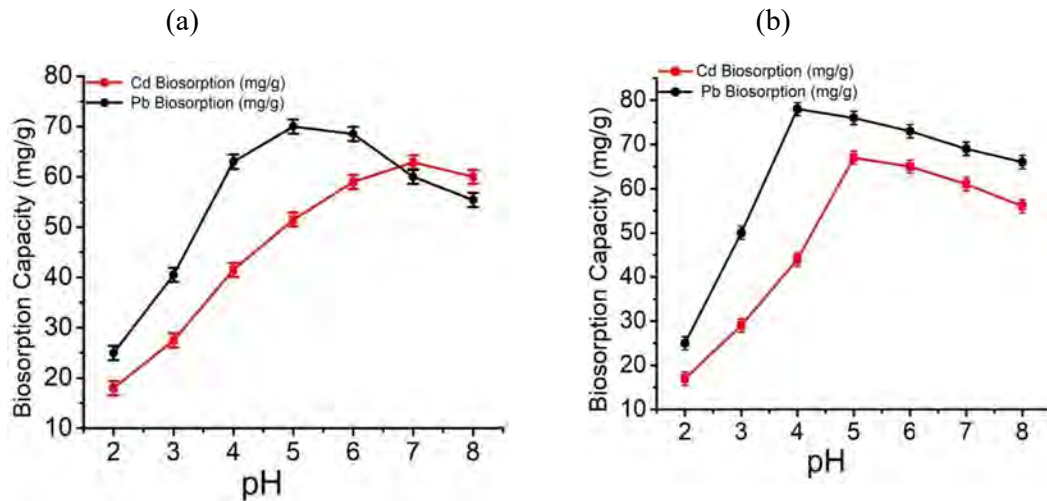


Figure 3.4: (a) Effect of pH on Pb and Cd ions biosorption by dried biomass of *F. muscicola*; (b) effect of pH on Pb and Cd ions biosorption by dried biomass of *Nostoc* sp.

3.3.3. Effect of contact time

Contact time is an important factor in metal ions adsorption. Fig. 3.5a shows the biosorption of Cd and Pb dry biomass of *F. muscicola* a function of contact time (5 to 120 min). Initially the metal adsorption rate was quite high. For both Pb and Cd the equilibrium time reached at 60 and 90 minutes, respectively. Therefore, all further studies were conducted at 60 and 90 minutes. In case of *Nostoc* sp., maximum biosorption of both Cd and Pb occurred at 60 minutes (Figure 3.5b). A previous study on biomass of *Anabaena sphaerica* reported maximum biosorption of Cd at 60 minutes and Pb at 90 minutes (Abdel-Aty et al., 2013). Similarly, 90 minute was reported as optimum Pb biosorption time in case of *Oedogonium* sp. (Gupta and Rastogi, 2008). Another study described the maximum biosorption of Cd at 60 min on to the dry biomass of *Chlorella vulgaris* and *Oscillatoria* sp. H1 (Katircioğlu et al., 2008; Kumar et al., 2018b). Results of current study are in line with the earlier studies, which found that highest biosorption of Pb and Cd occurred at contact time of 60 minutes (Sarı and Tuzen, 2008; Tüzün et al., 2005a). When the contact time was increased beyond the optimum, it resulted in decline of biosorption capacity of both strains. The decline in biosorption after the optimal contact time can be explained by the desorption of metal ions from the biomass surface (Saif et al., 2012). Consequently, the respective optimum contact time was selected for further investigations in these species.

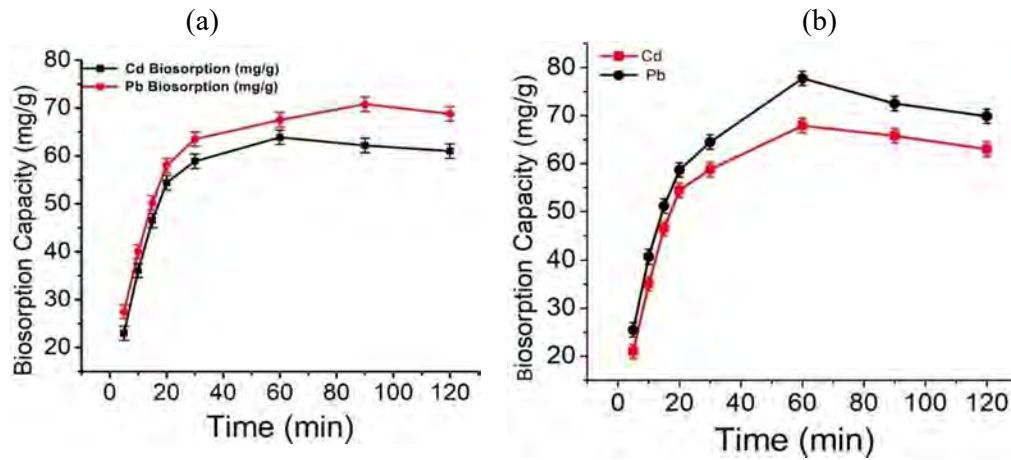


Figure 3.5: (a) Effect of contact time on Pb and Cd ions biosorption by dried biomass of *F. muscicola*; (b) effect of contact time on Pb and Cd ions biosorption by dried biomass of *Nostoc* sp.

3.3.4. Biosorption kinetics

Biosorption rate of metals on dried biomass of both strains was investigated using pseudo first order, pseudo second order and intra particles diffusion kinetic models. Pseudo first order kinetics primarily relies on the weak interactions between the adsorbent and adsorbate, predominantly governed by physisorption forces (Yuh-Shan, 2004), and pseudo second order kinetic largely controls chemisorption interactions (Ho and McKay, 1998). In addition to these, Intraparticle diffusion kinetic model was also described (Weber Jr and Morris, 1963). Equation 3, 4 and 5 represents pseudo 1st, pseudo 2nd order and intra particle diffusion kinetic models, respectively.

$$\ln(q_e - q_t) = \ln q_e - K_1 t \quad (3)$$

In this equation (3), q_t denotes the quantity of metal ions adsorbed (mg/g) at a specific time, whereas q_e is the amount of metal ions adsorbed (mg/g) onto the adsorbent at equilibrium. The rate constant associated with pseudo first order is denoted by the parameter K_1 (1/min). This study involves plotting $\log(q_e - q_t)$ against time (t) to get the rate constant and correlation coefficient for pseudo first order. These crucial parameters were primarily derived from the slope and intercept obtained during this investigation. The Pseudo second order is represented in equation 4 as follows:

$$\frac{t}{q_e} = \frac{1}{K_2 q_e^2} + \frac{1}{q_e} \quad (4)$$

Pseudo second order rate constant, denoted as K_2 (g/mg min), is calculated by making a plot t/q_t versus t . Following equation describes the linear form of Intraparticle diffusion kinetic model:

$$qt = k_{id} t^{0.5} + C \quad (5)$$

In equation 5, The term " K_{id} " corresponds to the rate constant for intraparticle diffusion, shown in milligrams per gram multiplied by the square root of minutes ($\text{mg}/(\text{g min}^{0.5})$). Lastly, the intercept is represented by the symbol " C ."

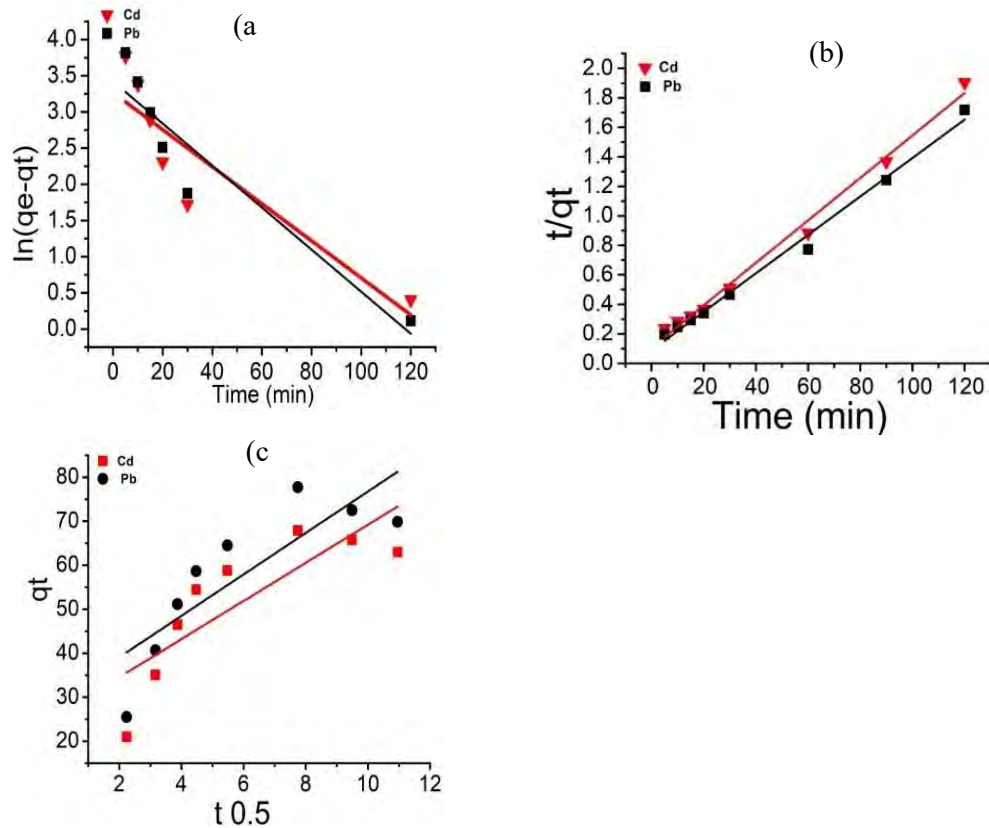


Figure 3.6: (a) Pseudo first order; (b) Pseudo second order; (c) Intraparticle diffusion kinetics for the biosorption of Pb and Cd by dried biomass of *F. muscicola*.

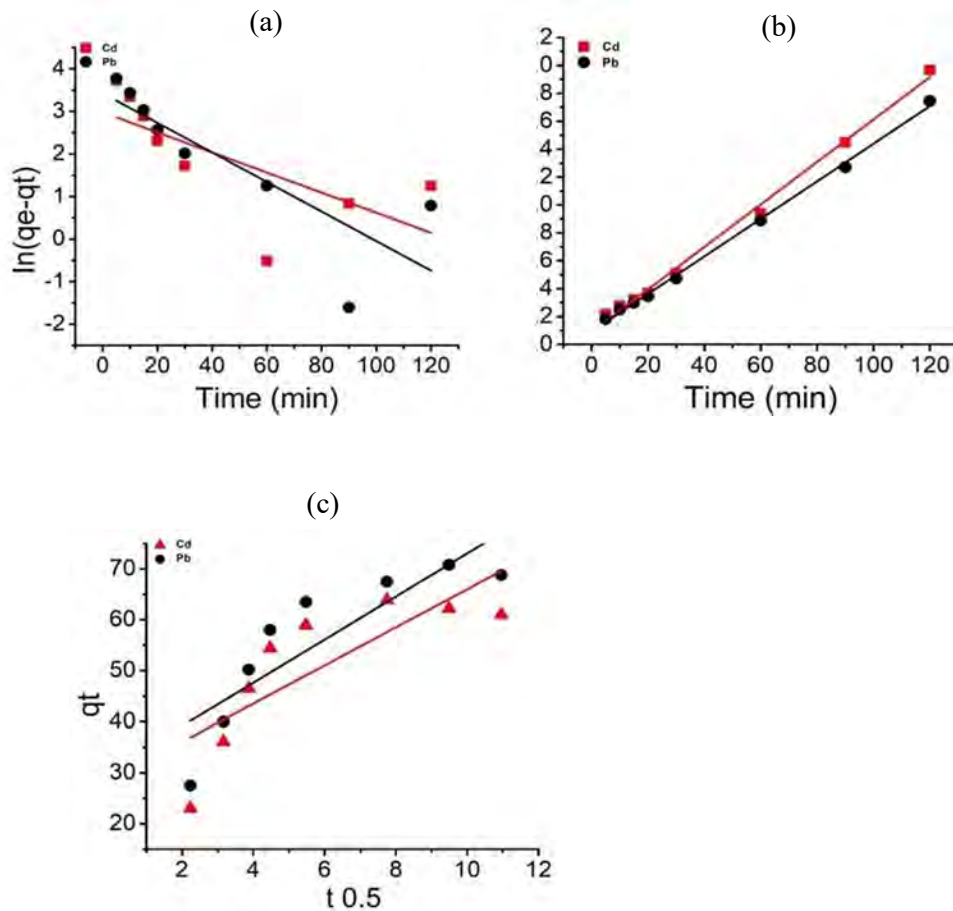


Figure 3.7: (a) Pseudo first order; (b) Pseudo second order; (c) Intraparticle diffusion kinetics for the biosorption of Cd and Pb by the dried biomass of *Nostoc* sp.

The linear representations of pseudo first-order, pseudo second-order and intraparticle diffusion kinetic models have been described in Fig. 3.6a, Fig. 3.6b and Fig. 3.6c, respectively for the biosorption of cadmium and lead onto the biomass of *F. muscicola*. While the Fig. 3.7a, Fig. 3.7b and Fig. 3.7c, describes the linear form plots of pseudo 1st order, pseudo 2nd order and intraparticle diffusion kinetic models for the biosorption Pb and Cd on to the dried biomass of *Nostoc* sp. Table 3.1 describes the parameters of kinetic models with their calculated values obtained from the biosorption of Pb and Cd by dried biomass of *F. muscicola* and *Nostoc* sp. In the kinetic modelling R^2 and q_e values of the biosorption data suggested that the pseudo second order was a suitable representation of the biosorption rates for Cd and Pb. Fitting of the pseudo second order suggest the chemisorption process (Bayo, 2012;

Ho and McKay, 1998). While the pseudo 1st order and intraparticle diffusion kinetic models did not follow the biosorption of Pb and Cd on to the dried biomass of both cyanobacteria strains with low R² values. More over in case of pseudo 1st order the experimental q_e and calculated q_e biosorption values were not close to each other. The findings showed that pseudo second-order kinetic model effectively described the biosorption process of both metals onto the dried biomass of *F. muscicola* and *Nostoc* sp. Earlier studies also reported the fitting well of the pseudo 2nd order on the biosorption of metals (Gupta and Rastogi, 2008; Mirghaffari et al., 2015; Tuzun et al., 2005b). In general, it is very important to evaluate equilibrium time by using experimental data and kinetic models to ascertain the rate at which various mechanisms, including chemical reaction, mass transfer and particle diffusion to administrate the biosorption process (Ho and McKay, 1998; Ozdes et al., 2011).

Table 3.1. Parameters of kinetic models

Kinetics models	Parameters	<i>F. muscicola</i>		<i>Nostoc sp.</i>	
		Cd	Pb	Cd	Pb
Pseudo first order	q _e (mg ⁻¹)	19.652	30.753	26.206	30.569
	K ₁ (min ⁻¹)	-0.0003	-0.0002	-0.0004	-0.0003
	R ²	0.411	0.644	0.770	0.863
Pseudo second order	q _e (mg ⁻¹)	65.659	74.23	69.492	76.923
	K ₂ (gmg ⁻¹ min ⁻¹)	0.0025	0.0019	0.00196	0.00192
	R ²	0.994	0.997	0.991	0.990
Intraparticle diffusion	K _i (mg g ⁻¹ h ^{-0.5})	3.748	4.242	0.158	0.632
	R ²	0.592	0.698	0.148	0.651

3.3.5. Effect of initial metal concentrations

Figures 3.8a and 3.8b elucidate the influence of initial metal concentrations on the biosorption of Cd and Pb onto the dried biomass of *F. muscicola* and *Nostoc* sp. Throughout the concentration range of 20 to 120 mg/L, the biosorption of both heavy metals exhibited an increasing trend before becoming constant.

Elevation in the concentrations of metal ions within the solution enhances the driving force for the translocation from the bulk solution to the biomass, thereby improve the biosorption capacity of the biosorbent (Satya et al., 2020). However, in the case of *Nostoc* sp. there was a minor drop in the capacity of biomass at metal ions concentrations of 120 mg/L. At higher metal ion concentrations, the biomass binding sites become saturated, the metal ions may remain un-adsorbed in the solution. This is consistent with the findings of the previously reported research (El-Sheekh et al., 2019b; Sun et al., 2012). Furthermore a preference to Pb sorption over Cd has been reported too (Abdel-Aty et al., 2013; Mirghaffari et al., 2015). The present data revealed such preferences in case of *F. muscicola* and *Nostoc* sp. too. Similarly comparing the species, *Nostoc* sp. showed higher capacity to remove Cd and Pb compared to *F. muscicola*.

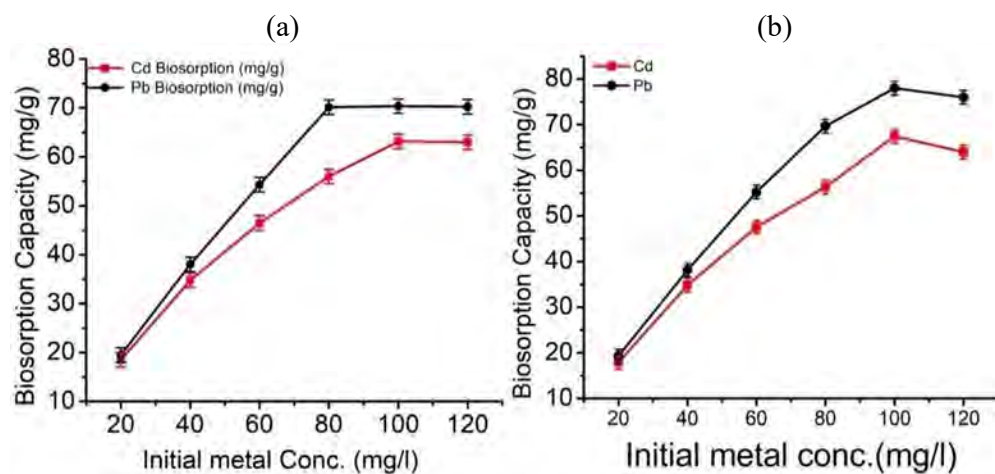


Figure 3.8: (a) Effect of initial metal concentrations on the biosorption of Cd and Pb by dried biomass of *F. muscicola*; (b) effect of initial metal concentrations on the biosorption of Cd and Pb by dried biomass of *Nostoc* sp.

3.3.6. Biosorption Isotherms

The Langmuir model measures the formation of an adsorbate monolayer on adsorbent surface and this model describes the distribution of metal ions when the liquid and solid phase are in equilibrium (Langmuir, 1918). Freundlich isotherm is suitable for describing multilayer biosorption processes on surfaces that exhibit heterogeneity (Freundlich, 1906) and Temkin isotherm model explains the interaction between the adsorbent and adsorbate. This model postulates that the heat of biosorption, which is a function of temperature, declines linearly rather than logarithmically, while disregarding conditions of extremely low and high concentrations (Temkin and Pyzhev, 1940). Using OriginPro 8.5 software, the data were fitted with linear regression analysis to establish the isotherms parameters. Equation (6) represents the Langmuir's isotherm as follows:

$$\frac{1}{q_e} = \frac{1}{K_L q_{\max}} \cdot \frac{1}{C_e} + \frac{1}{q_{\max}} \quad (6)$$

$$R_L = \frac{1}{1 + C_i \times K_L}$$

In equation 6, q_e is biosorption capacity (mg/g), C_e (mg/L) is concentrations of metals at equilibrium, C_i is the initial metal concentration, K_L (L/mg) shows the Langmuir's isotherm constant and q_{\max} (mg/g) represents the maximum biosorption capacity, R_L is the separation factor.

Linear form of Freundlich's isotherm is described in the following equation (7):

$$\text{Log}q_e = \text{Log}K_f + \frac{1}{n} \text{log}C_e \quad (7)$$

In equation 7, q_e is biosorption capacity (mg/g) K_f (mg/g) represents the Freundlich's constant used to evaluate the biosorption capacity and $1/n$ represents the biosorption intensity.

Temkin isotherm model equation (8):

$$q_e = \frac{RT}{b_T} \ln (A_T C_e)$$

$$B_T = \frac{RT}{b_T}$$

$$q_e = B_T \ln(AT) + B_T \ln(C_e) \quad (8)$$

In equation 8, Temkin equilibrium binding constant is denoted by A_T , Temkin isotherm constant by b_T . R^2 stand for the coefficient of correlation constant, B is the heat of adsorption constant, and T is the temperature.

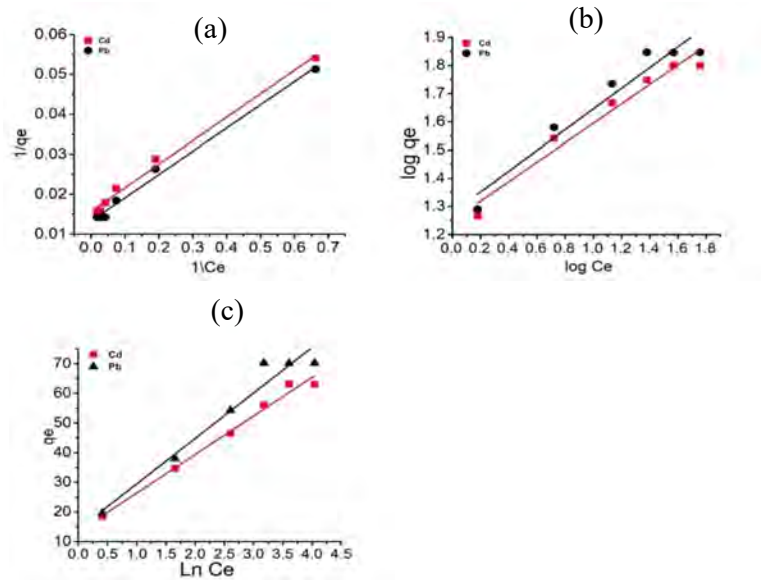


Figure 3.9: (a) Langmuir (b); Freundlich (c); Temkin isotherm models for the biosorption of Cd and Pb by dried biomass of *F. muscicola*.

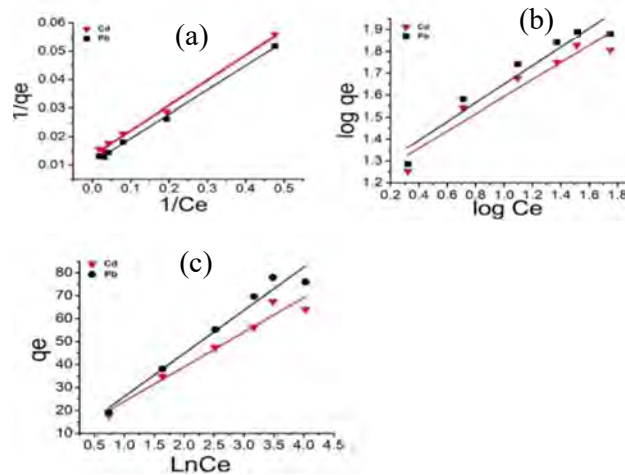


Figure 3.10: (a) Langmuir; (b) Freundlich; (c) Temkin, isotherm models for biosorption of Cd and Pb by dried biomass of *Nostoc* sp.

Liner form plots of Langmuir, Freundlich and Temkin isotherm models are shown in figure 3.9a, 3.9b and 3.9c, respectively for the biosorption of Cd and Pb by the dried biomass of *F. muscicola*. While the figure 3.10a, 3.10b and 3.10c shows the Liner form plots of Langmuir, Freundlich and Temkin isotherm models, respectively for the biosorption of Cd and Pb by dried biomass of *Nostoc* sp.

Parameters calculated from the isotherm models using biosorption experimental data are described in Table 3.2. Data showed that Langmuir isotherm model fitted well to the experimental biosorption data with high R^2 values. It suggests that the biosorption took place as a homogenous monolayer on biosorbent. Earlier studies also showed that biosorption of metals on the biosorbent surface took place as a homogenous monolayer (Ozer and Ozer, 2003; Tuzun et al., 2005b). Theoretical biosorption capacity (q_{\max}) of the biosorbent *F. muscicola* dried biomass was 63.572 mg/g for Cd and 70.274 mg/g for Pb which were very close to the experimental values 63.15 and 70.37 mg/g for Cd and Pb, respectively. Similarly, theoretical biosorption capacity (q_{\max}) of the biosorbent *Nostoc* sp. dried biomass were 83.963 and 75.757 mg/g for Pb and Cd, respectively and the biosorption capacity of biomass were 78 mg/g and 67.45 and for Pb and Cd, respectively. q_{\max} values anticipated from the Langmuir model agreed with the experimental values. The values of separation factor R_L also favour the sorption phenomenon (Table 3.2). Temkin isotherm model described well to the biosorption of Cd using *F. muscicola* dried biomass. The coefficient of correlation (R^2) was 0.984. Comparative analysis of Cd and Pb biosorption by *F. muscicola* and *Nostoc* sp. dried biomass with other biosorbents suggested that biosorbents used in this study are better than many of the biosorbents described previously (Table 3.4).

Table 3.2. Parameters of Isotherm models

Isotherm models		<i>F. muscicola</i>		<i>Nostoc sp.</i>	
	Parameters	Cd	Pb	Cd	Pb
Langmuir	q _{max} (mg/g)	63.572	70.274	75.757	83.963
	K _L (L/mg)	0.267	0.755	0.149	0.428
	R _L	0.0360	0.013	0.0627	0.0098
	R ²	0.989	0.985	0.993	0.998
Freundlich	K _f (mg/g)	17.788	28.986	15.915	27.664
	1/n	0.344	0.278	0.391	0.328
	R ²	0.951	0.832	0.897	0.844
Temkin	K _T	2.788	14.726	1.752	7.228
	B _T	13.013	11.745	15.796	14.68
	R ²	0.984	0.887	0.947	0.928

3.3.7. Desorption and reusability

Pb and Cd biosorption results showed that biosorbents used in this study possess the potential for sequestering the metals from the aqueous solution. To establish the desorption-to-biosorption ratio (D/B), experiments were conducted over three cycles as described in Table 3.3. Upon employing 0.1M HCL, desorption of both metals was found up to 90% (Table 3.3). Following the initial biosorption-desorption cycle; there was a little drop in the biosorption capacity of *F. muscicola* and *Nostoc sp.* dried biomass. According to Tuzun et al., (2005b) after 6 cycles, the *C. reinhardtii* microalgae biomass lost some of its capacity to adsorb Cd and Pb ions. Decline in the biosorption potential of biomass could be due to the eluent used for desorption of metals and consequently losing the binding sites on the surface of biomass. Cost effectiveness of this process depends on determining how much of the dried biosorbent may be reused. As a result, variations in the ratio of desorption to biosorption were utilized to assess this potential (Akar et al., 2013; Kumar and Gaur, 2011; Luo and Xiao, 2010). However, the desorption process is important as it assists in the recovery of economically important metals (Pérez-Rama et al., 2010; Rangsayatorn et al., 2002; Rodrigues et al., 2012).

Table 3.3. Borption-desorption of Cd and Pb by dried biomass of *F. muscicola* and *Nostoc* sp.

Strains	Heavy metals	Cycles	Biosorption (mg/g)	Desorption (mg/g)	Ratio, D/B (mg/g)	Desorption (%)
<i>F. muscicola</i>	Cd	1	63.51	57.231	0.901	90.1
		2	60.233	54.5	0.90	90
		3	56.272	51.561	0.916	91.6
	Pb	1	70.251	63.29	0.90	90
		2	67.01	61.134	0.91	91
		3	62.56	56.217	0.898	89.8
<i>Nostoc</i> sp.	Cd	1	65.65	61.22	0.932	93.2
		2	62	57.5	0.927	92.7
		3	57.02	52.11	0.913	91.3
	Pb	1	74.49	71.4	0.958	95.8
		2	69.22	64.45	0.931	93.1
		3	60	56	0.933	93.3

Table 3.4. Comparison of maximum biosorption capacities of *F. muscicola* and *Nostoc* sp. dried biomass with other biosorbents

Algal Strain	Cd (biosorption capacity), mg/g	Pb (biosorption capacity), mg/g	Reference
<i>Anabaena sphaerica</i>	111.100	121.950	(Abdel-Aty et al., 2013)
<i>Scenedesmus quadricauda</i>	135.100	333.3	(Mirghaffari et al., 2015)
<i>Ulva lactuca</i>	29.2	34.7	(Sarı and Tuzen, 2008)
<i>Rhizopus arrhizus</i>	27	56	(Rakhshae et al., 2006)
<i>Pinus sylvestris</i>	19.1	22.2	(Fourest and Roux, 1992)
<i>F. muscicola</i>	63.572	70.274	Current study
<i>Nostoc</i> sp.	75.757	83.963	Current study

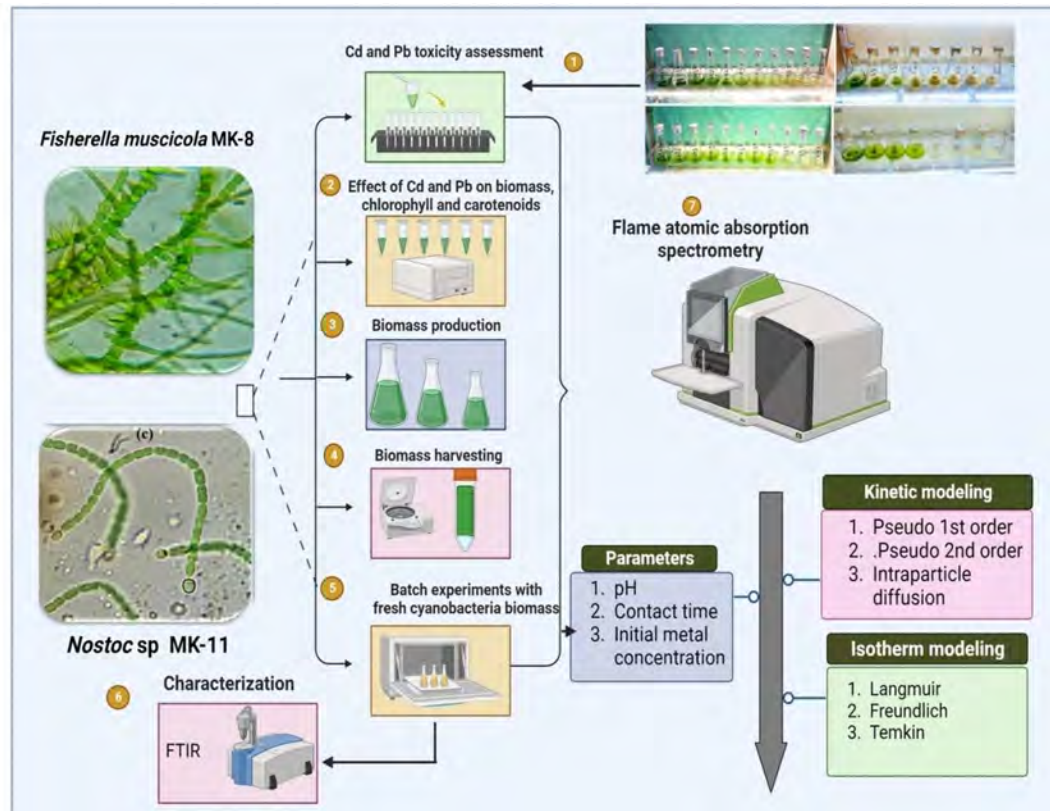
In conclusion

- Removal of heavy metals with cyanobacteria is effective and green technology to treat wastewater.
- *Nostoc* sp. was more effective than *F. muscicola* in bio-removal of Cd and Pb from aqueous solutions.
- Mechanism of Cd and Pb ions binding to dried biomass of both cyanobacteria species was chemisorption and homogeneous.
- Reusability of dried biomass of *F. muscicola* and *Nostoc* sp. is revealed. The process may help to reclaim economically important metals.

CHAPTER 4

Comparative studies on growth and biosorption of Cd and Pb from aqueous solutions by fresh biomass of *Fischerella muscicola* and *Nostoc* sp.: Kinetic and Isotherm modeling

Graphical Abstract



Graphical abstract: Graphical representation of comparative studies on growth and biosorption of Cd and Pb by fresh biomass of *Fischerella muscicola* and *Nostoc sp.*

Summary

Increasing industrialization has intensified heavy metal pollution, posing severe threats to environmental and human health. This study investigated the fresh biomass potential of two cyanobacteria, *Fischerella muscicola* (branched heterocystous cyanobacterium) and *Nostoc* sp. (un-branched heterocystous cyanobacterium) as biosorbents for the removal of Cd and Pb from aqueous solution. Furthermore, the effects of Cd and Pb on the growth, biomass and photosynthetic pigments were investigated. *Fischerella muscicola* tolerated Cd and Pb stress up to 1.5 and 30 mg/L, respectively. While, *Nostoc* sp. tolerated Cd and Pb stress up to 1.75 and 45 mg/L, respectively. Exposure of these strains to different concentrations of Cd and Pb showed inhibitory effects on the growth, biomass, chlorophyll and carotenoids. Studying the biosorption process, the effects of initial metal concentrations, pH and contact time were optimized. Biosorption experimental data was analyzed with three kinetics (Pseudo first order, Pseudo second order and intraparticle) and isotherms (Langmuir, Freundlich and Temkin) models to assess the mechanism and rate of biosorption. Modeling results showed the Pseudo second order and Langmuir isotherm models as best fit to the experimental biosorption data. Modeling analysis suggested that the binding of metals to the biomass in case of both the strains was chemisorption in nature and homogeneous in manner. Langmuir isotherm calculated maximum biosorption capacity of *F. muscicola* fresh biomass as 84.38 and 75.30 mg/g for Pb and Cd, respectively. Similarly, Langmuir isotherm calculated *Nostoc* sp. maximum biosorption capacity as 86.73 and 81.69 for Cd and Pb, respectively. The results showed that *Nostoc* sp. exhibited a greater efficacy in the removal of Cd and Pb from aqueous solutions compared to *F. muscicola*. Further characterization through FTIR analysis showed that living biomass of both strains possessed the functional groups which are instrumental in heavy metals binding and removal. Hence both freshwater cyanobacterial strains may be deployed in removing heavy metals from aqueous solutions and their reusability potentials render them as a sustainable solution for pollution treatment.

4.1. Introduction

Urbanization and industrialization are two significant phenomena that cause emission of various environmental contaminants globally. Because of their toxicity and inability to decompose, heavy metals are regarded as the most dangerous of these environmental pollutants. In particular, the general health of humans and other living things is negatively impacted by the heavy metals build-up in the environment (Meitei and Prasad, 2013; Sari et al., 2011; Verma et al., 2016). Reports indicate that the industrial sector is responsible for the annual discharge of 300 to 400 million tons of heavy metals, solvents, toxic sludge and various other waste materials into aquatic environments (United Nations World Water Assessment Programme, 2006). The US Environmental Protection Agency (EPA) released a comprehensive list of contaminants in 1978 which are extremely dangerous to both human health and the survival of organisms. This record specifically includes heavy metals such as Cd, chromium, zinc, mercury, Pb, copper, and nickel (Sari et al., 2011). Incorporation of heavy metals into the human body is supported by three alternate routes which include air, water and food.

Occurrence of trace amounts of heavy metals within the human body has an important role in metabolic processes but higher amounts have toxic effects causing health hazards (Gupta et al., 2016). Heavy metals, whether they possess direct toxicity or they accumulate indirectly in sediments and aquatic organisms, have the potential to enter human body via food chain (Bo et al., 2015; Dadar et al., 2016; Kumar et al., 2015). The transfer of heavy metals from lower to upper trophic levels as well as acquisition in tissues of living organisms can consequently result in increased concentration. Heavy metals possess the potential to impact the biochemical properties, structure and growth of microorganisms. It is accomplished by modifying cell membranes which disturbs the functioning of membranes. Furthermore, oxidative phosphorylation and enzyme activity can be inhibited by heavy metals modifying the structure of nucleic acids. Heavy metals can also disrupt the osmotic balance, induce lipid peroxidation, and denature proteins (Xie et al., 2016).

Cd, chromium, Pb and mercury are at the top of the poisonous hierarchy among various metal ions (Abbas et al., 2014). It has been found that arsenic, Pb, and mercury are associated with various kinds of cancers (Conti et al., 2015; Ryan et al., 2000). Pb is a natural component of earth's lithosphere and is commonly present in small

quantities within terrestrial substrates, flora, and aqueous bodies (Evans, 1921). It is an important pollutant of terrestrial and aquatic ecosystems. Air (15%), water (20%) and food (65%), and serves as a source for Pb intake. Slightly acidic pH of water increases the susceptibility of contamination by Pb due to higher probability of tube corrosion. Therefore, it necessitates the regular and proper testing of pH of drinking water systems (Sciacca and Conti, 2009; Ryan et al., 2000). It is well recognized that Cd is one of the most hazardous contaminants and it has a long biological half-life in living organisms ((approximately thirty years) making it as an accumulative toxic substance (Goering et al., 1995). When present in trace amounts, vital human organs like the lungs and liver are not harmed by it but its accumulation within an organism displaces the indispensable metals required for cellular metabolism hence halting the enzymatic activities and as a result harming to cell membrane (Duque et al., 2019). The International Agency for Research on Cancer has classified Cd as a class I human's carcinogen (Waalkes, 2000). Cd predominantly impedes the light-dependent photosynthesis phase and incorporation of carbon in photoautotrophs which produce oxygen, thus causing reduced growth and primary productivity as a consequence of their capacity to remove oxidized proteins (Deckert, 2005) and the existence of cellular mechanisms that restrict the transportation and cycling of toxicants (Malec et al., 2011). There is a rising global concern about removing heavy metals from water and Cd contamination because it poses a risk to both human and ecosystem health and industrial waste composition management (Galiulin et al., 2001).

Heavy metal-polluted wastewater can be purified using a variety of conventional techniques, including coagulation/flocculation, chemical precipitation, adsorption on chelating or ion exchange resins and membrane filtering. These techniques are frequently costly, inefficient-particularly at low concentrations-high energy and maintenance requirements, and can produce hazardous byproducts (Acien et al., 2016; Azimi et al., 2017; Fazlzadeh et al., 2017). Therefore, there is a need to develop methods for effective elimination of pollutants with the goal of enhancing the process of water treatment, reducing the operational expenses and acquisition as well as minimizing the carbon footprint that is associated with large-scale treatment facilities (Gupta and Rastogi, 2008).

Alternatively, removal of heavy metals based on biological materials including algae, fungi, bacteria, and yeast as biosorbents to remove organic pollutants and heavy metals (Barquilha et al., 2017; Camere and Karana, 2018). Recently, prokaryotic and eukaryotic algae have been found reliable and comparatively inexpensive biosorbents (Olal, 2016). Heavy metals have lethal effects on microalgae causing modifications in pigment composition, reducing growth rates of algae, gross protein and carbohydrate content (Fawzy, 2016). Algae harbor various enzymes (including catalase, glutathione reductase, superoxide dismutase and ascorbate peroxidase) and non-enzymatic constituents (such as ascorbate and glutathione) which serve to safeguard cells from damage due to reactive oxygen species triggered by the stress of heavy metals. There by augmenting the efficacy of antioxidant enzymes (Gao et al., 2017). Green and blue-green algae have been reported as having the high capacity to assimilate metal ions within their cellular structures (Sivakami et al., 2015). Comparatively cyanobacteria contain an additional advantage to other microorganisms in terms of basic nutrient requirements, broader surface area of expanded mucilage and durable binding affinity (Davis et al., 2003). Utilization of cyanobacteria is becoming a dominating practice in waste management because it can effectively plunge the presence of heavy metals in industrial waste. Due to their deleterious nature, these heavy metals have emerged as global threat and concern (Anjana et al., 2007; Cain et al., 2008; El-Enany and Issa, 2000). Thus its urgent need for the developments of efficient, economical and ecofriendly technologies to remove these toxic pollutants from the polluted environment. The present investigation details the biosorption of Cd and Pb ions from aqueous solutions utilizing the fresh biomass of newly isolated cyanobacteria, specifically *Fischerella muscicola* and *Nostoc* sp.

The objectives of this research were to utilize the fresh biomass of *F. muscicola* and *Nostoc* sp. as biosorbents to remove the Pb and Cd from the aqueous solutions. To study the impact of contact time, pH and initial metal concentrations on the biosorption and to assess the experimental data using Kinetic (Pseudo first order, Pseudo second order and, Intraparticle diffusion) and Isotherm (Langmuir, Freundlich and Temkin) models and decipher the possible mechanism of remediation.

4.2. Materials and Methods

4.2.1. Culturing and assessment of Cd and Pb toxicity effects on growth

Cyanobacteria strains, *F. muscicola* and *Nostoc* sp. were cultivated in Erlenmeyer flasks containing BG₁₁ media (Rippka et al., 1979) and cultures were kept at 25 ± 2 °C under white LED lights and harvested for additional analysis at the optimum growth using centrifugation for 15 minutes at 4000 rpm. Cd chloride and Pb acetate were used a source of Cd and Pb in aqueous solutions. Initially 1000 mg/L of Pb and Cd ions stock solutions were synthesized by separately mixing Cd chloride and Pb acetate in dH₂O (distilled water) and then sterilized using a Millipore 0.22 µm filter paper. To obtain the required concentrations, Cd and Pb solutions were added to the culture media in accordance with the experiment's specifications. For assessment of Cd and Pb toxicity effects on *F. muscicola* and *Nostoc* sp. growth, a set of media (100 ml total volume) with increasing Cd and Pb ions concentrations (Cd: 0, 0.25, 0.5, 0.75, 1, 1.25, 1.5, 1.75, 2, 2.5 and 3 mg/L and Pb: 0, 15, 30, 45, 60, 90 and 120 mg/L) were inoculated with aliquots of *F. muscicola* and *Nostoc* sp. suspension of cells up to the initial OD₇₅₀ = 0.05. Growth of cyanobacteria was estimated by measuring an optical density at 750 nm using an ultraviolet visible (UV-Vis) spectrophotometer (Chandrashekharaiah et al., 2021).

4.2.2. Measurement of photosynthetic pigments

In photosynthetic pigment assays, 1 ml of cell suspension was extracted by centrifuging the mixture at 15000g for 7 minutes. Supernatant was discarded and pellet of the cells was mixed with 1 milliliter of pre-cooled (-20°C) methanol. The mixture was then incubated in dark at 4°C for a minimum of 60 minutes, or until the colour of the pellet turned white. The absorbance of the supernatant was measured at 470, 665, and 720 nm (Wellburn, 1994). Chlorophyll *a* and carotenoids concentrations were measured using equation 1 and 2, respectively (Wang et al., 2021)

$$\text{Chl } a \text{ } [\mu\text{g/ml}] = 12.9447 \times (A_{665} - A_{720}) \quad (1)$$

$$\text{Total carotenoids } [\mu\text{g/ml}] = [1000 \times (A_{470} - A_{720}) - 2.86 \times (\text{Chl } a \text{ } [\mu\text{g/ml}])]/221 \quad (2)$$

4.2.3. Measurement of dry weight

The assessment of cyanobacteria biomass was carried out by following Abd El- Hameed et al. (2018). Adequate agitation was applied to the cyanobacteria

suspension or culture flasks, and representative samples of the cyanobacteria suspension were achieved. Consequently, from the culture media the cyanobacteria cells were separated using a centrifuge at 4000 rpm for 10 minutes. The obtained biomass was re-mixed in distilled water and again centrifuged for 10 minutes. After washing with distilled water, the cells were transferred to a pre-weighed glass dish. The biomass was dried in an oven at 65 to 70 °C until two successive weight measurements of the dish, taken at intervals, yielded a consistent value. Weighing was performed when the pre-weighed glass dish was cooled to room temperature in a desiccator. The dry weight of each cell replicate was determined by subtracting the weight of the dried sample from the initial weight of the glass dish, with the measurement expressed per unit volume.

4.2.4. Batch biosorption experiments

Biosorption studies were performed using fresh biomass of *F. muscicola* and *Nostoc* sp. as biosorbents and Pb and Cd ions as adsorbates. One gramme of the biosorbent was dissolved in 100 milliliters (ml) of an aqueous solution containing metal ions at a concentration of 100 milligrams (mg) per liter in a 250 ml conical flask. In the current study, effect of different factors such as pH (ranging from 2-8), initial metal ions concentration (20- 120 mg/L) and contact time (5-120 minutes) on the biosorption of metal ions onto the biosorbents were studied. Mixture of metal ions and biosorbents were stirred at 150 rpm using an orbital shaker for a predetermined period at 25 °C. Whatman-40 filter paper was used to filter the solution and Initial and final metal concentrations in the filtrate were determined using Agilent Flame Atomic Adsorption Spectrometer (FAAS). Biosorption capacity (mg/g) of fresh biomass was calculated using equation 3.

$$q_e = \frac{(C_i - C_e)}{w} \times V \quad (3)$$

4.2.5. Biosorbent characterization

FTIR was used for the characterization of biomass before and after the biosorption process. FTIR identified the surface functional groups present in the biomass, while the analysis of non-treated and metals-treated cyanobacterial cell morphology was assessed using Light microscopy.

4.2.6. Data analysis

Each experiment was performed in triplicates and the results were presented as the mean of three values. The data shown in figures and tables (Fig. 4.3; Fig.4.4; Fig. 4.5; Fig. 4.6; Fig. 4.8; Fig. 4.9. Fig. 4.10; Fig. 4.11; Fig. 4.12; Fig. 4.13; Fig. 4.14 and Table 4.1; Table 4.2) describe the average values along with the standard deviations calculated for all the repeated measurements. The data were statistical analyzed using OriginPro 8.5 (OriginLab Corporation, Northampton, Massachusetts, USA) and Microsoft Office Excel (2010) software.

4.3. Results and Discussion

4.3.1. Effects of Cd and Pb on growth of *Fischerella muscicola* and *Nostoc* sp.

To investigate the tolerance of *F. muscicola* and *Nostoc* sp. to Pb and Cd stress, experiments were performed observing the growth response of cyanobacteria cells ($OD_{750} = 0.05$) at different Cd and Pb concentrations. Fig 4.1a and 4.1b show the culturing images of *F. muscicola* and Fig 4.1c and 4.1d show the culturing images of *Nostoc* sp. under various concentrations of Cd and Pb, respectively. Visuals of culturing clearly show an inverse impact of the initial concentrations of Cd and Pb on the growth of cells. The growth declined at low and high concentrations of heavy metals and eventually led to cell death (Fig 4.1a, b, c and d). Furthermore, various concentrations of Cd and Pb affected the morphology of both the cyanobacterial strains. Figure 4.2a, b and c shows the microscopic images of *F. muscicola* under control (0 mg/L), Cd (3 mg/L) and Pb (120mg/L) conditions, respectively. Similarly, Figure 4.2d, e and f show the microscopic images of *Nostoc* sp. under control (0 mg/L), Cd (3 mg/L) and Pb (120 mg/L) stress conditions respectively.



Figure 4.1: Visuals of Cd and Pb stress on growth of cyanobacteria strains: (a) Growth (12 days culturing) visuals of *F. muscicola* in BG₁₁ media with different Cd concentrations; (b) Growth (12 days culturing) visuals of *F. muscicola* in BG₁₁ media with different Pb concentrations; (c) Growth (12 days culturing) visuals of *Nostoc* sp. in BG₁₁ media with different Cd concentrations; (d) Growth (12 days culturing) visuals of *Nostoc* sp. in BG₁₁ media with different Pb concentrations.

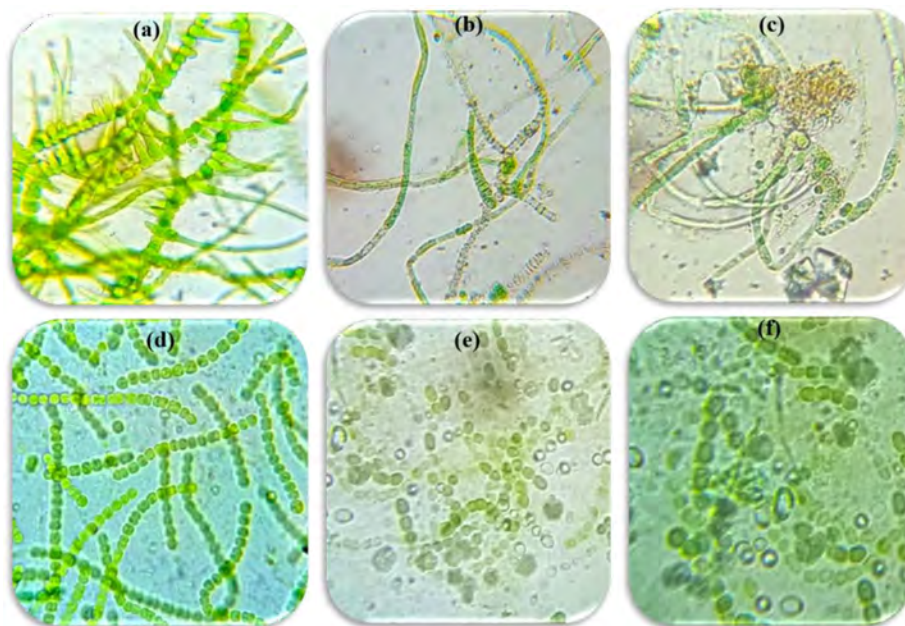


Figure 4.2: Microscopic images of Cd and Pb stress on the morphology of cyanobacteria strains: (a) Morphology of *F. muscicola* (4 days culturing) in BG₁₁ media with Cd (0mg/L); (b) Morphology of *F. muscicola* (4 days culturing) in BG₁₁ media with Cd (3 mg/L); (c) Morphology of *F. muscicola* (4 days culturing) in BG₁₁ media with Pb (120 mg/L); (d) Morphology of *Nostoc* sp. (4 days culturing) in BG₁₁ media with Cd(0 mg/L); (e) Morphology of *Nostoc* sp. (4 days culturing) in BG₁₁ media with Cd (3 mg/L); (f) Morphology of *Nostoc* sp. (4 days culturing) in BG₁₁ media with Pb (120 mg/L).

The cells of the both cyanobacteria strains grew well under the control conditions whereas the growth rate of strains under different metal concentrations gradually dropped with increase in concentrations of Cd and Pb as assessed over a period of 12-days. At Cd concentrations of 1.5 mg/L, the biomass of *F. muscicola* did not show any significant increase even on the extension of time. However, the strain revealed tolerance to Cd stress @ 1.5 mg/L. Similarly, at a Pb concentration of 30 mg/L, the cell biomass of *F. muscicola* did not show any significant increase even with dilated cultivation time and the strain tolerated Pb stress up to 30 mg/L. The highest biomass yield (OD₇₅₀) experienced a substantial decline when exposed to Cd at a concentration of 3.0 mg/L and Pb at a concentration of 120 mg/L, indicating that inhibitory effects of Cd and Pb on cyanobacteria growth were dose dependent. Figure 4.3a and 4.3b shows the growth curves of *F. muscicola* under different concentrations

of Cd and Pb, respectively.

Similarly, *Nostoc* sp. showed decent growth in the control conditions and declined under different concentrations of Pb and Cd over a twelve-day period of culturing. At Cd concentrations of 1.75 mg/L, the cell biomass did not show a significant increase with the extension of cultivation time, and the strain revealed tolerance to Cd stress up to 1.75 mg/L. In the same way, when the concentration of Pb reached upto 45 mg/L, the cell biomass did not show a notable rise when the cultivation duration was extended. Furthermore, *Nostoc* sp. showed tolerance to Pb stress up to 45 mg L⁻¹. Exposure to Cd at a concentration of 3.0 mg L⁻¹ and Pb at a concentration of 120 mg L⁻¹ resulted in a significant decrease in the biomass yield, suggesting that the effects of Cd and Pb on cyanobacteria growth were dose-dependent. Figures 4.3c and 4.3d depict the growth curves of *Nostoc* sp. at various amounts of Cd and Pb, including the control group. Analysis of the growth curves of both strains indicates that *Nostoc* sp. exhibited greater tolerance to Cd and Pb stress in comparison to *F. muscicola*. Growth rate of *Nostoc* sp. was also higher than the *F. muscicola*. In a previous study it has been described that higher concentrations of Pb showed the inhibitory effects for growth of two cyanobacteria, *Anabaena variabilis* and *Nostoc muscorum* (Abd El- Hameed et al., 2018). Similarly in another study it has been described that Cd exerted toxic effects on the metabolic system of *Synechocystis* sp. PCC6803 and reduced the growth (Shen et al., 2021).

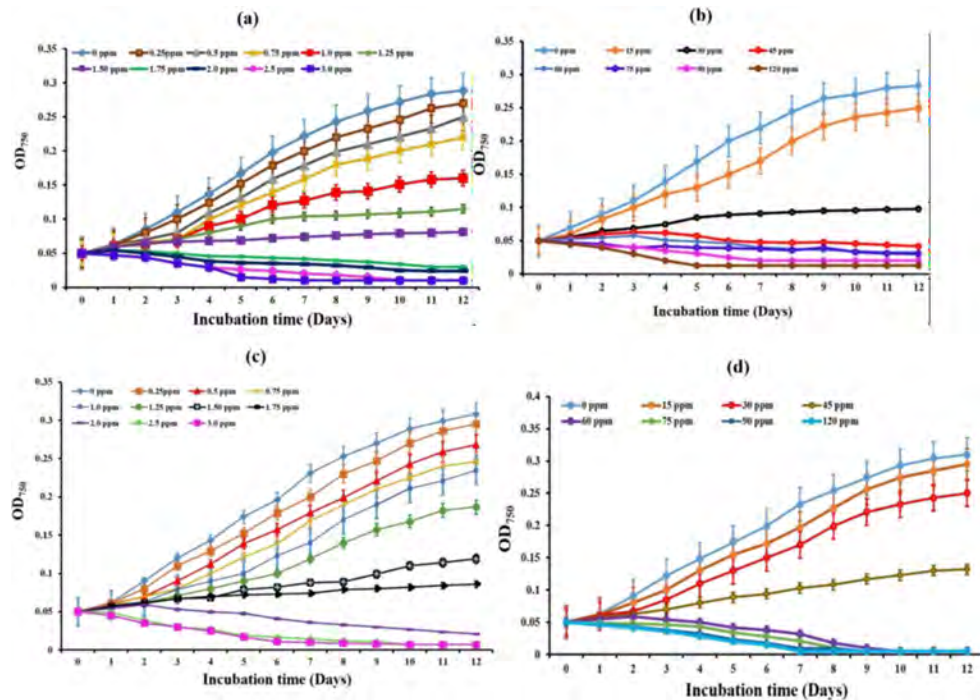


Figure 4.3: Growth curves of two cyanobacteria strains: (a) growth curve of *F. muscicola* under control and various concentrations of Cd; (b) growth curve of *F. muscicola* under control and various concentrations of Pb; (c) growth curve of *Nostoc* sp. under control and various concentrations of Cd; (d) growth curve of *Nostoc* sp. under control and various concentrations of Pb.

4.3.2. Effects of Cd and Pb on biomass

Cd and Pb stress exert the effects on the biomass of the cyanobacteria. As illustrated in Figure 4.4a and 4.4b, amount of biomass of *F. muscicola* varied during the incubation period under various concentrations of Cd (0, 1.5 and 3 mg/L) and Pb (0, 30 and 120 mg/L). Similarly, as illustrated in Figure 4.4c and 4.4d, biomass of *Nostoc* sp. varied during the incubation period based on the concentrations of Cd (0, 1.75 and 3 mg L⁻¹) and Pb (0, 45 and 120 mg/L). After 96 hours of incubation, the biomass of both strains was highest in the control treatment @ 0 mg/L (Cd and Pb) and lowest in the highest concentrations @ 3 mg/L of Cd and 120 mg/L of Pb. In the control treatment the biomass of *F. muscicola* was recorded as 83.12 mg/L while in the highest concentrations of Cd and Pb the biomass was recorded as 25.45 and 21.45 mg/L, respectively. Similarly, in the control treatment the biomass of *Nostoc* sp. was determined as 86.2 mg/L while in the highest concentrations of Cd and Pb the biomass

weight was recorded as 25.4 and 25.69 mg/L, respectively. According to a previous study (Arunakumara and Xuechen, 2007), high concentrations of metals could potentially reduced the growth due to the inhibition of various essential processes such as protein and nucleic acid synthesis, enzyme systems, respiration and photosynthesis. *F. muscicola* and *Nostoc* sp. biomass increased slowly at low Pb and Cd concentrations and biomass concentrations decreased drastically at higher concentrations of Cd and Pb. This was consistent with the findings of Hazarika et al. (2015), who discovered that high Pb concentrations inhibited the growth of biomass and also caused cell death. Wang et al. (2021) revealed that a high concentration of Cd had fatal effects on *Chlorella vulgaris* and reduced the biomass production.

Arunakumara and Xuecheng (2007) demonstrated that high concentrations of Pb impeded the growth of *Spirulina platensis*. Also, Chen and Pan (2005), demonstrated that *Spirulina* cells died due to growth inhibitions at high Pb concentrations.

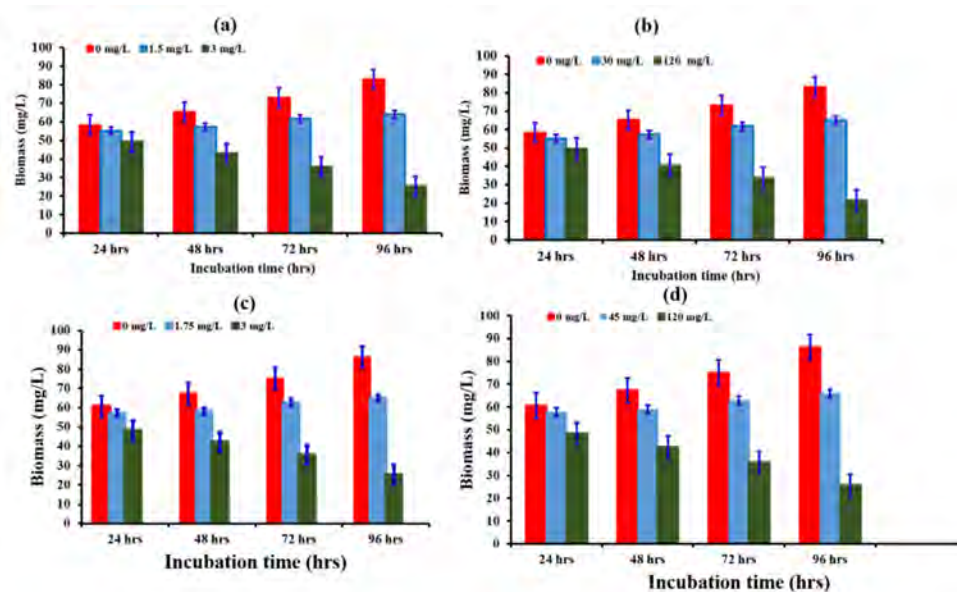


Figure 4.4: Effect of initial metal concentrations of Cd and Pb on biomass of two cyanobacteria strains: (a) effect of different initial concentrations of Cd on biomass of *F. muscicola*; (b) effect of various Pb concentrations on biomass of *F. muscicola*; (c) effect of various initial Cd concentrations on biomass of *Nostoc* sp.; (d) effect of different initial Pb concentration on biomass of *Nostoc* sp.

4.3.3. Effects of Cd and Pb on the photosynthetic pigments

Heavy metals toxicity assessment on photosynthetic pigments of *F. muscicola* and *Nostoc* sp. was carried out using various concentrations of Cd and Pb. It was found that there was a continuous increase in the chlorophyll *a* and carotenoids contents of both strains at control conditions. Photosynthetic pigments contents also increased at metals tolerant conditions but lower than the control conditions. While a consistent decrease in chlorophyll *a* was observed at highest concentrations of Cd and Pb. Production of photosynthetic pigments was considerably hindered at high concentrations, 3 mg L⁻¹ of Cd and 120 mg L⁻¹ of Pb. Figure 4.5a and 4.5b shows the chlorophyll *a* content of *F. muscicola* under control, tolerant and highest lethal concentrations of Cd and Pb. It is evident from the figures that maximum chlorophyll *a* was produced in the control treatments and lowest chlorophyll was produced in the highest lethal concentrations of Cd and Pb.

Figures 4.5c and 4.5d show that the carotenoids content of *F. muscicola* was high in the control treatment and average in the tolerant conditions and lowest at the high lethal concentrations of the Cd and Pb. Similarly, Fig 4.6a and 4.6b showed the chlorophyll *a* content of *Nostoc* sp. under control, tolerant and highest lethal concentrations of Cd and Pb. It is evident from the figures that maximum chlorophyll *a* was produced in the control treatments and lowest chlorophyll was produced in the highest lethal concentrations of Cd and Pb. Figures 4.6c and 4.6d show that the carotenoids content of *Nostoc* sp. was high in the control treatment and average in the tolerant conditions and lowest at high lethal concentrations. Previous studies show the harmful effects of Cd on cyanobacteria, with the concentration of Cd gradually increasing and leading to reduced content of chlorophyll and carotenoids (Shen et al., 2021). It has been found that, following seven days of exposure to varying amounts, an increase in the Pb concentration in *Synechococcus leopoliensis* growth medium caused a corresponding decrease in the amount of chlorophyll (Pinchasov et al., 2006). The results of this investigation are consistent with the earlier research on Pb bioaccumulation in algal cells (Rachlin et al., 1984; Poskuta et al., 1996; Starodub et al., 1987; Sing et al., 1993), It further suggests that an increase in the concentration of Pb and longer exposure time result in an increased toxicity of Pb on the biosynthesis of chlorophyll (Poskuta et al., 1996).

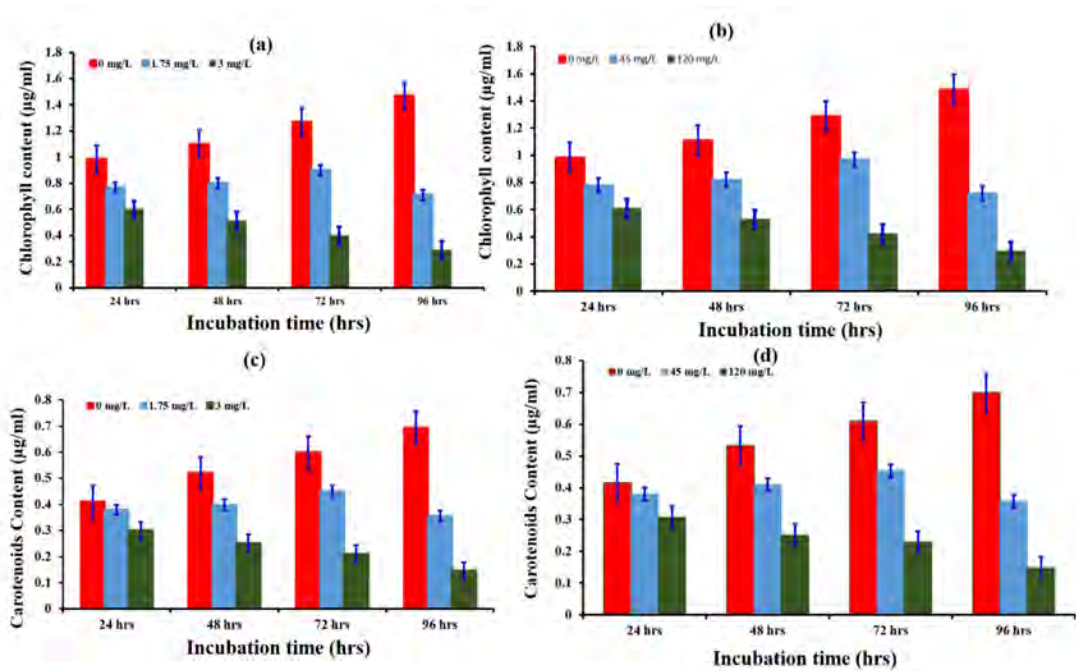


Figure 4.5: Effects of different concentrations of Cd and Pb on the photosynthetic pigments of two cyanobacteria strains: (a) effect of different Cd concentration on chlorophyll *a* content of *F. muscicola*; (b) effect of various concentrations of Pb on chlorophyll *a* content of *F. muscicola*; (c) effect of different Cd concentration on carotenoids content of *F. muscicola*; (d) effect of different concentrations of Pb on carotenoids content of *F. muscicola*.

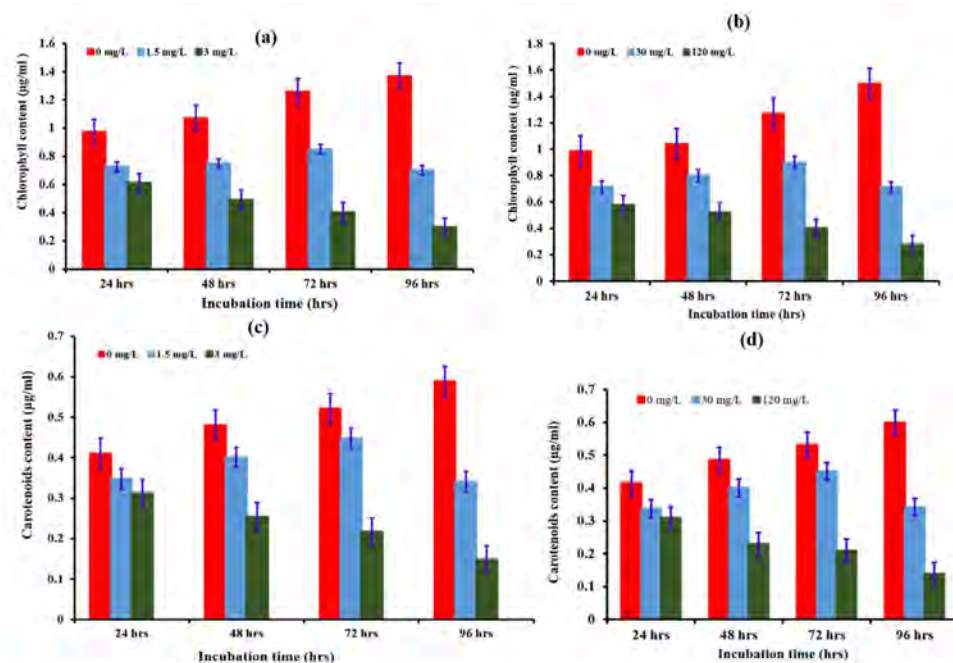


Figure 4.6: Effects of different concentrations of Cd and Pb on the photosynthetic pigments of two cyanobacteria strains: (a) effect of different Cd concentration on chlorophyll *a* content of *Nostoc* sp.; (b) effect of various concentrations of Pb concentration on chlorophyll *a* content of *Nostoc* sp.; (c) effect of different Cd concentration on carotenoids content of *Nostoc* sp.; (d) effect of different concentrations of Pb on carotenoids content of *Nostoc* sp.

4.3.4. FTIR

Figure 4.7aA, 4.7aB and 4.7aC show the FTIR spectra of *F. muscicola* untreated, Cd and Pb treated fresh biomass, respectively. Similarly, Fig 4.7bA, 4.7bB and 4.7bC represents the FTIR spectra of non-treated, Cd and Pb treated fresh biomass of *Nostoc* sp. The treatment of fresh biomass of cyanobacteria with Cd and Pb changed the absorption peaks which depicted the interaction of Cd and Pb ions with the functional groups of fresh biomass.

Figure 4.7aA, the spectrum of the untreated *F. muscicola* revealed numerous significant peaks at 3424, 3287, 2926, 2429, 1787, 1649, 1346, 1115, 1032, and 830 cm^{-1} . The broad band ranging from 3500 to 3050 cm^{-1} was indicative of the presence of O-H (hydroxyl) and N-H (amine) groups (Arif et al., 2021; Balaji et al., 2016). Detection of an absorption peak at 2926 cm^{-1} indicated the presence of carbon-hydrogen (C-H) stretching vibrations. This specific peak is linked to the stretching

vibrations of organic molecules of aliphatic C-H bonds (Sudhakar and Premalatha, 2015). Likewise, the absorption peak at 2429 cm^{-1} in the FTIR spectra linked to the stretching vibration of the carbon-nitrogen triple bond ($\text{C}\equiv\text{N}$, Cyano group). Moreover, the absorption peaks ranging from 1787 to 1649 cm^{-1} generally signifies the presence of a $\text{C}=\text{O}$ (carbonyl) functional group. These peaks are connected to the stretching vibration of the carbon-oxygen double bond ($\text{C}=\text{O}$) (Grace et al., 2020). Additionally, the peak observed at 1115 cm^{-1} wave number associated with the C-O stretching vibration in esters. Similarly, the peak at 1032 cm^{-1} associated with sulfoxide group ($\text{S}=\text{O}$) (Prabha and Anil, 2019).

Similarly, in the FTIR spectrum of non-treated *Nostoc* sp. biomass, numerous prominent peaks at wave numbers 3306, 2932, 2429, 1786, 1646, 1513, 1034, and 840 cm^{-1} were observed (Fig 4.7bA). The broad band ranging from 3500 to 3050 cm^{-1} was indicative of the presence of O-H (hydroxyl) and N-H (amine) groups (Arif et al., 2021; Balaji et al., 2016) and 3306 cm^{-1} is in the range of the presence of 3500 to 3050 cm^{-1} which indicates the presence of O-H and N-H functional groups. Peak at 2932 cm^{-1} corresponds to the existence of C-H stretching vibrations which is associated with the stretching vibrations of aliphatic C-H bonds present in organic compounds. Similarly the peak at 2429 cm^{-1} is linked to the stretching vibration of the carbon-nitrogen triple bond ($\text{C}\equiv\text{N}$). Peaks at 1786 cm^{-1} and 1646 cm^{-1} show the presence of $\text{C}=\text{O}$ (carbonyl) functional groups. Peak at 1513 cm^{-1} show the presence of N-O functional group. The peak at 1032 cm^{-1} corresponds to the sulfoxide group ($\text{S}=\text{O}$) and the peak 840 cm^{-1} show the bending of $\text{C}=\text{C}$ in alkene.

Specially, it has been found that the key functional groups engaged in the complexation of heavy metals are amines, hydroxyl, sulfoxide and carbonyl. These functional groups play a critical role in the binding and removal of heavy metals. Previously, the complexation of heavy metals by alcoholic and carboxylate groups in marine algal biomass was confirmed through the utilization of X-Ray Photoelectron Spectroscopy (XPS) (Sheng et al., 2004). Moreover, entirely functional groups cannot be deemed as responsible for removing heavy metals instead it is because of variety of different mechanisms (Volesky, 2003). The FTIR results of *F. muscicola* and *Nostoc* sp. fresh biomass indicated the presence of significant number of functional groups which indicated the presence of functional groups in both types of biomass facilitated the elimination of metals, rendering these strains viable candidates for the heavy

precipitation at high pH values and cause the decrease in the biosorption of metals. Significant increase in the acidity and alkalinity decreased the biosorption of Cd and Pb. At low pH, the observed phenomenon can be described to the intense competition of hydrogen ions on the surface of biosorbents due to protonation and the presence of positively charged adsorbate ions in acidic environment. The probable development of metal hydroxide precipitates in the solution causes a little drop in the adsorption of metal ions at higher pH (> 7) (El-Ashtoukhy et al., 2008). It is important to note that at high pH values, there may be precipitation between metal ions and hydroxide ions (Li et al., 2016). Consequently, all the biosorption experiments were conducted at pH 6 and 7 for Cd and Pb, respectively.

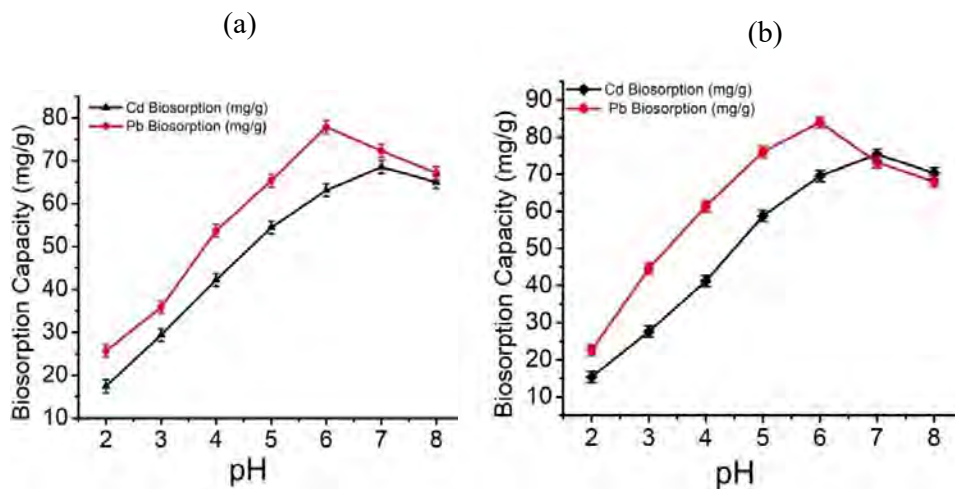


Figure 4.8: (a) Effect of pH on the biosorption of Cd and Pb by fresh biomass of *F. muscicola*; (b) Effect of pH on the biosorption of Cd and Pb by fresh biomass of *Nostoc sp.*

4.3.6. Effect of contact time on biosorption of Cd and Pb

This study examined the influence of contact duration the biosorption of Pb and Cd using the fresh biomass of *F. muscicola* and *Nostoc sp.*, with contact times ranging from 5 to 120 minutes, as illustrated in Figures 4.9a and 4.9b. With an increase in contact time between metal ions and biomass, the biosorption capacity of *F. muscicola* and *Nostoc sp.* increased to remove Cd and Pb from aqueous solutions. Initially, the biosorption process was fast, which can be credited to the presence of several active sites on the biosorbent material that instantly interacted with the heavy metal ions. Although, the accessibility of sites decreased over time, as these sites

became inhabited, consequent to slow biosorption of metals (Liu et al., 2016). Biosorption of Cd and Pb by fresh biomass of *F. muscicola* increased up to 120 minutes of contact time (Fig 4.9a). While the biosorption of Cd and Pb on to the fresh biomass of *Nostoc* sp. increased up to 90 and 120 minutes of contact time, respectively (Fig 4.9b). In previous studies, it has been described that the maximum biosorption of heavy metals on to the biomass of *S. obliquus* CNW-N (Chen et al., 2012), *Spirulina platensis* (Rangsayatorn et al., 2002), *Chlamydomonas reinhardtii* (Tüzün et al., 2005), and various brown algae (Montazer- Rahmati et al., 2011) occurred at 2 hours of contact time between metals and biosorbents. It is important to note that initial concentrations of heavy metals should not excessively be high due to toxicity of Pb and Cd on growth of algae. For instance, in this study, all concentrations of Cd and some of the Pb concentrations used for the biosorption experiments were higher than the tolerance level of cyanobacterial strains used in this study. Therefore, short-term heavy metals removal by *F. muscicola* and *Nostoc* sp. has an advantage in treating aqueous solutions containing high initial concentrations of heavy metals. Zhang et al. (2016) described that short-term removal of heavy metals by algae shows a distinct advantage in enhancing the removal rate which is important factor for industrial applications.

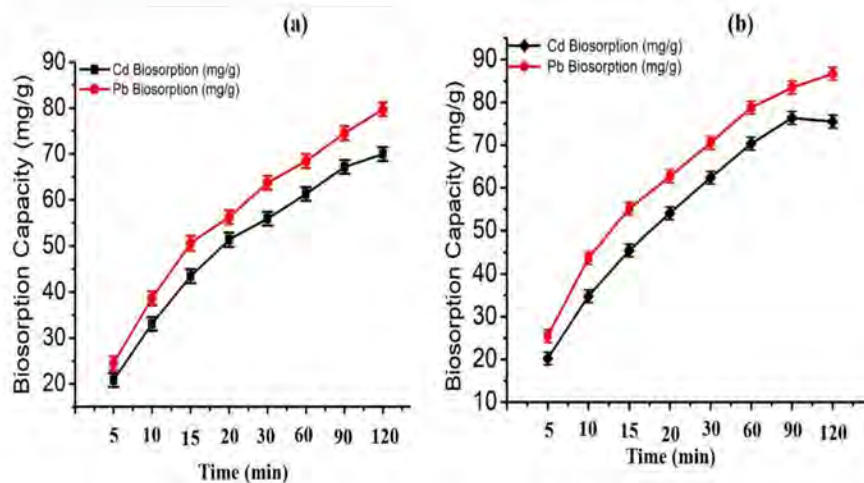


Figure 4.9: (a) Effect of contact time on Cd and Pb biosorption by fresh biomass of *F. muscicola*; (b) Effect of contact time on Cd and Pb biosorption by fresh biomass of *Nostoc* sp.

4.3.7. Kinetic study

Kinetic modeling plays crucial role in defining the dominant rate of biosorption and understanding the mechanism involved in the process. In this particular study, the mechanisms and rates of metal biosorption by the fresh biomass of *F. muscicola* and *Nostoc* sp. were investigated using kinetic models. The kinetic models of pseudo-first order, pseudo-second order and intraparticle diffusion are expressed through equations 4, 5, and 6, respectively.

$$\ln(q_e - q_t) = \ln q_e - K_1 t \quad (4)$$

$$\frac{t}{q_t} = \frac{1}{K_2 q_e^2} + \frac{1}{q_e} t \quad (5)$$

$$q_t = k_{id} t^{0.5} + C \quad (6)$$

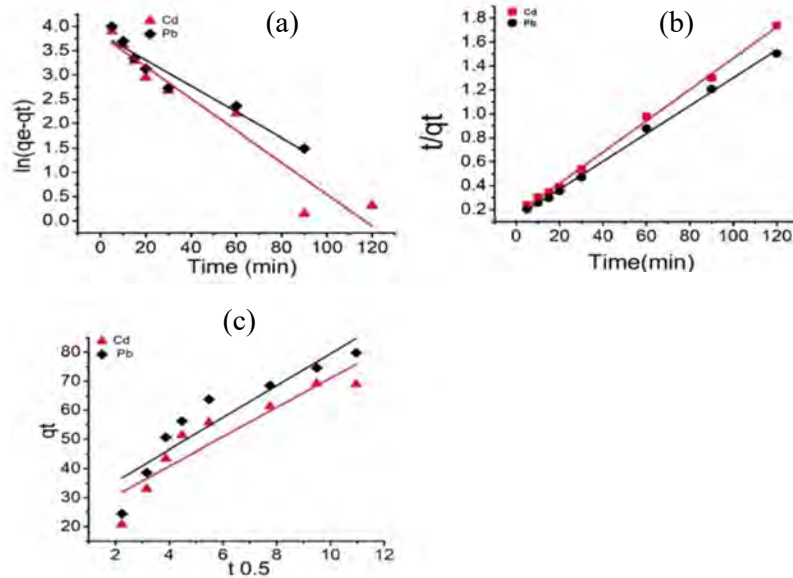


Figure 4.10: (a) Pseudo first order; (b) Pseudo second order; (c) Intraparticle diffusion, kinetics for the biosorption of Cd and Pb by fresh biomass of *F. muscicola*.

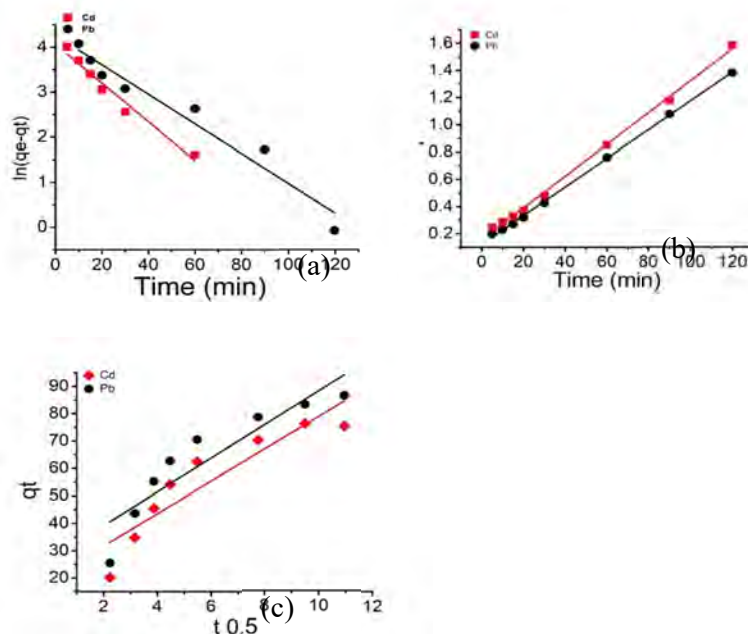


Figure 4.11: (a) Pseudo first order; (b) Pseudo second order; (c) Intraparticle diffusion, kinetics for the biosorption of Cd and Pb by fresh fresh biomass of *Nostoc* sp.

Linearized plots of equations 4-6 are depicted in Fig 4.10a, 4.10b, and 4.10c, respectively for the biosorption of Pb and Cd by *F. muscicola*. Similarly, Linearized plots of equations 4-6 are depicted in Fig 4.11a, 4.11b, and 4.11c, respectively for biosorption of Cd and Pb by fresh biomass of *Nostoc* sp. The kinetic parameters including rate constants, calculated biosorption capacity (mg/g) and correlation coefficients obtained from the plotted data are tabulated in Table 4.1. A comprehensive analysis of Table 4.1 reveals that the metals biosorption experimental data exhibited a remarkable fit to the pseudo-second-order kinetic model, as evidenced by the high R^2 values for Cd (0.997) and Pb (0.997) biosorption on to the fresh biomass of *F. muscicola* and high R^2 values for Cd (0.997) and Pb (0.999) biosorption on to the fresh biomass of *Nostoc* sp. The successful application of the pseudo-second-order model to the biosorption process indicates that Cd and Pb biosorption occurred through chemisorption process (Liu et al., 2012; Liu et al., 2016; Chen et al., 2018).

Table 4.1. Parameters of kinetic models

Kinetics models	Parameters	<i>F. muscicola</i>		<i>Nostoc sp.</i>	
		Cd	Pb	Cd	Pb
Pseudo first order	q_e (mg^{-1})	45.797	46.503	57.931	62.560
	K_1 (min^{-1})	-0.00036	-0.00022	-0.00048	-0.00038
	R^2	0.920	0.929	0.962	0.981
Pseudo second order	q_e (mg^{-1})	76.511	85.984	85.543	94.786
	K_2 ($\text{gmg}^{-1} \text{min}^{-1}$)	0.001	0.00098	0.00087	0.00091
	R^2	0.997	0.997	0.997	0.999
Intraparticle diffusion	K_i ($\text{mg g}^{-1} \text{min}^{-0.5}$)	5.035	5.499	5.917	6.161
	R^2	0.819	0.832	0.815	0.812

4.3.8. Effect of initial metal concentrations on biosorption

It was observed that as the concentrations of Cd ions increased from 20 to 100 mg/L, the biosorption capacity also increased from 19.2 to 70.37 mg/g, respectively. However, there was no further increase in the biosorption of Cd beyond 100 mg/L (Fig 4.12a). On the other hand, the biosorption of Pb continued to increase up to concentration of 120 mg/L. Similarly, as the concentrations of Pb ions increased from 20 to 120 mg/L, the biosorption capacity of the biosorbent also increased from 19.46 to 79.01 mg/g, respectively (Fig. 4.12b). The process of biosorbing metals onto the fresh biomass of *Nostoc sp.*, the effects of initial metal concentrations of Cd and Pb were investigated at pH 6 and 7, respectively. The biomass dosage for Cd and Pb was set at 1 g/L, and the contact periods were 90 minutes for Cd and 120 minutes for Pb (Fig 4.12b). The biosorption capacity increased from 18.34 to 75.33 mg/g as the concentrations of Cd metal ions increased (from 20 to 120 mg). Pb biosorption increased from 19.6 to 84.36 mg/g in a similar manner. An increase in the concentration of metal ions Pbs to a decrease in the barrier to mass transfer between metal ions and biosorbents, which in turn make the sites more accessible.

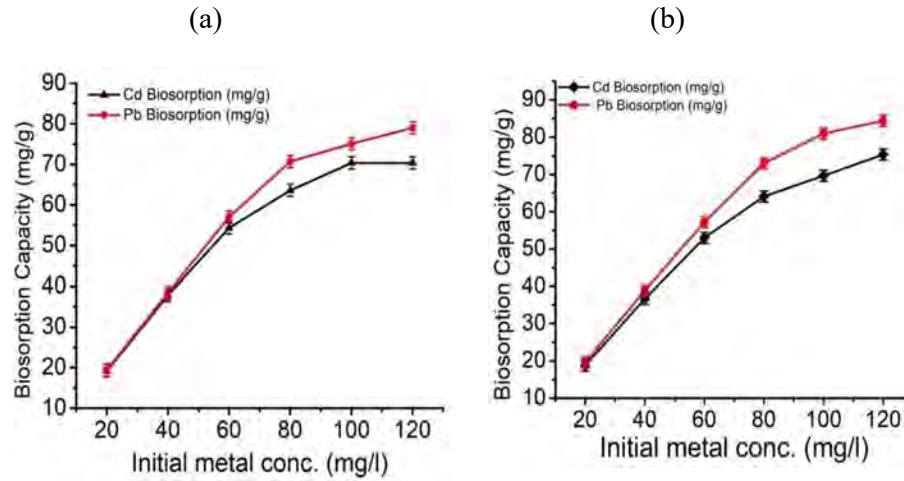


Figure 4.12: (a) Effect of initial metal concentrations on Cd and Pb the biosorption by the fresh biomass of *F. muscicola*; (b) Effect of initial metal concentrations on Cd and Pb ions biosorption by fresh biomass of *Nostoc* sp.

4.3.9. Isotherm study

Equilibrium data of Pb and Cd ions biosorption by *F. muscicola* and *Nostoc* sp. fresh biomass subjected to analysis using the Freundlich, Langmuir, and Temkin isotherm models. Langmuir model postulates that adsorption occurs in a monolayer fashion on the surface, where numerous accessible sites are present. Following equation (7) was used to obtain the parameters for Langmuir isotherm.

$$\frac{1}{q_e} = \frac{1}{K_L} \cdot \frac{1}{q_{\max}} \cdot \frac{1}{C_e} + \frac{1}{q_{\max}} \quad (7)$$

$$R_L = \frac{1}{1 + C_i \times K_L}$$

Freundlich isotherm model comprise the adsorption process on multilayer and heterogeneous surfaces (Freundlich, 1906). Such situations can be accounted for by employing the Freundlich isotherm equation (8).

$$\text{Log}q_e = \text{Log}K_f + \frac{1}{n} \text{log}C_e \quad (8)$$

In contrast to the logarithmic reduction, the Temkin model suggests that energy of adsorption decreases in a linear fashion as the adsorption sites become occupied (Temkin, 1940). The Temkin-Isotherm equation (8) can be described as follows:

$$q_e = \frac{RT}{b_T} \ln (A_T C_e) \quad (9)$$

$$q_e = B_T \ln (A_T) + B_T \ln (C_e)$$

$$B_T = \frac{RT}{b_T}$$

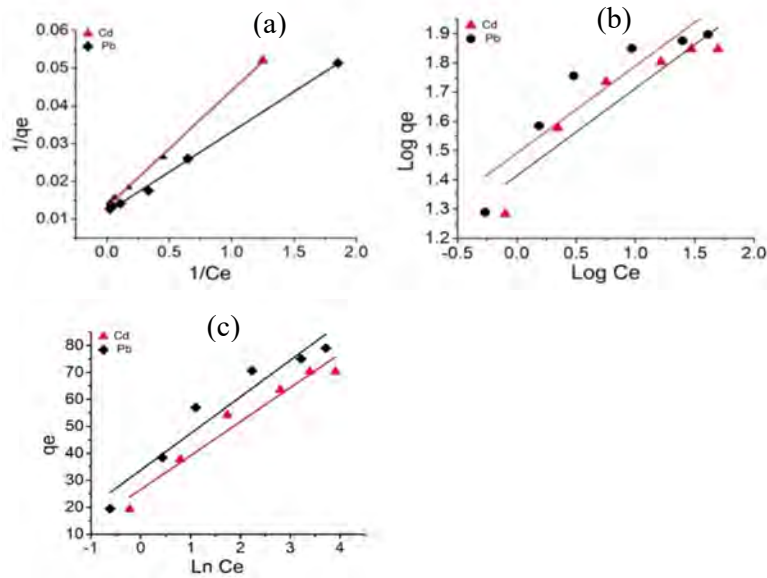


Figure 4.13: (a) Langmuir; (b) Freundlich; (c) Temkin, isotherm models for the biosorption of Cd and Pb by fresh biomass of *F. muscicola*.

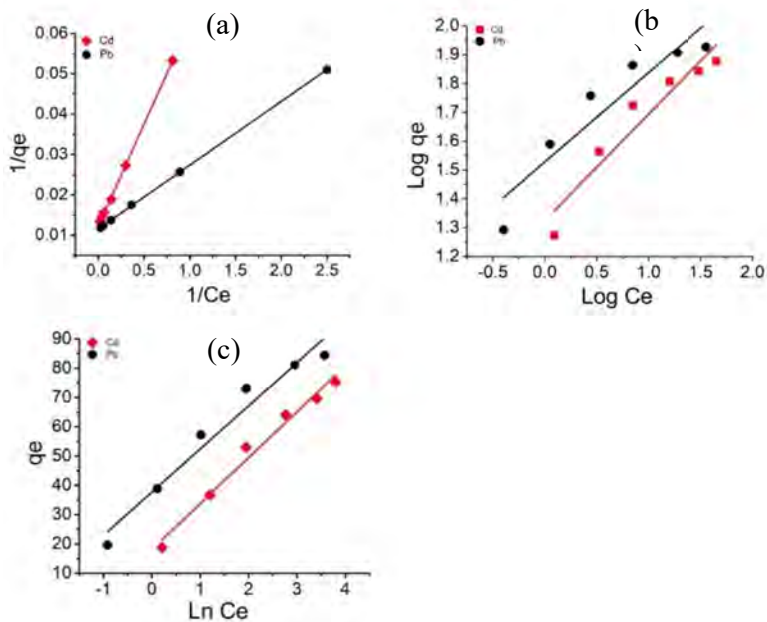


Figure 4.14: (a) Langmuir; (b) Freundlich; (c) Temkin, isotherm models for the biosorption of Cd and Pb by fresh biomass of *Nostoc* sp.

Figures 4.13a, 4.13b, and 4.13c exhibit the graphical representation of the isotherm models for biosorption of Cd and Pb by fresh biomass of *F. muscicola* and Fig 4.14a, 4.14b, and 4.14c exhibit the graphical representations of the isotherm models for biosorption of Cd and Pb by fresh biomass of *Nostoc* sp. Table 4.2 displays the entire information regarding the isotherm constants and correlation coefficients (R^2) acquired from the isotherm modeling. Based on the results, it was found that the Langmuir isotherm model provided the most accurate description of the data, as demonstrated by R^2 values (Table 4.2). This observation suggests that the biosorption process manifested itself consistently and transpired exclusively on the surface of the biosorbent in a homogenous manner (Liu et al., 2012).

The Langmuir isotherm model calculated maximum biosorption capacity of 75.301 mg/g for Cd and 84.38 mg/g for Pb for the biosorbent *F. muscicola*. Langmuir isotherm calculated *Nostoc* sp. maximum biosorption capacity as 81.699 mg/g for Cd and 86.730 mg/g for Pb. It showed that cyanobacterium *Nostoc* sp. removed more heavy metals from the contaminated aqueous solutions compared to the *F. muscicola*. A comparison between the maximum biosorption capacities of fresh cyanobacteria biomass employed in this study and other biosorbents documented in previous studies was also conducted (Mota et al., 2016; Fagundes-Klen et al., 2007; Hashim and Chu, 2004; Haghghi et al., 2017; Sarı and Tuzen, 2008; Abdel-Aty et al., 2013; Pavasant et al., 2006). It was observed that fresh cyanobacteria biomasses used in this research project were as more effective biosorbents than numerous other biosorbents reported previously (Table 4.3).

Table 4.2. Parameters of Isotherm models

Isotherm models		<i>F. muscicola</i>		<i>Nostoc sp.</i>	
	Parameters	Cd	Pb	Cd	Pb
Langmuir	q _{max} (mg/g)	75.301	84.38	81.699	86.730
	K _L (L/mg)	0.431	0.556	0.243	0.729
	R _L	0.0226	0.014	0.033	0.011
	R ²	0.998	0.997	0.999	0.999
Freundlich	K _f (mg/g)	25.952	30.984	21.191	33.747
	1/n	0.298	0.298	0.368	0.309
	R ²	0.848	0.807	0.892	0.850
Temkin	K _T	8.300	12.104	3.186	12.926
	B _T	12.577	13.564	15.649	14.732
	R ²	0.945	0.917	0.977	0.953

Table 4.3. Comparison of maximum biosorption capacities of *F. muscicola* and *Nostoc* sp. fresh biomass with other biosorbents.

Types of biosorbents	Maximum biosorption capacity (mg/g)	Reference
Cd		
<i>Cyanothece</i> sp. CCY 0110	16.5	(Mota et al., 2016)
<i>Nostoc sphaeroides</i>	116.28	(Jiang et al., 2016)
<i>Ulva lactuca</i>	29.20	Sarı and Tuzen, 2007
<i>Chlorella vulgaris</i>	62.30	(Kumar et al., 2015)
<i>Sargassum filipendula</i>	83.41	(Fagundes-Klen et al., 2007)
<i>Chlamydomonas reinhardtii</i>	42.71	(Tuzun et al., 2005)
<i>Cystoseira baccata</i>	56.2	(Lodeiro et al., 2006)
<i>Gracilaria edulis</i>	26.88	(Hashim and Chu, 2004)
<i>F. muscicola</i>	75.301	Current study
<i>Nostoc</i> sp.	81.699	Current study
Pb		
<i>Cyanothece</i> sp. CCY 0110	23.5	(Mota et al., 2016)
<i>Microcystis aeruginosa</i>	0.96	(Deng et al., 2020)
<i>Limnothrix</i> sp. KO05	82.18	(Haghighi et al., 2017)
<i>Ulva. Lactuca</i>	34.7	(Sarı and Tuzen, 2008)
<i>Rhizopus arrhizus</i>	56.0	(Fourest and Roux, 1992)
<i>Anabaena sphaerica</i>	121.95	(Abdel-Aty et al., 2013)
<i>Caulerpa lentillifera</i>	28.7	(Pavasant et al., 2006)
<i>F. muscicola</i>	84.38	Current study
<i>Nostoc</i> sp.	86.730	Current study

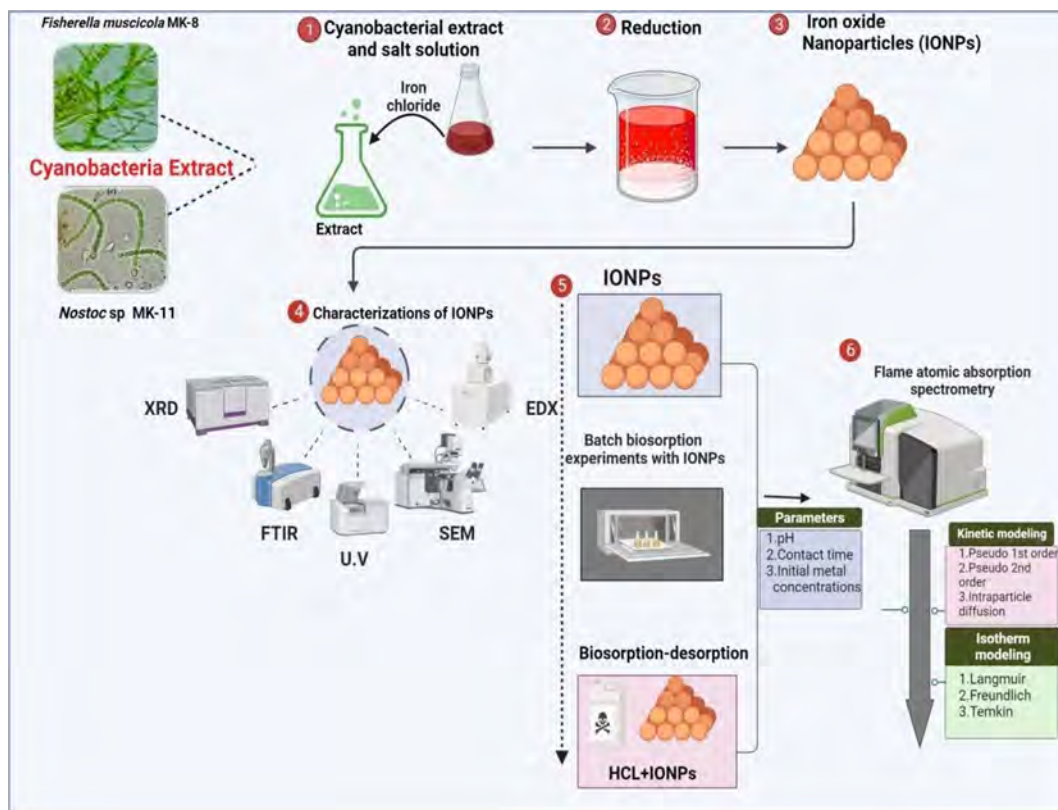
In conclusion results of current study show that:

- Cd and Pb affected the growth, biomass, chlorophyll *a* and carotenoids status in the cyanobacteria species (*F. muscicola* and *Nostoc* sp.).
- Both species have different level of tolerance against Cd and Pb toxicity. Interspecies Cd and Pb toxicity assessment identified *Nostoc* sp. as more tolerant compared to *F. muscicola*. The biosorption data showed fresh biomass of *Nostoc* sp. was found to be more effective than fresh biomass of *F. muscicola* to remove Pb and Cd from aqueous solutions.
- The mechanism of Cd and Pb ions binding to biomass of both cyanobacteria species was chemisorption and homogeneous.

CHAPTER 5

Fabrication of Iron Oxide Nanoparticles using *Fischerella muscicola* and *Nostoc* sp. extracts and their utility in adsorbing Cd and Pb from aqueous solutions.

Graphical Abstract



Graphical abstract: Graphical representation of Iron oxide nanoparticles synthesis, characterization and adsorption of Cd and Pb from aqueous solutions.

Summary

Water contamination is a worldwide issue consequent to the increasing human population and fast expansion of industrial activities. In the current study, Iron oxide nanoparticles were prepared using two cyanobacterial (*Fischerella muscicola* and *Nostoc* sp.) extracts and investigated for their capacity to remove Cd and Pb from aqueous solution. FTIR, XRD, UV-Vis, SEM, and EDX were employed to study chemical structure and surface morphological properties of the biosynthesized IONPs. The influence of pH, initial concentrations of metals, and contact duration on the adsorption of Pb and Cd ions onto iron oxide nanoparticles was examined. To analyze the adsorption mechanism, several kinetic models, including Pseudo first order, Pseudo second order, and Intraparticle diffusion kinetics, as well as isotherm models such as Langmuir, Freundlich, and Temkin, were employed to interpret the experimental data. Modeling results showed the Pseudo second order and Langmuir isotherm models as best fit to the experimental biosorption data.

Langmuir isotherm calculated maximum isotherm adsorption capacity of *F. muscicola* mediated IONPs as 93.370 and 94.161 mg/g for Cd and Pb, respectively. Similarly, the Langmuir isotherm determined the maximum adsorption capacities to be 118.764 mg/g for Pb and 105.932 mg/g for Cd. Following five cycles of adsorption and desorption, IONPs maintained their adsorption efficiency, exhibiting only a minimal reduction. Finding of this study revealed that *Nostoc* sp. mediated IONPS showed higher potentials of adsorbing Cd and Pb ions compare to *F. muscicola* mediated IONPs. Over all findings of this study suggest that both cyanobacteria have the potentials metabolites to cap the iron metal ions for the synthesis of IONPs and remove the Cd and Pb with significantly high potential. This shows that the Nanoparticles synthesized using cyanobacteria extract could be used for the potential industrial applications to remove heavy metals from the polluted environment in quick time.

5.1. Introduction

Heavy metals (HMs) are naturally found in the Earth crust. However, human activities like mining, agriculture, and industrial emissions contribute HMs into the environment (Sarker et al., 2022). These are well known environmental pollutants due to their toxic features, persistence, and ability to accumulate in living organisms (Ali et al., 2019). In various countries, the concentrations of HMs in ground water, soil, and several water bodies have surpassed permissible limits due to population growth, unplanned industrialization, urbanization, and insufficient management policies, offering a hidden risk to the human food chain (Khalid et al., 2017; Sarker et al., 2022; Rakib et al., 2022). Cd and Pb are heavy metals that are particularly hazardous environmental pollutants for both plant life and human health (Lou et al., 2013). Their pollution has a major negative impact on aquatic ecosystems and human well-being (Liu et al., 2022). Therefore, it is essential to mitigate Cd and Pb harmful impacts on the environment while also reducing their availability in the food chain.

Several traditional approaches have been employed to remove heavy metals from polluted water sources. These methods encompass an extensive array of techniques, which include physical, chemical, and conventional processes such as coagulation, membrane filtration, reverse osmosis, ion exchange, and electrolysis (Chen et al., 2020). However, the effectiveness of these traditional methods is limited when dealing with high metal concentrations and their large-scale applications become cost intensive. During traditional treatments secondary pollutants are released which pose adverse effects on the ecosystem and require further remediation processes (Barakat, 2011). Consequently, the development of cost-effective and sustainable techniques to remove heavy metals from water sources ensures the provision of safe and uncontaminated drinking water.

Recently, nano-bioremediation has been identified as a promising method for reducing heavy metal contamination in the environment. Innovative nanomaterial-based technologies have gained significant attention for environmental remediation. Notably, a variety of nanocomposite adsorbents for HMs removal from the field are now commercially accessible, including graphene, iron oxide nanoparticles, carbon nanotubes, and zero-valent iron (Soltani et al., 2014; Xu et al., 2012; Zhang and Pan 2014). These strategies typically provide a broader array of options for the management of pollutants in wastewater and groundwater (Yogalakshmi et al., 2020),

sediments contaminated with heavy metals and hydrocarbons (De Gisi et al., 2017), as well as inorganic or organic substances in the soil (Bharagava et al., 2020) by minimizing process intermediates, reducing related costs, and alleviating their negative environmental effects. As new technologies emerge, scientists and organizations have proposed a major growth in the application of nanomaterials to meet the growing demands in different application areas (Vazquez-Nunez and colleagues, 2020). Consequently, there is a necessity for innovative nanomaterials that exhibit enhanced efficacy in environmental remediation. Compared to other contemporary materials, nanomaterials exhibit enhanced absorption and catalytic abilities because of their larger specific surface areas, lower temperature needs for modification, adjustable pore sizes, reduced inter-particle diffusion distances, more adsorption sites, and diverse surface chemical properties (Wu et al., 2019).

IONPs have been employed frequently to remove HMs from polluted water because of their tiny size, high surface area, biocompatibility, and superparamagnetic characteristics (Xu et al., 2012). NPs are synthesized using a variety of physical and chemical techniques, including hydrothermal, laser ablation, sol-gel synthesis, and lithography etc., which require specific tools, expertise and may have harmful impacts on human health. On the contrary, biological techniques offer cost-effective, non-toxic, and biodegradable methods for NPs synthesis (Darroudi et al., 2014; Iravani, 2011; Nadagouda and Varma, 2008; Virkutyte and Varma 2011). These environment friendly techniques utilize less hazardous substances and natural resources such as bacteria, fungi, algae, and plant extracts (leaf, root, and flower) (; Rajiv et al., 2013; Shinde, 2015; Behravan et al., 2019). Successful synthesis of NPs using different salts as a precursor metals has been demonstrated, such as Ag, Au (Dash et al., 2014), Zn, Cu, Ti (Schabes-Retchkiman et al., 2006), Cd (Suresh, 2014), Fe (Minhas et al., 2023a), along with alginate (Asadi, 2014), have been identified in various studies.

Cyanobacteria are photosynthetic prokaryotes found in a variety of habitats (Singh et al., 2014). These have numerous applications in bioremediation, in dietary supplements, as biomedicine, in agriculture industry and serve as significant source of secondary metabolites with anticancer and antibacterial activities (Ai et al., 2020). Numerous studies show the use of cyanobacteria in NPs synthesis and reports suggest that they are excellent bio-systems for synthesizing the NPs both intracellularly and extracellularly (Pathak et al., 2019). Notably, in recent studies *Desertifilum* sp. and

Oscillatoria limnetica have been successfully used in NPs synthesis through cost-effective and eco-friendly methods highlighting their wide range applications in biomedical field (Hamida et al., 2020; Hamouda et al., 2021). However, studies on the biogenic synthesis of nano-sized iron are limited. For example, *Anabaena flos-aquae* and *Calothrix pulvinata* have been found to synthesize akaganeite (FeOOH) nanorods (Brayner et al., 2012). Literature shows that there are no studies on the adsorption of Pb and Cd by IONPs synthesized from the extract of cyanobacteria.

Therefore, in this study, IONPs were synthesized using cyanobacteria (*F. muscicola* and *Nostoc* sp.) extract and they were characterized using various analytical techniques. As-obtained functionalized IONPs were systematically investigated for their applications as Pb and Cd nano-adsorbents. The experimental factors, including contact time, pH, initial metal concentrations, were studied through batch methods. Many Kinetic and Isotherm models were used to study the rate and mechanism of Pb and Cd adsorption onto IONPs. Furthermore, the reusability of the nanoadsorbent was investigated.

5.2. Materials and Methods

5.2.1. Chemicals

To prepare salt solution, iron chloride hexahydrate ($\text{FeCl}_3 \cdot 6\text{H}_2\text{O}$) was used. Cd chloride (CdCl_2) and Pb nitrate ($\text{Pb}(\text{NO}_3)_2$) were used to synthesize metal ions solutions for the adsorption experiments. NaOH and HCl were used to adjust the pH of the media and other solutions.

5.2.2. Biogenic synthesis of cyanobacteria extract mediated IONPs

Using a pestle and mortar, cyanobacteria (*F. muscicola* and *Nostoc* sp.) biomass was crushed into a fine powder and sieved through a 100 μm mesh. Powdered biomass of both cyanobacteria was mixed with water separately in conical flasks and subjected to heating in a water bath for 24 hrs at 100°C to obtain the extracts. Subsequently, 100 mL of filtered extract was mixed with 3 g of iron chloride hexahydrate. A mixture of salt and cyanobacteria extract was continuously heated on a hot plate at 70 °C for 2 hrs. Changes in the color of solution were noted to confirm the synthesis of IONPs. After the completion of extract and salt solution reaction, centrifugation was performed at 3000 rpm for 30 minutes to isolate the IONPs from the solution. To eliminate impurities, IONPs pellet was washed three to four times

with double distilled water. The resulting dry powder, designated IONPs, was incubated at 75 °C for two hours. The dried material was ground into powder and calcined for two hours at 400 °C in an open-air furnace. Calcined IONPs were stored in a dry, cold, and dark condition for further investigation (Minhas et al., 2023a). Figure 5.1 shows the schematic presentation of biogenic synthesis of IONPs.



Figure 5.1: Biogenic synthesis of IONPs

5.2.3. Physio-chemical Characterizations of IONPs

Cyanobacteria mediated IONPs were subjected to comprehensive characterization using various analytical techniques such as UV-Vis, XRD, FTIR, EDX and SEM. A UV-visible spectrophotometer in the wavelength spectrum of 200 to 800 nanometers was used to evaluate the Surface Plasmon Resonance (SPR) of the IONPs and the biomolecules responsible for the reduction, stabilization, and capping of IONPs were identified using FTIR analysis (range 500-4000 cm^{-1}). Origin Pro 8.5 software was used to analyze the spectra of FTIR. IONPs surface appearance was determined using SEM. This technique provided valuable insights about the physical properties of the NPs. EDX analyses were performed to identify the presence of Fe and other elements associated to the IONPs and the values of EDX provided the information about the atomic content of the synthesized NPs, reflecting their atomic

structure. X-ray diffractometer was used for XRD analysis to check the purity of the prepared IONPs and the mean crystalline size of the synthesized IONPs was calculated using Scherrer equation.

5.2.4. Adsorption Batch study

Adsorption studies were performed using IONPs as adsorbents and Pb and Cd ions as adsorbates. One gramme of the adsorbent was dissolved in 100 milliliters (ml) of an aqueous solution containing metal ions at a concentration of 100 milligrams (mg) per liter in a 250 ml conical flask. In the current study, effect of different factors such as pH (ranging from 2-8), initial metal ions concentration (20-120 mg/L) and contact time (5-120 minutes) on the adsorption of metal ions onto the adsorbents were studied. Mixture of adsorbate and adsorbents were stirred at 150 rpm using an orbital shaker for a predetermined period at 25°C. Whatman-40 filter paper was used to filter the solution and Initial and final metal concentrations in the filtrate were determined using Agilent Flame Atomic Adsorption Spectrometer (FAAS). Adsorption capacity (mg/g) of IONPs was calculated using equation 1.

$$q_e = \frac{(C_i - C_e)}{w} \times V \quad (1)$$

5.2.5. Desorption and reusability

For the desorption and reusability studies, Cd and Pb loaded IONPs were dissolved in 0.1 M hydrochloric acid (HCL) solution for 1 hour at 150 rpm. Metals-loaded IONPs were rinsed three times with distilled water before to the desorption investigation to eliminate any loosely attached Cd and Pb ions from the surface of the adsorbents. Following the desorption investigation, supernatant was collected for further analysis and IONPs were carefully washed with distilled water after each cycle to neutralize and re-condition them for further adsorption and desorption studies.

Each experiment was performed in triplicates and the results were presented as the mean of three replicates. The data shown in figures and tables describe the average values plus or minus the standard deviations calculated from all the repeated measurements. The statistical analysis of the data was achieved using OriginPro 8.5 (OriginLab Corporation, Northampton, Massachusetts, USA) and Microsoft Office Excel (2010) software.

5.3. Results and Discussion

5.3.1. Physiochemical Characterizations

5.3.1.1. Colour indication

Biogenic synthesis of IONPs was conducted using cyanobacteria extract derived from *F. muscicola* and *Nostoc* sp. The dark brown color of the IONPs was observed following the reaction between the extract and the salt solution. The colors of the extract, salt solution, and IONPs are illustrated in Figures 5.2a (IONPs mediated by *F. muscicola*) and 5.2b (IONPs mediated by *Nostoc* sp.). The final dark brown color of extract and salt solution is a strong indication for successful fabrication of *F. muscicola* and *Nostoc* sp. mediated IONPs. Surface Plasmon resonance and the interaction of metal ions with bioactive compounds are responsible for the distinctive color change (Sharif et al., 2023). Figure 5.2c explains the biological reduction mechanism of Iron Oxide NPs using *F. muscicola* and *Nostoc* sp.

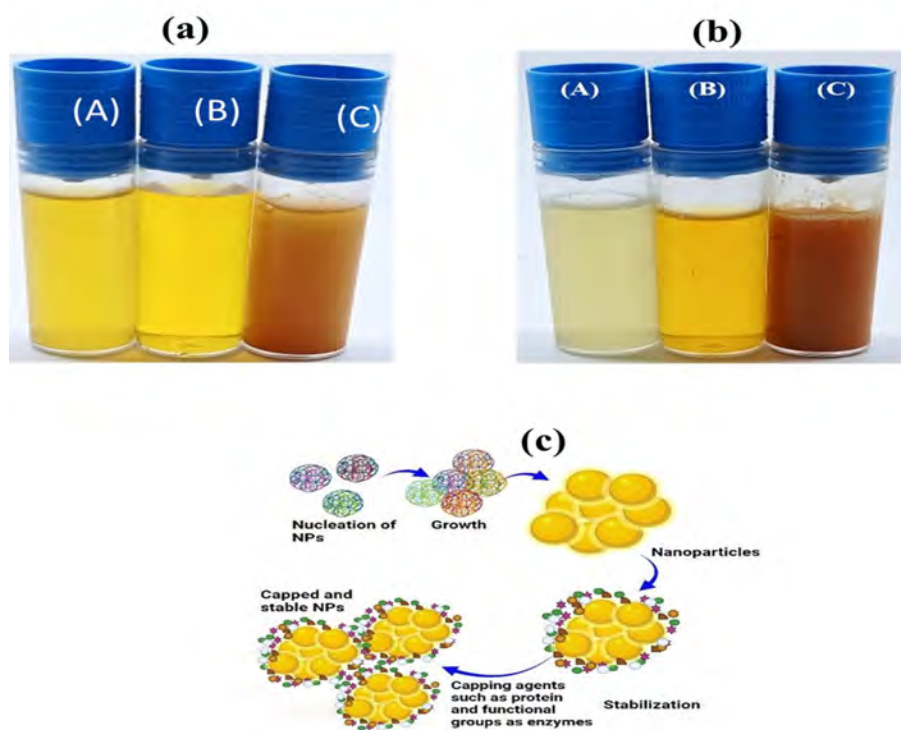


Figure 5.2: (aA) Extract of *F. muscicola*; (aB) Iron chloride hexahydrate salt solution; (aC) dark brown IONPs; (bA) extract of *Nostoc* sp.; (bB) Iron chloride hexahydrate salt solution; (bC) dark brown IONPs; (c) Biological reduction mechanism of Iron Oxide NPs using *F. muscicola* and *Nostoc* sp. extracts.

5.3.1.2. UV-visible spectroscopy

Confirmation of IONPs synthesis in solution was subsequently verified by conducting UV-visible spectroscopic analysis spanning the wavelength spectrum of 300-800 nm. The most prominent peak which indicated the successful synthesis of IONPs using extract of *F. muscicola* was found at 404 nm (Fig 5.3a). Similarly, the most prominent peak at 348 nm was found when the IONPs were synthesized using the extract of *Nostoc* sp. (fig 5.3b). These specific absorbance peaks correlate to the SPR characteristics of IONPs as depicted in Figures 5.3a and 5.3b. UVis analyses have a significant part in detailed characterization of IONPs, enabling the acquisition of crucial insights into their morphology, size, and stability (Abdel-Raouf et al., 2019). Notably, these findings align with the results described in previous studies (Minhas et al., 2023a).

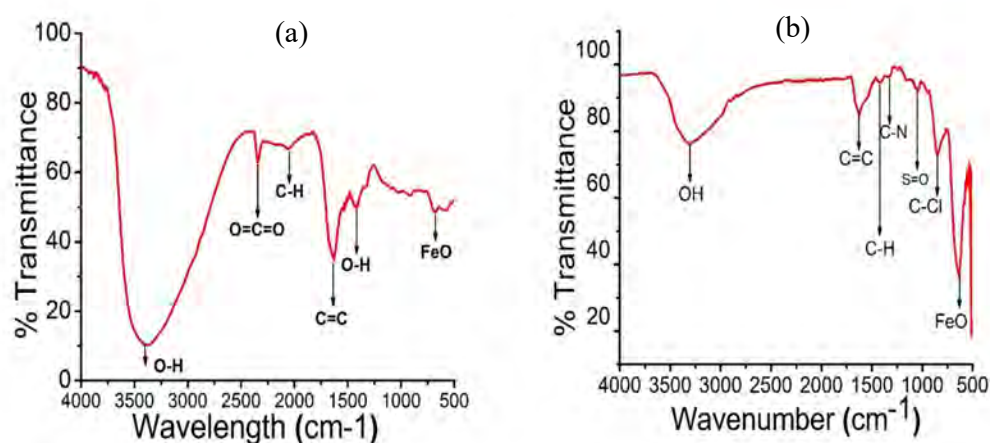


Figure 5.3: U. Vis spectra of IONPs: (a) U.V spectra of IONPs (*F. muscicola* mediated IONPs); (b) U.Vis spectra of IONPs (*Nostoc* sp. mediated IONPs).

5.3.1.3. FTIR

FTIR is a useful tool for identifying and characterizing chemicals, such as the functional group responsible for reduction and functioning as a capping agent in biosynthetic nanoparticles (Elrefaey et al., 2022). In the *F. muscicola* mediated synthesized IONPs, FT-IR analysis revealed major peaks at 3387, 2349, 1996, 1629, 1423, and 684, cm⁻¹ (Fig. 5.4a). The peaks at 3387 cm⁻¹ and 1423 cm⁻¹ were identified as OH stretching, H-bonded alcohols, and phenols, respectively, while the spectrum at 2349 cm⁻¹ was assigned to the stretching vibration of O=C=O and the peak at 1996 cm⁻¹ to the CH-aliphatic. Another band at 1629 cm⁻¹ could be linked to alkene C=C

stretching vibrations. The peak at 684 cm^{-1} was attributed to typical IONPs band absorption peaks.

FTIR results demonstrated the role of various chemicals in *F. muscicola* extract in the reduction, capping, and stabilization of biosynthesized IONPs (Fig. 5.4a). Similar studies have revealed that metal oxides exhibit absorption bands in the fingerprint regions below 1000 cm^{-1} due to inter-atomic vibrations (Naseer et al., 2020). Similarly, the FTIR analysis was conducted for the IONPs synthesized using extract of *Nostoc* sp. (Figure 5.4b). FTIR spectrum exhibited seven distinct peaks at wavenumbers of 3321, 1632, 1450, 1327, 1041, 848, and 631 cm^{-1} . Width of peaks may be attributed to both intra- and intermolecular hydrogen bonding interactions (Khalafi et al., 2019). Furthermore, this research revealed a distinct band at 1632 cm^{-1} that can be related to the C=C stretching vibration observed in alkenes. The presence of C-H stretching modes in asymmetric and symmetric carbohydrates or lipids, as previously reported by Duygu et al. (2012), was also indicated by the detection of a strong peak at 1450 cm^{-1} . FTIR analysis of the IONPs revealed the presence of sulfoxide and hydroxyl groups, as evidenced by distinct peaks at 1041 and 3321 cm^{-1} , respectively. These findings suggest the reduction of Fe^{+3} ions and the biogenic synthesis of IONPs (Iram et al., 2010). Additionally, peaks observed at 1327 cm^{-1} correspond to the C-N stretching mode associated with amino acids, while the peak at 848 cm^{-1} is indication of stretching vibration of C-Cl bonds (Hamza et al., 2018). Moreover, the absorption band at 631 cm^{-1} provides strong evidence for the successful formation of Fe-O bonds. Consistent with our results, previous studies on the FTIR spectroscopy of biosynthesized iron oxide nanoparticles have reported absorption bands at wavelengths such as 550 cm^{-1} (Minhas et al., 2023a), 618 cm^{-1} (Karpagavinayagam and Vedhi, 2019), 631 cm^{-1} (Hwang et al., 2014) and 634 cm^{-1} (Sodipo and Azlan, 2015). These collective findings from FTIR spectroscopy suggest that the *Nostoc* sp. and *F. muscicola* extracts possess organic compounds that serve as stabilizing, reducing and capping agents in the process of IONPs synthesis.

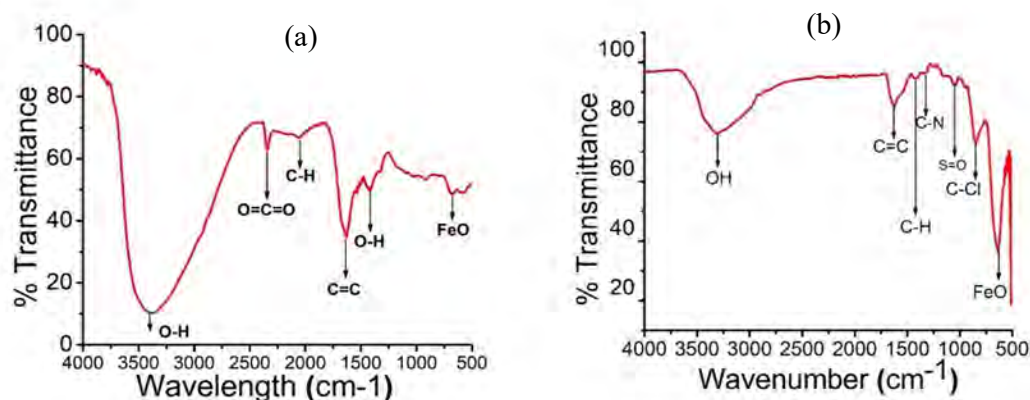


Figure 5.4: FTIR spectra of biogenic IONPs: (a) FTIR spectra of *F. muscicola* extract mediated IONPs; (b) FTIR spectra of *Nostoc* sp. extract mediated IONPs

5.3.1.4. X-ray diffraction

XRD is a useful tool for examining the crystalline form of IONPs and determining their crystalline size. The crystalline structure of *F. muscicola* mediated IONPs was investigated using an X-ray diffractometer. Before performing X-ray diffraction, biogenic IONPs were annealed at 400 °C. These biologically synthesized IONPs showed a good crystalline structure in their XRD pattern (Fig. 5.5a). Seven different peaks corresponding to 2 theta degrees were observed: 27.47°, 35.96°, 38.69°, 44.05°, 57.49°, 60.75°, and 65.84°. These peaks matched with (104), (110), (113), (202), (112), (214), and (300) planes. XRD pattern of IONPs agreed with the crystallographic planes characteristic of IONPs in a rhombohedral structure, which corresponds to the JCPDS Card No. 00-005-0586. The average crystalline size was found ≈ 28 nm using the Debye-Scherrer equation (Fig. 5.5b). It is important that the XRD spectra contain small peaks that may be linked to the crystallization of organic compounds on the surface of nanoparticles (Hameed et al., 2023; Khalafi et al., 2019).

Similarly, XRD analysis for the IONPs mediated by *Nostoc* sp. extract was also performed. A single pure rhombohedral hematite phase was identified by the XRD pattern, and it was aligned with Bragg peaks that were assigned to JCPDS Card No. 00-006-0694. The XRD distinct diffraction peaks of IONPs (Fig. 5.5c) synthesized by magnetic stirring were indexed at 2 theta values of 38.56°, 44.37°, 64.51°, and 81.72°, which were unambiguously associated with Bragg's reflections at planes 101, 110, 200, and 211, respectively. Additionally, the mean crystalline size of IONPs was calculated using the Scherrer equation, providing an average size of 18.21 nm (Fig. 5.5d) for each particle. This was accomplished by utilizing the high-intensity peak in

the (101) plane of the diffractogram. This analysis indicates the crystalline nature of the IONPs. The outcomes of this study are consistent with previously reported research on iron oxide nanoparticles synthesized through biological methods (Ondiek, 2016).

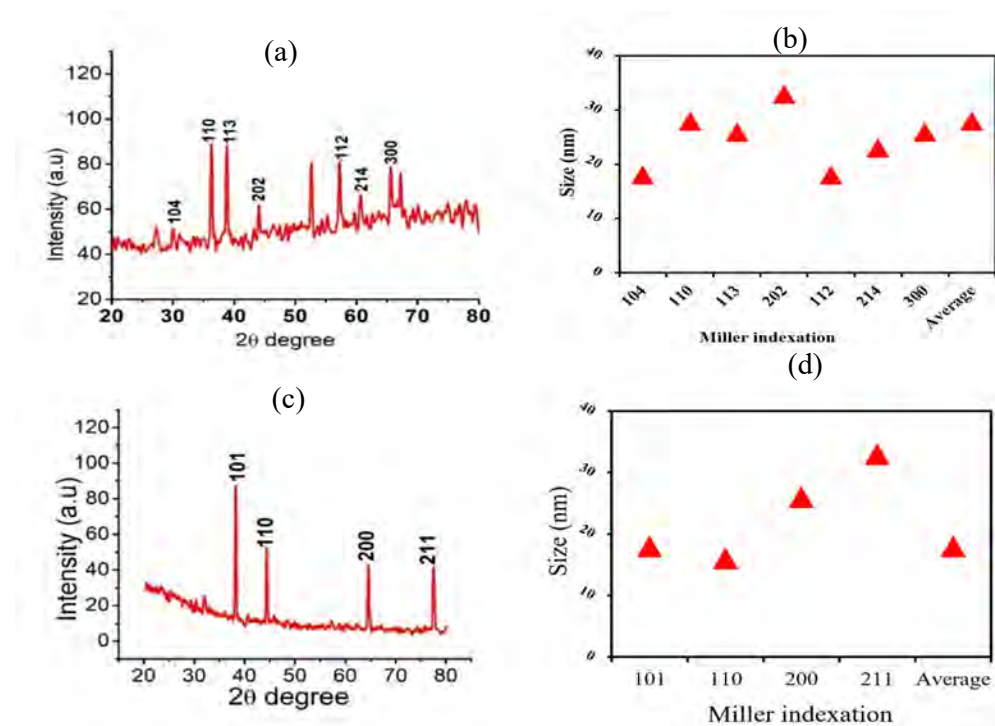


Figure 5.5: (a) XRD pattern of *F. muscicola* mediated IONPs; (b) Size calculation of *F. muscicola* mediated IONPs; (c) XRD pattern of *Nostoc* sp. mediated IONPs; (d) size calculation of *Nostoc* sp. mediated IONPs.

5.3.1.5. Energy dispersive X-Ray and Scanning electron microscopy

EDX analyses were conducted to determine the elemental composition of *F. muscicola* mediated IONPs (Fig 5.6a) and *Nostoc* sp. mediated IONPs (Fig 5.6b). EDX analysis showed that the *F. muscicola* mediated IONPs contained components including Zn, Na, Al, O, Ca, K, Fe and C and *Nostoc* sp. mediated IONPs contained K, Na, O, Cl, C and Fe. EDX spectrum also confirmed the successful synthesis of IONPs using the metabolites of *F. muscicola* and *Nostoc* sp. It also highlighted that Fe and O were the predominant constituents of the nanostructure. Notable abundance of both iron and oxygen in the EDX results relate the single phase purity of the IONPs, in alignment with the findings reported previously (Nair et al., 2023). The presence of additional peaks in the EDX spectrum for C, Na, Al, and K are due to capping agents

like sugars, amino acids, polysaccharides and proteins which are considered the principal components of cyanobacteria extracts. SEM was used to observe the surface morphological characteristics of IONPs. Figure 5.6c and 5.6b show the SEM images of the *F. muscicola* and *Nostoc* sp. mediated IONPs. The SEM analysis unveiled the spherical or agglomerated forms of *F. muscicola* mediated IONPs and shapes of the *Nostoc* sp. mediated IONPs was spherical or cubic.

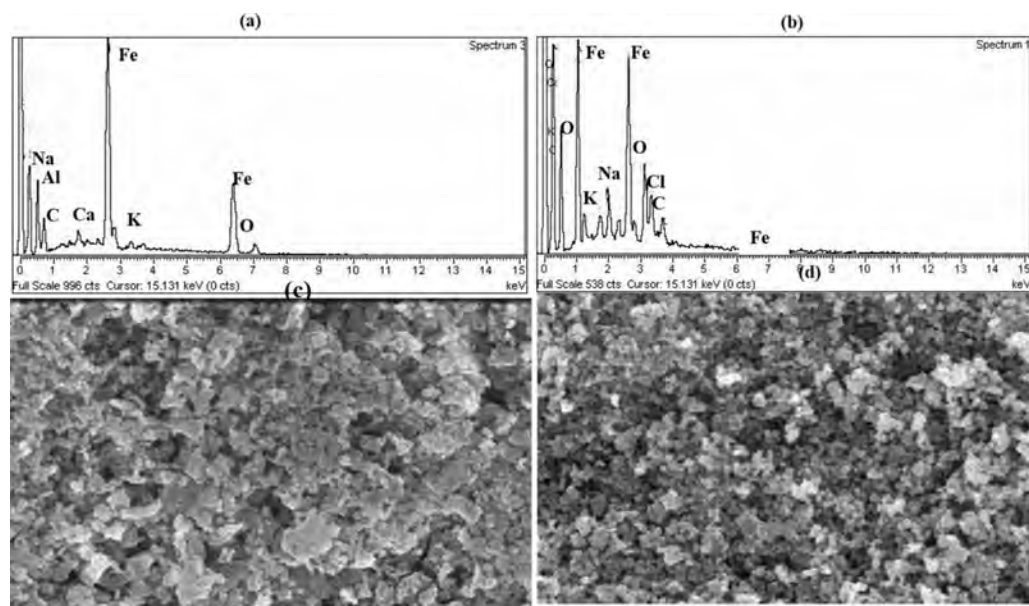


Figure 5.6: (a) EDX spectrum of *F. muscicola* mediated IONPs; (b) EDX spectrum of *Nostoc* sp. mediated IONPs; (c) SEM image of *F. muscicola* mediated IONPs; (d) SEM image of *Nostoc* sp. mediated IONPs

5.3.2. Impact of pH on the adsorption of metals

pH of the solution is critical in maintaining the surface charge characteristics of NPs and behavior of the metal ions. In this study, a systematic examination of metal ions adsorption onto the IONPs mediated by using *F. muscicola* extract and IONPs mediated by *Nostoc* sp. was conducted across a pH range from 2, 3, 4, 5, 6, 7 to 8. Effects of different pH on the adsorption of Cd and Pb ions on to the *F. muscicola* mediated IONPs and IONPs mediated by *Nostoc* sp. are shown in figure 9a and 9b, respectively. Results showed that the *F. muscicola* mediated IONPs had a limited ability to adsorb Cd and Pb in a low pH (2) environment, with removal capacity of about 15.5 and 29.13 mg/g for Cd and Pb, respectively. Similarly, the *Nostoc* sp. mediated IONPs also showed the limited adsorption of Pb and Cd with removal

capacity 27.57 and 20.9 mg/g, respectively. This behavior can be related to the competition between protons and metal ions for active binding sites on the surface of IONPs. These activesites get protonated at lower pH levels because of the presence of the additional protons, which reduces the ability of metal ions to bind with the adsorbent (Barros et al., 2007; Wang et al., 2012). Adsorption capacity of IONPs improved as the pH of the solution increased, achieving peak adsorption at pH 6 for Cd and pH 5 for Pb. This is illustrated in Figure 5.7a, which highlights the optimal pH conditions for these metals. *F. muscicola* mediated IONPs showed a remarkable adsorption capacity of 83.71 and 85.55 mg/g, respectively. Likewise, *Nostoc* sp. mediated IONPs removed remarkable concentrations of Cd and Pb with removal capacity of 85.44 mg/g for Cd and 95.13 mg/g for Pb Figure (5.7b).

However, it is essential to note that the adsorption of Cd ions began to decline after pH 6, and reduction in Pb ions adsorption was observed after pH 5. The presence of hydrolyzed Pb ions after pH 5 could be the reason for decreased Pb adsorption. It is interesting to note that depending on the pH, Pb may exist in a variety of various forms, including $\text{Pb}(\text{OH})^{3-}$, $\text{Pb}_3(\text{OH})_4^{2+}$, $\text{Pb}(\text{OH})^+$, $\text{Pb}_3(\text{OH})^{3+}$, $\text{Pb}_6(\text{OH})_8^{4+}$ and $\text{Pb}_6\text{O}(\text{OH})^{4+}$ (Breza and Manova, 2002). Beyond pH 5, Pb ions convert into $\text{Pb}(\text{OH})^{3-}$, and electrostatic repulsion strongly attracts $\text{Pb}(\text{OH})^{3-}$ to the negatively charged surface of the adsorbent (Ebrahim et al., 2016; Sarojini et al., 2021).

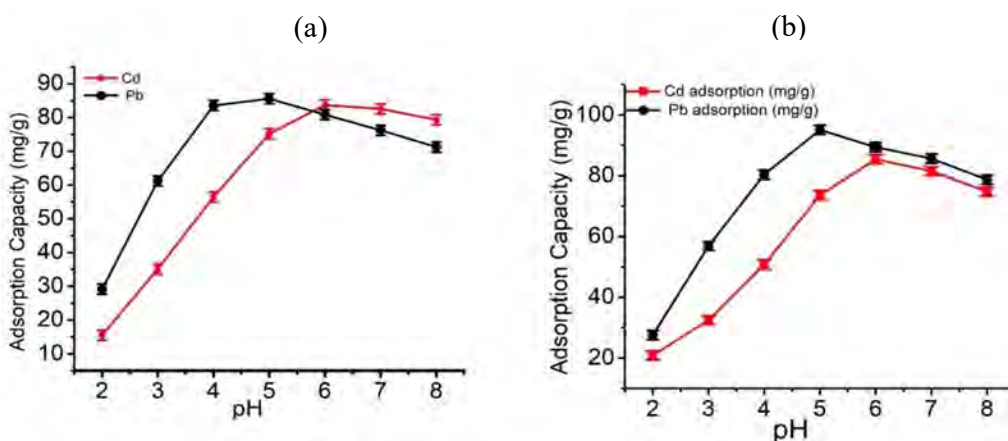


Figure 5.7: (a) impact of pH on the adsorption of Cd and Pb onto the *F. muscicola* mediated IONPs; (b) impact of pH on the adsorption of Cd and Pb onto *Nostoc* sp. mediated IONPs.

5.3.3. Impact of contact time on adsorption

Contact time is an important factor in metal ions adsorption. A comprehensive

investigation was performed to explore the influence of contact time adsorption over time periods ranging from 5 to 120 minutes. Initially the adsorption rate of metal ions on to the adsorbents was rapid as described in the Figure (5.8a and 5.8b) with distinct patterns. This behavior of metal ions adsorption on to the IONPs was due to free availability of adsorption sites in the initial phase of adsorption. The contact duration between the metal ions and the nanoadsorbent plays important role in the cost-effective treatment of wastewater. By increasing the duration of contact between contaminants and adsorbent, the adsorption efficiency significantly enhances because of the increased interaction between metals and chelation active sites. Typically, at the start of the adsorption process, the removal efficiency starts off fast and then builds up progressively. This happens because of the accessibility of the initial free active sites available for adsorption, which is progressively taken up by chelated metals over time (Dubey et al., 2016). *F. muscicola* mediated IONPs, the maximum adsorption of Pb was 86.208 mg/g at contact time of 90 minutes and the maximum adsorption of Cd was 82.433 mg/g at 120 minutes of contact time. While on the *Nostoc* sp. mediated IONPs, the maximum adsorption of Pb was 95.1 mg/g at contact time of 90 minutes and the maximum adsorption of Cd was 86.58 mg/g at 120 minutes of contact time. These findings show that IONPs have high adsorption capacity for the removal of Pb and Cd. Results of this study were found consistent with the previous studies showing the optimum adsorption at 120 minutes for Cd (Ameh, 2023; Jain et al., 2018) 90 minutes for Pb (Ameh, 2023).

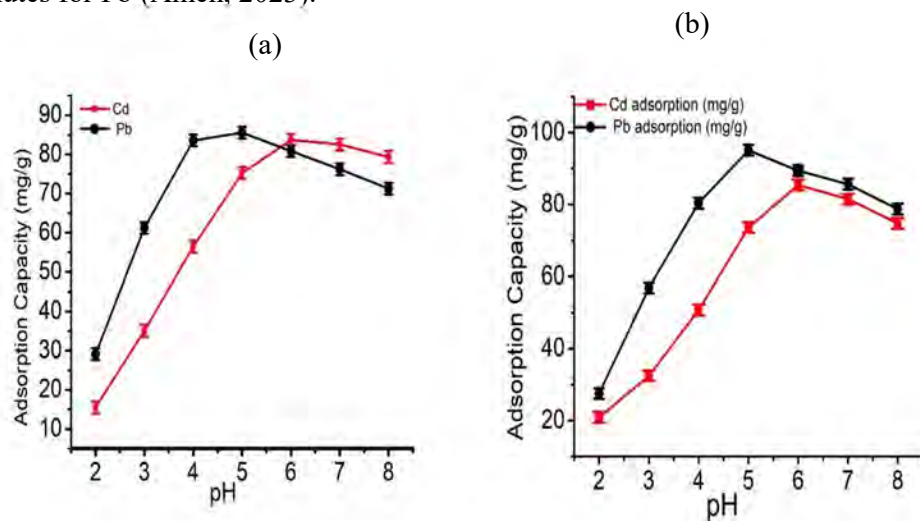


Figure 5.8: (a) Impact of contact time on the adsorption of Cd and Pb ions onto the *F. muscicola* mediated IONPs; (b) Impact of contact time on adsorption of Cd and Pb ions onto the *Nostoc* sp. mediated IONPs.

5.3.4. Kinetic modeling of the experimental data

The most crucial aspect to consider in any adsorption inquiry is the adsorption kinetics, which must be analyzed. Adsorption kinetics is the study of how a system's sorption properties, its reaction rate and sorption mechanism improve over time (Mohamed et al., 2023). In a liquid phase system, the rate of adsorption using solid adsorbent is significantly impacted by many physicochemical parameters throughout the adsorption process (Ghaedi et al., 2014). Extensive kinetics analysis on Cd and Pb ions adsorption on to the cyanobacteria mediated IONPs were conducted and used a variety of kinetic models as described below:

Pseudo first order kinetic model:

$$\ln(q_e - q_t) = \ln q_e - K_1 t \quad (2)$$

Pseudo-second- order kinetic model:

$$\frac{t}{q_e} = \frac{1}{K_2 q_e^2} + \frac{1}{q_e} \quad (3)$$

Intraparticle diffusion kinetic model:

$$q_t = k_{id} t^{0.5} + C \quad (4)$$

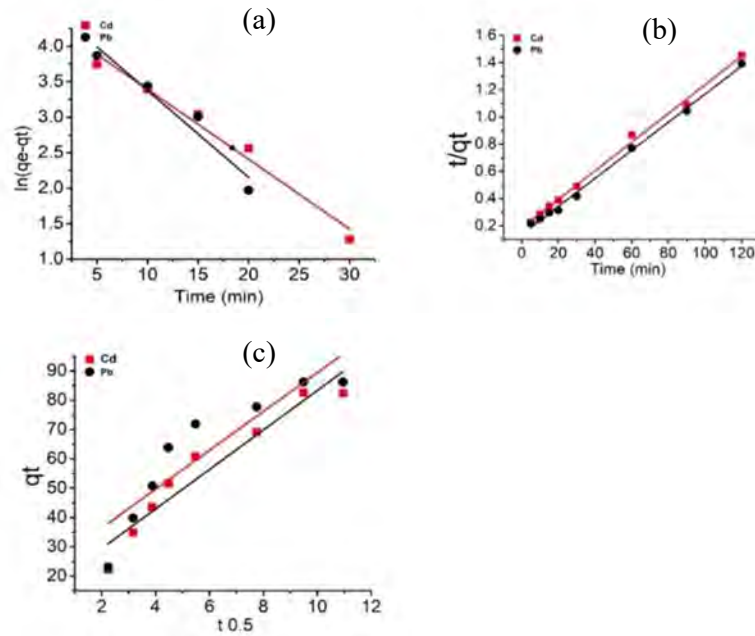


Figure 5.9: Pseudo 1st; order (b) Pseudo 2nd; (c) Intraparticle diffusion, kinetics for the adsorption of Pb and Cd onto the *F. muscicola* mediated IONPs.

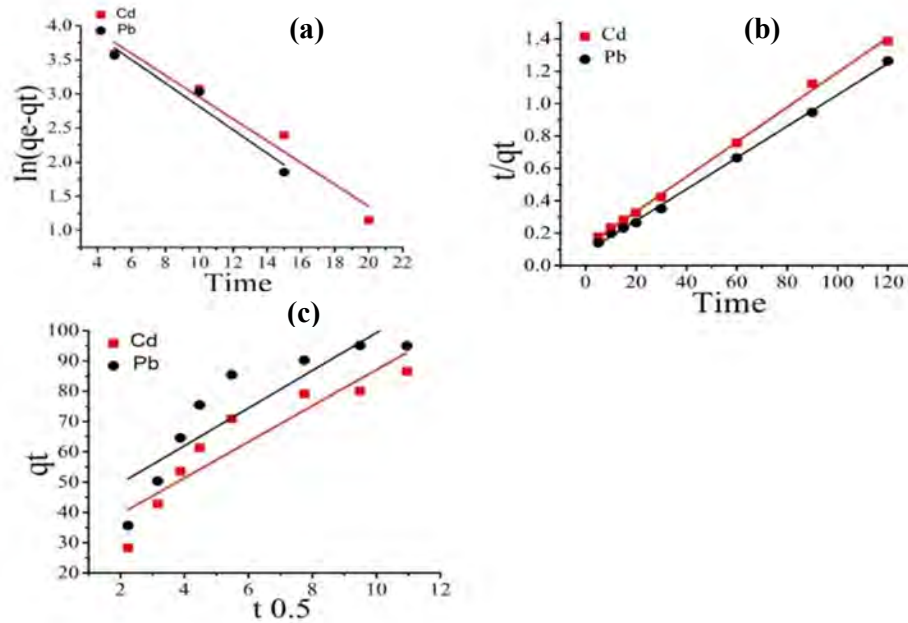


Figure 5.10: Pseudo 1st order; (b) Pseudo 2nd; (c) Intraparticle diffusion, kinetics for adsorption of Pb and Cd onto *Nostoc* sp. mediated IONPs.

Linearized plots for equation 2, 3, and 4 are shown in figures 5.9a, 5.9b, and 5.9c, respectively for Cd and Pb adsorption onto the *F. muscicola* mediated IONP. While figures 5.10a, 5.10b and 5.10c show the graphical representation of Pseudo first order, Pseudo second order and Intraparticle diffusion kinetic model for the adsorption of Cd and Pb onto the IONPs mediated by *Nostoc* sp. Table 5.1 displays the rate constants, kinetic parameters, and correlation coefficients obtained from the graphs of kinetic models. Kinetic modeling of the adsorption data showed significantly higher correlation coefficient (R^2) values obtained from the Pseudo second order models (Table 5.1). This indicates that the rate-regulating phase in the adsorption of Pb and Cd ions onto the Nano-adsorbent was chemisorption in nature involving valence forces and potential electron sharing or exchange between the adsorbates and adsorbents (Ho & McKay, 1999). Data in Table 5.1 shows low values of R^2 for Pseudo first order and intraparticle diffusion kinetic models indicating that these models were not suitable to describe the adsorption mechanism of Cd and Pb in the present case.

Table 5.1. Parameters of the pseudo first order, pseudo second order, and intraparticle diffusion kinetic models

Kinetics models		<i>F. muscicola</i>		<i>Nostoc sp.</i>	
	Parameters	Cd	Pb	Cd	Pb
Pseudo first order	q_e (mg^{-1})	79.716	99.733	94.99	92.489
	K_1 (min^{-1})	-0.00109	-0.001	-0.003	-0.001
	R^2	0.969	0.916	0.937	0.911
Pseudo second order	q_e (mg^{-1})	94.876	86.208	93.109	102.774
	K_2 ($\text{g mg}^{-1} \text{ min}^{-1}$)	0.0006	0.0007	0.0009	0.0011
	R^2	0.996	0.996	0.998	0.999
Intraparticle diffusion	K_i ($\text{mg g}^{-1} \text{ min}^{-0.5}$)	6.728	0.125	5.953	6.219
	R^2	0.916	0.801	0.824	0.748

5.3.5. Impact of initial metal concentrations on adsorption of Cd and Pb

Figure 5.11a and Figure 5.11b show the influence of initial metal concentrations of Cd and Pb ranging from 20, 40, 60, 80, 100 to 120 mg/L on the adsorption of Cd and Pb ions onto IONPs. It was found that metal ion adsorption

increased with increasing initial metal concentrations. The highest adsorption of Cd and Pb onto the surface of the *F. muscicola* IONPs occurred at the concentrations of 120 mg/L and maximum adsorption was 84.38 and 87.4 mg/g for Cd and Pb, respectively. While the maximum adsorption of Cd on to the *Nostoc* sp. IONPs was 85.55 mg/g) which was observed at 100 mg/L and the Pb ions maximum adsorption was at an initial concentration of 120 mg/L. However, it is important to note that the difference in the adsorption between the initial concentrations of 100 mg/L and 120 mg/L for Pb ions was relatively minimal. Consequently, we calculated the maximum Pb adsorption to be 95.02 mg/g at an initial concentration of 100 mg/L and 95.04 mg/g at a concentration of 120 mg/L. The difference in active binding sites accessibility can be attributed to Cd ions having lower accessibility than Pb ions, resulting in a difference in the adsorption capacities of IONPs for Cd and Pb ions. The results of this research demonstrate that when the concentration of metal ions in the solution increased it also increased Pb and Cd ions adsorption onto IONPs. As seen in earlier studies utilizing silicate porous materials as adsorbent for the adsorption of Cd, Cu and Pb ions, the adsorption capacity increased at greater starting concentrations of the adsorbates (Ouyang et al., 2019). The rise in adsorption capacity as a function of metal ion concentration is attributed to the increased concentration, which in turn generates a substantial driving force between the solid and liquid phases (Ali et al., 2019).

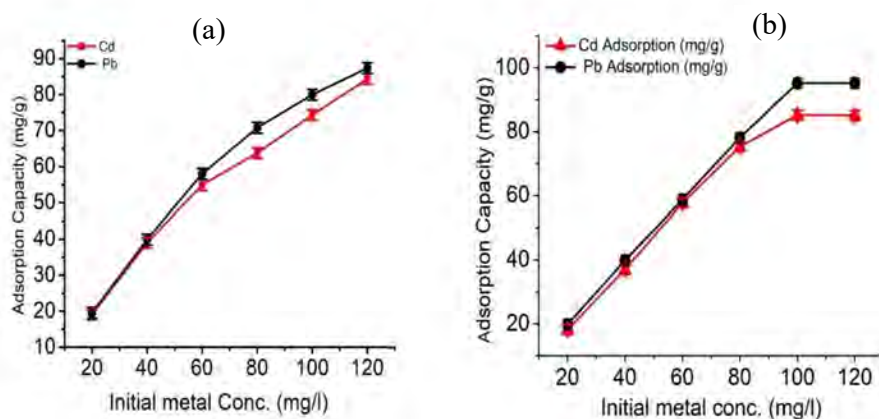


Figure 5.11: Impact of initial metal concentrations on the adsorption of Cd and Pb ions onto the *F. muscicola* mediated IONPs; (b) Impact of initial metal concentrations on adsorption of Cd and Pb ions onto the *Nostoc* sp. mediated IONP.

5.3.6. Isotherm study

One of the objectives of this research was to apply Langmuir (Langmuir, 1918), Freundlich (Freundlich, 1906), and Temkin (Tempkin and Pyzhev, 1940) isotherm models on Cd and Pb adsorption experimental data to study the isothermal behavior during the adsorption of Pb and Cd on to the IONPs.

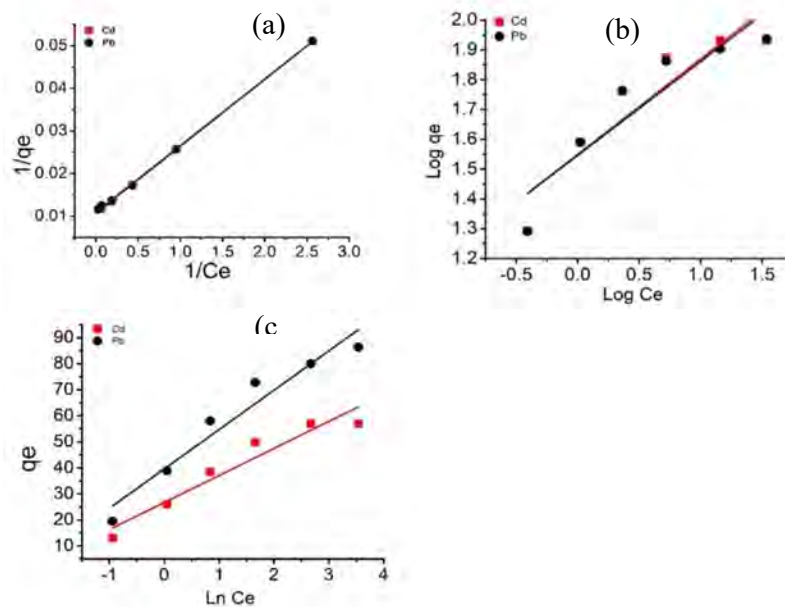


Figure 5.12: (a) Langmuir; (b) Freundlich; (c) Temkin, Isotherms for the adsorption of Pb and Cd onto the *F. muscicola* mediated IONPs

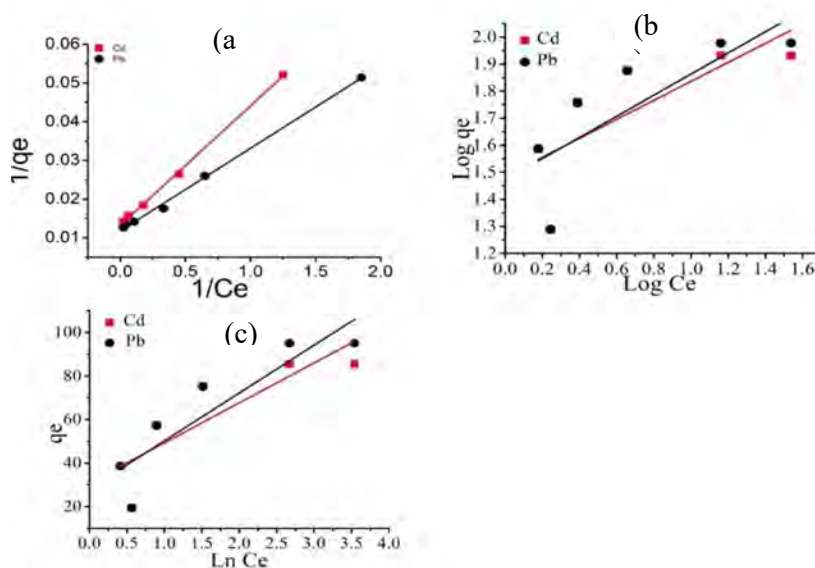


Figure 5.13: (a) Langmuir; (b) Freundlich; (c) Temkin, Isotherms for the adsorption of Pb and Cd onto the *Nostoc* sp. mediated IONPs.

Plots of the isotherm models are shown in Figures 5.12a, 5.12b and 5.12c for the adsorption of Pb and Cd onto the *F. muscicola* mediated IONPs. Similarly plots of the isotherm models are shown in Figures 5.13a, 5.13b and 5.13c for the adsorption of Pb and Cd *Nostoc* sp. mediated IONPs. The corresponding isotherm constants and correlation coefficients (R^2) are summarized in Table 5.2. The results on application of Langmuir model showed a notably higher R^2 value compared to the other isotherm models, signifying its fitness to the metal adsorption data and affirming the surface homogeneity of the adsorbent. Adsorption isotherm showed a well-fitted Langmuir isotherm at high residual Pb and Cd concentrations in the solution phase. It further indicated reduction of active sites on the adsorbents (Kaewsarn, 2002). Maximum adsorption capacities of *F. muscicola* mediated IONPs were estimated using the Langmuir isotherm as 93.370 mg/g for Cd and 94.161 mg/g for Pb, respectively. Likewise, the maximum adsorption capacities of *Nostoc* sp. mediated IONPs were estimated using the Langmuir isotherm as 105.932 mg/g for Cd and 118.764 mg/g for Pb, respectively. Additionally, the Freundlich isotherm model yielded $1/n$ values between 0 and 1 indicate a favorable adsorption environment. Findings of this study suggest that the adsorption mechanisms align more closely with the Langmuir model. Table 5.3 compared the maximum adsorption capacities observed in this investigation to those reported in the literature for nano-adsorbent (Chen et al., 2017; Ebrahim et al., 2016; Facchi et al., 2018; Gong et al., 2012; Kumari et al., 2015; Lin et al., 2018; Rajput et al., 2016; Recillas et al., 2011; Rusmin et al., 2017; Sarojini et al., 2021, Shalaby et al., 2014; Tran et al., 2010). In terms of maximum adsorption capacity, comparison show that the cyanobacteria mediated IONPs fabricated in this study and used as adsorbents outscored many other adsorbents (Rusmin et al., 2017; Facchi et al., 2018; Kumari et al., 2015; Tran et al., 2010).

Table 5.2. Parameters of Langmuir, Freundlich and Temkin isotherm models

Isotherm models		<i>F. muscicola</i> mediated IONPs		<i>Nostoc</i> sp. mediated IONPs	
	Parameters	Cd	Pb	Cd	Pb
Langmuir	q _{max} (mg/g)	93.370	94.161	105.932	118.764
	K _L (L/mg)	0.682	0.494	0.396	0.362
	R _L	0.012	0.016	0.0246	0.0268
	R ²	0.999	0.992	0.99	0.99
Freundlich	K _f (mg/g)	35.427	32.352	32.853	33.29
	1/n	0.320	0.304	0.346	0.427
	R ²	0.812	0.804	0.749	0.777
Temkin	K _T	9.114	11.113	8.626	5.697
	B _T	5.698	14.701	16.914	21.610
	R ²	0.953	0.933	0.853	0.805

Table 5.3. Comparison of maximum adsorption capacities of *F. muscicola* and *Nostoc* sp. mediated IONP with other adsorbents

Types of Adsorbents	Q _{max} (mg/g)	Reference
Adsorption of Pb		
Chitosan/magnetite nanocomposite	63.30	(Tran et al., 2010)
Fe ₃ O ₄ nanospheres	18.47	(Kumari et al., 2015)
Sulfonated magnetic nanoparticle	108.93	(Chen et al., 2017)
Polypyrrole iron-oxide seaweed nanocomposite	333.33	(Sarojini et al., 2021)
CHT/ALG/Fe ₃ O ₄ @SiO ₂ composite	245.28	(Facchi et al., 2018)
Polygorskite-iron oxide nanocomposite	26.70	(Rusmin et al., 2017)
Fe ₃ O ₄ nanoparticles	189	(Recillas et al., 2011)
<i>F. muscicola</i> IONPs	94.161	Current study
<i>Nostoc</i> sp. mediated IONPs	118.76	Current study

Chitosan coated magnetite Fe ₃ O ₄ Nanoparticles	39.6	(Shalaby et al., 2014)
Fe ₃ O ₄ nanomaterial	11.698	(Ebrahim et al., 2016)
IONPs	18.32	(Lin et al., 2018)
SCMNs	18.80	(Gong et al., 2016)
<i>F. muscicola</i> IONPs	93.370	Current study
<i>Nostoc</i> sp. mediated IONPs	105.932	Current study
Adsorption of Cd		
Chitosan coated magnetite Fe ₃ O ₄ Nanoparticles	39.6	(Shalaby et al., 2014)
Fe ₃ O ₄ nanomaterial	11.698	(Ebrahim et al., 2016)
IONPs	18.32	(Lin et al., 2018)
SCMNs	18.80	(Gong et al., 2016)
<i>F. muscicola</i> mediated IONPs	93.370	Current study
<i>Nostoc</i> sp. mediated IONPs	105.932	Current study

5.3.7. Desorption and Reusability

For economic viability the reusability of adsorbent in metal sequestration is crucial. It is depicted by the desorption and regeneration process in wastewater treatment (Kulkarni and Kaware, 2014). In large-scale operations, it is important to reduce the operational costs of the adsorption process. Therefore, it is recommended to reuse the adsorbent by recovering the metal ions from the solution. In acidic conditions, the bonding complex formed between the metals and the active sites of the nanoadsorbant can be desorbed, owing to a more favorable protonation of active sites. In this study, HCl (0.1M) was selected as the desorption effluent (Tan et al., 2012). Adsorption and desorption tests were run five times in this investigation to verify the reuse of IONPs. As illustrated in Fig 5.14a and 5.14b, IONPs retained high adsorption capacity even after undergoing five cycles of adsorption and desorption. After few cycles a slight decrease in adsorption capacity was observed which may be attributed to metals that were irreversibly binding or to the chelating agent losses during the cycles. Nonetheless, following five cycles of adsorption and desorption, the removal capacity of IONPs for Pb and Cd remained notably high. After five adsorption and

desorption cycles, the adsorption capacity of *F. muscicola* mediated IONPs was 91.87 and 80.41 mg/g for Pb and Cd, respectively and adsorption capacity of *Nostoc* sp. mediated IONPs was 92.77 and 88.35 mg/g for Pb and Cd, respectively. In several previous studies adsorption and desorption investigations were conducted to study the reusability of the adsorbent and recovery of economically important metals (Martín et al., 2018; Zeng et al., 2019; Naseem et al., 2019).

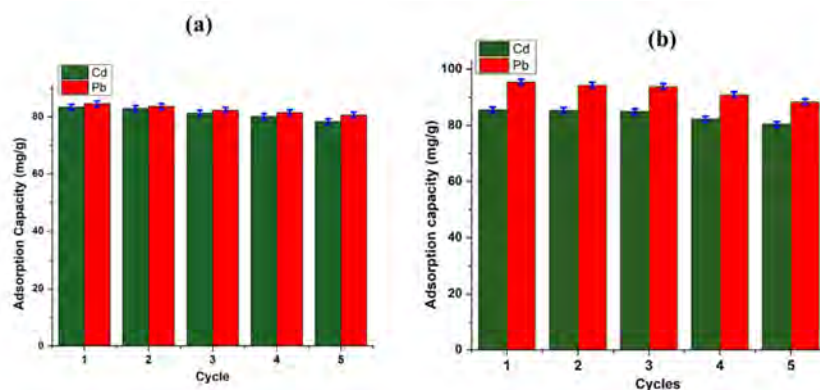


Figure 5.14: (a) Reusability of *F. muscicola* mediated IONPs; (b) Reusability of *Nostoc* sp. mediated IONPs.

In conclusion,

- Finding of this study show that Iron oxide nanoparticles were successfully synthesized from aqueous extract of cyanobacteria which are rich in functional biomolecules.
- *Nostoc* sp. mediated iron oxide nanoparticles were more (maximum adsorption capacity 118.764 mg/g and 105.932 mg/g Pb and Cd, respectively) efficient than *F. muscicola* mediated iron oxide nanoparticles (maximum adsorption capacity 94.161 and 93.370 mg/g for Pb and Cd, respectively).
- Mechanism of Pb and Cd ions binding on to the iron oxide nanoparticles mediated through *F. muscicola* and *Nostoc* sp. was chemisorption and homogeneous.
- Reusability study showed that IONPs have the potential to be reused and economically important metals can be recovered in aqueous conditions.

Synthesis and Conclusion

Pakistan possesses distinctive geographical and environmental conditions which promote extensive biodiversity, well documented in case of plants and animals. However, thallophytes including cyanophytes and the algal flora gained little attention. Lately, as urban areas are expanding with ancillary issues of wastewater and eutrophication, so is increasing the importance of planktonic life. Therefore the present study was commissioned to collect, isolate and characterize the native algal flora from wastewater bodies situated in the suburbs of Islamabad and Rawalpindi. Initial assessment of samples revealed presence of as many as 9 different heavy metals some of which especially Cd and Pb were found above the USA EPA mean permissible limits. The diversity of cyanobacteria in these samples was also high, with six new species including *Desertifilum thareense* MK-2, *Nodosilinea nodulosa* MK-4, *Fischerella muscicola* MK-8, *Westiellopsis prolifica* MK-9, *Desikacharya* sp. MK-7, *Synechocystis fuscopigmentosa* MK-13, all recorded for the first time from Pakistan.

Harnessing the benefit of available facility to culture and maintain cyanobacteria as axenic cultures is challenging and requires a careful and focused approach.

Known in the literature are the often-raised quantities of arsenic (As) with roadside samples; Hg, Pb with effluents of tanneries; Ni/Mn/Co/Cd/Pb with waste of batteries etc. The findings of present study expand the list to include Cd and Pb with sewage and e-wastewater sites in Islamabad and Rawalpindi. Further to this, utilizing the available facility to culture and maintain axenic cultures of cyanobacteria, several isolates were obtained and screened for Pb and Cd tolerance. Among these, *Nostoc* sp. was the most tolerant species followed by *F. muscicola*, which emphasized their potential for environmental bioremediation. Removal of heavy metals utilizing cyanobacteria is deemed effective and green technology to treat wastewater.

With all the experimental modelities employed for assessment, it can be stated with confidence that the capacity of two strains (with some level of subjectivity) to bioremediate Cd and Pb was average to high (avg. efficiency 70 to 80%). Comparison of the two strains revealed a higher capacity of *Nostoc* sp. as compared to *F. muscicola* mainly due to its surface chemistry. The NPs synthesis further enhanced the capacity by a factor of 20 to 30%. Therefore it is highly recommended to deploy

technology based biological solutions to address environmental issues.

Future Recommendations

1. Further explore diverse ecological niches in polluted water bodies of Pakistan to isolate and cultivate algae.
2. Species identified up to genus level are further needs to be characterized upto species level and for this other loci are needed to be amplified.
3. Investigate the potential integration of biological methods with other water treatment technologies, aiming to develop hybrid systems for more efficient metal removal.
4. Further experiments should focus on potential gene targets and produce knock outs or over expression for enhanced heavy metals tolerance.
5. Calcium-alginate treatment of living cells is suggested to increase the resistance potential against heavy metals when using the *Nostoc* sp. and *F. muscicola* for practical applications in large-scale water treatment systems for long duration.
6. Cyanobacteria dried biomass, fresh biomass and cyanobacteria based nanoparticles showed the significant potential. Conduct extensive field trials and environmental impact assessments in real-world polluted sites are required further validating the performance, feasibility and ecological safety of these biosorbents and nanoparticles.
7. These systems are suggested for effective removal of other pollutants.
8. Explore methods for modifying the surface properties of biomass and biosynthesized nanoparticles to improve their biosorption capacity and stability, ensuring sustained effectiveness over multiple adsorptions and desorption cycles.
9. Doping of IONPs with Polyvinylpyrrolidone (PVP) and Chitosan is suggested to increase the active metal binding sites on the surface of the nanoparticles to further enhance the heavy metals removal potential of these adsorbents.

Bibliography

- Abad, D., Albaina, A., Aguirre, M., Laza-Martínez, A., Uriarte, I., Iriarte, A., Villate, F., & Estonba, A. (2016). Is metabarcoding suitable for estuarine plankton monitoring? A comparative study with microscopy. *Marine Biology*, 163, 1-13.
- Abbas, S.H., Ismail, I.M., Mostafa, T.M., & Sulaymon, A.H. (2014). Biosorption of heavy metals: a review. *Journal of Chemical Science and Technology* 3(4), 74-102.
- Abbasi, B. A., Iqbal, J., Mahmood, T., Qyyum, A., & Kanwal, S. (2019). Biofabrication of iron oxide nanoparticles by leaf extract of *Rhamnus virgata*: Characterization and evaluation of cytotoxic, antimicrobial and antioxidant potentials. *Applied Organometallic Chemistry*, 33(7), 4947.
- Abd El-Hameed, M.M., Abuarab, M.E., Mottaleb, S.A., El-Bahbohy, R.M., & Bakeer, G.A. (2018). Comparative studies on growth and Pb (II) removal from aqueous solution by *Nostoc muscorum* and *Anabaena variabilis*. *Ecotoxicology and Environmental Safety*, 165, 637-644.
- Abdel-Aty, A.M., Ammar, N.S., Ghafar, H.H.A., & Ali, R.K. (2013). Biosorption of Cd and Pb from aqueous solution by fresh water alga *Anabaena sphaerica* biomass. *Journal of advanced research*, 4(4), 367-374.
- Abdel-Raouf, N., Al-Enazi, N.M., Ibraheem, I.B.M., Alharbi, R.M., & Alkhulaifi, M.M. (2019). Biosynthesis of silver nanoparticles by using of the marine brown alga *Padina pavonia* and their characterization. *Saudi Journal of Biological Sciences*, 26(6), 1207-1215.
- Abdollahi, Z., Taheri-Kafrani, A., Bahrani, S.A. & Kajani, A.A. (2019). PEGylated graphene oxide/superparamagnetic nanocomposite as a high-efficiency loading nanocarrier for controlled delivery of methotrexate. *Journal of biotechnology*,

298, 88-97.

Abed, R. M., Dobretsov, S., & Sudesh, K. (2009). Applications of cyanobacteria in biotechnology. *Journal of applied microbiology*, 106(1), 1-12.

Abirhire, O., & Kadiri, M.O. (2011). Bioaccumulation of heavy metals using microalgae. *Asian Journal of Microbiology, Biotechnology and Environmental Sciences*, 13(1), 91-94.

Acien, F.G., Gómez-Serrano, C., Morales-Amaral, M.d.M., Fernández-Sevilla, J.M., & Molina- Grima, E. (2016). Wastewater treatment using microalgae: how realistic a might it be to significant urban wastewater treatment? *Applied Microbiology and Biotechnology*, 100, 9013-9022.

Adams, D.G., & Duggan, P.S. (2008). Cyanobacteria–bryophyte symbioses. *Journal of experimental botany*, 59(5), 1047-1058.

Adaramodu, A.A., Osuntogun, A., & Ehi-Eromosele, C. (2012). Heavy metal concentration of surface dust present in E-waste components: the Westminster electronic market, Lagos case study. *Resources and Environment*, 2(2), 9-13.

Adhiya, J., Cai, X., Sayre., R.T. & Traina, S.J. (2002). Binding of aqueous Cd by the lyophilized biomass of *Chlamydomonas reinhardtii*. *Colloids and Surfaces A: Physicochemical and Engineering Aspects*, 210(1), 1-11.

Afreen, R., Tyagi, S., Singh, G.P., & Singh, M. (2021). Challenges and perspectives of polyhydroxyalkanoate production from microalgae/cyanobacteria and bacteria as microbial factories: an assessment of hybrid biological system. *Frontiers in Bioengineering and Biotechnology*, 9, 624885.

Agarwal, A., Upadhyay, U., Sreedhar, I., Singh, S.A., & Patel, C.M. (2020). A review on valorization of biomass in heavy metal removal from wastewater. *Journal of Water Process Engineering*, 38, 101602.

- Agarwal, P., Soni, R., Kaur, P., Madan, A., Mishra, R., Pandey, J., Singh, S. and Singh, G. (2022). Cyanobacteria as a promising alternative for sustainable environment: Synthesis of biofuel and biodegradable plastics. *Frontiers in Microbiology*, 13, 939347.
- Ai, Y., Lee, S., & Lee, J. (2020). Drinking water treatment residuals from cyanobacteria bloom- affected areas: Investigation of potential impact on agricultural land application. *Science of the total environment*, 706, 135756.
- Aiba, S., & Ogawa, T. (1977). Assessment of growth yield of a blue-green alga, *Spirulina platensis*, in axenic and continuous culture. *Microbiology*, 102(1), 179-182.
- Ajmal Iqbal, I.A., Ahmad, H., Nadeem, M., Nisar, M., & Riaz, H. (2013). An efficient DNA extraction protocol for medicinal plants. *International Journal of Biosciences*, 3(7), 30- 35.
- Akar, T., Celik, S., Ari, A.G., & Akar, S.T. (2013). Removal of Pb²⁺ ions from contaminated solutions by microbial composite: combined action of a soilborne fungus *Mucor plumbeus* and alunite matrix. *Chemical Engineering Journal*, 215-216, 626-634.
- Alain, K., & Querellou, J. (2009). Cultivating the uncultured: limits, advances and future challenges. *Extremophiles*, 13, 583-594.
- Alam, S., Ullah, B., Khan, M.S., Rahman, N.u., Khan, L., Shah, L.A., Zekker, I., Burlakovs, J., Kallistova, A., & Pimenov, N. (2021). Adsorption kinetics and isotherm study of basic red 5 on synthesized silica monolith particles. *Water*, 13(20), 2803.
- Al-Amin, A., Parvin, F., Chakraborty, J., & Kim, Y.I. (2021). Cyanobacteria mediated heavy metal removal: A review on mechanism, biosynthesis, and removal

- capability. *Environmental Technology Reviews*, 10(1), 44-57.
- Al-Hasan, R., Al-Bader, D., Sorkhoh, N., & Radwan, S. (1998). Evidence for n-alkane consumption and oxidation by filamentous cyanobacteria from oil-contaminated coasts of the Arabian Gulf. *Marine Biology*, 130, 521-527.
- Al-Homaidan, A.A., Alabdullatif, J.A., Al-Hazzani, A.A., Al-Ghanayem, A.A., & Alabbad, A.F. (2015). Adsorptive removal of Cd ions by *Spirulina platensis* dry biomass. *Saudi Journal of Biological Sciences*, 22(6), 795-800.
- Ali Anvar, S.A., Nowruzi, B., & Afshari, G. (2023). A Review of the Application of Nanoparticles Biosynthesized by Microalgae and Cyanobacteria in Medical and Veterinary Sciences. *Iranian Journal of Veterinary Medicine*, 17(1), 1-18.
- Ali, I., Khan, A., Ali, A., Ullah, Z., Dai, D.Q., Khan, N., Khan, A., Al-Tawaha, A.R., & Sher, H. (2022). Iron and zinc micronutrients and soil inoculation of *Trichoderma harzianum* enhance wheat grain quality and yield. *Frontiers in Plant Science*, 13, 960948.
- Ali, I., Peng, C., & Naz, I. (2019). Removal of Pb and Cd ions by single and binary systems using phytogenic magnetic nanoparticles functionalized by 3-mercaptopropanoic acid. *Chinese Journal of Chemical Engineering*, 27(4), 949-964.
- Al-Khashman, O. A. (2007). Determination of metal accumulation in deposited street dusts in Amman, Jordan. *Environmental geochemistry and health*, 29, 1-10.
- Amadu, A.A., deGraft-Johnson, K.A.A., & Ameka, G.K. (2021). Industrial Applications of Cyanobacteria. *Cyanobacteria-Recent Advances in Taxonomy and Applications*.
- Ameh, P. (2023). Synthesized iron oxide nanoparticles from *Acacia nilotica* leaves for the sequestration of some heavy metal ions in aqueous solutions. *Journal of*

- Chemistry Letters*, 4(1), 38-51.
- Andersen, R.A. (2005). Algal culturing techniques. *Journal of Phycology*, 41, 906–908.
- Anjana, K., Kaushik, A., Kiran, B., & Nisha, R. (2007). Biosorption of Cr (VI) by immobilized biomass of two indigenous strains of cyanobacteria isolated from metal contaminated soil. *Journal of hazardous materials*, 148(1-2), 383-386.
- Anyanwu, B.O., Ezejiofor, A.N., Igweze, Z.N., & Orisakwe, O.E. (2018). Heavy metal mixture exposure and effects in developing nations: an update. *Toxics*, 6(4), 65.
- Ardal, E. (2014). Phycoremediation of pesticides using microalgae. Swedish University of Agricultural Sciences.
- Arief, V.O., Trilestari, K., Sunarso, J., Indraswati, N., & Ismadji, S. (2008). Recent progress on biosorption of heavy metals from liquids using low cost biosorbents: characterization, biosorption parameters and mechanism studies. *CLEAN–Soil, Air, Water*, 36(12), 937- 962.
- Arif, M., Li, Y., El-Dalatony, M.M., Zhang, C., Li, X., & Salama, E.-S. (2021). A complete characterization of microalgal biomass through FTIR/TGA/CHNS analysis: An approach for biofuel generation and nutrients removal. *Renewable energy*, 163, 1973-1982.
- Arunakumara, K., & Xuecheng, Z. (2007). How does Pb (Pb²⁺) at low concentrations effect on *Spirulina (Arthrospira) platensis*. *Tropical Agricultural Research and Extension*, 10, 47- 52.
- Asadi, A. (2014). Streptomycin-loaded PLGA-alginate nanoparticles: preparation, characterization, and assessment. *Applied Nanoscience*, 4, 455-460.
- Ashida, N., Ishii, S., Hayano, S., Tago, K., Tsuji, T., Yoshimura, Y., & Senoo, K.

- (2010). Isolation of functional single cells from environments using a micromanipulator: application to study denitrifying bacteria. *Applied microbiology and biotechnology*, 85, 1211-1217.
- Ashraf, S., Rizvi, N. B., Rasool, A., Mahmud, T., Huang, G. G., & Zulfajri, M. (2020). Evaluation of heavy metal ions in the groundwater samples from selected automobile workshop areas in northern Pakistan. *Groundwater for sustainable development*, 11, 100428.
- Assi, M.A., Hezmee, M.N.M., Sabri, M.Y.M., & Rajion, M.A. (2016) The detrimental effects of Pb on human and animal health. *Veterinary world*, 9(6), 660.
- Awasthi., A.K., Zeng, X., & Li, J. (2016). Environmental pollution of electronic waste recycling in India: a critical review. *Environmental Pollution*, 211, 259–270.
- Ayangbenro, A.S., & Babalola, O.O. (2017). A new strategy for heavy metal polluted environments: a review of microbial biosorbents. *International journal of environmental research and public health*, 14(1), 94.
- Azimi, A., Azari, A., Rezakazemi, M., & Ansarpour, M. (2017). Removal of heavy metals from industrial wastewaters: a review. *ChemBioEng Reviews*, 4(1), 37-59.
- Bailet, B., Apothéloz-Perret-Gentil, L., Baričević, A., Chonova, T., Franc, A., Frigerio, J.-M., Kelly, M., Mora, D., Pfannkuchen, M., & Proft, S. (2020). Diatom DNA metabarcoding for ecological assessment: Comparison among bioinformatics pipelines used in six European countries reveals the need for standardization. *Science of the total environment*, 745, 140948.
- Balaji, S., Kalaivani, T., Shalini, M., Gopalakrishnan, M., Rashith Muhammad, M.A., & Rajasekaran, C. (2016). Sorption sites of microalgae possess metal binding ability towards Cr (VI) from tannery effluents a kinetic and characterization

- study. *Desalination and Water Treatment*, 57(31), 14518-14529.
- Barakat, M. (2011). New trends in removing heavy metals from industrial wastewater. *Arabian Journal of Chemistry*, 4(4), 361-377.
- Barquilha, C., Cossich, E., Tavares, C., & Silva, E. (2017). Biosorption of nickel (II) and copper (II) ions in batch and fixed-bed columns by free and immobilized marine algae *Sargassum* sp. *Journal of Cleaner Production*, 150, 58-64.
- Barros, A.J.M., Prasad, S., Leite, V.D., & Souza, A.G. (2007). Biosorption of heavy metals in upflow sludge columns. *Bioresource Technology*, 98(7), 1418-1425.
- Batool, F., Iqbal, M.S., Khan, S.-U.-D., Khan, J., Ahmed, B., & Qadir, M.I. (2021). Biologically synthesized iron nanoparticles (FeNPs) from *Phoenix dactylifera* have anti-bacterial activities. *Scientific Reports*, 11(1), 22132.
- Bayo, J. (2012). Kinetic studies for Cd (II) biosorption from treated urban effluents by native grapefruit biomass (*Citrus paradisi* L.): The competitive effect of Pb (II), Cu (II) and Ni (II). *Chemical Engineering Journal*, 191, 278-287.
- Behravan, M., Panahi, A.H., Naghizadeh, A., Ziaee, M., Mahdavi, R., & Mirzapour, A. (2019). Facile green synthesis of silver nanoparticles using *Berberis vulgaris* leaf and root aqueous extract and its antibacterial activity. *International journal of biological macromolecules*, 124, 148-154.
- Beijerinck. (1890). Evaluation of Cd (II) toxicity in the presence of Cu(II), Co(II) and Zn(II) in synchronous culture of algae *Chlorella vulgaris* Beijerinck 1890, strain A8, Thesis, Medical University of Silesia, Sosnowiec-1998, Katowice, Poland.
- Berthold, D.E., Lefler, F.W., & Laughinghouse IV, H.D. (2021). Untangling filamentous marine cyanobacterial diversity from the coast of South Florida with the description of Vermifilaceae fam. nov. and three new genera: *Leptochromothrix* gen. nov., *Ophiophycus* gen. nov., and *Vermifilum* gen. nov.

Molecular Phylogenetics and Evolution, 160, 107010.

- Berthold, D.E., Lefler, F.W., & Laughinghouse, H.D. (2022). Recognizing novel cyanobacterial diversity in marine benthic mats, with the description of Sirenicapillariaceae fam. nov., two new genera, *Sirenicapillaria* gen. nov. and *Tigrinifilum* gen. nov., and seven new species. *Phycologia*, 61(2), 146-165.
- Bhakta, S., Das, S., & Adhikary, S. (2016). Algal diversity in hot springs of Odisha. *Nelumbo*, 58, 157-173.
- Bharagava, R. N., Saxena, G., & Mulla, S. I. (2020). Introduction to industrial wastes containing organic and inorganic pollutants and bioremediation approaches for environmental management. *Bioremediation of Industrial Waste for Environmental Safety I: Industrial Waste and Its Management*, 1-18. https://doi.org/10.1007/978-981-13-1891-7_1.
- Bhatt, P., Bhandari, G., Bhatt, K., & Simsek, H. (2022). Microalgae-based removal of pollutants from wastewaters: Occurrence, toxicity and circular economy. *Chemosphere*, 306, 135576.
- Bhattacharyya, K., Sen, D., Laskar, P., Saha, T., Kundu, G., Ghosh Chaudhuri, A. & Ganguly, S. (2021). Pathophysiological effects of Cd (II) on human health-a critical review. *Journal of Basic and Clinical Physiology and Pharmacology*, 34(3), 249-261.
- Billah, M.M., Kokushi, E., & Uno, S. (2019). Distribution, geochemical speciation, and bioavailable potencies of Cd, copper, Pb, and zinc in sediments from urban coastal environment in Osaka Bay, Japan. *Water, Air, & Soil Pollution*, 230(157), 1-13.
- Bischoff, H.C. (1963). Some soil algae from enchanted rock and related algal species. *Phycological Studies IV. University of Texas Publ. No. 6318(6318): 1-95*

- Bloch, K., & Ghosh, S. (2022). Integrated environmental technologies for wastewater treatment and sustainable development, pp. 533-548, *Elsevier*.
<https://doi.org/10.1016/B978-0-323-91180-1.00002-8>.
- Blank, C. E. (2013). Phylogenetic distribution of compatible solute synthesis genes support a freshwater origin for cyanobacteria. *Journal of Phycology*, 49(5), 880-895.
- Bo, L., Wang, D., Li, T., Li, Y., Zhang, G., Wang, C., & Zhang, S. (2015). Accumulation and risk assessment of heavy metals in water, sediments, and aquatic organisms in rural rivers in the Taihu Lake region, China. *Environmental Science and Pollution Research*, 22, 6721-6731.
- Bon, I.C., Salvatierra, L.M., Lario, L.D., Morató, J., & Pérez, L.M. (2021). Prospects in Cd-contaminated water management using free-living cyanobacteria (*Oscillatoria* sp.). *Water*, 13(4), 542.
- Bonthond, G., Shalygin, S., Bayer, T., & Weinberger, F. (2021). Draft genome and description of *Waterburya agarophytonicola* gen. nov. sp. nov. (Pleurocapsales, Cyanobacteria): a seaweed symbiont. *Antonie van Leeuwenhoek*, 114(12), 2189-2203.
- Boyer, S.L., Flechtner, V.R., & Johansen, J.R. (2001). Is the 16S-23S rRNA internal transcribed spacer region a good tool for use in molecular systematics and population genetics? A case study in cyanobacteria. *Molecular biology and evolution*, 18(6), 1057-1069.
- Bravakos, P., Kotoulas, G., Skaraki, K., Pantazidou, A., & Economou-Amilli, A. (2016). A polyphasic taxonomic approach in isolated strains of Cyanobacteria from thermal springs of Greece. *Molecular Phylogenetics and Evolution*, 98, 147-160.

- Brayner, R., Coradin, T., Beaunier, P., Grenèche, J.-M., Djediat, C., Yéprémian, C., Couté, A., & Fiévet, F. (2012). Intracellular biosynthesis of superparamagnetic 2-lines ferri-hydrate nanoparticles using *Euglena gracilis* microalgae. *Colloids and Surfaces B: Biointerfaces*, 93, 20-23.
- Breza, M., & Manová, A. (2002). On the structure of Pb (II) complexes in aqueous solutions. III. Hexanuclear clusters. *Collection of Czechoslovak chemical communications*, 67(2), 219-227.
- Briffa, J., Sinagra, E., & Blundell, R. (2020). Heavy metal pollution in the environment and their toxicological effects on humans. *Heliyon* 6(9), e04691.
- Burja, A. M., Banaigs, B., Abou-Mansour, E., Burgess, J. G., & Wright, P. C. (2001). Marine cyanobacteria—a prolific source of natural products. *Tetrahedron*, 57(46), 9347-9377.
- Caf, F. (2022). Biogenic Synthesis of Iron Oxide Nanoparticle Using *Padina pavonica* Extract: Application for Photocatalytic Degradation of Congo Red Dye, Neurotoxicity and Antioxidant Activity. *Turkish Journal of Fisheries and Aquatic Sciences*, 23(2). DOI .10.4194/TRJFAS21398.
- Cai, F. F., Chen, Y. X., Zhu, M. L., Li, X. C., & Li, R. (2017). *Desertifilum salkalinema* sp. nov. (Oscillatoriales, Cyanobacteria) from an alkaline pool in China. *Phytotaxa*, 292(3), 262-270.
- Cain, A., Vannela, R., & Woo, L.K. (2008) Cyanobacteria as a biosorbent for mercuric ion. *Bioresource Technology*, 99(14), 6578-6586.
- Callahan, B.J., McMurdie, P.J., & Holmes, S.P. (2017). Exact sequence variants should replace operational taxonomic units in marker-gene data analysis. *The ISME journal*, 11(12), 2639-2643.
- Camere, S., & Karana, E. (2018). Fabricating materials from living organisms: An

- emerging design practice. *Journal of Cleaner Production*, 186, 570-584.
- Capone, D. G., Burns, J. A., Montoya, J. P., Subramaniam, A., Mahaffey, C., Gunderson, T., & Carpenter, E. J. (2005). Nitrogen fixation by *Trichodesmium* spp. An important source of new nitrogen to the tropical and subtropical North Atlantic Ocean. *Global Biogeochemical Cycles*, 19(2), 1-17.
- Casamatta, D.A. (2011). A unique Pseudanabaenalean (cyanobacteria) genus *Nodosilinea* gen. nov. based on morphological and molecular data. *Journal of Phycology*, 47, 1397-1412.
- Castenholz, R.W. (2015). Cyanobacteria. *Bergey's Manual of Systematics of Archaea and Bacteria*, 1-2. DOI: 10.1002/9781118960608.
- Cellamare, M., Duval, C., Drelin, Y., Djediat, C., Touibi, N., Agogu , H., & Bernard, C. (2018). Characterization of phototrophic microorganisms and description of new cyanobacteria isolated from the saline-alkaline crater-lake Dziani Dzaha (Mayotte, Indian Ocean). *FEMS Microbiology Ecology*, 94(8), 108.
- Chandrashekharaiyah, P., Sanyal, D., Dasgupta, S., & Banik, A. (2021). Cd biosorption and biomass production by two freshwater microalgae *Scenedesmus acutus* and *Chlorella pyrenoidosa*: An integrated approach. *Chemosphere*, 269, 128755.
- Chang, J.S. (2020). Bioremediation of heavy metals using microalgae: Recent advances and mechanisms. *Bioresource Technology*, 303, 122886.
- Chang, JS., Kim, YH., & Kim KW (2008). The ars genotype characterization of arsenic-resistant bacteria from arsenic-contaminated gold–silver mines in the Republic of Korea. *Applied Microbiology and Biotechnology*, 80, 155-165.
- Chatterjee, A., & Abraham, J. (2019). Desorption of heavy metals from metal loaded sorbents and e-wastes: A review. *Biotechnology letters*, 41, 319-333.
- Chaubey, M.G., Patel, S.N., Sonani, R.R., Singh, N.K., Rastogi, R.P., & Madamwar,

- D. (2022). Antioxidant, Anti-aging and Anti-Neurodegenerative Biomolecules from Cyanobacteria. *Ecophysiology and Biochemistry of Cyanobacteria*, pp. 327-350. DOI. <https://doi.org/10.1007/978>.
- Chaudhary, R., Nawaz, K., Khan, A.K., Hano, C., Abbasi, B.H., & Anjum, S. (2020). An overview of the algae-mediated biosynthesis of nanoparticles and their biomedical applications. *Biomolecules*, 10(11), 1498.
- Chen, C.Y., Chang, H.W., Kao, P.C., Pan, J.L., & Chang, J.S. (2012). Biosorption of Cd by CO₂-fixing microalga *Scenedesmus obliquus* CNW-N. *Bioresource Technology*, 105, 74-80.
- Chen, H., & Pan, S. S. (2005). Bioremediation potential of spirulina: toxicity and biosorption studies of lead. *Journal of Zhejiang University-Science B*, 6(3), 171-174.
- Chen, K., He, J., Li, Y., Cai, X., Zhang, K., Liu, T., Hu, Y., Lin, D., Kong, L., & Liu, J. (2017). Removal of Cd and lead ions from water by sulfonated magnetic nanoparticle adsorbents. *Journal of colloid and interface science*, 494, 307-316.
- Chen, L., Wu, P., Chen, M., Lai, X., Ahmed, Z., Zhu, N., Dang, Z., Bi, Y., & Liu, T. (2018). Preparation and characterization of the eco-friendly chitosan/vermiculite biocomposite with excellent removal capacity for Cd and lead. *Applied Clay Science*, 159, 74-82.
- Chen, Q., Tang, Z., Li, H., Wu, M., Zhao, Q., & Pan, B. (2020). An electron-scale comparative study on the adsorption of six divalent heavy metal cations on MnFe₂O₄@ CAC hybrid: Experimental and DFT investigations. *Chemical Engineering Journal*, 381, 122656. <https://doi.org/10.1016/j.cej.2019.122656>.
- Chen, Z., Ma, W., & Han, M. (2008). Biosorption of nickel and copper onto treated

- alga(*Undaria pinnatifida*): application of isotherm and kinetic models. *Journal of hazardous materials*, 155(1-2), 327-333.
- Chen, Z.S., He, X., Li, Q., Yang, H., Liu, Y., Wu, L.N., Liu, Z.X, Hu, B.W., Wang, X.K.,(2022c). Low-temperature plasma induced phosphate groups onto coffee residue-derived porous carbon for efficient U(VI) extraction. *Journal of Environmental Science*, 122, 1- 13
- Cheng, S.Y., Show, P.L., Lau, B.F., Chang, J.S., & Ling, T.C. (2019). New prospects for modified algae in heavy metal adsorption. *Trends in biotechnology*, 37(11), 1255-1268.
- Chisholm, S.W., Olson, R.J., Zettler, E.R., Goericke, R., Waterbury, J.B., & Welschmeyer, N.A. (1988). A novel free-living prochlorophyte abundant in the oceanic euphotic zone. *Nature*, 334(6180), 340-343.
- Chittora, D., Meena, M., Barupal, T., Swapnil, P. & Sharma, K. (2020). Cyanobacteria as a source of biofertilizers for sustainable agriculture. *Biochemistry and biophysics reports*, 22, 100737.
- Choo, T., Lee, C., Low, K., & Hishamuddin, O. (2006). Accumulation of chromium (VI) from aqueous solutions using water lilies (*Nymphaea spontanea*). *Chemosphere*, 62(6), 961- 967.
- Chorus, I., & Welker, M. (2021). Toxic cyanobacteria in water: a guide to their public health consequences, monitoring and management, *Taylor & Francis*. DOI. 10.1201/9781003081449
- Chuanwei, Z., Hanjie, W., Yuxu, Z., Yizhang, L. & Rongfei, W. (2015). Isotopic geochemistry of Cd: a review. *Acta Geologica Sinica-English Edition*, 89(6), 2048-2057.
- Ciani, M., & Adessi, A. (2023). Cyanoremediation and phyconanotechnology:

- cyanobacteria for metal biosorption toward a circular economy. *Frontiers in Microbiology*, 14, 1166612.
- Cohen, Y. (2002) Bioremediation of oil by marine microbial mats. *International Microbiology*, 5, 189-193.
- Cohen, Y., Jørgensen, B. B., Revsbech, N. P., & Poplawski, R. (1986). Adaptation to hydrogen sulfide of oxygenic and anoxygenic photosynthesis among cyanobacteria. *Applied and Environmental Microbiology*, 51(2), 398-407.
- Collin, M.S., Venkatraman, S.K., Vijayakumar, N., Kanimozhi, V., Arbaaz, S.M., Stacey, R.S., Anusha, J., Choudhary, R., Lvov, V., & Tovar, G.I. (2022a) Bioaccumulation of lead (Pb) and its effects on human: A review. *Journal of Hazardous Materials Advances* 7, 100094. <https://doi.org/10.1016/j.hazadv.2022.100094>.
- Comte, K., Šabacká, M., Carré-Mlouka, A., Elster, J. & Komárek, J. (2007). Relationships between the Arctic and the Antarctic cyanobacteria; three *Phormidium*-like strains evaluated by a polyphasic approach. *FEMS microbiology ecology*, 59(2), 366-376.
- Congeevaram, S., Dhanarani, S., Park, J., Dexilin, M., & Thamaraiselvi, K. (2007). Biosorption of chromium and nickel by heavy metal resistant fungal and bacterial isolates. *Journal of hazardous materials*, 146(1-2), 270-277.
- Conti, G.O., Copat, C., Wang, Z., D'Agati, P., Cristaldi, A., & Ferrante, M. (2015). Determination of illegal antimicrobials in aquaculture feed and fish: an ELISA study. *Food Control*, 50, 937-941.
- Cordonier, A., Straub, F., Iseli, J., Esling, P., & Pawlowski, J. (2017). Taxonomy-free molecular diatom index for high-throughput eDNA biomonitoring. *Molecular ecology resources*, 17(6), 1231-1242.

- Costa, N.B., Kolman, M.A., & Giani, A. (2016). Cyanobacteria diversity in alkaline saline lakes in the Brazilian Pantanal wetland: a polyphasic approach. *Journal of Plankton Research*, 38(6), 1389-1403.
- Cui, J., Xie, Y., Sun, T., Chen, L., & Zhang, W. (2021). Deciphering and engineering photosynthetic cyanobacteria for heavy metal bioremediation. *Science of the total environment*, 761, 144111. <https://doi.org/10.1016/j.scitotenv.2020.144111>.
- Dadar, M., Adel, M., Ferrante, M., Nasrollahzadeh Saravi, H., Copat, C., & Oliveri Conti, G. (2016). Potential risk assessment of trace metals accumulation in food, water and edible tissue of rainbow trout (*Oncorhynchus mykiss*) farmed in Haraz River, northern Iran. *Toxin Reviews*, 35(3-4), 141-146.
- Dadheech, P. K., Mahmoud, H., Kotut, K., & Krienitz, L. (2014). *Desertifilum fontinale* sp. nov.(Oscillatoriales, Cyanobacteria) from a warm spring in East Africa, based on conventional and molecular studies. *Fottea, Olomouc*, 14(2), 129-140.
- Dadheech, P.K., Abed, R.M., Mahmoud, H., Mohan, M.K., & Krienitz, L. (2012). Polyphasic characterization of cyanobacteria isolated from desert crusts, and the description of *Desertifilum tharensense* gen. et sp. nov.(Oscillatoriales). *Phycologia*, 51(3), 260-270.
- Darroudi, M., Sabouri, Z., Oskuee, R.K., Zak, A.K., Kargar, H., & Abd Hamid, M.H.N. (2014). Green chemistry approach for the synthesis of ZnO nanopowders and their cytotoxic effects. *Ceramics International*, 40(3), 4827-4831.
- Das, N., Vimala, R. and Karthika, P. (2008) Biosorption of heavy metals—an overview. *Indian Journal of Biotechnology*, 7(2), 159-169.
- Dash, S.S., Majumdar, R., Sikder, A.K., Bag, B.G., & Patra, B.K. (2014). *Saraca indica* bark extract mediated green synthesis of polyshaped gold nanoparticles

- and its application in catalytic reduction. *Applied Nanoscience*, 4, 485-490.
- Davis, T.A., Volesky, B., & Mucci, A. (2003). A review of the biochemistry of heavy metal biosorption by brown algae. *water research*, 37(18), 4311-4330.
- De Gisi, S., Minetto, D., Lofrano, G., Libralato, G., Conte, B., Todaro, F., & Notarnicola, M. (2017). Nano-scale zero valent iron (nZVI) treatment of marine sediments slightly polluted by heavy metals. *Chemical Engineering Transactions*, 60, 139-144.
- De Philippis, R., & Micheletti, E. (2017). Handbook of advanced industrial and hazardous wastes anagement. 931-964, *CRC Press*.
<https://doi.org/10.1016/j.envres.2021.111630>.
- Deb, D., Mallick, N., & Bhadoria, P. (2021). Engineering culture medium for enhanced carbohydrate accumulation in *Anabaena variabilis* to stimulate production of bioethanol and other high-value co-products under cyanobacterial refinery approach. *Renewable Energy*, 163, 1786-1801.
- Deckert, J. (2005). Cd toxicity in plants: is there any analogy to its carcinogenic effect in mammalian cells? *Biometals*, 18, 475-481.
- Deng, J., Fu, D., Hu, W., Lu, X., Wu, Y., & Bryan, H. (2020). Physiological responses and accumulation ability of *Microcystis aeruginosa* to zinc and Cd: implications for bioremediation of heavy metal pollution. *Bioresource Technology*, 303, 122963.
- Desikachary, T. V. (1959). *Cyanophyta*. New Delhi: Indian Council of Agricultural Research.
- Devi, M., Devi, S., Sharma, V., Rana, N., Bhatia, R.K., & Bhatt, A.K. (2020). Green synthesis of silver nanoparticles using methanolic fruit extract of *Aegle marmelos* and their antimicrobial potential against human bacterial pathogens. *Journal of*

- traditional and complementary medicine*, 10(2), 158-165.
- Devi, N.D., Sun, X., Hu, B., & Goud, V.V. (2023). Bioremediation of domestic wastewater with microalgae-cyanobacteria co-culture by nutritional balance approach and its feasibility for biodiesel and animal feed production. *Chemical Engineering Journal*, 454(2), 140197.
- Dhaliwal, S. S., Singh, J., Taneja, P. K., & Mandal, A. (2020). Remediation techniques for removal of heavy metals from the soil contaminated through different sources: a review. *Environmental Science and Pollution Research*, 27, 1319-1333.
- Dhir, B. (2014). Potential of biological materials for removing heavy metals from wastewater. *Environmental Science and Pollution Research*, 21, 1614-1627.
- Dirbaz, M., & Roosta, A. (2018). Adsorption, kinetic and thermodynamic studies for the biosorption of Cd onto microalgae *Parachlorella* sp. *Journal of Environmental Chemical Engineering*, 6(2), 2302-2309.
- Dixit, R., Wasiullah, X., Malaviya, D., Pandiyan, K., Singh, U.B., Sahu, A., Shukla, R., Singh, B.P., Rai, J.P., & Sharma, P.K. (2015). Bioremediation of heavy metals from soil and aquatic environment: an overview of principles and criteria of fundamental processes. *Sustainability*, 7(2), 2189-2212.
- Dönmez, G., & Aksu, Z. (2002). Removal of chromium (VI) from saline wastewaters by *Dunaliella* species. *Process biochemistry*, 38(5), 751-762.
- Doyle, J. J., & Doyle, J. L. (1987). A rapid DNA isolation procedure for small quantities of freshleaf tissue. *Phytochemical bulletin*, 9, 11-15.
- Dubey, R., Bajpai, J., & Bajpai, A. K. (2016). Chitosan-alginate nanoparticles (CANPs) as potential nanosorbent for removal of Hg (II) ions. *Environmental Nanotechnology, Monitoring & Management*, 6, 32-44.

- Duffus, J. H. (2002). " Heavy metals" a meaningless term?(IUPAC Technical Report). *Pure and applied chemistry*, 74(5), 793-807.
- Duque, D., Montoya, C., & Botero, L.R. (2019). Cd tolerance evaluation of three strains of microalgae of the genus *Ankistrodesmus*, *Chlorella* and *Scenedesmus*. *Revista Facultad de Ingeniería Universidad de Antioquia*, (92), 88-95.
- Duygu, D.Y., Udoh, A.U., Ozer, T.B., Akbulut, A., Erkaya, I.A., Yildiz, K., & Guler, D. (2012). Fourier transform infrared (FTIR) spectroscopy for identification of *Chlorella vulgaris* Beijerinck 1890 and *Scenedesmus obliquus* (Turpin) Kützing 1833. *African Journal of Biotechnology*, 11(16), 3817-3824.
- Ebrahim, S.E., Sulaymon, A.H., & Saad Alhares, H. (2016). Competitive removal of Cu^{2+} , Cd^{2+} , Zn^{2+} , and Ni^{2+} ions onto iron oxide nanoparticles from wastewater. *Desalination and Water Treatment*, 57(44), 20915-20929.
- Efthymiou, L., Mavragani, A., & Tsagarakis, K.P. (2016). Quantifying the effect of macroeconomic and social factors on illegal E-waste trade. *International Journal of Environmental Research and Public Health* 13(789), 1-13.
- El-Ashtoukhy, E.S., Amin, N., & Abdelwahab, O. (2008). Removal of lead (II) and copper (II) from aqueous solution using pomegranate peel as a new adsorbent. *Desalination* 223(1- 3), 162-173.
- El-Bestawy, E. A., Abd El-Salam, A. Z., & Mansy, A. E. R. H. (2007). Potential use of environmental cyanobacterial species in bioremediation of lindane-contaminated effluents. *International Biodeterioration & Biodegradation*, 59(3), 180-192.
- El-Enany, A., & Issa, A. (2000). Cyanobacteria as a biosorbent of heavy metals in sewage water. *Environmental toxicology and pharmacology*, 8(2), 95-101.
- Elrefaey, A.A.K., El-Gamal, A.D., Hamed, S.M., & El-belely, E.F. (2022). Algae-

- mediated biosynthesis of zinc oxide nanoparticles from *Cystoseira crinite* (Fucales; Sargassaceae) and its antimicrobial and antioxidant activities. *Egyptian Journal of Chemistry*, 65(4), 231-240.
- El-Sheekh, M., El Sabagh, S., Abou El-Souod, G., & Elbeltagy, A. (2019a). Biosorption of Cd from aqueous solution by free and immobilized dry biomass of *Chlorella vulgaris*. *International Journal of Environmental Research*, 13, 511-521.
- Encarnação, T., Ramos, P., Mohammed, D., McDonald, J., Lizzul, M., Nicolau, N., da Graça Campos, M., & Sobral, A.J. (2023). Marine Organisms: A solution to environmental pollution? Uses in bioremediation and in biorefinery, pp. 5-28, Springer. DOI. <https://doi.org/10.1007/978>
- Esenkulova, S., Sutherland, B.J., Tabata, A., Haigh, N., Pearce, C.M., & Miller, K.M. (2020). Correction: Operational taxonomic unit comparing metabarcoding and morphological approaches to identify phytoplankton taxa associated with harmful algal blooms. *Facets*, 5(1), 921-921
- Evans, J.W. (1921). (1) Economic Mineralogy: A Practical Guide to the Study of Useful Minerals (2) Mineralogy: An Introduction to the Study of Minerals and Crystals. *Nature Publishing Group UK London*, 107, 646–647.
- Facchi, D.P., Cazetta, A.L., Canesin, E.A., Almeida, V.C., Bonafé, E.G., Kipper, M.J., & Martins, A.F. (2018). New magnetic chitosan/alginate/Fe₃O₄@ SiO₂ hydrogel composites applied for removal of Pb (II) ions from aqueous systems. *Chemical Engineering Journal*, 337, 595-608.
- Fagundes-Klen, M., Ferri, P., Martins, T., Tavares, C., & Silva, E. (2007). Equilibrium study of the binary mixture of Cd–zinc ions biosorption by the *Sargassum filipendula* species using adsorption isotherms models and neural

- network. *Biochemical Engineering Journal*, 34(2), 136-146.
- Faiz, Y., Tufail, M., Javed, M. T., & Chaudhry, M. M. (2009). Road dust pollution of Cd, Cu, Ni, Pb and Zn along Islamabad expressway, Pakistan. *Microchemical Journal*, 92(2), 186-192.
- Farhat, A., Mohammadzadeh, A., Balali-Mood, M., Aghajanpoor-Pasha, M., & Ravanshad, Y. (2013). Correlation of blood lead level in mothers and exclusively breastfed infants: A study on infants aged less than six months. *Asia Pacific Journal of Medical Toxicology*, 2, 150-2.
- Fawzy, M.A. (2016). Phycoremediation and adsorption isotherms of Cd and copper ions by *Merismopedia tenuissima* and their effect on growth and metabolism. *Environmental toxicology and pharmacology*, 46, 116-121.
- Fazlzadeh, M., Khosravi, R., & Zarei, A. (2017). Green synthesis of zinc oxide nanoparticles using *Peganum harmala* seed extract, and loaded on *Peganum harmala* seed powdered activated carbon as new adsorbent for removal of Cr (VI) from aqueous solution. *Ecological Engineering*, 103, 180-190.
- Feng, L., Yan, H., Dai, C., Xu, W., Gu, F., Zhang, F., Li, T., Xian, J., He, X., & Yu, Y. (2020). The systematic exploration of Cd-accumulation characteristics of maize kernel in acidic soil with different pollution levels in China. *Science of the total environment*, 729, 138972.
- Finger, M., Palacio-Barrera, A.M., Richter, P., Schlembach, I., Büchs, J.
- Rosenbaum, M.A. (2022). Tunable population dynamics in a synthetic filamentous coculture. *Microbiology Open*, 11(5), 1324.
- Fourest, E., & Roux, J.C. (1992). Heavy metal biosorption by fungal mycelial by-products: mechanisms and influence of pH. *Applied Microbiology and Biotechnology*, 37, 399-403.
- Freundlich, H. (1906). Over the adsorption in

- solution. *The Journal of Physical Chemistry*, 57(385471), 1100-1107.
- Galiulin, R.V., Bashkin, V.N., Galiulina, R.R., & Birch, P. (2001). A Critical Review: Protection from Pollution by Heavy Metals- Phytoremediation of Industrial Wastewater. *Land Contamination & Reclamation*, 9(4), 349-358.
- Gao, Q., Wong, Y., & Tam, N.F. (2017). Antioxidant responses of different microalgal species to nonylphenol-induced oxidative stress. *Journal of Applied Phycology*, 29 1317-1329.
- Gautam, P.K., Gautam, R.K., Banerjee, S., Chattopadhyaya, M., & Pandey, J. (2016). Heavy metals in the environment: fate, transport, toxicity and remediation technologies. *Nova Science Publishers*, 60, 101-130.
- Geitler, L., & Rabenhorst, L. (1932). Cyanophyceae, pp. 1060-1061, Akademische Verlag, Leipzig, Germany.
- Genchi, G., Sinicropi, M.S., Lauria, G., Carocci, A., & Catalano, A. (2020). The effects of Cd toxicity. *International journal of environmental research and public health*, 17(11), 3782.
- Ghaedi, A.M., Panahimehr, M., Nejad, A.R.S., Hosseini, S.J., Vafaei, A., & Baneshi, M.M. (2018). Factorial experimental design for the optimization of highly selective adsorption removal of lead and copper ions using metal organic framework MOF-2 (Cd). *Journal of Molecular Liquids*, 272, 15-26.
- Ghaedi, M., Ansari, A., Habibi, M. H., & Asghari, A. R. (2014). Removal of malachite green from aqueous solution by zinc oxide nanoparticle loaded on activated carbon: kinetics and isotherm study. *Journal of Industrial and Engineering Chemistry*, 20(1), 17-28.
- Ghaly, A., Ananthashankar, R., Alhattab, M. & Ramakrishnan, V.V. (2014). Production, characterization and treatment of textile effluents: a critical review.

- Chemical Engineering & Process Technology Journal*, 5(1), 1-19.
- Glibert, P. M. (2017). Eutrophication, harmful algae and biodiversity—Challenging paradigms in a world of complex nutrient changes. *Marine Pollution Bulletin*, 124(2), 591-606.
- Goering, P., Waalkes, M., & Klaassen, C. (1995). Toxicology of metals: biochemical aspects, *Toxicology of metals*, 115, 189-214.
- Goher, M.E., AM, A.E.-M., Abdel-Satar, A.M., Ali, M.H., Hussian, A.E., & Napiórkowska- Krzebietke, A. (2016). Biosorption of some toxic metals from aqueous solution using non-living algal cells of *Chlorella vulgaris*. *Journal of Elementology*, 21(3), 703-714.
- Gomont, M.A. (1892) Monographie des oscillariées:(nostocacées homocystées), G. Masson
- Gong, J., Chen, L., Zeng, G., Long, F., Deng, J., Niu, Q., & He, X. (2012). Shellac-coated iron oxide nanoparticles for removal of Cd (II) ions from aqueous solution. *Journal of Environmental Sciences*, 24(7), 1165-1173.
- Goswami, S., Syiem, M.B., & Pakshirajan, K. (2015). Cd removal by *Anabaena doliolum* Ind1 isolated from a coal mining area in Meghalaya, India: associated structural and physiological alterations. *Environmental Engineering Research*, 20(1), 41-50.
- Goyer, R.A. (1990). Transplacental transport of lead. *Environmental Health Perspectives*, 89, 101-105.
- Grace, C.E.E., Lakshmi, P.K., Meenakshi, S., Vaidyanathan, S., Srisudha, S., & Mary, M.B. (2020). Biomolecular transitions and lipid accumulation in green microalgae monitored by FTIR and Raman analysis. *Spectrochimica Acta Part A: Molecular and Biomolecular Spectroscopy*, 224, 117382.
- Grossmann, L., Hinrichs, J., & Weiss, J. (2020). Cultivation and downstream

- processing of microalgae and cyanobacteria to generate protein-based technofunctional food ingredients. *Critical Reviews in Food Science and Nutrition*, 60(17), 2961-2989.
- Gupta, S.K., Ansari, F.A., Shriwastav, A., Sahoo, N.K., Rawat, I., & Bux, F. (2016). Dual role of *Chlorella sorokiniana* and *Scenedesmus obliquus* for comprehensive wastewater treatment and biomass production for bio-fuels. *Journal of Cleaner Production*, 115, 255-264.
- Gupta, V., & Rastogi, A. (2008). Equilibrium and kinetic modelling of Cd (II) biosorption by nonliving algal biomass *Oedogonium* sp. from aqueous phase. *Journal of hazardous materials*, 153(1-2), 759-766.
- Gupta, V.K., & Rastogi, A. (2008). Biosorption of lead (II) from aqueous solutions by non-living algal biomass *Oedogonium* sp. and *Nostoc* sp. a comparative study. *Colloids and Surfaces B: Biointerfaces*, 64(2), 170-178.
- Hagemann, M., & Hess, W. R. (2018). Systems and synthetic biology for the biotechnological application of cyanobacteria. *Current opinion in biotechnology*, 49, 94-99.
- Haghighi, O., Shahryari, S., Ebadi, M., Modiri, S., Zahiri, H.S., Maleki, H., & Noghabi, K.A. (2017). *Limnothrix* sp. KO05: A newly characterized cyanobacterial biosorbent for Cd removal: the enzymatic and non-enzymatic antioxidant reactions to Cd toxicity. *Environmental toxicology and pharmacology*, 51, 142-155.
- Hajjaligol, S., Taher, M., & Malekpour, A. (2006). A new method for the selective removal of Cd and zinc ions from aqueous solution by modified clinoptilolite. *Adsorption Science & Technology*, 24(6), 487-496.
- Hallenbeck, P.C. (2017). Modern topics in the phototrophic prokaryotes:

- environmental and applied aspects*, Springer. DOI. <https://doi.org/10.1007/978-3-319-46261-5>
- Hamed, S.M., El-Gaml, N.M., & Eissa, S.T. (2022). Integrated biofertilization using yeast with cyanobacteria on growth and productivity of wheat. Beni-Suef University. *Journal of Basic and Applied Sciences*, 11(1), 112.
- Hameed, H., Waheed, A., Sharif, M.S., Saleem, M., Afreen, A., Tariq, M., Kamal, A., Al-Onazi, W.A., Al Farraj, D.A., & Ahmad, S. (2023). Green Synthesis of Zinc Oxide (ZnO) Nanoparticles from Green Algae and Their Assessment in Various Biological Applications. *Micromachines*, 14(5), 928.
- Hamida, R.S., Abdelmeguid, N.E., Ali, M.A., Bin-Meferij, M.M., & Khalil, M.I. (2020). Synthesis of silver nanoparticles using a novel cyanobacteria *Desertifilum* sp. extract: Their antibacterial and cytotoxicity effects. *International journal of nanomedicine*, 15, 49-63.
- Hamouda, R.A., & El-Naggar, N.E.-A. (2021). Cyanobacteria-based microbial cell factories for production of industrial products. In *Microbial cell factories engineering for production of biomolecules*. Academic Press, 277-302. <https://doi.org/10.1016/B978-0-12-821477-0.00007-6>.
- Hamza, M.F., Roux, J.C., & Guibal, E. (2018). Uranium and europium sorption on amidoxime- functionalized magnetic chitosan micro-particles. *Chemical Engineering Journal*, 344, 124-137.
- Hashim, M., & Chu, K. (2004). Biosorption of Cd by brown, green, and red seaweeds. *Chemical Engineering Journal*, 97(2-3), 249-255.
- Hayat, M.T., Nauman, M., Nazir, N., Ali, S., & Bangash, N. (2019). Environmental Hazards of Cd: Past, Present, and Future. Cd toxicity & tolerance in plants, from plant Physiology to Remediation. *Academic Press*, 163-183.

<https://doi.org/10.1016/B978-0-12-814864-8.00007-3>.

- Hazarika, J., Pakshirajan, K., Sinharoy, A., & Syiem, M.B. (2015). Bioremoval of Cu (II), Zn (II), Pb (II) and Cd (II) by *Nostoc muscorum* isolated from a coal mining site. *Journal of Applied Phycology*, 27, 1525-1534.
- Hedges, S. B., Chen, H., Kumar, S., Wang, D. Y., Thompson, A. S., & Watanabe, H. (2001). A genomic timescale for the origin of eukaryotes. *BMC Evolutionary Biology*, 1(1), 1-10.
- Heimann, K., & Cirés, S. (2015). N₂-Fixing Cyanobacteria: Ecology and Biotechnological Applications. Handbook of Marine Microalgae, Biotechnology Advances. *Academic Press*, 501-515.
- Henze, M., van Loosdrecht, M.C., Ekama, G.A., & Brdjanovic, D. (2008). Biological wastewatertreatment. *International Water Association publishing*.
- Ho, Y. S., & McKay, G. (1999). Pseudo-second order model for sorption processes. *Process biochemistry*, 34(5), 451-465.
- Ho, Y.S., & McKay, G. (1998). A comparison of chemisorption kinetic models applied to pollutant removal on various sorbents. *Process Safety and Environmental Protection*, 76(4), 332-340.
- Hoffman, D., Rattner, B., Burton Jr, G. and Cairns Jr, J. (2002). Bioaccumulation And Bioconcentration In Aquatic Organisms. Handbook of Ecotoxicology. *CRC Press*, 901- 916.
- Holland, H.D. (2002). Volcanic gases, black smokers, and the Great Oxidation Event. *Geochimica et Cosmochimica acta*, 66(21), 3811-3826.
- Huang, H., Xu, X., Shi, C., Liu, X., & Wang, G. (2018). Response of taste and odor compounds to elevated cyanobacteria biomass and temperature. *Bulletin of environmental contamination and toxicology*, 101, 272-278.

- Huang, L.T.Y., Cao, H., Ma, J.Z., & Wang, X.X. (2022). Efficient removal of Pb(II) by UiO-66- NH₂: a combined experimental and spectroscopic studies. *Environmental Nanotechnology, Monitoring & Management*, 18:100741. <https://doi.org/10.1016/j.enmm.2022.100741>.
- Huang, Z., Mo, S., Yan, L., Wei, X., Huang, Y., Zhang, L., Zhang, S., Liu, J., Xiao, Q. & Lin, H.(2021). A simple culture method enhances the recovery of culturable actinobacteria from coastal sediments. *Frontiers in Microbiology*, 12, 675048.
- Huber, P., Diovisalvi, N., Ferraro, M., Metz, S., Lagomarsino, L., Llamas, M.E., Royo-Llonch, M., Bustingorry, J., Escaray, R., & Acinas, S.G. (2017). Phenotypic plasticity in freshwater picocyanobacteria. *Environmental Microbiology*, 19(3), 1120-1133.
- Humbert, J. F., & Fastner, J. (2016). Ecology of cyanobacteria. *Handbook of cyanobacterial monitoring and cyanotoxin analysis*, 9-18. <https://doi.org/10.1002/9781119068761.ch 2>.
- Hussain, A., Rehman, F., Rafeeq, H., Waqas, M., Asghar, A., Afsheen, N., & Iqbal, H. M. (2022). In-situ, Ex-situ, and nano-remediation strategies to treat polluted soil, water, and air–A review. *Chemosphere*, 289, 133252.
- Hwang, S., Umar, A., Dar, G., Kim, S., & Badran, R. (2014). Synthesis and characterization of iron oxide nanoparticles for phenyl hydrazine sensor applications. *Sensor Letters*, 12(1), 97-101.
- Igwe, J., & Abia, A. (2006). A bioseparation process for removing heavy metals from waste water using biosorbents. *African Journal of Biotechnology*, 5(11), 1684-5315.
- Ikeuchi, M. and Tabata, S. (2001). *Synechocystis sp.* PCC 6803 a useful tool in the study of the genetics of cyanobacteria. *Photosynthesis research*, 70, 73-83.

- Iqbal, M., Breivik, K., Syed, J.H., Malik, R.N., Li, J., Zhang, G., & Jones, K.C. (2015). Emerging issue of e-waste in Pakistan: a review of status, research needs and data gaps. *Environmental Pollution*, 207, 308-318.
- Iram, M., Guo, C., Guan, Y., Ishfaq, A., & Liu, H. (2010). Adsorption and magnetic removal of neutral red dye from aqueous solution using Fe₃O₄ hollow nanospheres. *Journal of hazardous materials*, 181(1-3), 1039-1050.
- Iravani, S. (2011). Green synthesis of metal nanoparticles using plants. *Green Chemistry* 13(10), 2638-2650.
- Ishii, S., Segawa, T., & Okabe, S. (2013). Simultaneous quantification of multiple food-and waterborne pathogens by use of microfluidic quantitative PCR. *Applied and environmental microbiology*, 79(9), 2891-2898.
- Jacob, J.M., Karthik, C., Saratale, R.G., Kumar, S.S., Prabakar, D., Kadirvelu, K. & Pugazhendhi, A. (2018). Biological approaches to tackle heavy metal pollution: a survey of literature. *Journal of environmental management*, 217, 56-70.
- Jain, M., Yadav, M., Kohout, T., Lahtinen, M., Garg, V.K., & Sillanpää, M. (2018). Development of iron oxide/activated carbon nanoparticle composite for the removal of Cr (VI), Cu (II) and Cd (II) ions from aqueous solution. *Water Resources and Industry*, 20, 54-74.
- Jasser, I., Callieri, C., Meriluoto, J., Spoof, L., & Codd, G. (2017). Handbook of cyanobacterial monitoring and cyanotoxin analysis.
- Jezberová, J., & Komárková, J. (2007). Morphometry and growth of three *Synechococcus*-like picoplanktic cyanobacteria at different culture conditions. *Hydrobiologia*, 578, 17-27.
- Jiang, J., Zhang, N., Yang, X., Song, L., & Yang, S. (2016). Toxic metal biosorption by macrocolonies of cyanobacterium *Nostoc sphaeroides* Kützinger. *Journal of*

- Applied Phycology*, 28, 2265-2277.
- Johansen, J.R., Bohunicka, M., Lukesova, A., Hrckova, K., Vaccarino, M.A., & Chesarino, N.M. (2014). Morphological and molecular characterization within 26 strains of the genus *Cylindrospermum* (Nostocaceae, Cyanobacteria), with descriptions of three new species. *Journal of Phycology*, 50(1), 187-202.
- John, D.M., Whitton, B.A., & Brook, A.J. (2002). The freshwater algal flora of the British Isles: An identification guide to freshwater and terrestrial algae. *Cambridge University Press*.
- Joint, I., Mühling, M., & Querellou, J. (2010). Culturing marine bacteria—an essential prerequisite for biodiscovery. *Microbial biotechnology*, 3(5), 564-575.
- Jupp, B.P., Fowler, S.W., Dobretsov, S., van der Wiele, H., & Al-Ghafri, A. (2017). Assessment of heavy metal and petroleum hydrocarbon contamination in the Sultanate of Oman with emphasis on harbours, marinas, terminals and ports. *Marine Pollution Bulletin*, 121(1-2), 260-273.
- Kabirnatay, S., Nematzadeh, G.A., Talebi, A.F., Saraf, A., Suradkar, A., Tabatabaei, M., & Singh, P. (2020). Description of novel species of *Aliinostoc*, *Desikacharya* and *Desmonostoc* using a polyphasic approach. *International Journal of Systematic and Evolutionary Microbiology*, 70(5), 3413-3426.
- Kadirvelu, K., Thamaraiselvi, K., & Namasivayam, C. (2001). Removal of heavy metals from industrial wastewaters by adsorption onto activated carbon prepared from an agricultural solid waste. *Bioresource Technology*, 76(1), 63-65.
- Kaewsarn, P. (2002). Biosorption of copper (II) from aqueous solutions by pre-treated biomass of marine algae *Padina* sp. *Chemosphere*, 47(10), 1081-1085.
- Kaleem, M., Minhas, L.A., Hashmi, M.Z., Ali, M.A., Mahmoud, R.M., Saqib, S., Nazish, M., Zaman, W., & Samad Mumtaz, A. (2023). Biosorption of Cd and

- Lead by Dry Biomass of *Nostoc* sp. MK-11: Kinetic and Isotherm Study. *Molecules*, 28(5), 2292.
- Kaneko, T., Sato, S., Kotani, H., Tanaka, A., Asamizu, E., Nakamura, Y., Miyajima, N., Hirose, M., Sugiura, M., & Sasamoto, S. (1996). Sequence analysis of the genome of the unicellular cyanobacterium *Synechocystis* sp. strain PCC6803. II. Sequence determination of the entire genome and assignment of potential protein-coding regions. *DNA research*, 3(3), 109-136.
- Karpagavinayagam, P., & Vedhi, C. (2019). Green synthesis of iron oxide nanoparticles using *Avicennia marina* flower extract. *Vacuum*, 160, 286-292.
- Katircioğlu, H., Aslım, B., Türker, A.R., Atıcı, T., & Beyatlı, Y. (2008). Removal of Cd (II) ion from aqueous system by dry biomass, immobilized live and heat-inactivated *Oscillatoria* sp. H1 isolated from freshwater (Mogan Lake). *Bioresource Technology*, 99(10), 4185-4191.
- Kermarrec, L., Franc, A., Rimet, F., Chaumeil, P., Humbert, J.F. & Bouchez, A. (2013). Next-generation sequencing to inventory taxonomic diversity in eukaryotic communities: a test for freshwater diatoms. *Molecular ecology resources*, 13(4), 607-619.
- Kertesz, M.A., Cook, A.M., & Leisinger, T. (1994). Microbial metabolism of sulfur and phosphorus-containing xenobiotics. *FEMS Microbiology Reviews*, 15(2-3), 195-215.
- Khalafi, T., Buazar, F., & Ghanemi, K. (2019). Phycosynthesis and enhanced photocatalytic activity of zinc oxide nanoparticles toward organosulfur pollutants. *Scientific Reports*, 9(1), 6866.
- Khalid, S., Shahid, M., Niazi, N.K., Murtaza, B., Bibi, I., & Dumat, C. (2017). A comparison of technologies for remediation of heavy metal contaminated soils.

- Journal of Geochemical Exploration*, 182, 247-268.
- Khan, Z. I., Ashraf, M., Ahmad, K., & Akram, N. A. (2011). A study on the transfer of Cd from soil to pasture under semi-arid conditions in Sargodha, Pakistan. *Biological trace element research*, 142, 143-147.
- Koller, M. (2017). Advances in Polyhydroxyalkanoate (PHA) Production. *Bioengineering*, 4 (4), 88.
- Komárek, J. (2005). Cyanoprokaryota 2. Teil/2nd part: oscillatoriales. *Susswasserflora von Mitteleuropa*, 19, 1-759.
- Komarek, J. (2006). Cyanobacterial taxonomy: current problems and prospects for the integration of traditional and molecular approaches. *Algae*, 21(4), 349-375.
- Komárek, J. (2014) Modern classification of cyanobacteria. Cyanobacteria: An economic perspective, 21-39
- Komárek, J. (2016). A polyphasic approach for the taxonomy of cyanobacteria: principles and applications. *European Journal of Phycology*, 51(3), 346-353.
- Komárek, J. (2016b). Review of the cyanobacterial genera implying planktic species after recent taxonomic revisions according to polyphasic methods: state as of 2014. *Hydrobiologia*, 764, 259-270.
- Komárek, J., & Anagnostidis, K. (1989). Modern approach to the classification system of Cyanophytes 4-Nostocales. *Algological Studies/Archiv für Hydrobiologie*, 247-345.
- Komárek, J., Kaštovský, J., & Jezberová, J. (2011). Phylogenetic and taxonomic delimitation of the cyanobacterial genus *Aphanothece* and description of *Anathece* gen. nov. *European Journal of Phycology*, 46(3), 315-326.
- Komárek, J., Kaštovský, J., Mareš, J., & Johansen, J. (2014). Taxonomic classification of cyanoprokaryotes (cyanobacterial genera) Taxonomic

- classification of cyanoprokaryotes (cyanobacterial genera) 2014, using a polyphasic approach. *Preslia*, 86, 295-233.
- Korelusova, J., Kas̆tovský, J. & Komárek, J. (2009). Heterogeneity Of The Cyanobacterial Genus *Synechocystis* And Description Of A New Genus, *Geminocystis* 1. *Journal of Phycology*, 45(4), 928-937.
- Kulkarni, S. & Kaware, J. (2014). Regeneration and recovery in adsorption-a review. *The International Journal of Innovative Research in Science, Engineering and Technology*, 1(8), 61-64.
- Kumar, D., & Gaur, J. (2011). Metal biosorption by two cyanobacterial mats in relation to pH, biomass concentration, pretreatment and reuse. *Bioresource Technology*, 102(3), 2529- 2535.
- Kumar, K., Mella-Herrera, R.A., & Golden, J.W., (2010). Cyanobacterial heterocysts. *Cold Spring Harbor perspectives in biology*, 2(4), a000315
- Kumar, K.S., Dahms, H.U., Won, E.J., Lee, J.S. & Shin, K.H. (2015). Microalgae—a promising tool for heavy metal remediation. *Ecotoxicology and Environmental Safety*, 113, 329- 352.
- Kumar, M., Singh, A.K. & Sikandar, M. (2018a). Study of sorption and desorption of Cd (II) from aqueous solution using isolated green algae *Chlorella vulgaris*. *Applied WaterScience*, 8(8), 225.
- Kumar, S., Stecher, G., Li, M., Knyaz, C. & Tamura, K. (2018b). MEGA X: molecular evolutionary genetics analysis across computing platforms. *Molecular biology and evolution*, 35(6), 1547.
- Kumar, V., Sinha, A.K., Rodrigues, P.P., Mubiana, V.K., Blust, R., & De Boeck, G. (2015). Linking environmental heavy metal concentrations and salinity gradients with meta accumulation and their effects: A case study in 3 mussel

- species of Vitória estuary and Espírito Santo bay, Southeast Brazil. *Science of the total environment*, 523, 1-15.
- Kumari, M., Pittman Jr, C.U., & Mohan, D. (2015). Heavy metals [chromium (VI) and lead (II)] removal from water using mesoporous magnetite (Fe₃O₄) nanospheres. *Journal of colloid and interface science*, 442, 120-132.
- Kurmayer, R., Deng, L., & Entfellner, E. (2016). Role of toxic and bioactive secondary metabolites in colonization and bloom formation by filamentous cyanobacteria *Planktothrix*. *Harmful algae*, 54, 69-86.
- Langmuir, I. (1918). The adsorption of gases on plane surfaces of glass, mica and platinum. *Journal of the American Chemical society*, 40(9), 1361-1403.
- Laus, R., Costa, T.G., Szpoganicz, B., & Fávere, V.T. (2010). Adsorption and desorption of Cu (II), Cd (II) and Pb (II) ions using chitosan crosslinked with epichlorohydrin-triphosphate as the adsorbent. *Journal of hazardous materials*, 183(1-3), 233-241.
- Lee, A.H., & Nikraz, H. (2014). BOD: COD ratio as an indicator for pollutants leaching from landfill. *Journal of Clean Energy Technologies*, 2(3), 263-266.
- Lee, E. (2016). *Molecular systematics of cyanobacteria* (Doctoral dissertation, Murdoch University).
- Lee, R.E. (2018). *Phycology*. Cambridge university press.
- Lefler, F.W., Berthold, D.E., & Laughinghouse IV, H.D. (2023). Cyanoseq: A database of cyanobacterial 16S rRNA gene sequences with curated taxonomy. *Journal of Phycology*, 59(3), 470-480.
- Lefler, F.W., Berthold, D.E., & Laughinghouse IV, H.D. (2021). The occurrence of *Affixifilum* gen. nov. and *Neolyngbya* (Oscillatoriaceae) in South Florida (USA), with the description of *A. floridanum* sp. nov. and *N. biscaynensis* sp. nov.

- Journal of Phycology*, 57(1), 92- 110.
- Lengke, M.F., Fleet, M.E., & Southam, G. (2006). Synthesis of platinum nanoparticles by reaction of filamentous cyanobacteria with platinum (IV)-chloride complex. *Langmuir*, 22(17), 7318-7323.
- Leong, Y.K. Lengke, M.F., Fleet, M.E., & Southam, G. (2006). Synthesis of platinum nanoparticles by reaction of filamentous cyanobacteria with platinum (IV) chloride complex. *Langmuir*, 22(17), 7318-7323.
- Li, H., Alsanea, A., Barber, M. and Goel, R. (2019). High-throughput DNA sequencing reveals the dominance of pico-and other filamentous cyanobacteria in an urban freshwater Lake. *Science of the total environment* 661, 465-480.
- Li, M., Zhang, Z., Li, R., Wang, J.J., & Ali, A. (2016). Removal of Pb (II) and Cd (II) ions from aqueous solution by thiosemicarbazide modified chitosan. *International journal of biological macromolecules*, 86, 876-884.
- Li, X., Huo, S., & Xi, B. (2020). Updating the resolution for 16S rRNA OTUs clustering reveals the cryptic cyanobacterial genus and species. *Ecological Indicators* 117, 106695.
- Li, Z., & Brand, J. (2007). *Leptolyngbya nodulosa* sp. nov.(Oscillatoriaceae), a subtropicalmarine cyanobacterium that produces a unique multicellular structure. *Phycologia*, 46(4),396-401.
- Lin, J., Su, B., Sun, M., Chen, B., & Chen, Z. (2018). Biosynthesized iron oxide nanoparticles used for optimized removal of Cd with response surface methodology. *Science of the total environment*,t 627, 314-321.
- Lindberg, P., Park, S., & Melis, A. (2010). Engineering a platform for photosynthetic isoprene production in cyanobacteria, using *Synechocystis* as the model organism. *Metabolic engineering*, 12(1), 70-79.

- Lipok, J., Owsiak, T., Młynarz, P., Forlani, G., & Kafarski, P. (2007). Phosphorus NMR as a tool to study mineralization of organophosphonates-the ability of *Spirulina* spp. to degrade glyphosate. *Enzyme and Microbial Technology*, 41(3), 286-291.
- Lipok, J., Wiczorek, D., Jewgiński, M., & Kafarski, P. (2009). Prospects of in vivo ³¹P NMR method in glyphosate degradation studies in whole cell system. *Enzyme and Microbial Technology*, 44(1), 11-16.
- Liu, J., Zheng, L., Li, Y., Free, M., & Yang, M. (2016). Adsorptive recovery of palladium (II) from aqueous solution onto cross-linked chitosan/montmorillonite membrane. *RSC advances*, 6(57), 51757-51767.
- Liu, L., Li, C., Bao, C., Jia, Q., Xiao, P., Liu, X., & Zhang, Q. (2012). Preparation and characterization of chitosan/graphene oxide composites for the adsorption of Au (III) and Pd (II). *Talanta*, 93, 350-357.
- Liu, T., Lawluyv, Y., Shi, Y., Ighalo, J.O., He, Y., Zhang, Y., & Yap, P.S. (2022). Adsorption of Cd and lead from aqueous solution using modified biochar: A review. *Journal of Environmental Chemical Engineering*, 10(1), 106502.
- Liu, X.L., Ma R, Zhuang, L., Hu, B.W., Chen, J.R., Liu, X.Y., & Wang, X.K. (2021a). Recent developments of doped g-C₃N₄ photocatalysts for the degradation of organic pollutants. *Critical Reviews in Environmental Science and Technology*, 51:751–790
- Lodeiro, P., Barriada, J.L., Herrero, R., & De Vicente, M.S. (2006). The marine macroalga *Cystoseira baccata* as biosorbent for Cd (II) and lead (II) removal: kinetic and equilibrium studies. *Environmental Pollution*, 142(2), 264-273.
- Löffelhardt, W., & Bohnert, H. J. (1994). Molecular biology of cyanelles. In *The molecular biology of cyanobacteria*, 1, 65-89.

- Lou, Y., Luo, H., Hu, T., Li, H., & Fu, J. (2013). Toxic effects, uptake, and translocation of Cd and Pb in *perennial ryegrass*. *Ecotoxicology*, 22, 207-214.
- Luo, J.M., & Xiao, X. (2010). Biosorption of Cd (II) from aqueous solutions by industrial fungus *Rhizopus cohnii*. *Transactions of nonferrous metals society of China*, 20(6), 1104-1111.
- Lyra, C., Suomalainen, S., Gugger, M., Vezie, C., Sundman, P., Paulin, L., & Sivonen, K. (2001). Molecular characterization of planktic cyanobacteria of *Anabaena*, *Aphanizomenon*, *Microcystis* and *Planktothrix* genera. *International Journal of Systematic and Evolutionary Microbiology*, 51(2), 513-526.
- Mack, C., Wilhelmi, B., Duncan, J., & Burgess, J. (2007). Biosorption of precious metals. *Biotechnology advances*, 25(3), 264-271.
- Mahdavi, M., Namvar, F., Ahmad, M.B., & Mohamad, R. (2013). Green biosynthesis and characterization of magnetic iron oxide (Fe₃O₄) nanoparticles using seaweed (*Sargassum muticum*) aqueous extract. *Molecules*, 18(5), 5954-5964.
- Mai, T., Johansen, J. R., Pietrasiak, N., Bohunická, M., & Martin, M. P. (2018). Revision of the Synechococcales (Cyanobacteria) through recognition of four families including Oculatellaceae fam. nov. and Trichocoleaceae fam. nov. and six new genera containing 14 species. *Phytotaxa*, 365, 1–59.
- Mala, J.G.S., Nair, B.U., & Puvanakrishnan, R. (2006). Bioaccumulation and biosorption of chromium by *Aspergillus niger* MTCC 2594. *The Journal of General and Applied Microbiology*, 52(3), 179-186.
- Malec, P., Mysliwa-Kurdziel, B., Prasad, M., Waloszek, A., & Strzałka, K. (2011). Role of aquatic macrophytes in biogeochemical cycling of heavy metals, relevance to soil- sediment continuum detoxification and ecosystem health. *Detoxification of heavy metals*, 30, 345-368.

- Mandhata, C.P., Bishoyi, A.K., Sahoo, C.R., Maharana, S., & Padhy, R.N. (2023). Insight to biotechnological utility of phytochemicals from cyanobacterium *Anabaena* sp.: An overview. *Fitoterapia*, 169, 105594.
- Mandhata, C.P., Sahoo, C.R., & Padhy, R.N. (2022). Biomedical applications of biosynthesized gold nanoparticles from cyanobacteria: An overview. *Biological Trace Element Research*, 200(12), 5307-5327.
- Mareš, J. (2018). Multilocus and SSU rRNA gene phylogenetic analyses of available cyanobacterial genomes, and their relation to the current taxonomic system. *Hydrobiologia*, 811(1), 19-34.
- Martín-Betancor, K., Rodea-Palomares, I., & Muñoz-Martín, M.A. (2015). Construction of a self-luminescent cyanobacterial bioreporter that detects a broad range of bioavailable heavy metals in aquatic environments. *Frontiers in Microbiology*, 6(1), 11.
- Masindi, V., & Muedi, K.L. (2018). Environmental contamination by heavy metals. *Heavy metals*, 10, 115-132.
- Matheickal, J.T., & Yu, Q. (1999). Biosorption of lead (II) and copper (II) from aqueous solutions by pre-treated biomass of Australian marine algae. *Bioresource technology*, 69(3), 223-229.
- McElroy, M.E., Dressler, T.L., Titcomb, G.C., Wilson, E.A., Deiner, K., Dudley, T.L., Eliason, E.J., Evans, N.T., Gaines, S.D., & Lafferty, K.D. (2020). Calibrating environmental DNA metabarcoding to conventional surveys for measuring fish species richness. *Frontiers in Ecology and Evolution*, 8, 276.
- Meeks, J.C., & Elhai, J. (2002). Regulation of cellular differentiation in filamentous cyanobacteria in free-living and plant-associated symbiotic growth states. *Microbiology and molecular biology reviews*, 66(1), 94-121.

- Mehta, S., & Gaur, J. (2005). Use of algae for removing heavy metal ions from wastewater: progress and prospects. *Critical reviews in biotechnology*, 25(3), 113-152.
- Meitei, M.D., & Prasad, M. (2013). Lead (II) and Cd (II) biosorption on *Spirodela polyrhiza* (L.) Schleiden biomass. *Journal of Environmental Chemical Engineering*, 1(3),200-207.
- Mezynska, M., & Brzóska, M.M. (2018). Environmental exposure to Cd-A risk for health of the general population in industrialized countries and preventive strategies. *Environmental Science and Pollution Research*, 25, 3211-3232.
- Minhas, L.A., Kaleem, M., Minhas, M.A.H., Waqar, R., Al Farraj, D.A., Alsaigh, M.A., Badshah, H., Haris, M. and Mumtaz, A.S. (2023a). Biogenic Fabrication of Iron Oxide Nanoparticles from *Leptolyngbya* sp. L-2 and Multiple In Vitro Pharmacogenetic Properties. *Toxics*, 11(7), 561.
- Minhas, L.A., Mumtaz, A.S., Kaleem, M., Farraj, D.A., Kamal, K., Minhas, M.A.H., Waqar, R. and Mahmoud, R.M. (2023b). Green Synthesis of Zinc Oxide Nanoparticles Using *Nostoc* sp. and Their Multiple Biomedical Properties. *Catalysts*, 13(3), 549.
- Mirghaffari, N., Moeini, E., & Farhadian, O. (2015). Biosorption of Cd and Pb ions from aqueous solutions by biomass of the green microalga, *Scenedesmus quadricauda*. *Journal of Applied Phycology*, 27, 311-320.
- Mishra, A.K., Tiwari, D., & Rai, A.N. (2018). Cyanobacteria: from basic science to applications. London, Academic Press, an imprint of Elsevier.
- Mitra, S., Patra, P., Pradhan, S., Debnath, N., Dey, K.K., Sarkar, S., Chattopadhyay, D., & Goswami, A. (2015). Microwave synthesis of ZnO@mSiO₂ for detailed antifungal mode of action study: understanding the insights into oxidative stress.

Journal of colloid and interface science, 444, 97-108.

- Mmereki, D., Li, B., Baldwin, A., & Hong, L. (2016). The generation, composition, collection, treatment and disposal system, and impact of E-waste. In Mihai F-C (ed) E-waste in transition from pollution to resource. *InTech* (pp. 65–93). doi:[10.5772/61332](https://doi.org/10.5772/61332).
- Mohamed, A., Atta, R. R., Kotp, A. A., Abo El-Ela, F. I., Abd El-Raheem, H., Farghali, A., & Mahmoud, R. (2023). Green synthesis and characterization of iron oxide nanoparticles for the removal of heavy metals (Cd²⁺ and Ni²⁺) from aqueous solutions with Antimicrobial Investigation. *Scientific Reports*, 13(1), 7227.
- Montazer-Rahmati, M.M., Rabbani, P., Abdolali, A., & Keshtkar, A.R. (2011). Kinetics and equilibrium studies on biosorption of Cd, lead, and nickel ions from aqueous solutions by intact and chemically modified brown algae. *Journal of hazardous materials*, 185(1), 401-407.
- Monteiro, C.M., Castro, P.M., & Malcata, F.X. (2012). Metal uptake by microalgae: underlying mechanisms and practical applications. *Biotechnology progress*, 28(2), 299-311.
- Moreno-Jiménez, E., Meharg, A.A., Smolders, E., Manzano, R., Becerra, D., Sánchez-Llerena, J., Albarrán, Á., & López-Piñero, A. (2014). Sprinkler irrigation of rice fields reduces grain arsenic but enhances Cd. *Science of the total environment*, 485, 468-473.
- Mota, R., Rossi, F., Andrenelli, L., Pereira, S.B., De Philippis, R., & Tamagnini, P. (2016). Released polysaccharides (RPS) from *Cyanothece* sp. CCY 0110 as biosorbent for heavy metals bioremediation: interactions between metals and RPS binding sites. *Applied Microbiology and Biotechnology*, 100, 7765-7775.

- Mur, L., Skulberg, O., & Utkilen, H. (1999). Cyanobacteria in the Environment [w:] Toxic Cyanobacteria in Water: A guide to their public health consequences, monitoring and management, Chorus I., Bartram J.(red.). WHO., London.
- Mustafa, S., Bhatti, H.N., Maqbool, M., & Iqbal, M. (2021). Microalgae biosorption, bioaccumulation and biodegradation efficiency for the remediation of wastewater and carbon dioxide mitigation: Prospects, challenges and opportunities. *Journal of Water Process Engineering*, 41, 102009.
- Nadagouda, M.N., & Varma, R.S. (2008). Green synthesis of silver and palladium nanoparticles at room temperature using coffee and tea extract. *Green Chemistry*, 10(8), 859-862.
- Nair, M.S., Rajarathinam, R., Velmurugan, S., Devakumar, J., Karthikayan, J., & Saravanakumar, S.P. (2023). Phycocyanin-conjugated chitosan-coated iron oxide nanoparticles for the separation of *Escherichia coli* cells. *Biomass Conversion and Biorefinery*, 1-12. <https://doi.org/10.1007/s13399-023-04529-7>
- Nandagopal, P., Steven, A. N., Chan, L. W., Rahmat, Z., Jamaluddin, H., & Mohd Noh, N. I. (2021). Bioactive metabolites produced by cyanobacteria for growth adaptation and their pharmacological properties. *Biology*, 10(10), 1061.
- Naseem, K., Begum, R., Wu, W., Usman, M., Irfan, A., Al-Sehemi, A. G., & Farooqi, Z. H. (2019). Adsorptive removal of heavy metal ions using polystyrene-poly (N-isopropyl methacrylamide-acrylic acid) core/shell gel particles: adsorption isotherms and kinetic study. *Journal of Molecular Liquids*, 277, 522-531.
- Naseer, M., Aslam, U., Khalid, B., & Chen, B. (2020). Green route to synthesize Zinc Oxide Nanoparticles using leaf extracts of *Cassia fistula* and *Melia azadarach* and their antibacterial potential. *Scientific Reports*, 10(1), 9055.
- Ngo, T. T., Nguyen, B. L. T., Duong, T. A., Nguyen, T. H. T., Nguyen, T. L., Kieu,

- K. T., & Pham, H. T. (2022). Polyphasic evaluation and cytotoxic investigation of isolated cyanobacteria with an emphasis on potent activities of a *Scytonema* strain. *Frontiers in Microbiology*, *13*, 1025755.
- Norena-Caro, D.A., Malone, T.M., & Benton, M.G. (2021). Nitrogen sources and iron availability affect pigment biosynthesis and nutrient consumption in *Anabaena* sp. UTEX2576. *Microorganisms*, *9*(2), 431.
- Nozzi, N.E., Oliver, J.W. and Atsumi, S. (2013). Cyanobacteria as a platform for biofuel production. *Frontiers in bioengineering and biotechnology* *1*, 7.
- Nübel, U., Garcia-Pichel, F., & Muyzer, G. (1997). PCR primers to amplify 16S rRNA genes from cyanobacteria. *Applied and environmental microbiology*, *63*(8), 3327-3332.
- Obasi, P.N., & Akudinobi, B.B. (2020). Potential health risk and levels of heavy metals in water resources of lead–zinc mining communities of Abakaliki, southeast Nigeria. *Applied Water Science*, *10*(7), 1-23.
- Olal, F.O. (2016). Biosorption of selected heavy metals using green algae, *Spirogyra* species. *Journal of Natural Sciences Research*, *6*, 14.
- Olguín, E.J., & Sánchez-Galván, G. (2012). Heavy metal removal in phytoremediation and phycoremediation: the need to differentiate between bioadsorption and bioaccumulation. *New biotechnology*, *30*(1), 3-8.
- Ondiek, J.K. (2016). Synthesis and characterization of iron nanoparticles using banana peels extracts and their application in Aptasensor. Ph.D. Thesis, University of Nairobi.
- Ouyang, D., Zhuo, Y., Hu, L., Zeng, Q., Hu, Y., & He, Z. (2019). Research on the adsorption behavior of heavy metal ions by porous material prepared with silicate tailings. *Minerals*, *9*(5), 291.

- Oyebamiji, O.O., Boeing, W.J., Holguin, F.O., Ilori, O., & Amund, O. (2019). Green microalgae cultured in textile wastewater for biomass generation and biodegradation of heavy metals and chromogenic substances. *Bioresource Technology Reports*, 7, 100247.
- Ozdes, D., Duran, C., & Senturk, H.B. (2011). Adsorptive removal of Cd (II) and Pb (II) ions from aqueous solutions by using Turkish illitic clay. *Journal of environmental management*, 92(12), 3082-3090.
- Ozer, A. & Ozer, D. (2003). Comparative study of the biosorption of Pb (II), Ni (II) and Cr (VI) ions onto *S. cerevisiae*: determination of biosorption heats. *Journal of hazardous materials*, 100(1-3), 219-229.
- Padmaja, M., Bhavani, R. & Pamila, R. (2018). Adsorption of Cd from aqueous solutions using low cost materials-a review. *International Journal of Engineering & Technology*, 7,26-29.
- Paerl, H. W., Gardner, W. S., Havens, K. E., Joyner, A. R., McCarthy, M. J., Newell, S. E., & Scott, J. T. (2016). Mitigating cyanobacterial harmful algal blooms in aquatic ecosystems impacted by climate change and anthropogenic nutrients. *Harmful Algae*, 54, 213-222.
- Paerl, H.W., & Paul, V.J. (2012). Climate change: links to global expansion of harmful cyanobacteria. *Water research*, 46(5), 1349-1363.
- Pak, T., Archilha, N. L., & de Lima Luz, L. F. (2019). Nanotechnology-based remediation of groundwater. *Nanotechnology characterization tools for environment, health, and safety*, 145-165.
- Palinska, K.A., Deventer, B., Hariri, K., & Lotocka, M. (2011). A taxonomic study on *Phormidium*-group (cyanobacteria) based on morphology, pigments, RAPD molecular markers and RFLP analysis of the 16S rRNA gene fragment. *Fottea*,

- 11(1), 41-55.
- Pandey, S., Dubey, S.K., Kashyap, A.K., & Jain, B.P. (2022). Cyanobacteria-mediated heavy metal and xenobiotics bioremediation. *Cyanobacterial Lifestyle and Its Applications in Biotechnology*, 335-350.
- Pathak, J., Ahmed, H., Singh, D.K., Pandey, A., Singh, S.P. & Sinha, R.P. (2019). Recent developments in green synthesis of metal nanoparticles utilizing cyanobacterial cell factories. *Nanomaterials in plants, algae and microorganisms*, 237-265.
- Pavasant, P., Apiratikul, R., Sungkhum, V., Suthiparinyanont, P., Wattanachira, S., & Marhaba, T. F. (2006). Biosorption of Cu^{2+} , Cd^{2+} , Pb^{2+} , and Zn^{2+} using dried marine green macroalga *Caulerpa lentillifera*. *Bioresource technology*, 97(18), 2321-2329.
- PCRWR (2016). Water quality status of major cities of Pakistan. Islamabad Capital Territory, Pakistan: PCRWR.
- Pekkoh, J., Duangjan, K., Phinyo, K., Kaewkod, T., Ruangrit, K., Thurakit, T., Pumas, C., Pathom-aree, W., Cheirsilp, B., & Gu, W. (2023). Turning waste CO₂ into value-added biorefinery co-products using cyanobacterium *Leptolyngbya* sp. KC45 as a highly efficient living photocatalyst. *Chemical Engineering Journal*, 460, 141765.
- Pérez-Rama, M., Torres, E., Suárez, C., Herrero, C., & Abalde, J. (2010). Sorption isotherm studies of Cd (II) ions using living cells of the marine microalga *Tetraselmis suecica* (Kylin) Butch. *Journal of environmental management*, 91(10), 2045-2050.
- Pinchasov, Y., Berner, T. & Dubinsky, Z. (2006). The effect of lead on photosynthesis, as determined by photoacoustics in *Synechococcus leopoliensis*

- (Cyanobacteria). *Water, air, and soil pollution*, 175, 117-125.
- Poskuta, J., Parys, E., & Romanowska, E. (1996). Toxicity of lead to photosynthesis, accumulation of chlorophyll, respiration and growth of *Chlorella pyrenoidosa*. Protective role of dark respiration. *Acta physiologiae plantarum*, 18(2), 165-171.
- Prabha, L.R., & Anil, K. (2019). Identification of functional groups in leaf, stem and root extracts of *Andrographis paniculata* by FTIR. *Research Journal of Chemistry and Environment*, 23(12), 106-110.
- Pradhan, J.K., & Kumar, S. (2014). Informal e-waste recycling: environmental risk assessment of heavy metal contamination in Mandoli industrial area, Delhi, India. *Environmental Science and Pollution Research*, 21(13), 7913-7928.
- Premanandh, J., Priya, B., Teneva, I., Dzhambazov, B., Prabakaran, D., & Uma, L. (2006). Molecular characterization of marine cyanobacteria from the Indian subcontinent deduced from sequence analysis of the phycoerythrin operon (*cpeB-IGS-cpeA*) and 16S-23S ITS region. *The Journal of Microbiology*, 44(6), 607-616.
- Prescott, G.W. (1978). How to know the fresh water algae W. M. C. Brown Company publishers. pp. 12-267. Dubuque, Iowa, USA.
- Pure & Fergusson, J.E. (1990). The heavy elements: chemistry, environmental impact and health effects. *Applied chemistry*, 74(5), 793-807.
- Qiu, M., Liu, L., Ling, Q., Cai, Y., Yu, S., Wang, S., & Wang, X. (2022). Biochar for the removal of contaminants from soil and water: a review. *Biochar*, 4(1), 19.
- Rachlin, J.W., Jensen, T.E., & Warkentine, B. (1984). The toxicological response of the alga *Anabaena flos-aquae* (Cyanophyceae) to Cd. *Archives of Environmental Contamination and Toxicology*, 13, 143-151.
- Radkova, M., Stefanova, K., Uzunov, B., Gartner, G., & Stoyneva-Gartner, M.

- (2020). Morphological and molecular identification of microcystin-producing cyanobacteria in nine shallow Bulgarian water bodies. *Toxins*, 12(1), 39.
- Raghukumar, C., Vipparthy, V., David, J., & Chandramohan, D. (2001). Degradation of crude oil by marine cyanobacteria. *Applied Microbiology and Biotechnology*, 57, 433-436.
- Raize, O., Argaman, Y., & Yannai, S. (2004). Mechanisms of biosorption of different heavy metals by brown marine macroalgae. *Biotechnology and bioengineering*, 87(4), 451-458.
- Rajaniemi, P., Hrouzek, P., Kaštovska, K., Willame, R., Rantala, A., Hoffmann, L., Komárek, J., & Sivonen, K. (2005). Phylogenetic and morphological evaluation of the genera *Anabaena*, *Aphanizomenon*, *Trichormus* and *Nostoc* (Nostocales, Cyanobacteria). *International Journal of Systematic and Evolutionary Microbiology*, 55(1), 11-26.
- Rajiv, P., Rajeshwari, S., & Venckatesh, R. (2013). Bio-Fabrication of zinc oxide nanoparticles using leaf extract of *Parthenium hysterophorus* L. and its size-dependent antifungal activity against plant fungal pathogens. *Spectrochimica Acta Part A: Molecular and Biomolecular Spectroscopy*, 112, 384-387.
- Tran, S., Pittman Jr, C.U., & Mohan, D. (2016). Magnetic magnetite (Fe₃O₄) nanoparticle synthesis and applications for lead (Pb²⁺) and chromium (Cr⁶⁺) removal from water. *Journal of colloid and interface science*, 468, 334-346.
- Rakhshae, R., Khosravi, M., & Ganji, M.T. (2006). Kinetic modeling and thermodynamic study to remove Pb (II), Cd (II), Ni (II) and Zn (II) from aqueous solution using dead and living *Azolla filiculoides*. *Journal of hazardous materials*, 134(1-3), 120-129.
- Rakib, M.R.J., Rahman, M.A., Onyena, A.P., Kumar, R., Sarker, A., Hossain, M.B.,

- Islam, A.R.M.T., Islam, M.S., Rahman, M.M., & Jolly, Y.N. (2022). A comprehensive review of heavy metal pollution in the coastal areas of Bangladesh: abundance, bioaccumulation, health implications, and challenges. *Environmental Science and Pollution Research*, 29(45), 67532-67558
- Rangsayatorn, N., Upatham, E., Kruatrachue, M., Pokethitiyook, P., & Lanza, G. (2002). Phytoremediation potential of *Spirulina (Arthrospira) platensis*: biosorption and toxicity studies of Cd. *Environmental Pollution*, 119(1), 45-53.
- Rasheed, H., Altaf, F., Anwaar, K., & Ashraf, M. (2021). Drinking Water Quality in Pakistan: Current Status and Challenges. Pakistan Council of Research in Water Resources (PCRWR), Islamabad, pp. 141.
- Ratte, H.T. (1999). Bioaccumulation and toxicity of silver compounds: a review. *Environmental toxicology and chemistry: an international journal*, 18(1), 89-108.
- Recillas, S., García, A., González, E., Casals, E., Puentes, V., Sánchez, A. & Font, X. (2011). Use of CeO₂, TiO₂ and Fe₃O₄ nanoparticles for the removal of lead from water: Toxicity of nanoparticles and derived compounds. *Desalination*, 277(1-3), 213-220.
- Rezasoltani, S., & Champagne, P. (2023). An integrated approach for the phytoremediation of Pb (II) and the production of biofertilizer using nitrogen-fixing cyanobacteria. *Journal of Hazardous Materials* 445, 130448.
- Riani, P., & Futeri, R. (2023). Penentu jenis media terhadap efektivitas pertumbuhan jamur trichoderme harzianum. *Journal kimia saintek dan pendidikan*, 7(1), 27-34.
- Rippka, R. (1988). Isolation and purification of cyanobacteria. *Methods in enzymology*, 167, 3- 27.
- Rippka, R., Deruelles, J., Waterbury, J.B., Herdman M., & Stanier R.Y. (1979). Generic assignments, strain histories and properties of pure cultures of

- cyanobacteria. *Microbiology*. 111(1), 1–61.
- Ritchie, R.J. (2006). Consistent sets of spectrophotometric chlorophyll equations for acetone, methanol and ethanol solvents. *Photosynthesis research*, 89, 27-41.
- Robertson, B.R., Tezuka, N., & Watanabe, M.M. (2001). Phylogenetic analyses of *Synechococcus* strains (cyanobacteria) using sequences of 16S rDNA and part of the phycocyanin operon reveal multiple evolutionary lines and reflect phycobilin content. *International Journal of Systematic and Evolutionary Microbiology*, 51(3), 861-871.
- Robinson, B.H. (2009). E-waste: an assessment of global production and environmental impacts. *Science of Total Environment*, 408, 183-191.
- Rodrigues, M.S., Ferreira, L.S., de Carvalho, J.C.M., Lodi, A., Finocchio, E., & Converti, A. (2012). Metal biosorption onto dry biomass of *Arthrospira (Spirulina) platensis* and *Chlorella vulgaris*: multi-metal systems. *Journal of hazardous materials*, 217, 246-255.
- Rouhani, F., & Morsali, A. (2018). Goal-directed design of metal organic frameworks for Hg(II) and Pb(II) adsorption from aqueous solutions. *Chemistry – A European Journal*, 24, 17170–17179
- Roy, D., Greenlaw, P.N., & Shane, B.S. (1993). Adsorption of heavy metals by green algae and ground rice hulls. *Journal of Environmental Science & Health*, 28(1), 37-50.
- Rusmin, R., Sarkar, B., Tsuzuki, T., Kawashima, N., & Naidu, R. (2017). Removal of lead from aqueous solution using superparamagnetic palygorskite nanocomposite: Material characterization and regeneration studies. *Chemosphere* 186, 1006-1015.
- Ryan, P.B., Huet, N., & MacIntosh, D.L. (2000). Longitudinal investigation of

- exposure to arsenic, Cd, and lead in drinking water. *Environmental Health Perspectives*, 108(8), 731-735.
- Saber, A. A., Cantonati, M., Mareš, J., Anesi, A., & Guella, G. (2017). Polyphasic characterization of *Westiellopsis prolifica* (Hapalosiphonaceae, Cyanobacteria) from the El-Farafra Oasis (Western Desert, Egypt). *Phycologia*, 56(6), 697-709.
- Saeed, M.U., Hussain, N., Shahbaz, A., Hameed, T., Iqbal, H.M., & Bilal, M. (2022). Bioprospecting microalgae and cyanobacteria for biopharmaceutical applications. *Journal of Basic Microbiology*, 62(9), 1110-1124.
- Saif, M.M.S., Kumar, N.S., & Prasad, M. (2012). Binding of Cd to *Strychnos potatorum* seed proteins in aqueous solution: adsorption kinetics and relevance to water purification. *Colloids and Surfaces B: Biointerfaces*, 94, 73-79.
- Salam, H.A., Rajiv, P., Kamaraj, M., Jagadeeswaran, P., Gunalan, S., & Sivaraj, R. (2012). Plants: green route for nanoparticle synthesis. *International Research Journal of Biological Sciences*, 1(5), 85-90.
- Sanchez-Baracaldo, P., Hayes, P., & BLANK, C.E. (2005). Morphological and habitat evolution in the Cyanobacteria using a compartmentalization approach. *Geobiology*, 3(3), 145-165.
- Santi, I., Kasapidis, P., Karakassis, I., & Pitta, P. (2021). A comparison of DNA metabarcoding and microscopy methodologies for the study of aquatic microbial eukaryotes. *Diversity*, 13(5), 180.
- Saraf, A.G., Dawda, H.G., & Singh, P. (2019). *Desikacharya* gen. nov., a phylogenetically distinct genus of Cyanobacteria along with the description of two new species, *Desikacharya nostocoides* sp. nov. and *Desikacharya soli* sp. nov., and reclassification of *Nostoc* thermotolerans to *Desikacharya thermotolerans* comb. nov. *International Journal of Systematic and Evolutionary*

- Microbiology*, 69(2), 307-315.
- Sari, A., & Tuzen, M. (2008). Biosorption of Pb (II) and Cd (II) from aqueous solution using green alga (*Ulva lactuca*) biomass. *Journal of Hazardous Materials*, 152(1), 302-308.
- Sari, A., Uluozlü, Ö.D., & Tüzen, M. (2011). Equilibrium, thermodynamic and kinetic investigations on biosorption of arsenic from aqueous solution by algae (*Maugeotia genuflexa*) biomass. *Chemical Engineering Journal*, 167(1), 155-161.
- Sarkar, M. M., Rohani, M. F., Hossain, M. A. R., & Shahjahan, M. (2022). Evaluation of Heavy Metal Contamination in Some Selected Commercial Fish Feeds Used in Bangladesh. *Biological Trace Element Research*, **200**, 844–854.
- Sarker, A., Al Masud, M.A., Deepo, D.M., Das, K., Nandi, R., Ansary, M.W.R., Islam, A.R.M.T., & Islam, T. (2023). Biological and green remediation of heavy metal contaminated water and soils: A state-of-the-art review. *Chemosphere*, 332, 138861.
- Sarojini, G., Venkateshbabu, S., & Rajasimman, M. (2021). Facile synthesis and characterization of polypyrrole-iron oxide-seaweed (PPy-Fe₃O₄-SW) nanocomposite and its exploration for adsorptive removal of Pb (II) from heavy metal bearing water. *Chemosphere*, 278, 130400.
- Sarojini, Y. (1996). Seasonal changes in phytoplankton of sewage and receiving harbour waters at Visakhapatnam. *Phykos*, 35(1&2), 171-182.
- Sathiyavimal, S., Vasantharaj, S., Veeramani, V., Saravanan, M., Rajalakshmi, G., Kaliannan, T., Al-Misned, F.A., & Pugazhendhi, A. (2021). Green chemistry route of biosynthesized copper oxide nanoparticles using *Psidium guajava* leaf extract and their antibacterial activity and effective removal of industrial dyes.

- Journal of Environmental Chemical Engineering*, 9(2), 105033.
- Satya, A., Harimawan, A., Haryani, G.S., Johir, M., Nguyen, L.N., Nghiem, L.D., Vigneswaran, S., Ngo, H.H., & Setiadi, T. (2021). Fixed-bed adsorption performance and empirical modeling of Cd removal using adsorbent prepared from the cyanobacterium *Aphanothece* sp. cultivar. *Environmental Technology & Innovation*, 21, 101194.
- Satya, A., Harimawan, A., Haryani, G.S., Johir, M.A.H., Vigneswaran, S., Ngo, H.H., & Setiadi, T. (2020). Batch study of Cd biosorption by carbon dioxide enriched *Aphanothece* sp. dried biomass. *Water*, 12(1), 264.
- Schaechter, M. (2009). *Encyclopedia of microbiology*, Academic Press.
- Schaefer, H.R., Dennis, S., & Fitzpatrick, S. (2020). Cd: Mitigation strategies to reduce dietary exposure. *Journal of food science*, 85(2), 260-267.
- Schulz-Vogt, H.N., Angert, E.R., & Garcia-Pichel, F. (2007). Giant bacteria. eLS. doi: 10.1002/9780470015902.a0020371.
- Sciacca, S., & Conti, G.O. (2009). Mutagens and carcinogens in drinking water, 2, 157-162,
- Sciuto, K., Rascio, N., Andreoli, C., & Moro, I. (2011). Polyphasic characterization of ITD-01, a cyanobacterium isolated from the Ischia Thermal District (Naples, Italy). *Fottea*, 11(1), 31-39.
- Selatnia, A., Boukazoula, A., Kechid, N., Bakhti, M., Chergui, A., & Kerchich, Y. (2004). Biosorption of lead (II) from aqueous solution by a bacterial dead *Streptomyces rimosus* biomass. *Biochemical Engineering Journal*, 19(2), 127-135.
- Selvasembian, R., Gwenzi, W., Chaukura, N., & Mthembu, S. (2021). Recent advances in the polyurethane-based adsorbents for the decontamination of

- hazardous wastewaterpollutants. *Journal of Hazardous Materials*, 417, 125960.
- Selvasembian, R., Gwenzi, W., Chaukura, N., & Mthembu, S. (2021). Recent advances in the polyurethane-based adsorbents for the decontamination of hazardous wastewaterpollutants. *Journal of Hazardous Materials*, 417, 125960.
- Sendall, B.C., & McGregor, G.B. (2018). Cryptic diversity within the Scytonema complex: Characterization of the paralytic shellfish toxin producer *Heteroscytonema crispum*, and the establishment of the family Heteroscytonemataceae (Cyanobacteria/Nostocales). *Harmful algae*, 80, 158-170.
- Shah, M. H., Shaheen, N., Jaffar, M., & Saqib, M. (2004). Distribution of lead in relation to size of airborne particulate matter in Islamabad, Pakistan. *Journal of environmental management*, 70(2), 95-100.
- Shalaby, T.I., Fikrt, N., Mohamed, M., & El Kady, M. (2014). Preparation and characterization of iron oxide nanoparticles coated with chitosan for removal of Cd (II) and Cr (VI) from aqueous solution. *Water science and technology*, 70(6), 1004-1010.
- Sharif, M.S., Hameed, H., Waheed, A., Tariq, M., Afreen, A., Kamal, A., Mahmoud, E.A., Elansary, H.O., Saqib, S., & Zaman, W. (2023). Biofabrication of Fe₃O₄ nanoparticles from *spirogyra hyalina* and *ajuga bracteosa* and their antibacterial applications. *Molecules*, 28(8), 3403.
- Sharma, A., Shukla, S., & Kumar, S. (2022). Application of cyanobacteria in soil health and rhizospheric engineering. In *Rhizosphere Engineering*, (pp. 113-127). Academic Press. <https://doi.org/10.1016/B978-0-323-89973-4.00024-7>.
- Shen, L., Chen, R., Wang, J., Fan, L., Cui, L., Zhang, Y., Cheng, J., Wu, X., Li, J., & Zeng, W. (2021). Biosorption behavior and mechanism of Cd from aqueous

- solutions by *Synechocystis* sp. PCC6803. *RSC advances* 11(30), 18637-18650.
- Shen, L., Li, Z., Wang, J., Liu, A., Li, Z., Yu, R., Wu, X., Liu, Y., Li, J., & Zeng, W. (2018). Characterization of extracellular polysaccharide/protein contents during the adsorption of Cd (II) by *Synechocystis* sp. PCC6803. *Environmental Science and Pollution Research*, 25, 20713-20722.
- Sheng, P.X., Ting, Y.-J.P., Chen, J.P., & Hong, L. (2004). Sorption of lead, copper, Cd, zinc, and nickel by marine algal biomass: characterization of biosorptive capacity and investigation of mechanisms. *Journal of colloid and interface science*, 275(1), 131-141.
- Shinde, S.S. (2015). Antimicrobial activity of ZnO nanoparticles against pathogenic bacteria and fungi. *JSM Nanotechnol Nanomed*, 3(1), 1033.
- Shishido, T.K., Kaasalainen, U., Fewer, D.P., Rouhiainen, L., Jokela, J., Wahlsten, M., Fiore, M.F., Yunes, J.S., Rikkinen, J., & Sivonen, K. (2013). Convergent evolution of [D- Leucine1] microcystin-LR in taxonomically disparate cyanobacteria. *BMC Evolutionary Biology*, 13(1), 1-16.
- Singh, A., Mehta, S., & Gaur, J. (2007). Removal of heavy metals from aqueous solution by common freshwater filamentous algae. *World Journal of Microbiology and Biotechnology*, 23(8), 1115-1120.
- Singh, J.B., Prasad, S.M., Rai, L.C., & Kumar, H.D. (1993). Response of the cyanobacterium *Nostoc muscorum* to chromium and lead: the effect on phosphorus metabolism. *The Journal of General and Applied Microbiology*, 39(6), 559-570.
- Singh, J.S., Kumar, A., Rai, A.N., & Singh, D.P., (2016). Cyanobacteria: a precious bio-resource in agriculture, ecosystem, and environmental sustainability. *Frontiers in Microbiology*, 7,529.

- Singh, K.B., Kaushalendra, Verma, S., Lalnunpuii, R., & Rajan, J.P. (2023). Current Issues and Developments in Cyanobacteria-Derived Biofuel as a Potential Source of Energy for Sustainable Future. *Sustainability*, 15(13), 10439.
- Singh, P.K., Fillat, M.F., & Kumar, A. (2021). Cyanobacterial lifestyle and its applications in biotechnology, Academic Press.
- Singh, R., Parihar, P., Singh, M., Bajguz, A., Kumar, J., Singh, S., & Prasad, S. M. (2017). Uncovering potential applications of cyanobacteria and algal metabolites in biology, agriculture and medicine: current status and future prospects. *Frontiers in microbiology*, 8, 515.
- Singh, Y., Khattar, J., Singh, D., Rahi, P., & Gulati, A. (2014). Limnology and cyanobacterial diversity of high altitude lakes of Lahaul-Spiti in Himachal Pradesh, India. *Journal of biosciences*, 39, 643-657.
- Sivakami, R., Mahalakshmi, M., & Premkishore, G. (2015). Removal of heavy metals by biosorption using cyanobacteria isolated from freshwater pond. *International Journal of Current Microbiology and Applied Sciences*, 4(12), 655-660.
- Skeffington, A.W., Grimm, A., Schönefeld, S., Petersen, K., & Scheffel, A. (2020). An Efficient Method for the Plating of Haploid and Diploid *Emiliana huxleyi* on Solid Medium1. *Journal of Phycology*, 56(1), 238-242.
- Sodipo, B. K., & Azlan, A. A. (2015, April). Superparamagnetic iron oxide nanoparticles incorporated into silica nanoparticles by inelastic collision via ultrasonic field: role of colloidal stability. In *AIP conference proceedings* (Vol. 1657, No. 1). AIP Publishing.
- Soltani, R.D.C., Khorramabadi, G.S., Khataee, A., & Jorfi, S. (2014). Silica nanopowders/alginate composite for adsorption of lead (II) ions in aqueous solutions. *Journal of the Taiwan Institute of Chemical Engineers*, 45(3), 973-980.

- Song, Q., & Li, J. (2014). A systematic review of the human body burden of e-waste exposure in China. *Environment international*, 68, 82-93.
- Sorkhoh, N., Al-Hasan, R., Khanafer, M., & Radwan, S. (1995). Establishment of oil-degrading bacteria associated with cyanobacteria in oil-polluted soil. *Journal of Applied Bacteriology*, 78(2), 194-199.
- Stal, L. J. (1995). Physiological ecology of cyanobacteria in microbial mats and other communities. *New Phytologist*, 131(1), 1-32.
- Stal, L. J. (2012). Cyanobacterial mats and stromatolites. In *Ecology of cyanobacteria II: their diversity in space and time* (pp. 65-125). Dordrecht: Springer Netherlands.
- Stal, L. J., & Moezelaar, R. (1997). Fermentation in cyanobacteria. *FEMS microbiology reviews*, 21(2), 179-211.
- Stanier, R. Y., & Cohen-Bazire, G. (1977). Phototrophic prokaryotes: the cyanobacteria. *Annual review of microbiology*, 31(1), 225-274.
- Starodub, M., Wong, P. & Mayfield, C. (1987). Short term and long term studies on individual and combined toxicities of copper, zinc and lead to *Scenedesmus quadricauda*. *Science of the total environment*, 63, 101-110.
- Strunecký, O., Ivanova, A.P. & Mareš, J. (2023). An updated classification of cyanobacterial orders and families based on phylogenomic and polyphasic analysis. *Journal of Phycology*, 59(1), 12-51.
- Sudhakar, K., & Premalatha, M. (2015). Characterization of micro algal biomass through FTIR/TGA/CHN analysis: application to *Scenedesmus* sp. *Energy Sources, Part A: Recovery, Utilization, and Environmental Effects*, 37(21), 2330-2337. <https://doi.org/10.1080/15567036.2013.825661>.
- Suhani, I., Sahab, S., Srivastava, V., & Singh, R.P. (2021). Impact of Cd pollution on

- foodsafety and human health. *Current Opinion in Toxicology*, 27, 1-7.
- Sun, D.T., Peng, L., Reeder, W.S., Moosavi, S.M., Tiana, D., Britt, D.K., Oveisi, E., & Queen, W.L. (2018). Rapid, selective heavy metal removal from water by a metal-organic framework/polydopamine composite. *ACS central science* 4(3), 349-356.
- Sun, J., Ji, Y., Cai, F., & Li, J. (2012). Heavy Metal Removal Through Biosorptive Pathways. *Advances in water treatment and pollution prevention*, 95-145.
- Suresh, S. (2014). Studies on the dielectric properties of CdS nanoparticles. *Applied Nanoscience*, 4, 325-329.
- Tamura, K., Peterson, D., Peterson, N., Stecher, G., Nei, M., & Kumar, S. (2011). MEGA5: molecular evolutionary genetics analysis using maximum likelihood, evolutionary distance, and maximum parsimony methods. *Molecular biology and evolution*, 28(10), 2731-2739.
- Tan, H.T., Yusoff, F.M., Khaw, Y.S., Nazarudin, M.F., Noor Mazli, N.A.I., Ahmad, S.A., Shaharuddin, N.A., & Toda, T. (2023). Characterisation and selection of freshwater cyanobacteria for phycobiliprotein contents. *Aquaculture International*, 31(1), 447-477.
- Tan, Y., Chen, M., & Hao, Y. (2012). High efficient removal of Pb (II) by amino-functionalized Fe₃O₄ magnetic nano-particles. *Chemical engineering journal*, 191, 104-111.
- Tanabe, Y., Sano, T., Kasai, F., & Watanabe, M.M. (2009). Recombination, cryptic clades and neutral molecular divergence of the microcystin synthetase (mcy) genes of toxic cyanobacterium *Microcystis aeruginosa*. *BMC Evolutionary Biology*, 9, 1-14.

- Tapolczai, K., Keck, F., Bouchez, A., Rimet, F., Kahlert, M. & Vasselon, V. (2019). Diatom DNA metabarcoding for biomonitoring: strategies to avoid major taxonomical and bioinformatical biases limiting molecular indices capacities. *Frontiers in Ecology and Evolution* 7, 409.
- Tchounwou, P.B., Yedjou, C.G., Patlolla, A.K., & Sutton, D.J. (2012). Heavy metal toxicity and the environment. *Molecular, clinical and environmental toxicology: environmental toxicology*, 3, 133-164.
- Temkin, M. (1940). Kinetics of ammonia synthesis on promoted iron catalysts. *Acta physiochim*, 12, 327-356.
- Tempkin, M., & Pyzhev, V. (1940). Kinetics of ammonia synthesis on promoted iron catalyst. *Acta physicochimica U.R.S.S*, 12(1), 327.
- Thangaraj, B., Rajasekar, D. P., Vijayaraghavan, R., Garlapati, D., Devanesan, A. A., Lakshmanan, U., & Dharmar, P. (2017). Cytomorphological and nitrogen metabolic enzyme analysis of psychrophilic and mesophilic *Nostoc* sp.: a comparative outlook. *3 Biotechnology*, 7, 1-10.
- Tran, H.V., Dai Tran, L., & Nguyen, T.N. (2010). Preparation of chitosan/magnetite composite beads and their application for removal of Pb (II) and Ni (II) from aqueous solution. *Materials Science and Engineering*, 30(2), 304-310.
- Tripathy, B., Dash, A., & Das, A.P. (2022). Detection of environmental microfiber pollutants through vibrational spectroscopic techniques: recent advances of environmental monitoring and future prospects. *Critical Reviews in Analytical Chemistry*, 1-11. <https://doi.org/10.1080/10408347.2022.2144994>
- Tüzün, I., Bayramoğlu, G., Yalçın, E., Başaran, G., Celik, G., & Arica, M.Y. (2005a). Equilibrium and kinetic studies on biosorption of Hg (II), Cd (II) and Pb (II) ions onto microalgae *Chlamydomonas reinhardtii*. *Journal of Environmental*

- Management*, 77(2), 85-92.
- Uyeda, J.C., Harmon, L.J., & Blank, C.E. (2016). A comprehensive study of cyanobacterial morphological and ecological evolutionary dynamics through deep geologic time. *PloS one*, 11(9), 162539.
- Vasantharaj, S., Sathiyavimal, S., Saravanan, M., Senthilkumar, P., Gnanasekaran, K., Shanmugavel, M., Manikandan, E., & Pugazhendhi, A. (2019). Synthesis of ecofriendly copper oxide nanoparticles for fabrication over textile fabrics: characterization of antibacterial activity and dye degradation potential. *Journal of Photochemistry and Photobiology B: Biology*, 191, 143-149.
- Vasselon, V., Domaizon, I., Rimet, F., Kahlert, M., & Bouchez, A. (2017). Application of high- throughput sequencing (HTS) metabarcoding to diatom biomonitoring: Do DNA extraction methods matter? *Freshwater Science*, 36(1), 162-177.
- Vazquez-Martinez, J., Gutierrez-Villagomez, J.M., Fonseca-Garcia, C., Ramirez-Chavez, E., Mondragón-Sánchez, M.L., Partida-Martinez, L., Johansen, J.R., & Molina-Torres, J. (2018). *Nodosilinea chupicuarensis* sp. nov. (Leptolyngbyaceae, Synechococcales) a subaerial cyanobacterium isolated from a stone monument in central Mexico. *Phytotaxa*, 334(2), 167–182-167–182.
- Vázquez-Núñez, E., Molina-Guerrero, C. E., Peña-Castro, J. M., Fernández-Luqueño, F., & de la Rosa-Álvarez, M. G. (2020). Use of nanotechnology for the bioremediation of contaminants: A review. *Processes*, 8(7), 826.
- Verma, A., Kumar, S., & Kumar, S. (2016). Biosorption of lead ions from the aqueous solution by *Sargassum filipendula*: Equilibrium and kinetic studies. *Journal of Environmental Chemical Engineering*, 4(4), 4587-4599.
- Verma, A., Kumar, S., & Kumar, S. (2016). Biosorption of lead ions from the

- aqueous solution by *Sargassum filipendula*: Equilibrium and kinetic studies. *Journal of Environmental Chemical Engineering*, 4(4), 4587-4599.
- Vijayakumar, S. (2012). Potential applications of cyanobacteria in industrial effluents-a review. *Journal of Bioremediation & Biodegradation*, 3 (6): 1-6.
- Vilchez, C., Garbayo, I., Lobato, M.V., & Vega, J. (1997). Microalgae-mediated chemicals production and wastes removal. *Enzyme and Microbial Technology*, 20(8), 562-572.
- Vilchez, Carlos, et al. "Microalgae-mediated chemicals production and wastes removal." *Enzyme and Microbial Technology* 20.8 (1997): 562-572.
- Virkutyte, J., & Varma, R.S. (2011). Green synthesis of metal nanoparticles: biodegradable polymers and enzymes in stabilization and surface functionalization. *Chemical Science*, 2(5), 837-846.
- Volesky, B. (2003). Biosorption process simulation tools. *Hydrometallurgy*, 71(1-2), 179-190.
- Vu, C.H.T., Lee, H.-G., Chang, Y.K., & Oh, H.-M. (2018). Axenic cultures for microalgal biotechnology: establishment, assessment, maintenance, and applications. *Biotechnology advances*, 36(2), 380-396.
- Vuorio, K., Mäki, A., Salmi, P., Aalto, S.L., & Tirola, M. (2020). Consistency of targeted metatranscriptomics and morphological characterization of phytoplankton communities. *Frontiers in Microbiology*, 11, 96.
- Waalkes, M.P. (2000). Cd carcinogenesis in review. *Journal of inorganic biochemistry*, 79(1-4), 241-244.
- Waheed, A., Baig, N., Ullah, N., & Falath, W. (2021). Removal of hazardous dyes, toxic metal ions and organic pollutants from wastewater by using porous hyper-cross-linked polymeric materials: A review of recent advances. *Journal of*

- Environmental Management*, 287, 112360.
- R., Hopkin, S.P., & Peakall, D.B. (2012). Principles of ecotoxicology, CRC press.
- Wan, X., Zeng, W., Cai, W., Lei, M., Liao, X., & Chen, T. (2023). Progress and future prospects in co-planting with hyperaccumulators: Application to the sustainable use of agricultural soil contaminated by arsenic, Cd, and nickel. *Critical Reviews in Environmental Science and Technology*, 24(23),1-20.
- Wang, L., Liu, J., Filipiak, M., Mungunkhuyag, K., Jedynek, P., Burczyk, J., Fu, P., & Malec, P. (2021). Fast and efficient Cd biosorption by *Chlorella vulgaris* K-01 strain: The role of cell walls in metal sequestration. *Algal Research*, 60, 102497.
- Wang, S., Shi, L., Yu, S., Pang, H., Qiu, M., Song, G., Fu, D., Hu, B., & Wang, X.X. (2022b). Effect of shewanella oneidensis MR-1 on U(VI) sequestration by montmorillonite. *Journal of Environmental Radioactivity*, 242, 106798.
- Wang, Y., Ma, X., Li, Y., Li, X., Yang, L., Ji, L., & He, Y. (2012). Preparation of a novel chelating resin containing amidoxime–guanidine group and its recovery properties for silver ions in aqueous solution. *Chemical Engineering Journal* 209, 394-400.
- Weber Jr, W.J., & Morris, J.C. (1963). Kinetics of adsorption on carbon from solution. *Journal of the sanitary engineering division*, 89(2), 31-59.
- Wellborn, A.R. (1994). The spectral determination of chlorophylls a and b, as well as total carotenoids, using various solvents with spectrophotometers of different resolution. *Journal of plant physiology*, 144(3), 307-313.
- Whitton, B. A., & Potts, M. (2007). *The ecology of cyanobacteria: their diversity in time and space*. Springer Science & Business Media.
- Whitton, B.A. (2000). Soils and Rice-Fields. In: Whitton, B.A., Potts, M. (eds) *The Ecology of Cyanobacteria*. Springer, Dordrecht. <https://doi.org/10.1007/0-306->

46855-7_8.

- Whitton, B.A. (2012). Ecology of cyanobacteria II: their diversity in space and time, Springer Science & Business Media.
- Wilmotte, A., & Herdman M. (2001). Phylogenetic relationships among the cyanobacteria based on 16S rRNA sequences. In: *Bergey's Manual of Systematic Bacteriology* (Eds D.R. Boone, R.W. Castenholz & G.M. Garrity), pp. 487–493. Springer-Verlag, New York.
- Wolk, C., Ernst, A., Elhai, J.i., & Bryant, D. (1994). The molecular biology of cyanobacteria. *Kluwer Academic Publishers*, 769-823.
- Wong, F.C.Y., & Meeks, J.C. (2002). Establishment of a functional symbiosis between the cyanobacterium *Nostoc punctiforme* and the bryophyte *Anthoceros punctatus* requires genes involved in nitrogen control and initiation of heterocyst differentiation. *Microbiology*, 148(1), 315-323.
- Woodhouse, J.N., Kinsela, A.S., Collins, R.N., Bowling, L.C., Honeyman, G.L., Holliday, J.K., & Neilan, B.A. (2016). Microbial communities reflect temporal changes in cyanobacterial composition in a shallow ephemeral freshwater lake. *The International Society for Microbial Ecology journal*, 10(6), 1337-1351.
- World Water Assessment Programme (United Nations). (2006). *Water: A shared responsibility*, (Vol. 2). Berghahn Books.
- Wu, K., Su, D., Liu, J., Saha, R., & Wang, J. P. (2019). Magnetic nanoparticles in nanomedicine: a review of recent advances. *Nanotechnology*, 30(50), 502003.
- Wu, Q., Chen, J., Clark, M., & Yu, Y. (2014). Adsorption of copper to different biogenic oyster shell structures. *Applied Surface Science*, 311, 264-272.
- Wu, W., He, Q., & Jiang, C. (2008). Magnetic iron oxide nanoparticles: synthesis and surface functionalization strategies. *Nanoscale research letters*, 3, 397-415.

- Xie, Y., Fan, J., Zhu, W., Amombo, E., Lou, Y., Chen, L., & Fu, J. (2016). Effect of heavy metals pollution on soil microbial diversity and bermudagrass genetic variation. *Frontiers in Plant Science*, 7, 755.
- Xu, P., Zeng, G. M., Huang, D. L., Feng, C. L., Hu, S., Zhao, M. H., & Liu, Z. F. (2012). Use of iron oxide nanomaterials in wastewater treatment: a review. *Science of the total environment*, 424, 1-10.
- Xu, P., Zeng, G.M., Huang, D.L., Lai, C., Zhao, M.H., Wei, Z., Li, N.J., Huang, C., & Xie, G.X. (2012). Adsorption of Pb (II) by iron oxide nanoparticles immobilized *Phanerochaete chrysosporium*: equilibrium, kinetic, thermodynamic and mechanisms analysis. *Chemical Engineering Journal*, 203, 423-431.
- Yadav, A.P.S., Dwivedi, V., Kumar, S., Kushwaha, A., Goswami, L., & Reddy, B.S. (2020). Cyanobacterial extracellular polymeric substances for heavy metal removal: a mini review. *Journal of Composites Science*, 5(1), 1.
- Ye, S., Zeng, G., Wu, H., Liang, J., Zhang, C., Dai, J., & Yu, J. (2019). The effects of activated biochar addition on remediation efficiency of co-composting with contaminated wetland soil. *Resources, Conservation and Recycling*, 140, 278-285.
- Yogalakshmi, K. N., Das, A., Rani, G., Jaswal, V., & Randhawa, J. S. (2020). Nano-bioremediation: a new age technology for the treatment of dyes in textile effluents. *Bioremediation of Industrial Waste for Environmental Safety: Volume I: Industrial Waste and Its Management*, 313-347.
- Yu, C., Shao, J., Sun, W., & Yu, X. (2020). Treatment of lead contaminated water using synthesized nano-iron supported with bentonite/graphene oxide. *Arabian Journal of Chemistry*, 13(1), 3474-3483.
- Yuh-Shan, H. (2004). Citation review of Lagergren kinetic rate equation on

- adsorption reactions. *Scientometrics*, 59(1), 171-177.
- Yuvakkumar, R., Suresh, J., Saravanakumar, B., Nathanael, A.J., Hong, S.I., & Rajendran, V. (2015). Rambutan peels promoted biomimetic synthesis of bioinspired zinc oxide nanochains for biomedical applications. *Spectrochimica Acta Part A: Molecular and Biomolecular Spectroscopy*, 137, 250-258.
- Zahra, Z., Choo, D.H., Lee, H., & Parveen, A. (2020). Cyanobacteria: Review of current potentials and applications. *Environments*, 7(2), 13.
- Zamora-Ledezma, C., Negrete-Bolagay, D., Figueroa, F., Zamora-Ledezma, E., Ni, M., Alexis, F., & Guerrero, V.H. (2021). Heavy metal water pollution: A fresh look about hazards, novel and conventional remediation methods. *Environmental Technology & Innovation* 22, 101504.
- Zavřel, T., Očenášová, P., & Červený, J. (2017). Phenotypic characterization of *Synechocystis* PCC 6803 substrains reveals differences in sensitivity to abiotic stress. *PloS one*, 12(12), e0189130.
- Zhang, X., Zhao, X., Wan, C., Chen, B., & Bai, F. (2016). Efficient biosorption of Cd by the self-flocculating microalga *Scenedesmus obliquus* AS-6-1. *Algal Research*, 16, 427- 433.
- Zhang, Y., & Pan, B. (2014). Modeling batch and column phosphate removal by hydrated ferric oxide-based nanocomposite using response surface methodology and artificial neural network. *Chemical Engineering Journal*, 249, 111-120.
- Zhao, G., Li, J., Ren, X., Chen, C., & Wang, X. (2011). Few-layered graphene oxide nanosheets as superior sorbents for heavy metal ion pollution management. *Environmental Science & Technology*, 45, 10454–10462
- Zhu, W., Naidu, A.G., Wu, Q., Yan, H., Zhao, M., Wang, Z., & Liang, H. (2022). Simultaneous electrocatalytic hydrogen production and hydrazine removal from

acidic waste water. *Chemical Engineering Science*, 258, 117769.

Zinicovscaia, I., Cepoi, L., Povar, I., Chiriac, T., Rodlovskaya, E., & Culicov, O.A. (2018). Metal uptake from complex industrial effluent by cyanobacteria *Arthrospira platensis*. *Water, Air, & Soil Pollution*, 229, 1-10.

Author List of Publications Ph.D. Research

1. **Kaleem, M.**, Minhas, L. A., Hashmi, M. Z., Ali, M. A., Mahmoud, R. M., Saqib, S., & Samad Mumtaz, A. (2023). Biosorption of Cd and Lead by Dry Biomass of Nostoc sp. MK-11: Kinetic and Isotherm Study. *Molecules*, 28(5), 2292 ([Link](#))
2. **Kaleem, M.**, Minhas, L. A., Hashmi, M. Z., Farooqi, H. M. U., Waqar, R., Kamal, K., & Mumtaz, A. S. (2023). Biogenic Synthesis of Iron Oxide Nanoparticles and Experimental Modeling Studies on the Removal of Heavy Metals from Wastewater. *Journal of Saudi Chemical Society*, 101777. ([Link](#))

Rest of other Publications

1. **Kaleem, M.**, Hashmi, M. Z., & Mumtaz, A. S. (2022). Can algae reclaim polychlorinated biphenyl-contaminated soils and sediments? In *Biological Approaches to Controlling Pollutants* (pp. 273-283). Woodhead Publishing. ([Link](#))
2. Minhas, L.A., **Kaleem, M.**, Farooqi, H.M.U., Kausar, F., Waqar, R., Bhatti, T., Aziz, S., Jung, D.W. and Mumtaz, A.S., 2024. Algae-derived bioactive compounds as potential nutraceuticals for cancer therapy: A comprehensive review. *Algal Research*, p.103396. ([Link](#))
3. Minhas, L.A.; **Kaleem, M.**; Jabeen, A.; Ullah, N.; Farooqi, H.M.U.; Kamal, A.; Inam, F.; Alrefaei, A.F.; Almutairi, M.H.; Mumtaz, A.S. Synthesis of Silver Oxide Nanoparticles: A Novel Approach for Antimicrobial Properties and Biomedical Performance, Featuring *Nodularia haraviana* from the Cholistan Desert. *Microorganisms* 2023, 11, 2544
4. Minhas, L. A., **Kaleem, M.**, Minhas, M. A. H., Waqar, R., Al Farraj, D. A., Alsaigh, M. A., & Mumtaz, A. S. (2023). Biogenic Fabrication of Iron Oxide Nanoparticles from *Leptolyngbya* sp. L-2 and Multiple In Vitro Pharmacogenetic

- Properties. *Toxics*, 11(7), 561. ([Link](#))
5. Minhas, L. A., Mumtaz, A. S., **Kaleem, M.**, Waqar, R., & Annum, J. (2023). A prospective study on morphological identification and characterization of freshwater green algae based on the microscopic technique in District Rawalpindi. *Pakistan Journal of Agricultural Research*, 36(1), 20-35. ([Link](#))
 6. Minhas, L. A., Mumtaz, A. S., **Kaleem, M.**, Farraj, D. A., Kamal, K., Minhas, M. A. H., & Mahmoud, R. M. (2023). Green Synthesis of Zinc Oxide Nanoparticles Using *Nostoc* sp. and Their Multiple Biomedical Properties. *Catalysts*, 13(3), 549. ([Link](#))
 7. Waqar, R., **Kaleem, M.**, Iqbal, J., Minhas, L. A., Haris, M., Chalgham, W., ... & Mumtaz, A. S. (2023). Kinetic and Equilibrium Studies on the Adsorption of Lead and Cd from Aqueous Solution Using *Scenedesmus* sp. *Sustainability*, 15(7), 6024. ([Link](#))
 8. Waqar R, Rahman S, Iqbal J, **Kaleem M**, Minhas LA, Ullah N, Kausar F, Chalgham W, Al- Misned FA, El-Serehy HA, et al. Biosorption Potential of *Desmodesmus* sp. for the Sequestration of Cd and Lead from Contaminated Water. *Sustainability*. 2023;15(15):11634. <https://doi.org/10.3390/su151511634>. ([Link](#))
 9. Inam, F., Mumtaz, A. S., **Kaleem, M.**, & Sajid, I. (2022). Morphogenetic variation and assorted biological activities in true branching Nostocales strains of Cholistan oasis, Pakistan. *Journal of Basic Microbiology*, 62(5), 634-643. ([Link](#))
 10. Kausar, F., Kim, K. H., Farooqi, H. M. U., Farooqi, M. A., **Kaleem, M.**, Waqar, R., & Mumtaz, A. S. (2021). Evaluation of antimicrobial and anticancer activities of selected medicinal plants of Himalayas, Pakistan. *Plants*, 11(1), 48. ([Link](#))
 11. Hashmi, M. Z., **Kaleem, M.**, Farooq, U., Su, X., Chakraborty, P., & Rehman, S.

- U. (2022). Chemical remediation and advanced oxidation process of polychlorinated biphenyls in contaminated soils: a review. *Environmental Science and Pollution Research*, 29(16), 22930-22945. ([Link](#))
12. Badshah, H., Nisa, S. U., Ali, M. A., Alwahibi, M. S., Kamal, A., **Kaleem, M.**, & Mumtaz, A. S. (2023). Bio-Concentration and Influence of Environmental Factors on Accumulation of Heavy Metals in Edible Autumn Morel (*Morchella galilaea*) of Low Elevation. *Metals*, 13(3), 472. ([Link](#))
13. Khan, A. S., Ahmad, M., Gilani, S. A. A., Zafar, M., Butt, M. A., Lubna, ... & **Kaleem, M.** (2021). Taxonomic implications of macro and micromorphological characters in the genus *Brachythecium* (Brachytheciaceae, Bryopsida) from the Western Himalayas: A combined light and scanning electron microscopic analysis. *Microscopy Research and Technique*, 84(12), 3000-3022. ([Link](#))
14. Ullah, N., Mumtaz, A.S., Minhas, L.A., **Kaleem, M.**, Waqar, R., Jabeen, A., Hanif, A., Morpho-taxonomic identification and seasonal correlation between algal diversity and water physio-chemical parameters in District Bajaur Khyber Pakhtunkhwa. *Pakistan Journal of Agriculture Research*, 36(3): 193-206
15. Jabeen, A., Mumtaz, A., **Kaleem, M.**, Minhas LA., & Ullah, N. (2023). Taxonomic Identification of Microalgae of District Jhelum through Light Microscopy

Appendix (I)

Composition of Bol's Basal medium

Stock solution(SL)	Components	Concentration (gm/L dH ₂ O)
Macronutrients (10ml vol)		
SL I	NaNO ₃	25
SL II	CaCl ₂ .2H ₂ O	2.5
SL III	NaCl	2.5
SL IV	K ₂ HPO ₄	7.5
SL V	KH ₂ PO ₄	17.5
SL VI	MgSO ₄ .7H ₂ O	7.5
Trace Elements Solution (1 ml)		
SL VII	ZnSO ₄ .7H ₂ O	8.82
	MnCl ₂ .4H ₂ O	1.44
	MoO ₃	0.71
	CuSO ₄ .5H ₂ O	1.57
	Co(NO ₃) ₂ .6H ₂ O	0.49
Boron Solution (1 ml)		
SL VIII	H ₃ BO ₃	11.42
Alkaline EDTA Solution (1 ml)		
SL IX	EDTA	50
	KOH	31
Acidified Ferric Solution (1ml)		
SL X	FeSO ₄ .7H ₂ O	4.98
	H ₂ SO ₄	1ml (to acidify)

Appendix (II)

Compositions of BG-11 medium

Stock solutions (SL)	Component	gm/L	Volume
SL I	Na ₂ MgEDT A	0.1	10 ml
	Ferric Ammoniu mCitrate	0.6	
	Citric acid	0.6	
	CaCl ₂ .2H ₂ O	3.6	
SL II	MgSO ₄ .7H ₂ O	7.5	10 ml
SL III	K ₂ HPO ₄ .3H ₂ O	4.0	10 ml
SL IV	Micronutrient media		
	Component	gm/L	1 ml
	H ₃ BO ₃	2.86	
	MnCl ₂ . 4H ₂ O	1.81	
	ZnSO ₄ . 7H ₂ O	0.222	
	CuSO ₄ . 5H ₂ O	0.079	
	NaMoO ₄ . 2H ₂ O	0.391	
	COCl ₂ .6H ₂ O	0.050	

Appendix (III)

Composition of Spirulina medium

Stock Solution (SL)	Components	Concentration (gm)	Volume (500ml)
SL 1	NaHCO ₃	13.61	500
	Na ₂ CO ₃	4.03	
	K ₂ HPO ₄	0.50	
SL 11	NaNO ₃	2.5	500
	NaCl	1	
	K ₂ SO ₄	1	
	MgSO ₄ .7H ₂ O	0.20	
	CaCl ₂ .2H ₂ O	0.04	
	FeSO ₄ .7H ₂ O	0.01	
	EDTA (triplex)	0.08	
	Micronutrient solution	5 ml	

Appendix (IV)

Composition of CTAB buffer

Component	Amount (gm/100ml)
CTAB	2.00 gm
NaCl	8.19 gm
TRIS HCl	1.2 gm
EDTA	0.58 gm

Appendix (V)

10X CTAB composition

NaCl	4.1 gm
CTAB	10 gm
Distilled water	100 ml

Appendix (VI)**3M Sodium Acetate solution**

Component	Quantity (gm/100ml)
Sodium acetate	60 or 24.6 gm
Distilled water	100 ml

Appendix (VII)**10X TBE buffer composition**

Tris Base	108 gm
0.5 M EDTA	40 ml
Boric acid	55 gm
Distilled water	1 Litre

Appendix (VIII)**1% agarose gel composition**

10 X TBE	10 ml
dH ₂ O	90 ml
Agarose	1 gm
Ethidium Bromide	2 µl

Appendix (IX)**Chloroform Isoamyl alcohol (24:1)**

Chloroform	24 ml
Isoamyl alcohol	1 ml

Appendix (X)**10% SDS solution:**

Dissolve 10 gm SDS in 100 ml of dH₂O

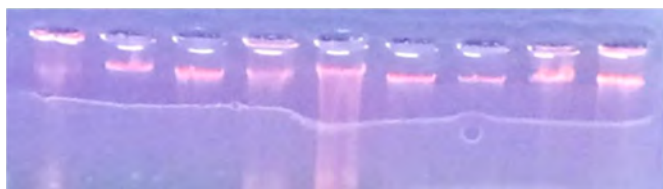
Appendix (XI)

6X Loading Dye composition

Tris HCl	10 Mm
EDTA	60 Mm
Glycerol	60%
Xylene cyanol FF	0.03 %
Bromophenol blue	0.03 %

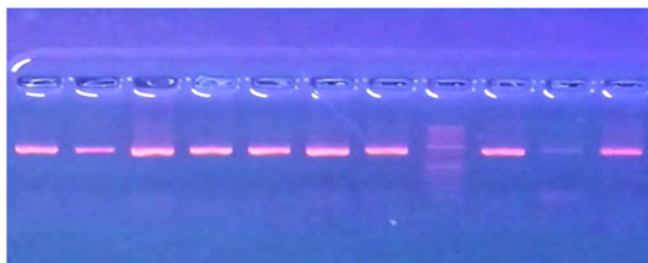
Appendix (XII)

DNA bands of axenic cyanobacteria strains



Appendix (XIII)

PCR DNA bands of cyanobacteria axenic strains



Turnitin Originality Report

Genetic Characterization of Selected Cyanobacteria and their Role in Remediating Environmental Pollutants by Muhammad Kaleem .

From Quick Submit (Quick Submit)

- Processed on 16-Sep-2024 10:28 PKT
- ID: 2455483791
- Word Count: 40678

Similarity Index

19%

Similarity by Source

Internet Sources:


10%

Publications:

16%

Student Papers:

5%


Professor
Department of Microbiology
Quaid-i-Azam University Islamabad

sources:

- 1 < 1% match (Internet from 10-Nov-2014)
<http://dns2.asia.edu.tw/~ysho/YSHO-English/Database/C.docx>
- 2 < 1% match (Internet from 27-May-2016)
<http://dns2.asia.edu.tw/~ysho/YSHO-English/Database/J-1.docx>
- 3 < 1% match (Internet from 04-Aug-2014)
<http://dns2.asia.edu.tw/~ysho/YSHO-English/Database/A.docx>
- 4 < 1% match (Internet from 01-Aug-2024)
<https://WWW.MDPI.COM/2071-1050/15/15/11634>
- 5 < 1% match (Internet from 09-Jul-2024)
<https://WWW.MDPI.COM/2076-2607/12/6/1217>
- 6 < 1% match (Internet from 11-Oct-2022)
<https://www.mdpi.com/1996-1944/13/2/481/htm>
- 7 < 1% match (Internet from 17-Jul-2024)
<https://WWW.MDPI.COM/2073-4441/16/10/1449>
- 8 < 1% match (Internet from 14-Oct-2022)
<https://www.mdpi.com/2076-3417/11/7/3125/htm>
- 9 < 1% match (Internet from 21-Jun-2023)
<https://www.mdpi.com/2073-4360/13/6/921>
- 10 < 1% match (Internet from 12-Mar-2024)
<https://WWW.MDPI.COM/1420-3049/25/22/5429>
- 11 < 1% match (Internet from 12-Jun-2024)
<https://www.mdpi.com/2310-2861/10/4/243>
- 12 < 1% match (Internet from 05-Jul-2024)
<https://WWW.MDPI.COM/2073-4395/12/10/2500>
- 13 < 1% match (Internet from 02-May-2023)
<https://www.mdpi.com/2073-4441/15/9/1688>
- 14 < 1% match (Internet from 30-Jun-2022)
https://link.springer.com/article/10.1007/s10570-019-02328-w?code=628e5216-cbf0-4708-a5a6-85dd85271a2f&error=cookies_not_supported
- 15 < 1% match (Internet from 29-Aug-2022)
https://link.springer.com/article/10.1007/s11356-022-19127-9?code=b0c71d21-855c-4937-aa65-7b696c529c01&error=cookies_not_supported

Focal Person (Turnitin)
Quaid-i-Azam University
Islamabad





Biogenic synthesis of iron oxide nanoparticles and experimental modeling studies on the removal of heavy metals from wastewater

Muhammad Kaleem^a, Lubna Anjum Minhas^a, Muhammad Zaffar Hashmi^b, Hafiz Muhammad Umer Farooqi^c, Rooma Waqar^a, Khalid Kamal^d, Rawa Saad Aljalud^e, Khaloud Mohammed Alarjani^e, Abdul Samad Mumtaz^{a*}

^a Department of Plant Sciences, Faculty of Biological Sciences, Quaid-i-Azam University, Islamabad 45320, Pakistan

^b Institute of Molecular Biology and Biotechnology, The University of Lahore, Pakistan

^c Board of Governors Regenerative Medicine Institute, Cedars-Sinai Medical Center, West Hollywood, Los Angeles, CA 90048, USA

^d Department of Chemistry, Faculty of Natural Sciences, Kohat University of Science and Technology, Pakistan

^e Department of Botany and Microbiology, College of Science, King Saud University, Riyadh 11451, Saudi Arabia

ARTICLE INFO

Keywords:

Nano-bioremediation
Cyanobacteria
Iron oxide nanoparticles
Cd
Pb
Adsorption

ABSTRACT

Water pollution is a major global challenge due to the fast expansion of industrial activities and the increasing human population. Certain heavy metals can be exceedingly hazardous and contribute significantly to water contamination. In this study, iron oxide nanoparticles (IONPs) were synthesized using cyanobacteria extract to remove heavy metals (Cd and Pb) from the wastewater. To characterize the IONPs, several analytical techniques were employed such as Ultraviolet-visible spectroscopy revealed a SPR (surface plasmon resonance) peak at 348 nm and FTIR (Fourier transform infrared) spectral analysis showed the OH, C-H and S=O functional groups which confirmed the biomolecules responsible for the biogenic synthesis and stability. The surface morphology of the biogenic IONPs was investigated using SEM (scanning electron microscopy) which revealed their nearly spherical or cubic shape. Additionally, XRD (X-ray diffraction) analysis confirmed the crystallinity of IONPs, with a crystalline size measuring 13.21 nm. Effects of contact time, pH, initial metal ions concentrations, and IONPs dosage were studied on the adsorption of Cd and Pb ions. Different adsorption kinetics and isotherm models were applied to the experimental data. Pseudo second-order kinetic and Langmuir isotherm models were well fitted to the adsorption of Cd and Pb onto the IONPs. Higher correlation coefficients (R^2) values of Langmuir isotherm (R^2 : 0.990 for Cd and Pb adsorption) and Pseudo second-order kinetic (R^2 : 0.998 and 0.999 for Cd and Pb adsorption, respectively) were found, which indicated the favorable interaction between the metal ions and adsorbent. Langmuir isotherm calculated maximal adsorption capacities of 105.932 and 110.764 mg/g for Cd and Pb, respectively. Recyclability of IONPs was conducted and after five adsorption/desorption cycles, IONPs retained their adsorption efficiency with negligible decline. After five cycles, IONPs removal efficiency was up to 80.41 and 88.35 % for Cd and Pb, respectively. Results of this study indicate that cyanobacteria-mediated IONPs were efficient adsorbent for Pb and Cd removal from contaminated aqueous solution.

1. Introduction

Heavy metals (HMs) are naturally found in the earth crust. However, human activities like mining, agriculture, and industrial emissions contribute to release of these HMs into the environment [1]. The concentration of heavy metals in soil, groundwater, and various water

bodies is exceeding the acceptable limits in many countries as a result of unplanned urbanization, industrialization, population growth, and poor management policies leading to a hidden threat to the human food chain [1–3]. Cadmium and Lead are considered the most lethal environmental pollutants because they are not only dangerous to plants but also to humans. Their pollution is a serious environmental issue that harms

* Corresponding author.

E-mail addresses: mkaleem@ksj.sci.edu.sa (M. Kaleem), lubnaminhas@ksj.sci.edu.sa (L. Anjum Minhas), hashmi_ghar@yahoocdn.com (M. Zaffar Hashmi), umerf.farooqi@csis.org (H.M. Umer Farooqi), 444203472@student.ksu.edu.sa (R. Saad Aljalud), kalarjani@ksu.edu.sa (K.M. Alarjani), asmumtaz@ksu.edu.sa (A. Samad Mumtaz).

<https://doi.org/10.1016/j.jscs.2023.101777>

Received 10 October 2023; Received in revised form 1 December 2023; Accepted 4 December 2023

Available online 7 December 2023

1319-6103/© 2023 The Authors. Published by Elsevier B.V. on behalf of King Saud University. This is an open access article under the CC BY-NC-ND license (<http://creativecommons.org/licenses/by-nc-nd/4.0/>).

Article

Biosorption of Cadmium and Lead by Dry Biomass of *Nostoc* sp. MK-11: Kinetic and Isotherm Study

Muhammad Kaleem ¹, Lubna Anjum Minhas ¹, Muhammad Zafar Hashmi ², Mohammad Ajmal Ali ³, Rania M. Mahmoud ⁴, Saddam Saqib ^{5,6}, Moona Nazish ⁷, Wajid Zaman ^{8,*} and Abdul Samad Mumtaz ^{1,4,*}

¹ Department of Plant Sciences, Quaid-i-Azam University, Islamabad 45320, Pakistan

² Department of Chemistry, COMSATS University, Islamabad 43550, Pakistan

³ Department of Botany and Microbiology, College of Science, King Saud University, Riyadh 11451, Saudi Arabia

⁴ Department of Botany, Faculty of Science, University of Fayoum, Fayoum 63514, Egypt

⁵ State Key Laboratory of Systematic and Evolutionary Botany, Institute of Botany, Chinese Academy of Sciences, Beijing 100093, China

⁶ University of Chinese Academy of Sciences, Beijing 100049, China

⁷ Department of Botany, Rawalpindi Women University, Rawalpindi 46000, Pakistan

⁸ Department of Life Sciences, Yeungnam University, Gyeongsan 38541, Republic of Korea

* Correspondence: wajidzaman@yu.ac.kr (W.Z.); asmumtaz@qu.edu.pk (A.S.M.)



Citation: Kaleem, M.; Minhas, L.A.; Hashmi, M.Z.; Ali, M.A.; Mahmoud, R.M.; Saqib, S.; Nazish, M.; Zaman, W.; Samad Mumtaz, A. Biosorption of Cadmium and Lead by Dry Biomass of *Nostoc* sp. MK-11: Kinetic and Isotherm Study. *Molecules* **2023**, *28*, 2292. <https://doi.org/10.3390/molecules28052292>

Academic Editor: Federico Menegazzo

Received: 13 February 2023

Revised: 26 February 2023

Accepted: 27 February 2023

Published: 1 March 2023



Copyright © 2023 by the authors. Licensee MDPI, Basel, Switzerland. This article is an open access article distributed under the terms and conditions of the Creative Commons Attribution (CC BY) license (<https://creativecommons.org/licenses/by/4.0/>).

Abstract: Cadmium (Cd) and lead (Pb) are global environmental pollutants. In this study, *Nostoc* sp. MK-11 was used as an environmentally safe, economical, and efficient biosorbent for the removal of Cd and Pb ions from synthetic aqueous solutions. *Nostoc* sp. MK-11 was identified on a morphological and molecular basis using light microscopic, 16S rRNA sequences and phylogenetic analysis. Batch experiments were performed to determine the most significant factors for the removal of Cd and Pb ions from the synthetic aqueous solutions using dry *Nostoc* sp. MK11 biomass. The results indicated that the maximum biosorption of Pb and Cd ions was found under the conditions of 1 g of dry *Nostoc* sp. MK-11 biomass, 100 mg/L of initial metal concentrations, and 60 min contact time at pH 4 and 5 for Pb and Cd, respectively. Dry *Nostoc* sp. MK-11 biomass samples before and after biosorption were characterized using FTIR and SEM. A kinetic study showed that a pseudo second order kinetic model was well fitted rather than the pseudo first order. Three isotherm models Freundlich, Langmuir, and Temkin were used to explain the biosorption isotherms of metal ions by *Nostoc* sp. MK-11 dry biomass. Langmuir isotherm, which explains the existence of monolayer adsorption, fitted well to the biosorption process. Considering the Langmuir isotherm model, the maximum biosorption capacity (q_{max}) of *Nostoc* sp. MK-11 dry biomass was calculated as 75.757 and 83.963 mg g⁻¹ for Cd and Pb, respectively, which showed agreement with the obtained experimental values. Desorption investigations were carried out to evaluate the reusability of the biomass and the recovery of the metal ions. It was found that the desorption of Cd and Pb was above 90%. The dry biomass of *Nostoc* sp. MK-11 was proven to be efficient and cost-effective for removing Cd and especially Pb metal ions from the aqueous solutions, and the process is eco-friendly, feasible, and reliable.

Keywords: biosorption; cadmium; lead; *Nostoc* sp. MK-11; kinetics; isotherms

1. Introduction

Heavy metal pollution is a severe global issue because of its non-biocompatibility, concealment, and high toxicity [1]. In general, mining, metal manufacturing, electronic electroplating, agricultural activities, and wastewater discharge from metallurgy are the major anthropogenic factors that contribute to the rising level of harmful metals in the environment [2–4]. A long-term exposure to heavy metals can cause irreversible damage to many biological systems [5].